Don E. Grissette
Vice President

Southern Nuclear
Operating Company, Inc.
40 Inverness Center Parkway
Post Office Box 1295
Birmingham, Alabama 35201

Tel 205.992.6474
Fax 205.992.0341

SOUTHERN COMPANY
Energy to Serve Your World℠

December 21, 2004

Docket No.: 50-425

NL-04-2413

U. S. Nuclear Regulatory Commission
ATTN: Document Control Desk
Washington, D. C. 20555-0001

Vogtle Electric Generating Plant
2R10 Steam Generator Tube Pull Test Results

Ladies and Gentlemen:

During Vogtle Electric Generating Plant (VEGP) Unit 2, Interval 2, Period 2, Outage 2 (2R10), the Steam Generator Maintenance Services Group of the Westinghouse Nuclear Services Division performed eddy current testing of two (2) Westinghouse Model F steam generators (SGs), numbers 2 and 3, in parallel from April 19 to May 10, 2004. The SG inspection results were included in the August 13, 2004, VEGP 2R10 Inservice Inspection (ISI) Summary Report.

The 2R10 ISI Summary Report stated that two tubes were pulled in SG 2 (row 11/column 60 and 12/59) for laboratory testing due to the discovery of circumferential crack indications. These tubes were cut below the second support plate on the Hot Leg side. Welded plugs were installed on the Hot Leg and mechanical plugs were installed on the Cold Leg. The pulled tubes were tested by Westinghouse, and the test results are enclosed as requested by the NRC staff.

This letter contains no NRC commitments. If you have any questions, please advise.

Sincerely,

Don E. Grissette

DEG/DRG/sdl

Enclosure: Vogtle Electric Generating Plant 2R10 Steam Generator Tube Pull Test Results

A047

cc: Southern Nuclear Operating Company
Mr. J. T. Gasser, Executive Vice President
Mr. W. F. Kitchens, General Manager – Plant Vogtle
RType: CVC7000

U. S. Nuclear Regulatory Commission
Dr. W. D. Travers, Regional Administrator (*w/o enclosure*)
Mr. C. Gratton, NRR Project Manager – Vogtle (*w/o enclosure*)
Mr. G. J. McCoy, Senior Resident Inspector – Vogtle (*w/o enclosure*)

SG-SGDA-04-45

STEAM GENERATOR PULLED TUBE EXAMINATION
VOGTLE 2R10

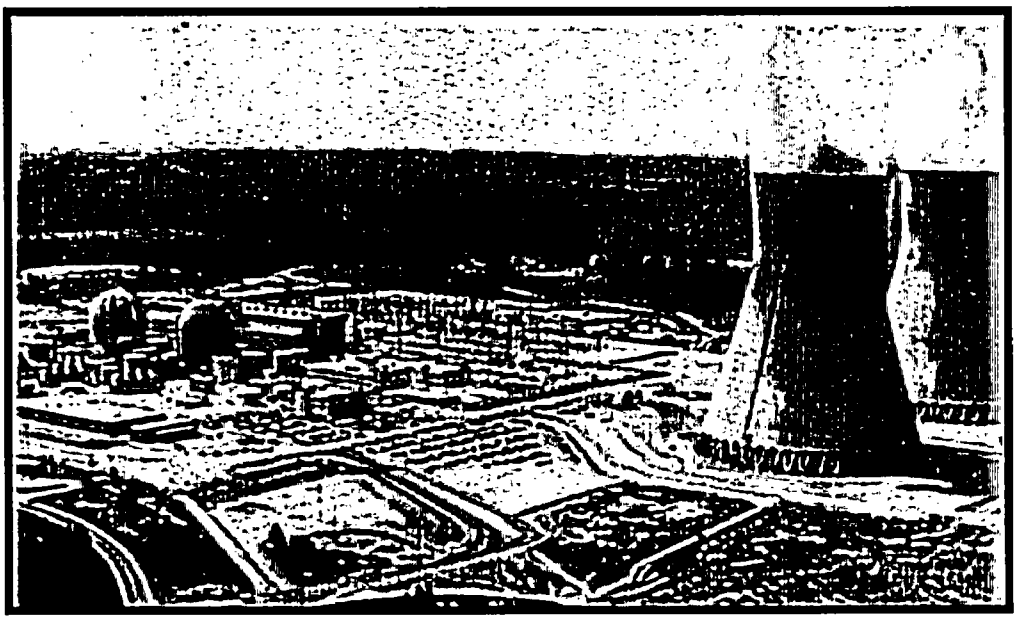

Prepared for
Southern Nuclear Operating Company

November 2004

Westinghouse Electric Company LLC
Nuclear Services

Table of Contents

Section	Description	Page
1	Summary and Conclusion	1-1
2	Introduction	2-1
3	Receipt Inspection	3-1
4	Sectioning Plans	4-1
5	Field and Laboratory Eddy Current Data Evaluation	5-1
6	Ultrasonic (Shear Wave) Data Evaluation	6-1
7	Post Pressurization Eddy Current Data Evaluation	7-1
8	Azimuthal Orientation of Signals	8-1
9	Laboratory Lamb Wave Data Evaluation	9-1
10	Deposit and OD Surface Analyses	10-1
11	Metallography	11-1
12	Tube Material Characterization	12-1

SECTION 1

SUMMARY AND CONCLUSION

During the Vogtle Unit 2 2R10 refueling outage, circumferential oriented flaw-like indications were reported at the top of tubesheet. The material of construction of the Vogtle 2 SG tubes is Alloy 600TT. Based on +Pt inspection data, the indications were reported to be within or at the hydraulic expansion transition at the top of the tubesheet (TTS) on the hot leg (HL) of the SG in all cases. A total of nine tubes in the four Vogtle 2 SGs were reported with flaw-like +Pt signals. Ultrasonic testing (UTEC) performed on 8 tubes in SG2 and SG3 corroborated 4 of the 6 +Pt circumferential indications (SCI) and, resolved as NDD, 2 tubes with PVN indications that masked the TSH region. The 2R10 outage was conducted after cumulative service equivalent to ~13.4 EFPY (effective full power years). As with all previous inspections, the condition of the Vogtle Unit 2 SGs as determined from the evaluation of the 2R10 inspection data met all industry and regulatory structural and leakage integrity guidance. Due to the unexpected identification of flaw-like indications in the Vogtle Unit 2 steam generators, two tubes were removed from Steam Generator 2 for detailed laboratory examination. The tubes were located at R12C59 HL and R11C60 HL and were cut below the 2nd tube support plate (2H).

The laboratory examination of the pulled tube sections, performed at the Westinghouse Remote Hot Cell Facility, included visual, eddy current, and ultrasonic inspections, as well as, detailed microchemistry and metallurgical evaluations. Both pulled tubes exhibited a ring of gray / brownish deposit at and slightly above the tube expansion transition. The height of this deposit was approximately ½ inch and was approximately 4 to 8 mils in thickness. A dark grayish deposit extending approximately 1 to 1 ½ inch above the collar deposit was noted on both tubes. A relatively thin and uniform gray oxide was noted on all remaining tube surfaces above the TTS region. Evidence of a white / grayish deposit was seen at two of the quatrefoil land to tube intersections on R12C59 HL. No evidence of a deposit at the quatrefoil land to tube intersection was noted on R11C60 HL.

All tubing sections were inspected using a 0.560 inch diameter differential bobbin coil probe. The tubes sections containing an area of interest were then cut into 12 inch lengths with the TTS or TSP intersection at their center. These sections were then inspected using +Pt, 3-Coil, and Ghent probes. After completing the eddy current examination of the tube sections, the two sections containing the TTS regions of (R12C59 HL and R11C60 HL) were ultrasonically (UTEC) inspected using techniques similar to those used in the field.

Laboratory eddy current and UTEC inspection efforts were not able to reproduce the field reported flaw-like indications. While many of the signals indicative of deposits remain, none of the field signals indicative of tube wall discontinuities were present in the laboratory.

Destructive examination of the TTS region of R12C59 HL – Piece 2B was performed to validate the laboratory E/C and UTEC inspection results. No destructive examinations were performed on the pulled sections from R11C60 HL. Piece 2B containing the TTS region will be available for future NDE development efforts, if required. Metallorgraphic examination of the top of tubesheet region of R12C59 HL showed no evidence of tube wall degradation. Microchemistry of the oxide deposit at the top of tubesheet and tube support plate showed no unexpected chemical species. Copper and lead were identified both within the oxide deposit as well as on the tube OD surfaces, however there was no indication of lead or copper induced corrosion initiation.

The results of the laboratory analyses of Vogtle Unit 2 pulled tubes showed that the flaw-like signals reported at the top of the tubesheet do not represent circumferential ODSCC in the hydraulic transitions. Even though it was not possible to determine the root cause of the field flaw-like signals, the likely rationale to explain the occurrence of the false positives centers on the nature and the non-homogeneity of scale/deposits on the tubes at the top of the HL tubesheet. The plugging of nine tubes on the basis of the TTS circumferential indications should be regarded as a precautionary action and that no results from the pulled tube examination were obtained that would warrant a change in the inspection or cleaning plans that prevailed prior to the 2R10 outage.

SECTION 2

INTRODUCTION

Vogtle Unit 2 is a four loop Westinghouse designed pressurized water reactor. The plant is owned and operated by the Southern Company and has accumulated 13.4 EFPY of operation prior to the 2R10 outage. The steam generators are Model F with thermal treated Alloy 600 tubing, full depth hydraulic expanded tube to tubesheet joints, and Type 405 stainless steel tube support plates (TSP's) with quatrefoil tube holes. The thermal treated Alloy 600 steam generator tubes are 11/16 inch in outer diameter and have a nominal wall thickness of 40 mils.

As summarized in the Degradation Assessment (Reference 2-1), the planned 2R10 inspection program was scheduled to be implemented in SG2 and SG3. The proposed inspection program included 100% bobbin examination, +Pt inspection of 50% of Row 1 and 2 U-bends, and +Pt inspection of the 50% of the hot leg (HL) top of the tubesheet (TTS) expansion transition region. During the +Pt inspection of the TTS region, OD circumferential indications were reported at a number off TTS locations resulting in an expansion of the +Pt inspection programs to 100% of HL tubes in all 4 SGs. No expansion of the +Pt program to the cold leg (CL) hydraulic transitions was required since the population of tubes with OD circumferential indications did not rise to the C-3 results category (Reference 2-2); the HL-CL temperature differential ~50° F is such that even if the HL indications did represent ODSCC, the large difference in the time anticipated to crack initiation in the CL hydraulic transitions supports limiting the inspection to the HL transitions. During the HL +Pt eddy current inspection, a total of nine (9) locations across the four (4) steam generators were identified with OD circumferential indications. There were two tubes identified with potential cracking in SGs 2, 3, and 4 and one tube with potential circumferential cracking in SG 1. Subsequent inspection using ultrasonic techniques, confirmed the reported OD circumferential indications in a number of the tubes. Table 2-1 provides a summary of the +Pt inspection history for the nine (9) location identified with OD circumferential indications at the hydraulic expansion transition. A tubesheet map showing the Row/ Column location of the nine (9) tubes is provided in Figure 2-1. Except for R46C89 HL in Steam Generator 3, all locations are clustered near the center of the bundle and within the area of the tubesheet where secondary side deposit buildup is more likely to occur due to reduce flow velocities. This area also corresponds to the "cut-out" region of the flow distribution baffle plate.

Due to the unexpected identification of flaw-like indications in the Vogtle Unit 2 steam generators, two tubes were removed from Steam Generator 2 for detailed laboratory

examination. The tubes were located at R12C59 HL and R11C60 HL and were cut below the 2nd tube support plate (2H). The bare holes were sealed with a welded plug. The removal of the tubes required elimination of the tube-to-tubesheet weld and TIG relaxation of the hydraulic expansion region, after which the tubes were pulled though the tubesheet. Both tubes were cut approximately 6 inches below the 2nd tube support plate. Both pulled tubes were located within the "cut-out" portion of the flow distribution baffle plate and therefore the pulled sections contained only the TTS and the 1st TSP intersections.

Following the removal from the steam generators, the pulled tube segments were transported to the Westinghouse Remote Hot Cell Metallographic Laboratory for destructive and nondestructive examinations. The evaluation effort consisted of the following activities:

- Verification of section identification – All pulled sections were measured for length and visually surveyed for landmark features (e.g. TTS and TSP intersections for comparison with tube pull records.
- Visual characterization of pulled tube sections – The purpose of this effort was to identify and characterize any tube degradation, characterize the appearance of any secondary side deposits, and identify any damage from the tube pulling process.
- Eddy current inspection – Full length bobbin examination and +Pt confirmation of all bobbin signals was performed on each pulled section. This information served to precisely locate all indications and to determine any differences from the pre-pull inspection.
- Ultrasonic inspections – The TTS regions of both pulled tubes were inspected using Shear Wave and Lamb Wave methods. The Shear Wave method was equivalent to the field inspection method, while the Lamb Wave method was employed based on its reduced sensitivity to OD deposits.
- OD profiling of tube sections at the TTS and TSP intersections using laser micrometer methods..
- ID profiling of the TTS expansion transition.
- Characterization of tubing material by chemistry, microhardness, residual stress, grain size, carbide distribution and Huey testing.
- SEM and EDS characterization of tube deposits at TTS and TSP areas.
- Metallography of R12C59 HL – Piece 2B to validate NDE findings.

The results of the various evaluations are summarized in the following sections. All examinations and testing presented in this report were treated as safety-related and were

performed in accordance with the Westinghouse Quality Assurance program, which satisfies the requirements of 10CFR50 Appendix B.

References:

2.1 LTR-SGDA-04-83 (SG-SGDA-04-14), SG Degradation Assessment for Vogtle Unit 2, 2R10 Refueling Outage, April 2004.

2-2 TR-1003138, "EPRI PWR SG Examination Guidelines", Revision 6, October 2002.

Table 2-1 - Summary of Inspection Results of Locations Identified With Top of Tubesheet Flaw-Like Signals: 2R10 (Spring 2004)

	Inspection Results					
SG # and Location	2R10 (2004)	2R09 (2002)	2R08 (2001)	2R07 (1999)	2R06 (1998)	2R05 (1996)
SG 1 R11C64	SCI - 31% Depth, 51.4° Extent: 0.30 volts on 300 kHz +Pt coil Crevice depth of 0.18" and an estimated sludge height of 1.00" to 1.50" by bobbin No UT performed Location stabilized and plugged	Signal not as pronounced as the current flaw-like signal	-	Signal not present	-	Signal not present
SG 2 R17C68	SCI – 17% Depth; 86.8° Extent; 0.42 volts on 300 kHz +Pt coil Crevice depth of 0.06" and an estimated sludge height of 0.00" by bobbin NDD by UT Location stabilized and plugged	-	Signal present but not flaw-like	-	Signal present but not flaw-like	-
SG 2 R12C59	SCI – 22% Depth; 41.8° Extent; 0.29 volts on 300 kHz +Pt coil Crevice depth of 0.10" and an estimated sludge height of 0.5" to 1.0" by bobbin MCI by UT Tube pulled for evaluation	-	-	-	Signal not present. - NDD	-

Table 2-1 (Cont'd) - Summary of Inspection Results of Locations Identified With Top of Tubesheet Flaw-Like Signals: 2R10 (Spring 2004)

	Inspection Results					
SG # and Location	2R10 (2004)	2R09 (2002)	2R08 (2001)	2R07 (1999)	2R06 (1998)	2R05 (1996)
SG 2 R11C60	SCI – 38% depth; 48.2° Extent; 0.19 volts on 300 kHz +Pt coil Crevice depth of 0.11" and an estimated sludge height of 2.10" to 2.50" by bobbin SCI by UT Tube pulled for evaluation	-	-	-	Signal not present. - NDD	-
SG 3 R14C56	SCI – 27% Depth; 59.5° Extent; 0.22 volts on 300 kHz +Pt coil Crevice depth of 0.28" and an estimated sludge height of 1.01" to 1.50" by bobbin SCI by UT Location stabilized and plugged	-	Signal not present. - NDD	-	Signal not present. - NDD	-
SG 3 R11C65	SCI – 0% Depth; 56.3° Extent; 0.25 volts on 300 kHz +Pt coil Crevice depth of 0.11" and an estimated sludge height of 1.01" to 1.50" by bobbin MCI by UT Location stabilized and plugged	-	-	-	Signal not present. - NDD	-

Table 2-1 (Cont'd) - Summary of Inspection Results of Locations Identified With Top of Tubesheet Flaw-Like Signals: 2R10 (Spring 2004)

	Inspection Results					
SG # and Location	2R10 (2004)	2R09 (2002)	2R08 (2001)	2R07 (1999)	2R06 (1998)	2R05 (1996)
SG 3 R46C89	SCI – 35% depth; 41.8° Extent; 0.11 volts on 300 kHz +Pt coil (Very small in amplitude – signal seen on all coils indicating a possible geometric response) Crevice depth of 0.10" and an estimated sludge height of 0.00" by bobbin NDD by UT Location stabilized and plugged	-	-	-	Signal not present. - NDD	-
SG 4 R14C67	SCI – 34% Depth; 64.3° Extent; 0.34 volts on 300 kHz +Pt coil Crevice depth of 0.19" and an estimated sludge height of 0.00" by bobbin No UT performed Location stabilized and plugged	Signal not present. - NDD	-	Signal not present. - NDD	-	Signal not present. - NDD
SG 4 R11C50	SCI – 34% Depth; 59.5° Extent; 0.21 volts on 300 kHz +Pt coil Crevice depth of 0.24" and an estimated sludge height of 1.00" to 1.50" by bobbin No UT performed Location stabilized and plugged	Signal not present. - NDD	-	Signal not present. - NDD	-	Signal not present. - NDD

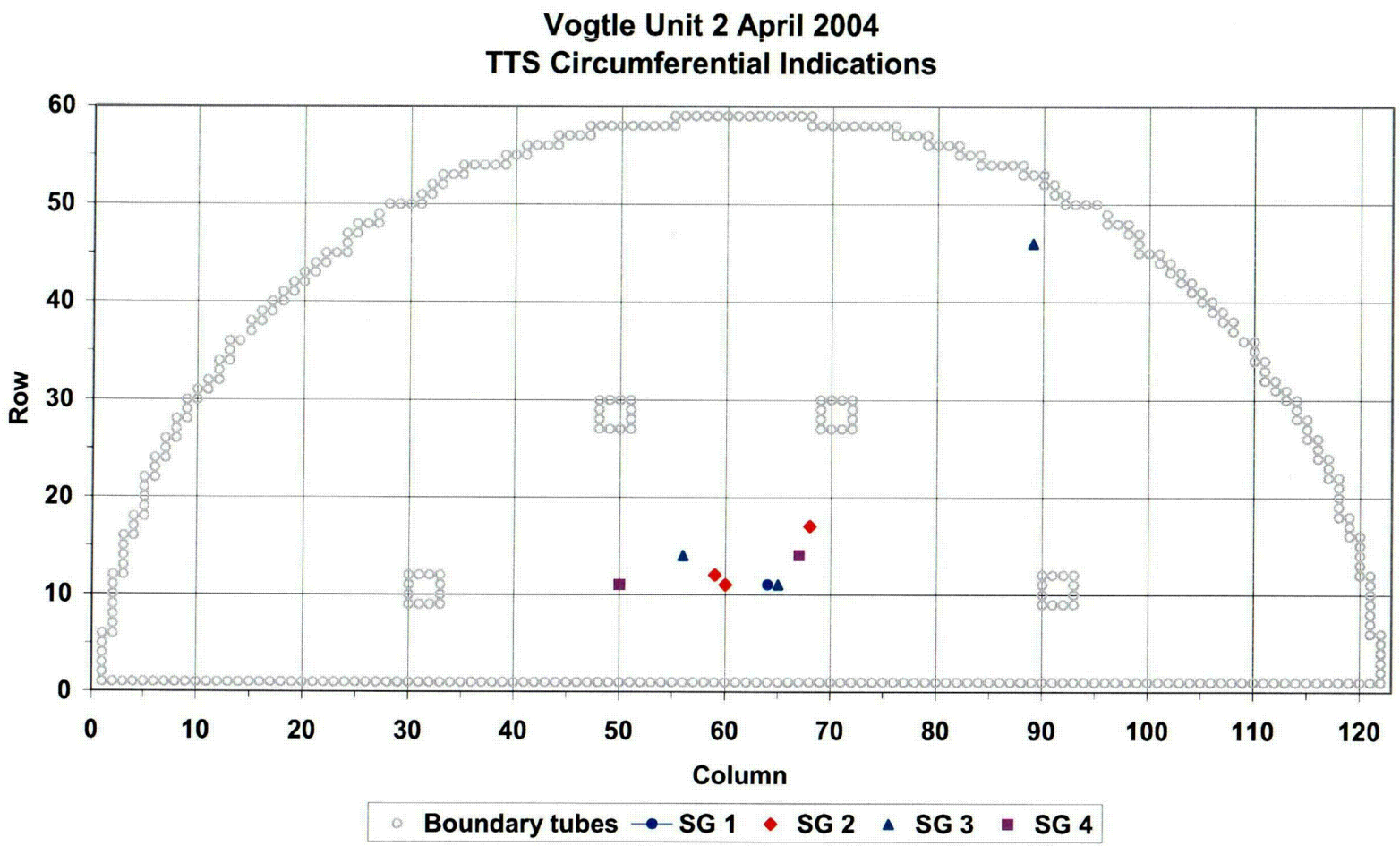

Figure 2-1 Tubesheet Mapping Showing the Row / Column Location of the TTS OD Circumferential Indications Reported During the Vogtle 2R10 +Pt Inspection Efforts.

col

SECTION 3

RECEIPT INSPECTION

The general appearance of the pulled tube sections removed from Steam Generator 2 at Vogtle Unit 2 as they were received at the Westinghouse Remote Hot Cell Metallographic Facility are described in this section. The information presented includes the lengths and locations of the tube sections, along with the general visual observations of the as-received condition.

3.1 Description of Tube Sections Received

Row 12 Column 59 tube (hereafter referred to as R12C59 HL) and Row 11 Column 60 (hereafter referred to as R11C60 HL) were cut at a distance of approximately 94 inches from the tube end and were cut into four sections each for shipment. Each pulled tube section received from Vogtle Unit 2 was measured for length to compare with site length data to verify tube piece identity and to provide data to aid in identifying the position of tube support plates. Each tube piece was visually inspected and surface features documented per the discussion provided below. Each pulled tube section was inspected to verify azimuthal markings to designate divider plate orientation. Table 3-1 provides a listing of the pieces and their respective lengths, and areas of interest.

3.2 Visual Observations

In addition to visual examination of the tube sections, low magnification photographs of the areas of interest were taken. The areas of interest included those areas identified in the field as having eddy current indications, UT reported indications, as well as those areas with OD surface anomalies or support structures, i.e., top of tubesheet, and tube support plates.

3.2.1 R12C59 HL and R11C60 HL – Freespan Areas – General Observations

All tube pieces were categorized as having relatively thin and uniform gray deposit. The gray deposits were the typical surface oxide formed during steam generator operation. Minimal evidence of deposit buildup or scale formation was seen on the freespan regions. Shallow axial scratches, randomly distributed around and along the tubes, were noted. The

scratches occasionally were down to bare metal, and appeared to have occurred during the tube removal process.

In the description of the observations, scratches and grooves are shallow, axial visual indications on the tube OD surface. The distinction between scratches and grooves in this examination is simply the width of the indication. Scratches are basically singular, narrow indications while grooves have a greater width and at times may consist of multiple scratches. As noted throughout the following discussion, reference is made to the fact that the scratch or groove was likely produced during the tube pulling operation. Scratches and grooves produced during the tube removal normally are characterized as being "shiny" (non-oxidized) and exhibiting a "ragged" surface appearance with evidence of "upset" material. Scratches and grooves produced during steam generator manufacturing are always covered with operational produced oxide deposits and are usually "rounded" and more "shallow" in appearance.

3.2.2 Tube R12C59 HL

Piece 1:

Piece 1 measured 5.75 inches and is the segment cut from the lower portion of the hydraulic expansion region. This segment was TIG relaxed in order to facilitate the tube removal process. This piece contained no area of interest and hence no photographs were taken.

Piece 2:

Piece 2 measured 26 inches and contained the upper portion of the hydraulic expansion region and the top of the tube sheet expansion transition (TTS). Photographs documenting the tube OD at the top of tubesheet and the OD deposit are presented in Figure 3-1. The photographs were taken at azimuthal locations corresponding to 0° [Figure 3-1(a)], 90° [Figure 3-1(b)], 180° [Figure 3-1(c), and 270° [Figure 3-1(d)] locations. The TTS was visible approximately 16 inches from the bottom of Piece 2. The lower portion, corresponding to the tube length expanded into the tubesheet, was "clean and shiny". Based on oxide formation, the hydraulic expansion transition was visible at and just above the "shiny" region which denoted the region of the hydraulic expansion in contact with the tubesheet. Longitudinal scratches, as well as light circumferential markings, were seen within this region. OD surface deposits were observed at and just above the expansion transition. These deposits were intact and rougher in texture than the deposit observed further up the tube. A brownish deposit, approximately ½ inch in height was observed at the TTS region. Above this region a dark grey deposit was noted. No evidence of

"spalling" or cracks within the deposit was noted. Minimal scratches or "rub" marks were noted. It appeared that this region passed through the tubesheet hole with minimal interference. The deposit above this region was lighter grey in appearance and thicker. Photographs presented in Figure 3-1 (e), (f), and (g) were taken at the azimuthal orientation were the +Pt field inspection reported an OD circumferential signal. Visual examination of this area showed no unusual OD deposit condition. Figure 3-1 (h) and (i) illustrates the OD surface appearance at 30° and 60° azimuthal orientation where the UT signal was reported during the field inspection. The azimuthal orientation of the field UT signal was determined to be 45° based on the laboratory evaluation of the eddy current signal characteristics of the OD deposits (Refer to Section 8). Local regions exhibiting minimal or no OD deposit were observed.

Piece 3:

Piece 3 measured 36 inches and contained the first tube support plate (1st TSP) intersection. Photographs documenting the general appearance of the deposit seen on the tube OD at the 1st tube support plate intersection are presented in Figure 3-2. The entire piece is covered with a thin, uniform grayish deposit. The texture of the deposit is relatively fine and no evidence of deposit "spalling" or "flaking" was noted. Evidence of the quatrefoil land to tube intersections was noted at 0° [Figure 3-2(a)], 90° [Figure 3-2(b)], and 180° [Figure 3-2(c)] azimuthal orientations. These areas are visible due to greater buildup of deposit corresponding to the quatrefoil land to tube intersection. No evidence of a thicker deposit was noted at the 270° [Figure 3-2(d)] orientation. There were also shiny scratches visible in oxidized areas. Intermittent longitudinal scratches, as well as light circumferential markings, were seen along the length of Piece 3. Except for the quatrefoil land to tube intersections, the OD deposit was relatively light over the entire length of Piece 3. A scribe mark showing the divider plate orientation was evident on Piece 3.

Piece 4:

Piece 4 measured 26 3/4 inches and represented the freespan area between the 1st and 2nd tube support plates. The OD deposit was relatively thin, uniform, and dark grey in color. Evidence of axial scratches due to pulling process was noted. This piece contained no area of interest and hence no photographs were taken.

3.2.3 Tube R11C60 HL

Piece 1:

Piece 1 measured 7.25 inches and is the segment cut from the lower portion of the hydraulic expansion region. This segment was TIG relaxed in order to facilitate the tube removal process. This piece contained no area of interest and hence no photographs were taken.

Piece 2:

Piece 2 measured 28 3/8 inches and contained the upper portion of the hydraulic expansion region and the top of the tube sheet expansion transition (TTS). Photographs documenting the tube OD at the top of tubesheet and the OD deposit are presented in Figure 3-3. The photographs were taken at azimuthal locations corresponding to 0° [Figure 3-3(a)], 90° [Figure 3-3(b)], 180° [Figure 3-3(c)], and 270° [Figure 3-3(d)] locations. The TTS was visible approximately 14 inches from the bottom of Piece 2. The lower portion, corresponding to the tube length expanded into the tubesheet, was "clean and shiny". Based on oxide formation, the hydraulic expansion transition was visible at and just above the "shiny" region which denoted the region of the hydraulic expansion in contact with the tubesheet. Longitudinal scratches, as well as light circumferential markings, were seen within this region. OD surface deposits were observed at and just above the expansion transition. These deposits were intact and rougher in texture than the deposit observed further up the tube. A brownish deposit, approximately ½ inch in height was observed at the TTS region. Above this region a dark grey deposit was noted. No evidence of "spalling" or cracks within the deposit was noted. Minimal scratches or "rub" marks were noted. It appeared that this region passed through the tubesheet hole with minimal interference. The deposit above this region was lighter grey in appearance and thicker. Photographs presented in Figure 3-3 (e), (f), and (g) were taken at the azimuthal orientations were the +Pt field inspection reported an OD circumferential signal. Visual examination of this area showed no unusual OD deposit condition. Photographs presented in Figure 3-3 (h) were taken at the azimuthal orientation where the UT examination reported a circumferential indication during the field inspection effort. Examination of the tube deposit at this azimuthal location showed an area of minimal to no OD deposit.

Piece 3:

Piece 3 measured 37 inches and contained the first tube support plate (TSP). The entire piece was covered with a thin, uniform grayish deposit. Photographs documenting the general appearance of the deposit seen on the tube OD at the 1st tube support plate

intersection are presented in Figure 3-4. The texture of the deposit was relatively fine with no evidence of deposit "spalling" or "flaking". No evidence of the quatrefoil land to tube intersections was noted at 0° [Figure 3-4(a)], 90° [Figure 3-4(b)], 180° [Figure 3-4(c)], and 270° [Figure 3-4(d)] azimuthal orientations. Intermittent longitudinal scratches, as well as light circumferential markings, were seen along the length of Piece 3.

Piece 4:
Piece 4 measured 21 5/8 inches and represented the freespan area between the 1st and 2nd tube support plates. The OD deposit was relatively thin, uniform, and dark grey in color. Evidence of axial scratches due to pulling process was noted. This piece contained no area of interest and hence no photographs were taken.

3.3 OD and ID Measurement Profiles

Field ECT data analysis indicated a general lack of tube deformation or geometrical anomalies at either the TTS or TSP regions. This is consistent with expectations for Model F steam generators such as those at Vogtle because of the use of hydraulic expansion and Type 405 stainless steel for the tube support plates. Laboratory testing was performed to confirm this analysis and to eliminate hydraulic expansion anomalies as a cause of the eddy current and UT signals.

OD laser micrometry was performed on the TTS and 1st TSP regions of both pulled tubes. The effort on the 1st TSP was undertaken to document any deposit buildup within the quatrefoil land to tube intersection and was not related to the circumferential ODSCC indications reported at the TTS region. Tube geometry assessments made from the laser micrometry data may be influenced by the presence of deposits on the outer surface of the tube. The raw data are collected in the form of radial data obtained from a mathematically averaged centerline for the tube section. Data is taken every 15° and approximately every 0.090" over a length sufficient to fully characterize the region of interest. Diametrical representations of these data were obtained by adding the appropriate radial measurements.

The ID diametrical profile of the tube expansion transition was determined by making a Silastic mold of the tube ID and profiling the mold by laser micrometry.

Figures 3-5 through 3-10 are plots of the OD laser micrometry data for the TTS and 1st TSP locations for the Vogtle Unit 2 pulled tubes. For the top of the tubesheet area, the respective figures illustrate both the 360 degree distribution of OD deposit, as well as, the average deposit thickness around the tube. The raw data were in the form of radial

distance from a mathematically average centerline of the tube section. Figures 3-5 and 3-6 provide data for the TTS area of R12C59 HL, while Figure 3-7 illustrates the distribution of OD deposit seen at the tube intersection and the 1st tube support plate. Figures 3-8 and 3-9 provide data for the TTS area of R11C60 HL, while Figure 3-10 illustrates the distribution of OD deposit seen at the tube intersection and the 1st tube support plate. For the TTS locations, the OD deposit thickness data are presented both as a geometrical plot as a function of axial and circumferential position and as a two dimensional display of the average deposit thickness as a function of axial position. The approximate location of the top of tubesheet is shown in each figure. For the 1st TSP regions, the data are shown only as a geometrical plot as a function of axial and circumferential position.

For the TTS region of both tubes, Figures 3-5, 3-6, 3-8, and 3-9, the OD deposit varies in thickness in both the circumferential and axial directions. The OD deposit at the TTS region varies in thickness from less than 50 μm to 200 μm. From the data displayed for the TTS area for both pulled tubes exhibit a "ring" of deposit of relatively uniform thickness above the top of the tubesheet and extending approximately 30 mm in elevation. Above this "ring", there is an area of reduced deposit thickness extending approximately 10 mm in elevation. Above this area of reduced OD deposit thickness, the thickness of the deposit tends to increase to a thickness similar to that observed at the TTS.

Figures 3-7 and 3-10 illustrate the OD deposit data obtained for the 1st tube support plate to tube intersections. Figure 3-7 is the data for R12C59 HL and Figure 3-10 is the data for R11C60 HL. For R12C59 HL, shown in Figure 3-7, the laser micrometry data clearly indicate a buildup of deposit corresponding to two of four quatrefoil land to tube intersections. A deposit thickness of approximately 0.045 mm was noted at the 0° azimuthal orientation and approximately 0.120 mm at the 90° azimuthal position. No evidence of buildup was noted for the other two quatrefoil land to tube intersections. For R11C60 HL, shown in Figure 3-10, there was no clear evidence of localized deposit buildup associated with the quatrefoil land to tube intersections.

In addition to characterizing the OD deposit thicknesses at the TTS and 1st TSP regions of both tubes, laser micrometry measurements were taken from the ID Silastic mold taken of the tube expansion transition of both pulled tubes. The results are presented as a three dimensional display, as well as, a two dimensional plot based on average ID radius. The ID tube profile R12C59 HL is presented in Figures 3-11 and 3-12, similar data for R11C60 HL are presented in Figures 3-13 and 3-14. There were no obvious geometrical anomalies noted. For both tubes, the expansion transitions were located at approximately the same

distance from the end of Piece 2B, and appeared to be uniform in diameter and exhibited an axial extent of approximately 6 to 8 mm for both expansion transitions.

Table 3-1
R12C59 HL and R11C60 HL Pulled Tube Sections

Location	Section Number	Area of Interest	Cut Length (Inch)	Pull Force (lbs)
R12C59 HL	1	-	5.75	3,618 (Breakaway) 1,604
	2	TTS	25.75	27
	3	1ST TSP	36.0	27
	4	-	26.5	27
			94.0 (Total)	
R11C60 HL	1	-	7.25	3, 270 (Breakaway) 1,428
	2	TTS	28.5	68 To 27
	3	1ST TSP	37.25	27
	4	-	21.25	27
			94.25 (Total)	

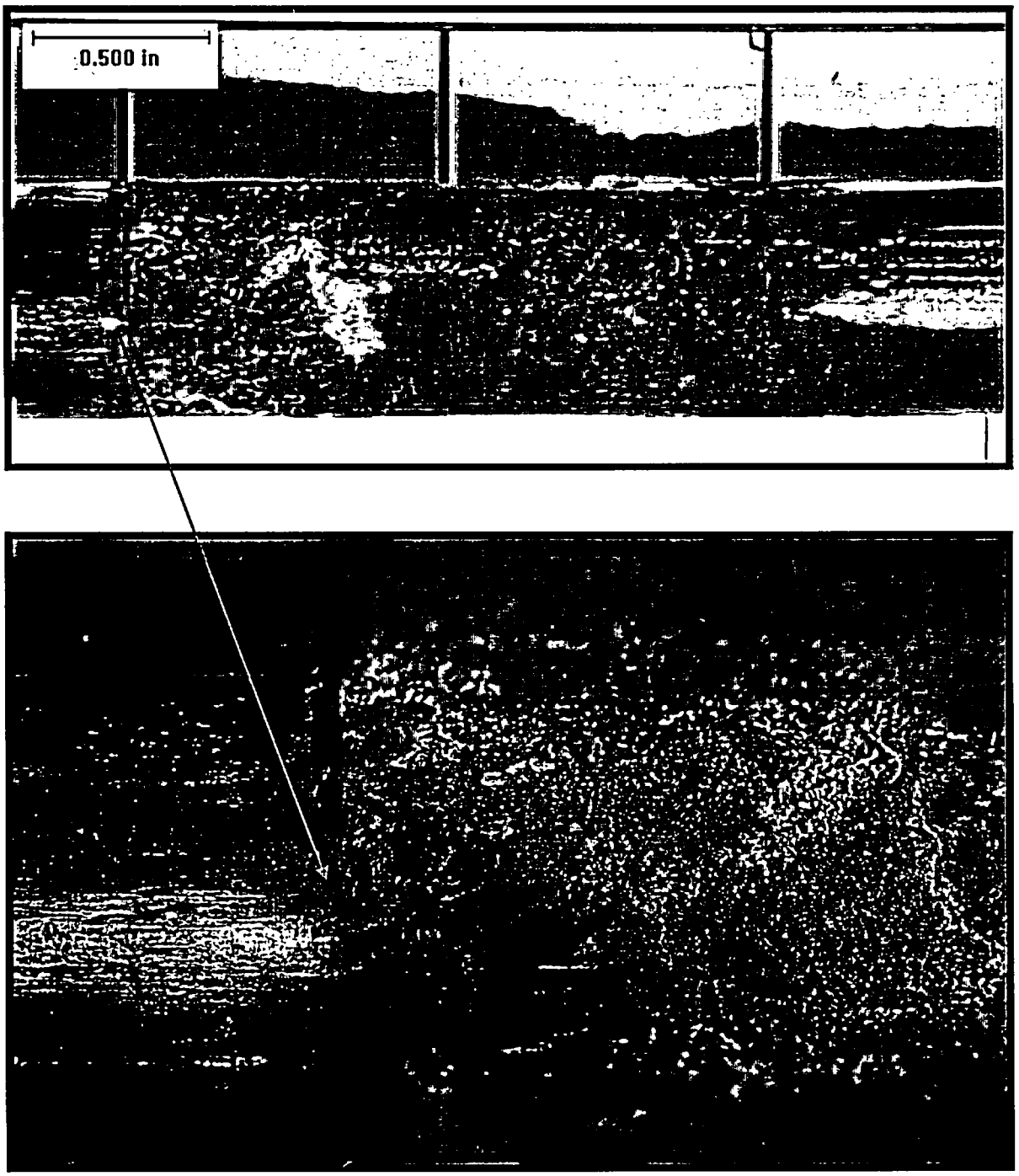

Figure 3-1 (a) General Appearance of OD Deposit Observed at Top of Tubesheet (TTS) on R12C59 HL – Piece 2B at 0° Azimuthal Orientation.

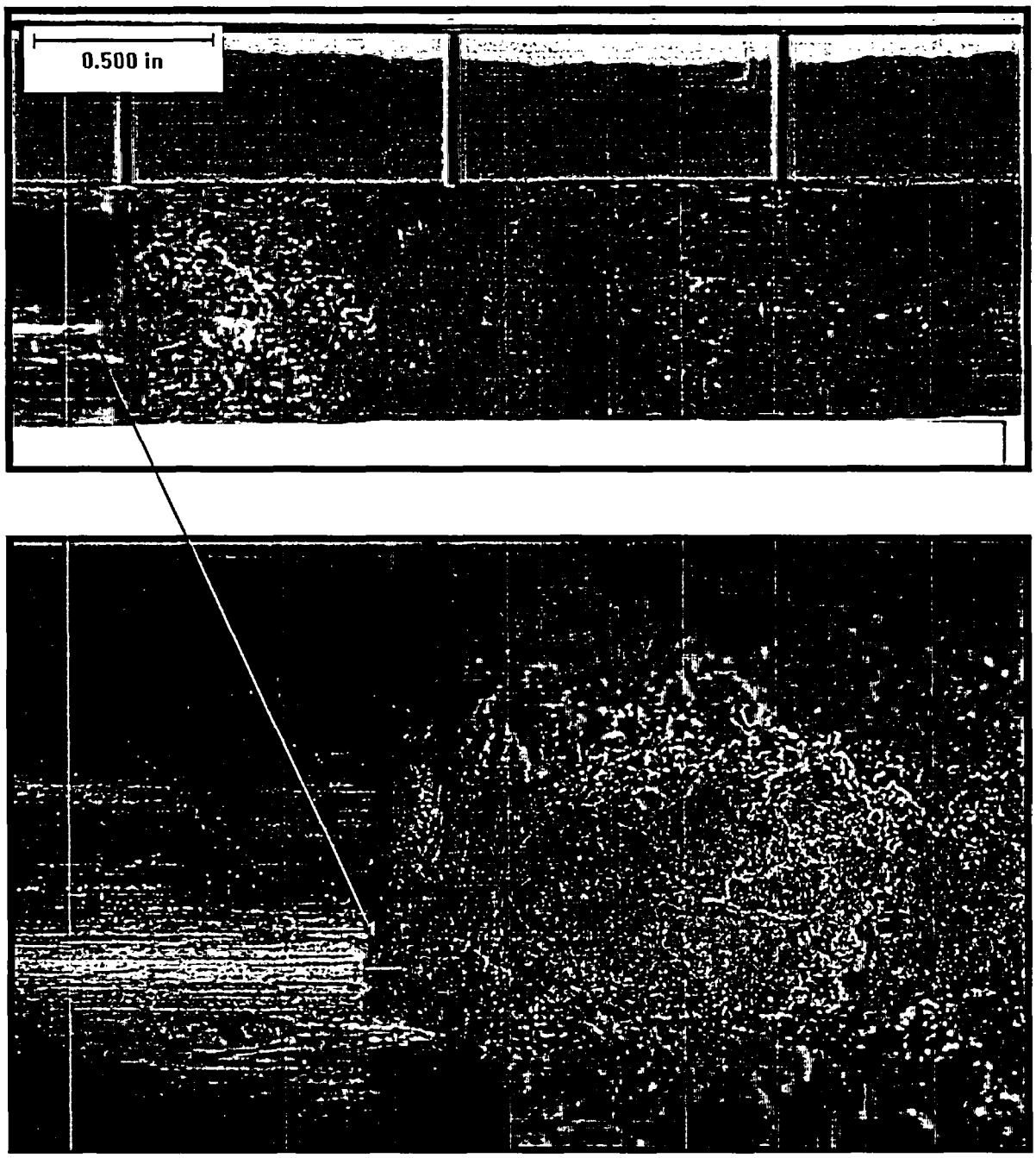

Figure 3-1 (b) General Appearance of OD Deposit Observed at Top of Tubesheet (TTS) on R12C59 HL – Piece 2B at 90° Azimuthal Orientation.

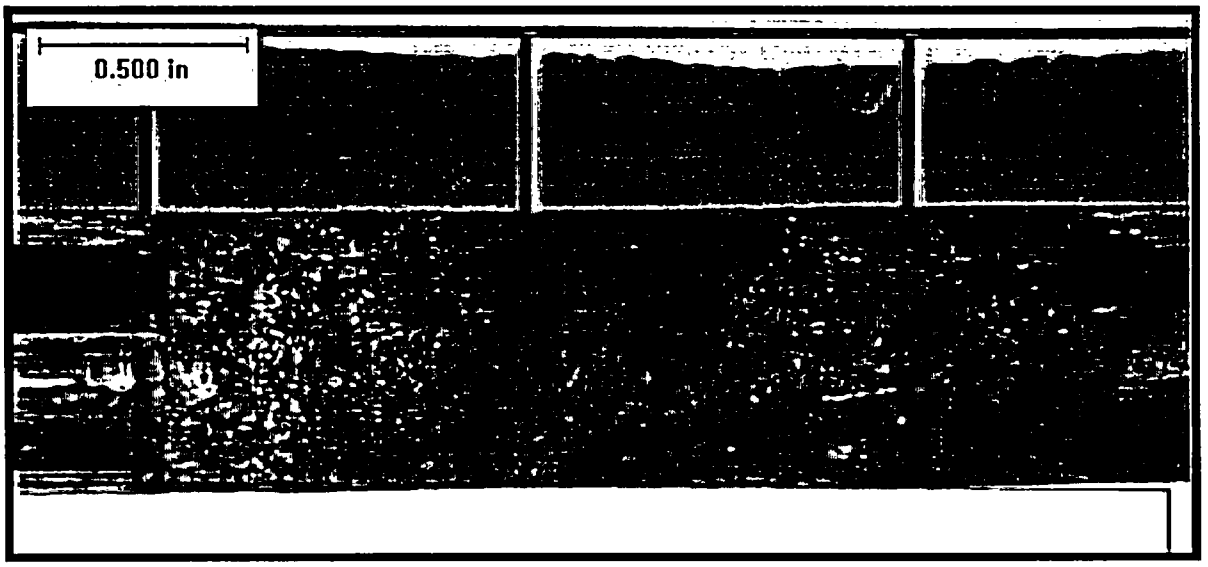

Figure 3-1 (c) General Appearance of OD Deposit Observed at Top of Tubesheet (TTS) on R12C59 HL – Piece 2B at 180° Azimuthal Orientation.

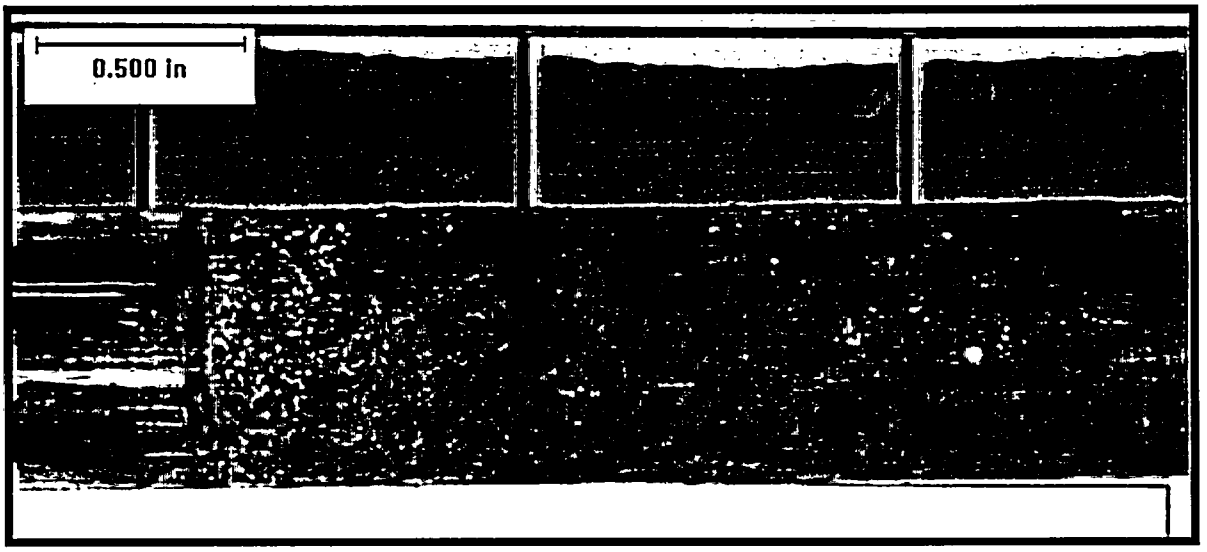

Figure 3-1 (d) General Appearance of OD Deposit Observed at Top of Tubesheet (TTS) on R12C59 HL – Piece 2B at 270° Azimuthal Orientation.

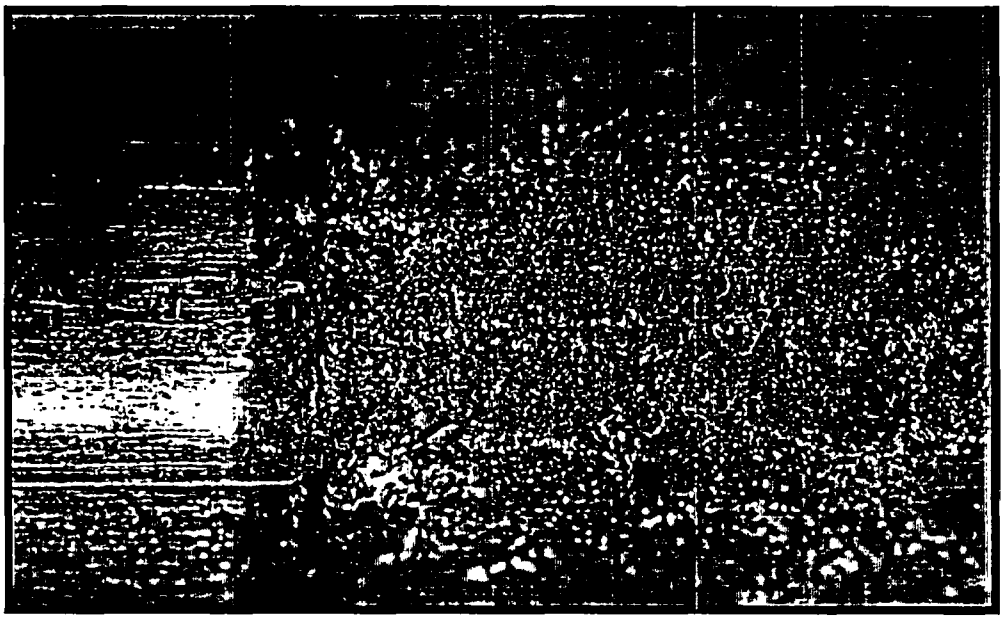

Figure 3-1 (e) General Appearance of OD Deposit Observed at Top of Tubesheet (TTS) on R12C59 HL – Piece 2B at 315° Azimuthal Orientation (Field +Pt Signal Response).

Figure 3-1 (f) General Appearance of OD Deposit Observed at Top of Tubesheet (TTS) on R12C59 HL – Piece 2B at 324° Azimuthal Orientation (Field +Pt Signal Response).

Figure 3-1 (g) General Appearance of OD Deposit Observed at Top of Tubesheet (TTS) on R12C59 HL – Piece 2B at the 335° Azimuthal Orientation (Field +Pt Signal Response).

Figure 3-1 (h) General Appearance of OD Deposit Observed at Top of Tubesheet (TTS) on R12C59 HL – Piece 2B at the 30° Azimuthal Orientation (Near Field UT Signal Response at 45°). Note: Area outlined shows minimal or no OD deposit.

Figure 3-1 (i) General Appearance of OD Deposit Observed at Top of Tubesheet (TTS) on R12C59 HL – Piece 2B at the 60° Azimuthal Orientation (Near Field UT Signal Response at 45°). Note: Area outlined shows minimal or no OD deposit.

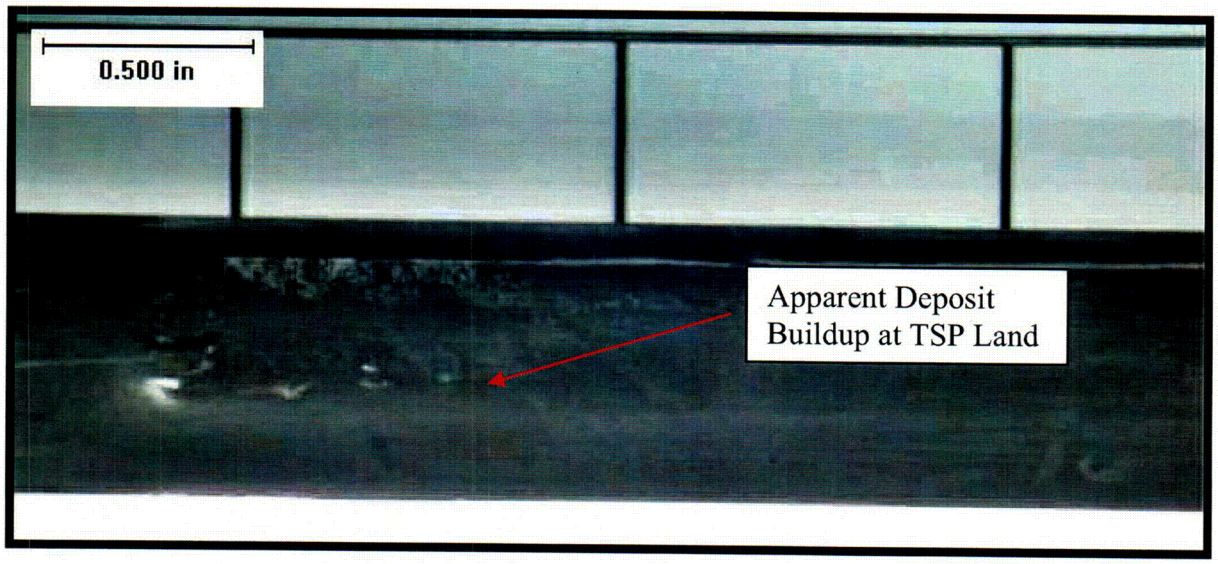

Figure 3-2 (a) General Appearance of OD Deposit Observed at Tube to Tube Support Plate (TSP) Intersection on R12C59 HL – Piece 3B at 0° Azimuthal Orientation.

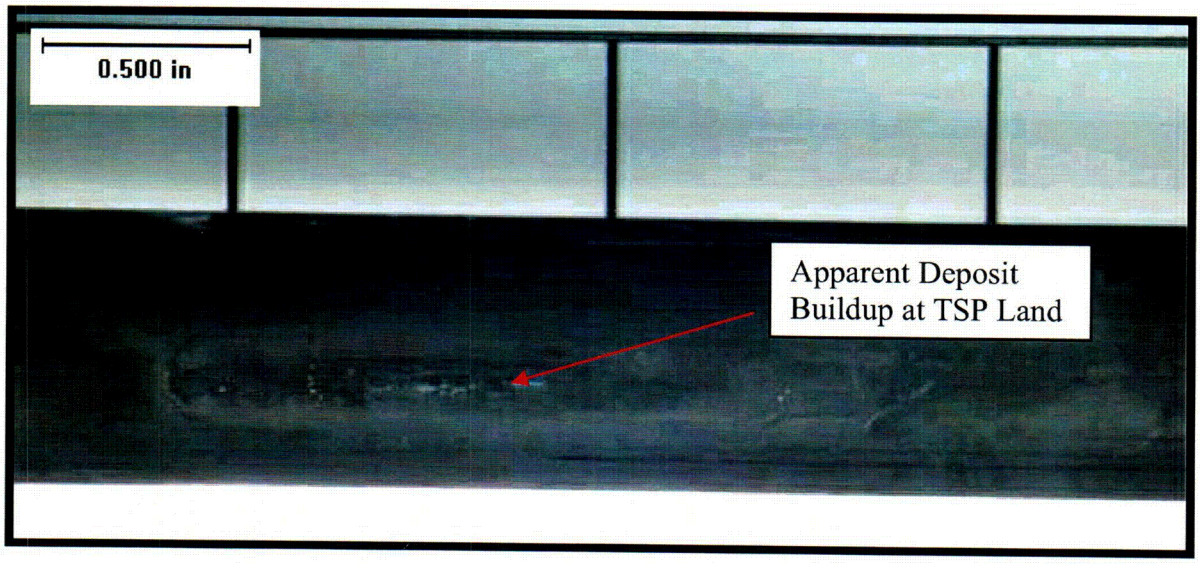

Figure 3-2 (b) General Appearance of OD Deposit Observed at Tube to Tube Support Plate (TSP) Intersection on R12C59 HL – Piece 3B at 90° Azimuthal Orientation.

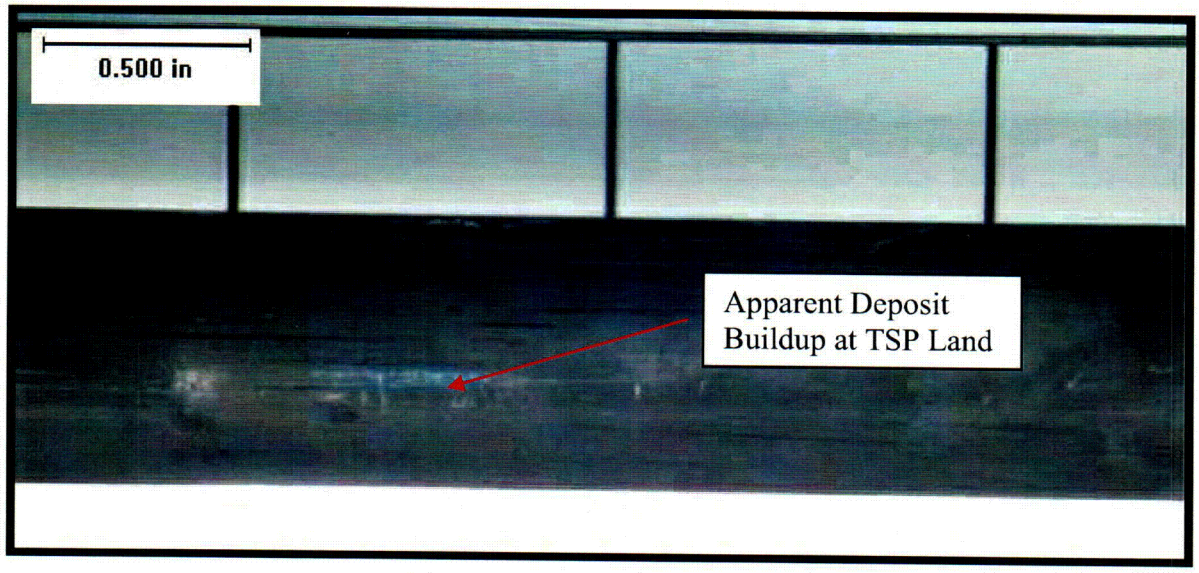

Figure 3-2 (c) General Appearance of OD Deposit Observed at Tube to Tube Support Plate (TSP) Intersection on R12C59 HL – Piece 3B at 180° Azimuthal Orientation.

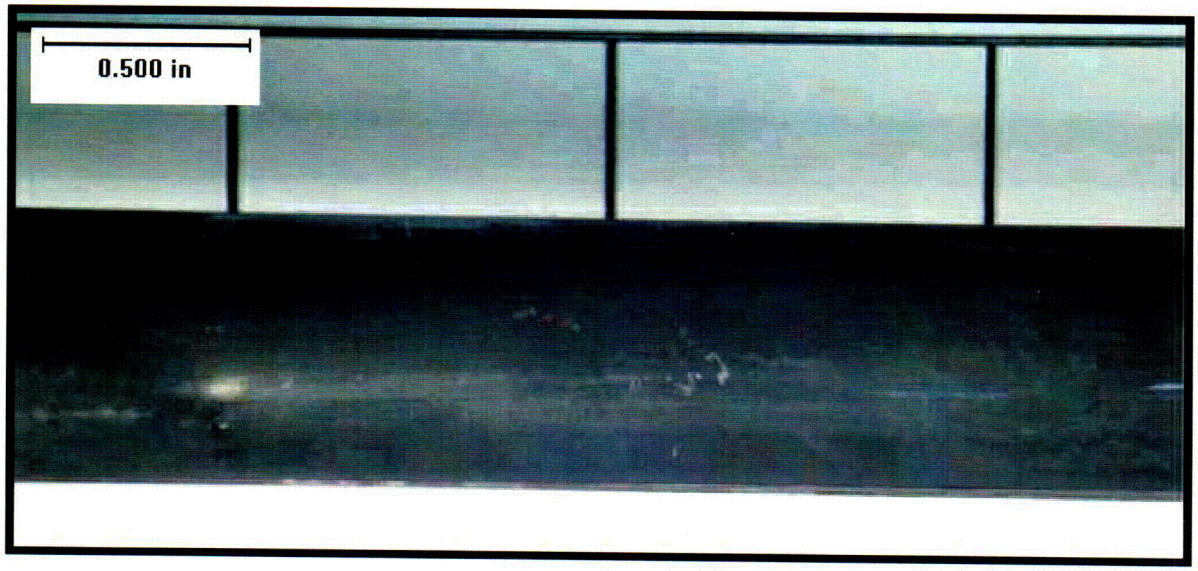

Figure 3-2 (d) General Appearance of OD Deposit Observed at Tube to Tube Support Plate (TSP) Intersection on R12C59 HL – Piece 3B at 270° Azimuthal Orientation.

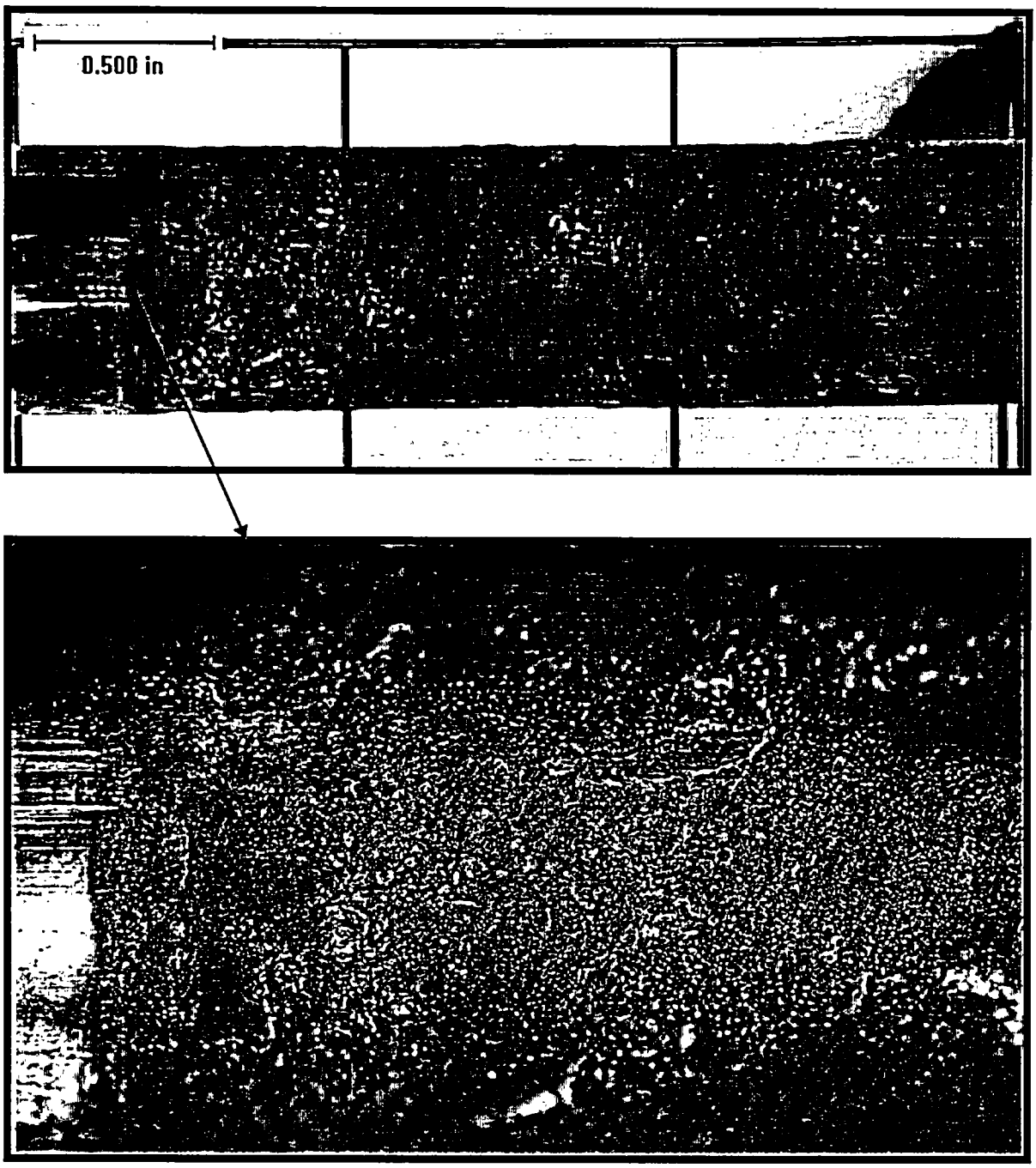

Figure 3-3 (a) General Appearance of OD Deposit Observed at Top of Tubesheet (TTS) on R11C60 HL – Piece 2B at 0° Azimuthal Orientation.

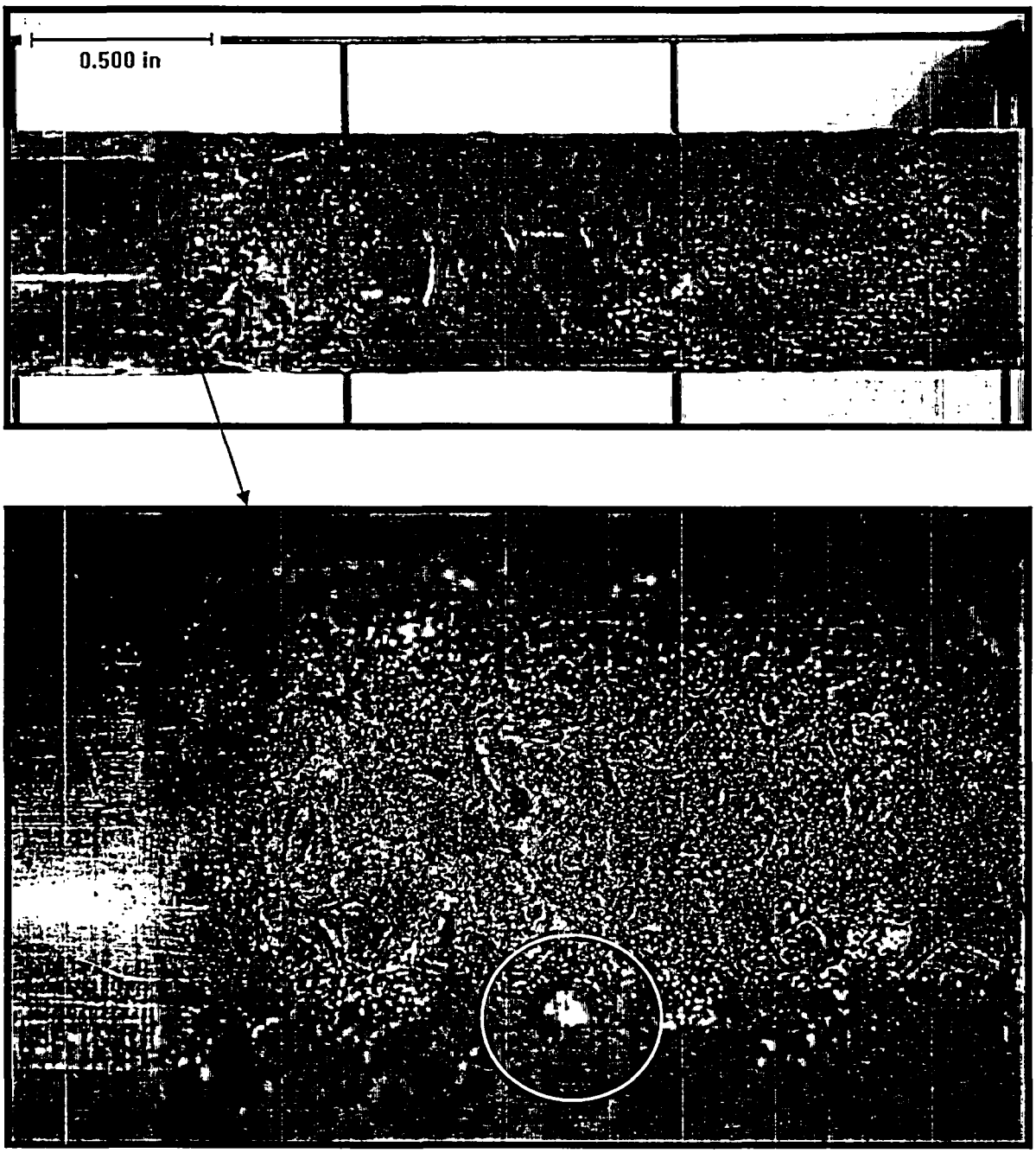

Figure 3-3 (b) General Appearance of OD Deposit Observed at Top of Tubesheet (TTS) on R11C60 HL – Piece 2B at 90° Azimuthal Orientation. Note: Area outlined shows minimal to no oxide deposit.

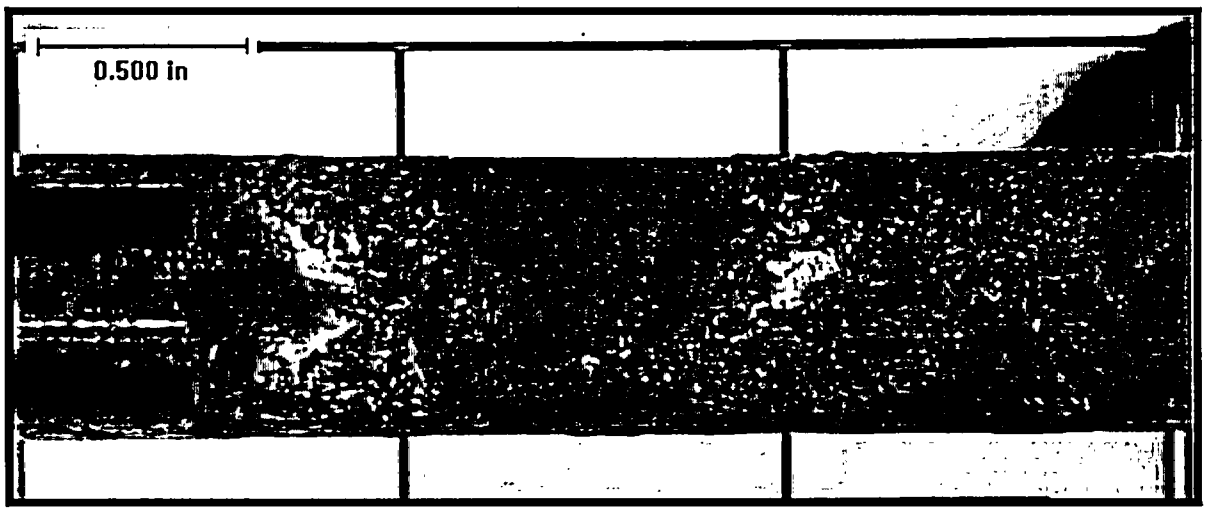

Figure 3-3 (c) General Appearance of OD Deposit Observed at Top of Tubesheet (TTS) on R11C60 HL – Piece 2B at 180° Azimuthal Orientation.

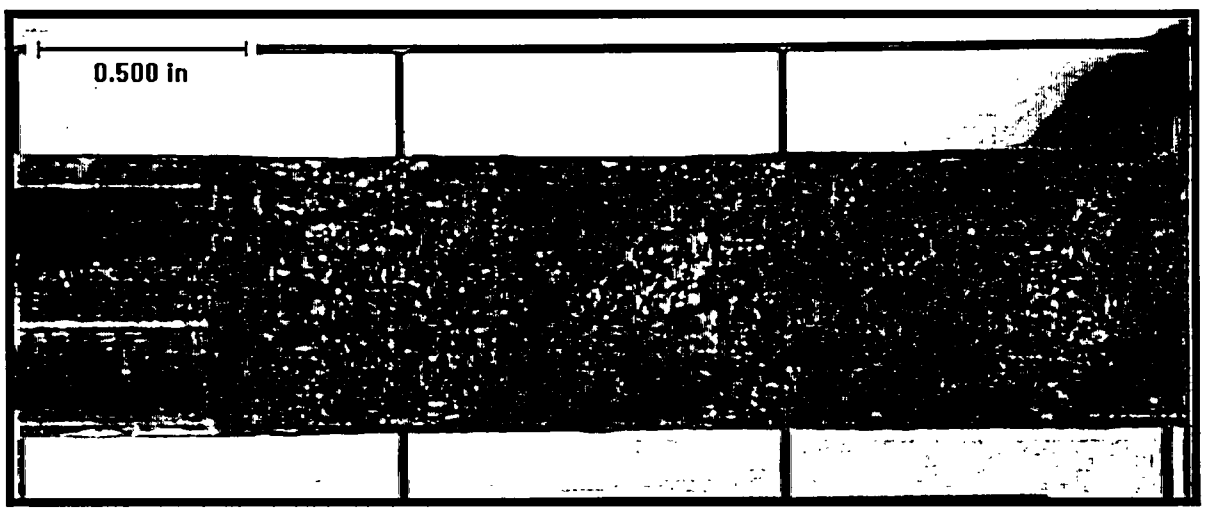

Figure 3-3 (d) General Appearance of OD Deposit Observed at Top of Tubesheet (TTS) on R11C60 HL – Piece 2B at 270° Azimuthal Orientation.

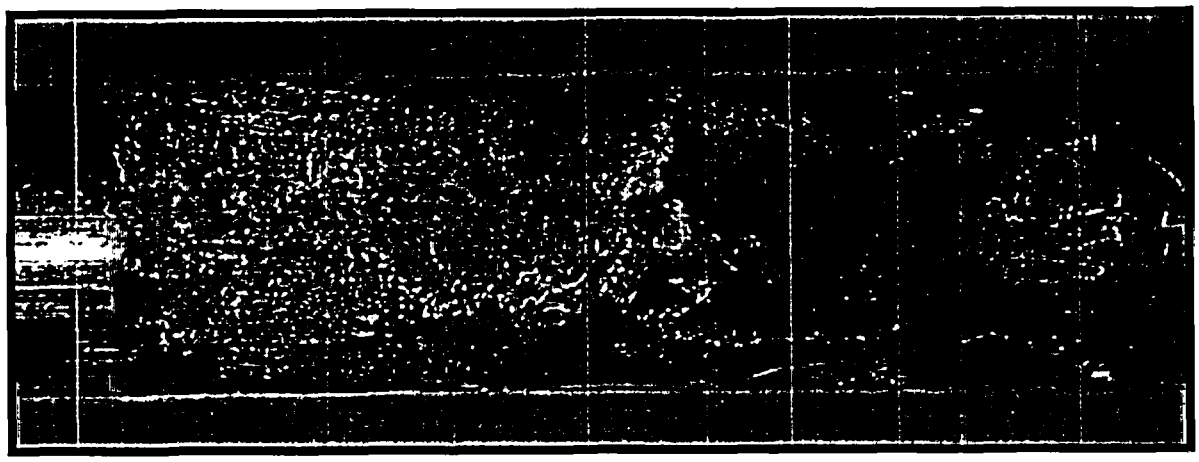

Figure 3-3 (c) General Appearance of OD Deposit Observed at Top of Tubesheet (TTS) for R11C60 HL – Piece 2B at 315° Azimuthal Orientation (Field +Pt signal response.

Figure 3-3 (f) General Appearance of OD Deposit Observed at Top of Tubesheet (TTS) for R11C60 HL – Piece 2B at 325° Azimuthal Orientation (Field +Pt signal response).

Figure 3-3 (g) General Appearance of OD Deposit Observed at Top of Tubesheet (TTS) for R11C60 HI – Piece 2B at 340° Azimuthal Orientation (Field +Pt signal response).

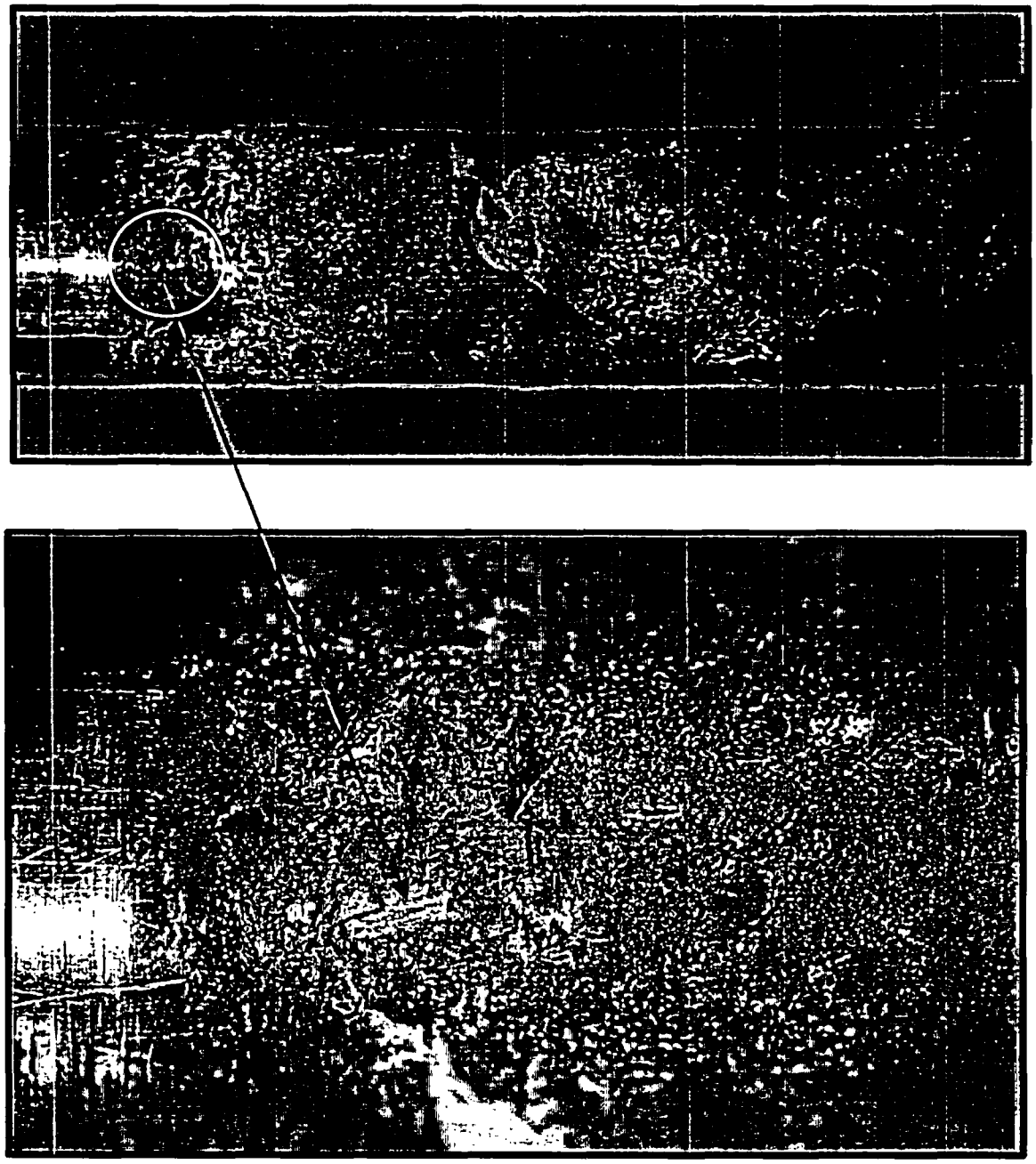

Figure 3-3 (h) General Appearance of OD Deposit Observed at Top of Tubesheet (TTS) for R11C60 HL – Piece 2B at 130° Azimuthal Orientation (Field UT signal response). Note: Area outlined shows minimal to no OD deposit.

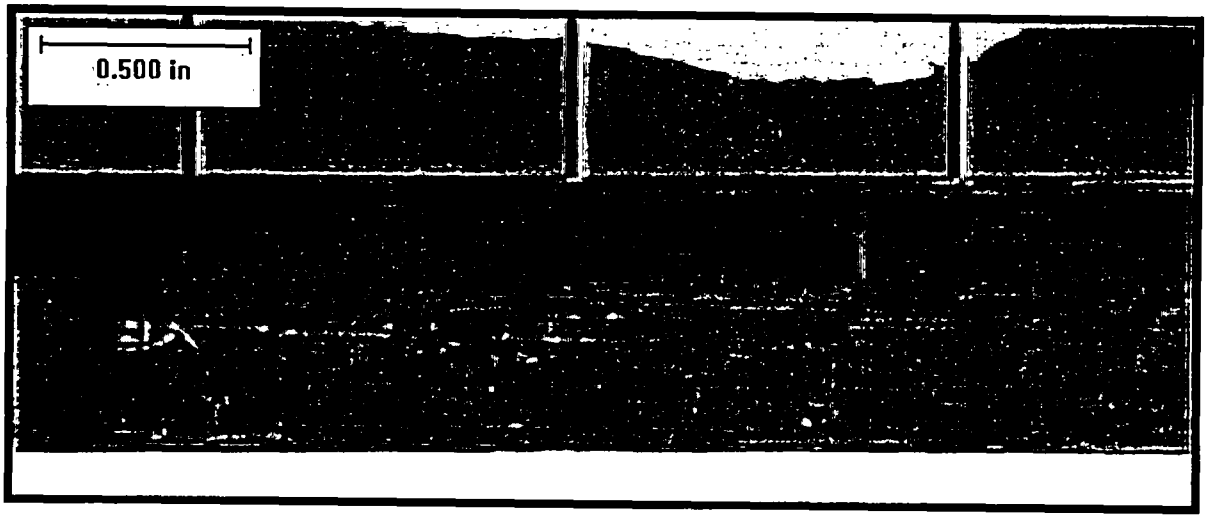

Figure 3-4 (a) General Appearance of OD Deposit Observed at Tube to Tube Support Plate (TSP) Intersection on R11C60 HL – Piece 3B at 0° Azimuthal Orientation.

No Evidence of Deposit Buildup at TSP Land Intersection

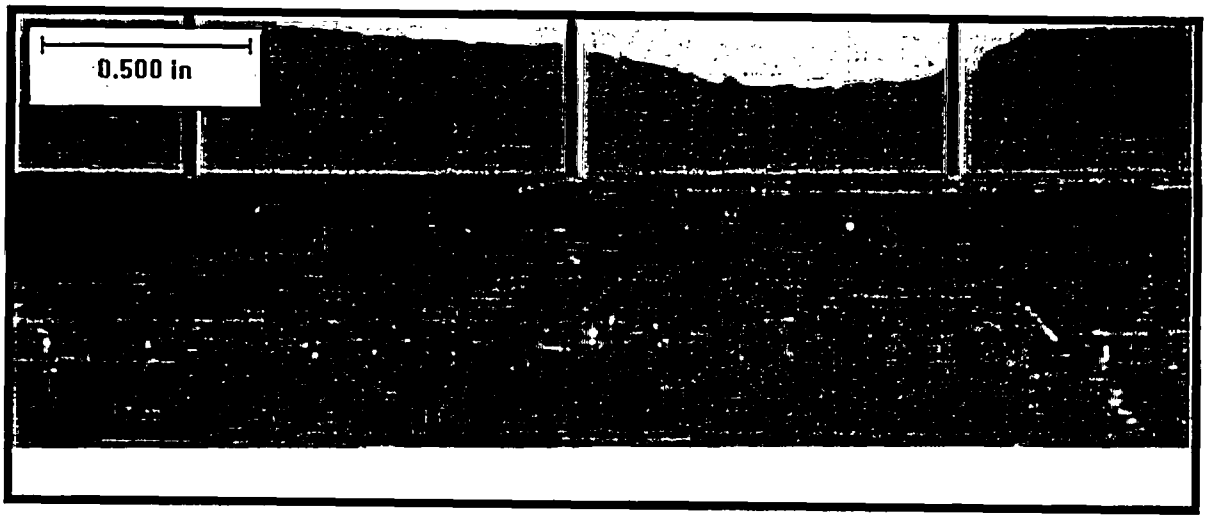

Figure 3-4 (b) General Appearance of OD Deposit Observed at Tube to Tube Support Plate (TSP) Intersection on R11C60 HL – Piece 3B at 90° Azimuthal Orientation.

No Evidence of Deposit Buildup at TSP Land Intersection

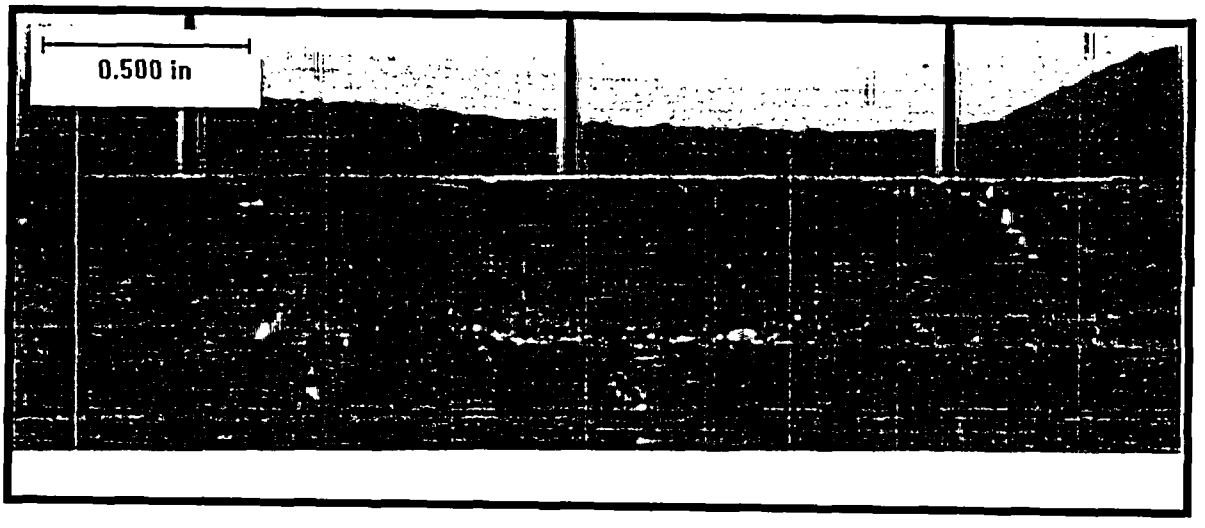

Figure 3-4 (c) General Appearance of OD Deposit Observed at Tube to Tube Support Plate (TSP) Intersection on R11C60 HL – Piece 3B at 180° Azimuthal Orientation.

No Evidence of Deposit Buildup at TSP Land Intersection

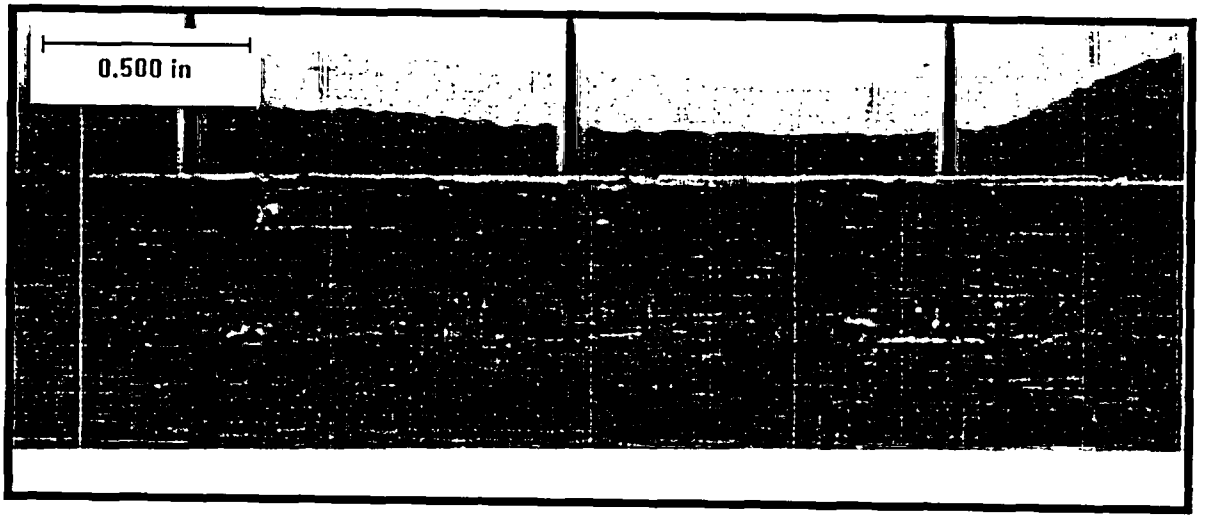

Figure 3-4 (d) General Appearance of OD Deposit Observed at Tube to Tube Support Plate (TSP) Intersection on R11C60 HL – Piece 3B at 270° Azimuthal Orientation.

No Evidence of Deposit Buildup at TSP Land Intersection

Figure 3-5 OD Dimensional Data Obtained by Laser Micrometry of the Top of Tubesheet Region of R12C59 HL - Piece 2B Showing OD Deposit Thickness as a Function of Axial and Circumferential Position. Position of the tubesheet is identified at approximately 153 mm.

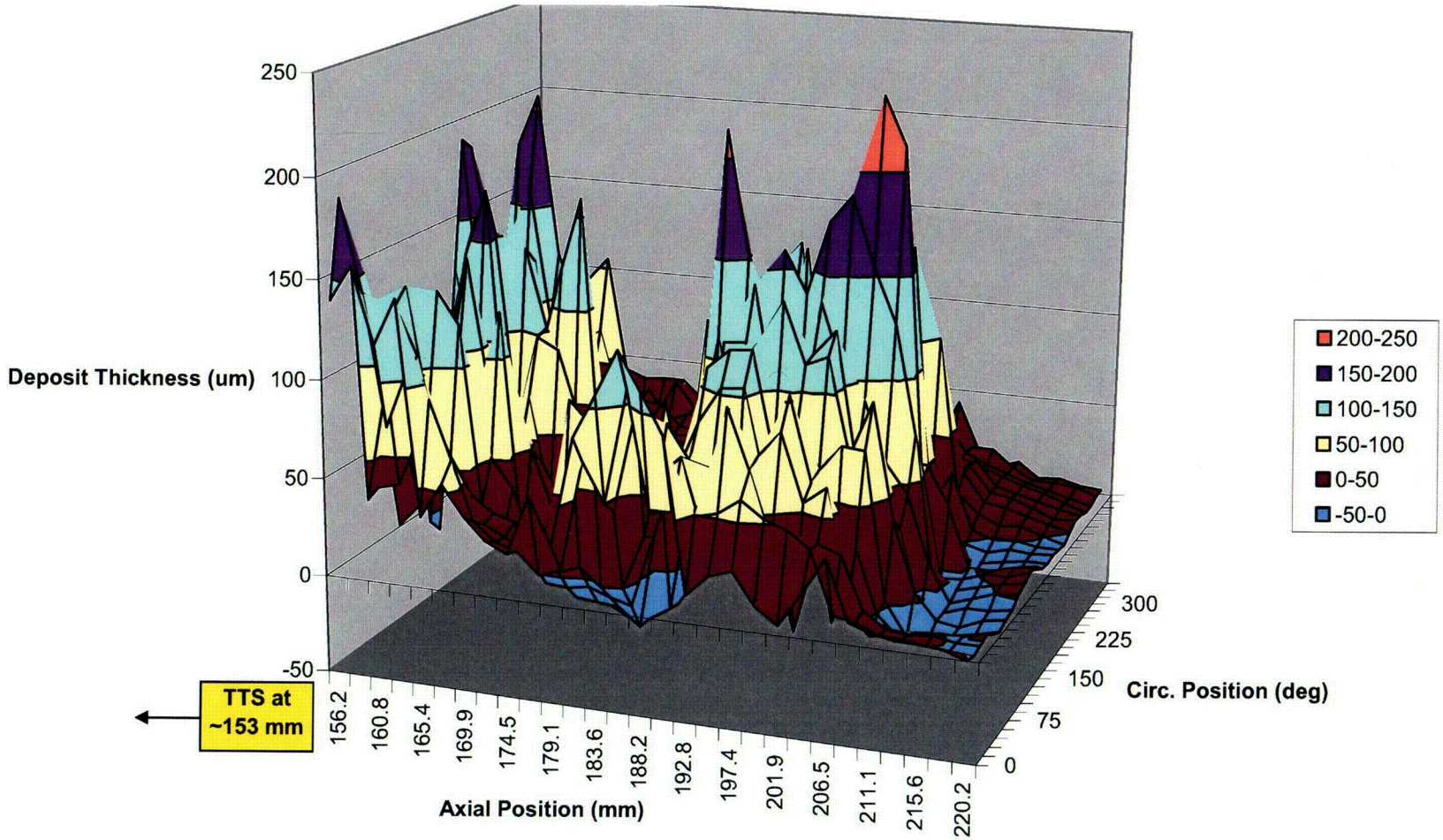

C02

Figure 3-6 Average OD Deposit Thickness Based on Dimensional Data Obtained by Laser Micrometry of the Top of the Tubesheet Region of R12C59 HL - Piece 2B as a Function of Axial Position. Position of the tubesheet is identified at approximately 153.

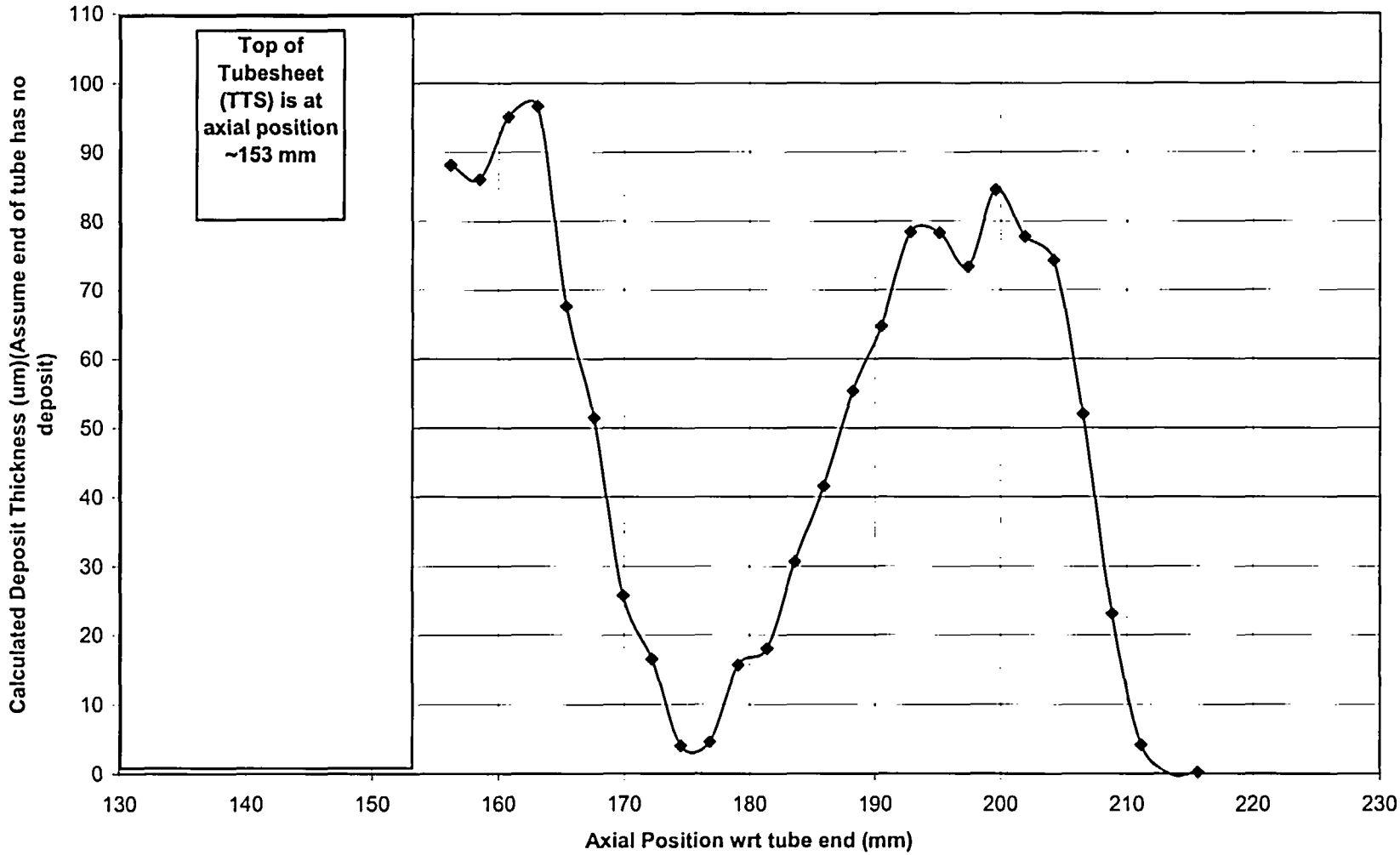

Figure 3- 7 OD Dimensional Data Obtained by Laser Micrometry of the Quatrefoil Tube Support Plate to Tube Intersection of R12C59 HL - Piece 3B Showing OD Deposit Thickness as a Function of Axial and Circumferential Position.

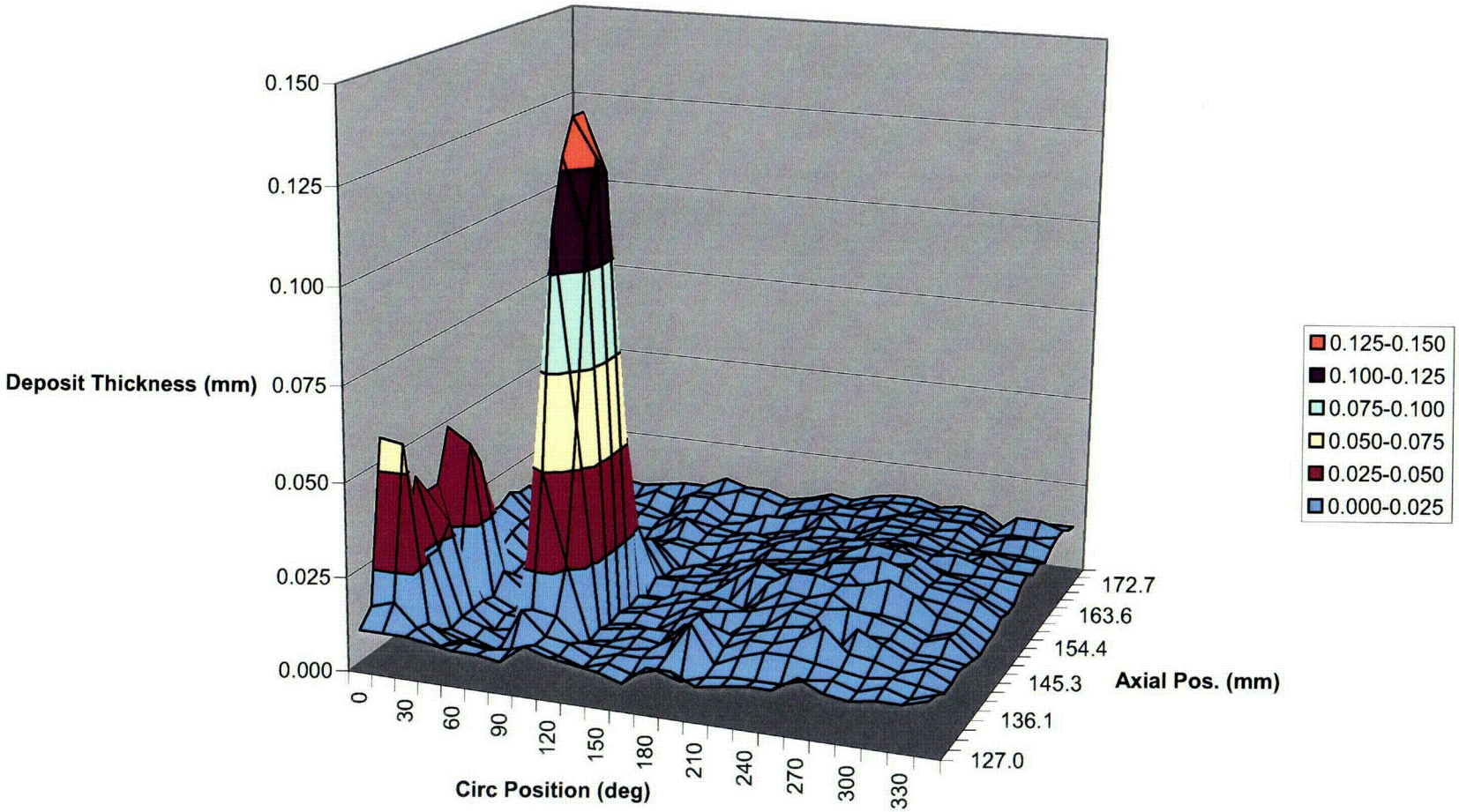

C03

Figure 3-8 OD Dimensional Data Obtained by Laser Micrometry of the Top of Tubesheet Region of R11C60 HL– Piece 2B Showing Deposit Thickness as a Function of Radial and Circumferential Position.

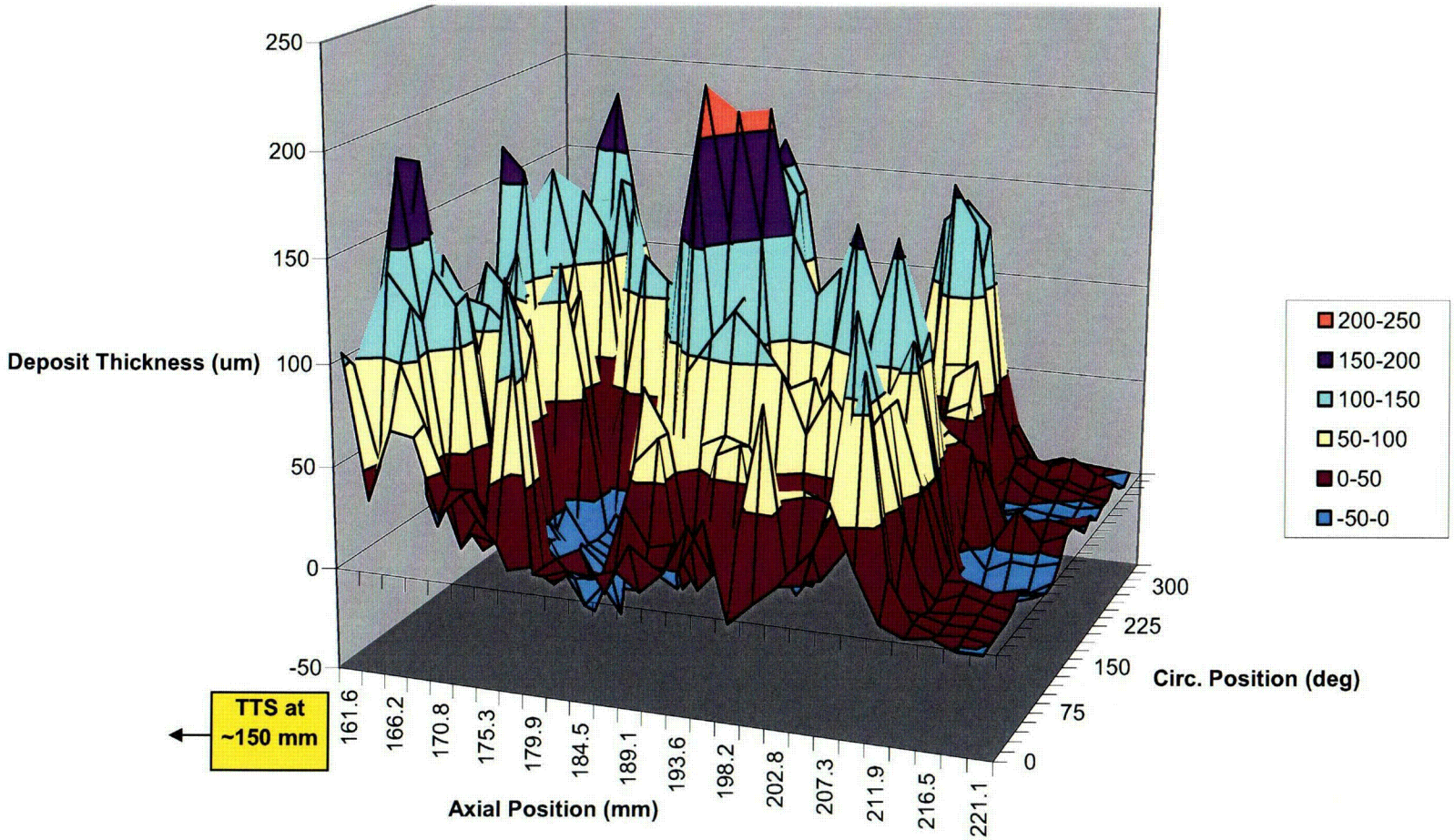

COX

Figure 3-9 Average OD Deposit Thickness Based on Dimensional Data Obtained by Laser Micrometry of the Top of Tubesheet Region of R11C60 HL - Piece 2B as a Function of Axial Position. Position of the tubesheet is identified at approximately 150 mm.

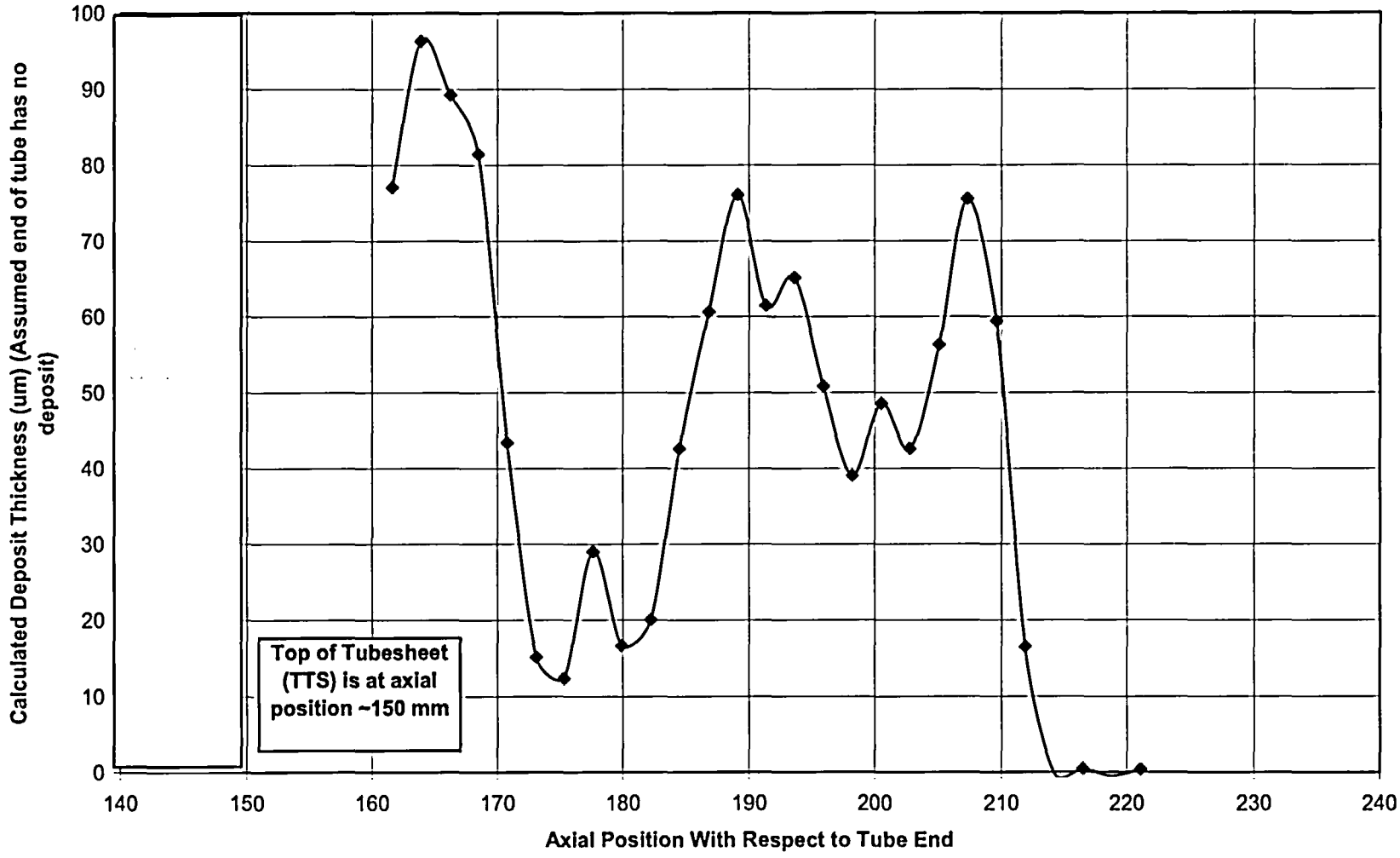

Figure 3- 10 OD Dimensional Data Obtained by Laser Micrometry of the Quatrefoil Tube Support Plate to Tube Intersection of R11C60 HL - Piece 3B Showing OD Deposit Thickness as a Function of Axial and Circumferential Position.

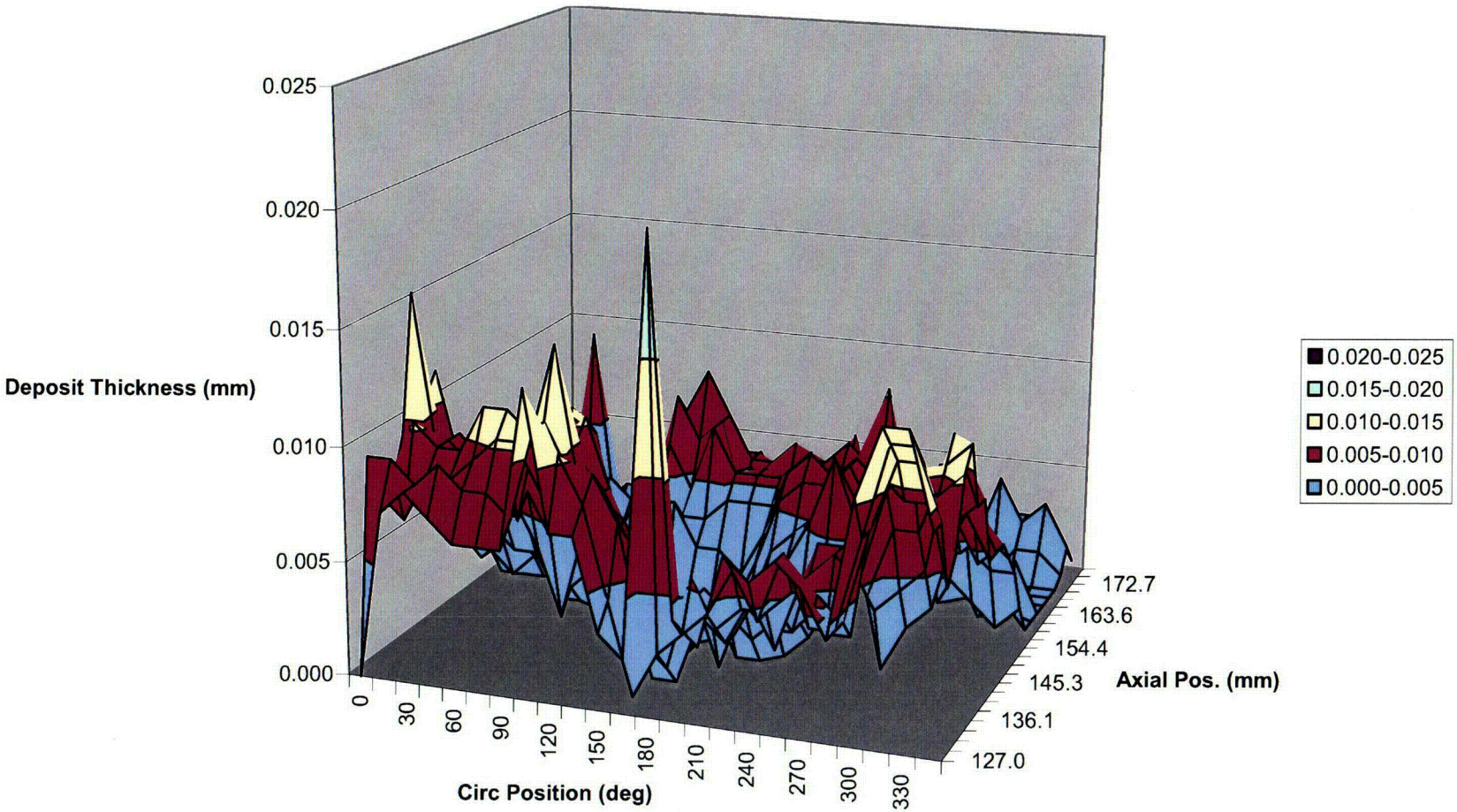

C05

Figure 3-11 ID Dimensional Data of Top of Tubesheet Expansion Transition of R12C59 HL - Piece 2B Obtained by Laser Micrometry of Silastic Mold.

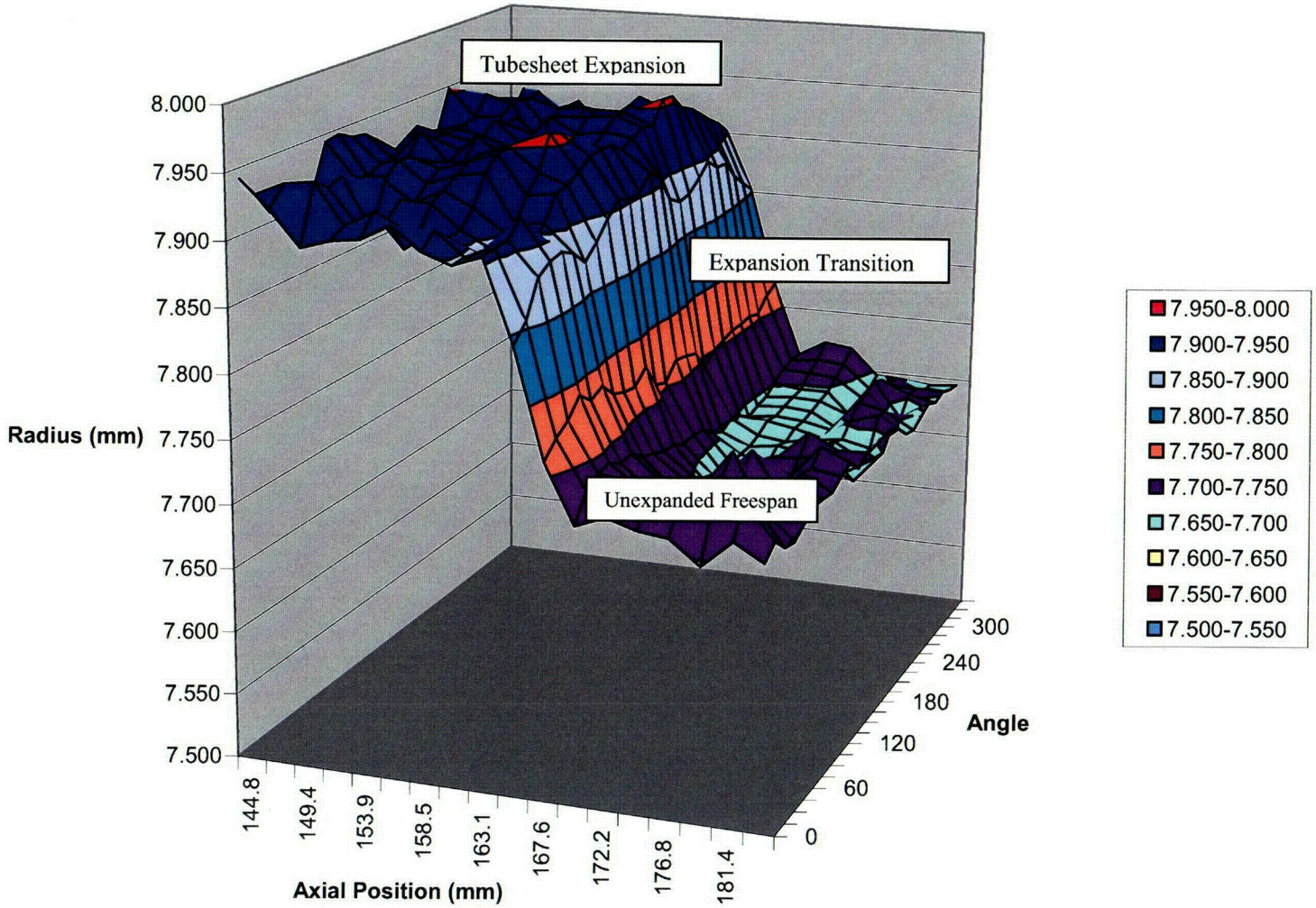

C06

Figure 3-12 Location of Expansion Transition for R12C59 HL Piece 2B Based on Average ID Radius Measurements Obtained by Laser Micrometry on ID Silastic Mold.

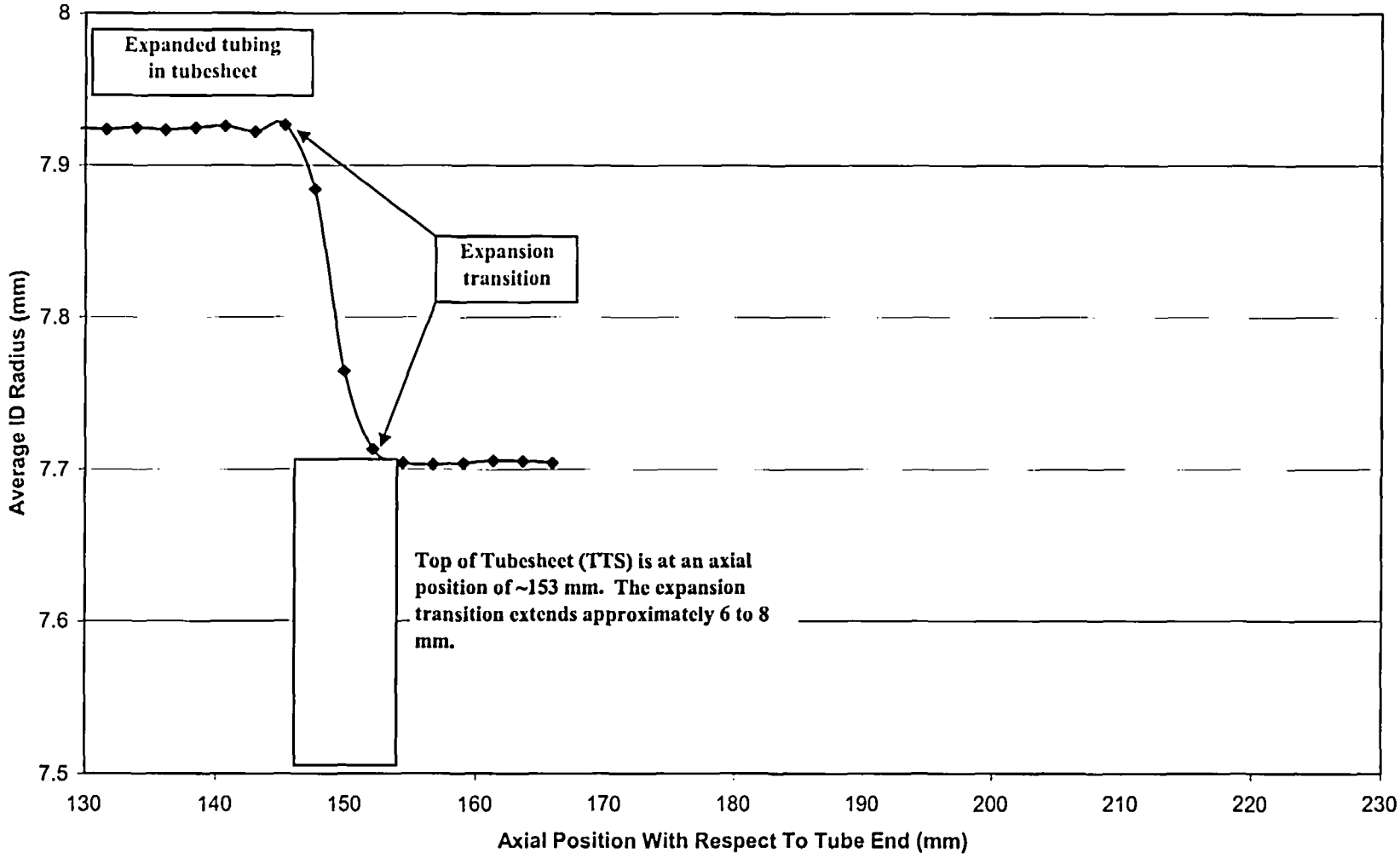

Figure 3-13 ID Dimensional Data of Top of Tubesheet Expansion Transition of R11C60 Piece 2B Obtained by Laser Micrometry of Silastic Mold.

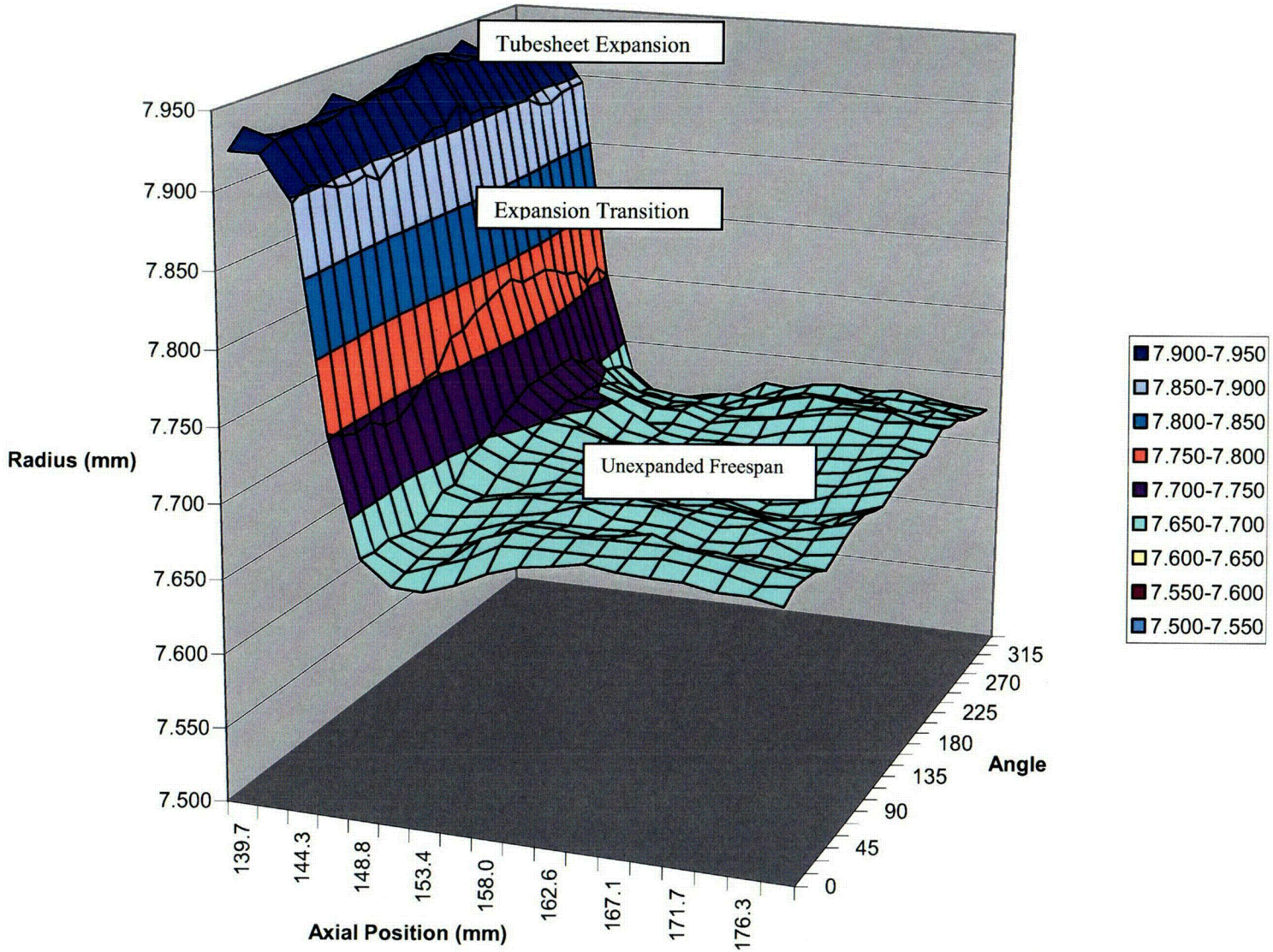

C07

Figure 3-14 Location of Expansion Transition for R11C60 HL Piece 2B Based on Average ID Radius Measurements Obtained by Laser Micrometry on ID Silastic Mold.

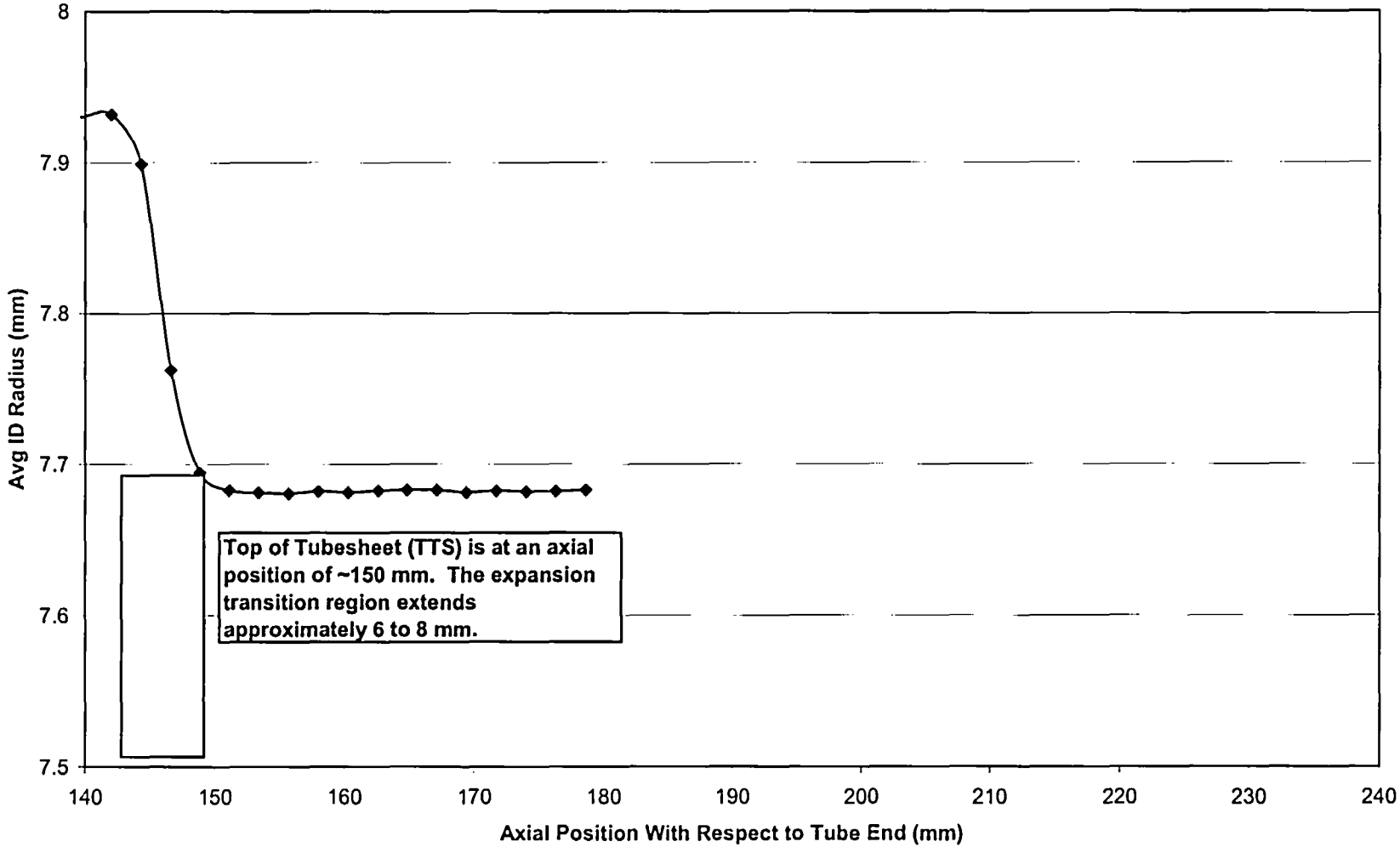

SECTION 4

SECTIONING PLANS

Following the receipt inspection of the tube segments, selected segments were cut into sample sizes that were applicable to a particular test. The 0° orientation mark and the top/bottom directions were maintained on each subsection by a small white paint mark. Section labeling was maintained in accordance with the standard laboratory procedure ("Steam Generator Tube Sample Identification," Westinghouse Science and Technology Department Procedure MR 0201, Rev 0, June 18, 2002).

Tables 4-1 through Table 4-5 lists the various evaluations performed on each pulled piece while Figures 4-1 through 4-5 present a description of which samples were used for each test and the locations of each sample on the parent segment. Included in each figure is an insert showing the azimuthal orientation used throughout the pulled tube examination. The 0° azimuthal position corresponds to the field scribe mark designating the position of the SG divider plate.

Chemistry-sensitive samples were cut using methods that would not contaminate the sample. Microstructure-sensitive samples were cut using methods that generated minimal heat.

In general, the ends of most sections were squared off and deburred prior to eddy current testing. The sections identified as Piece 1 from each of the two tubes were not tested in any way. These sections were from within the tubesheet region and had been significantly altered by the TIG weld heat-relaxation procedure that was performed to facilitate the removal of the tube through the tubesheet. Hence, sketches of these sections are not provided here.

In general, sections that contained a region of interest (top of the tubesheet or 1st tube support plate) were then cut to manageable length for additional NDE and other examinations.

Table 4-1
Disposition of Sections from R12C59 HL - Piece 1

Section	Area of Interest	Tests Performed
1	None	♦ Visual examination only – Piece 1 contained lower portion of hydraulic expansion which was TIG relaxed.

Table 4-2
Disposition of Sections from R12C59 HL - Piece 2
[See Figures 4-1, 4-1 (a), and 4-1 (b)]

Section	Area of Interest	Tests Performed
2	TTS	♦ OD Macro Photography ♦ Bobbin Coil and +Pt Inspection
2A	None	None
2B	TTS	♦ Ghent and Delta Coil Inspection ♦ UT Shear Wave Inspection ♦ UT Lamb Wave Inspection ♦ SEM and EDS Examination ♦ OD Taped at TTS ♦ 9,000 psi ID Pressurization ♦ +Pt Inspection ♦ SEM and EDS Examination
2B1	None	None
2B2	TTS	♦ OD Taped at TTS ♦ Axial Split at 90° and 270°
2B2A	TTS	♦ SEM and EDS of Tube Surface ♦ SEM, EDS, and XRD of OD Deposit
2B2A1	TTS	♦ Metallography @323°(Met #2664)
2B2A2	TTS	None
2B2A2A	TTS	♦ Metallography @90° (Met #2665)
2B2A2B	TTS	♦ Metallography @60° (Met #2666)
2B2A2C	TTS	♦ Metallography @30°(Met #2667)
2B2A2D	TTS	♦ Metallography @0°(Met #2668)
2B2A2E	TTS	♦ Metallography @300°(Met #2669)
2B2A2F	TTS	♦ Metallography @270°(Met #2670)
2B2B	TTS	♦ To be used for Chemical Cleaning Qualification
2B3	None	None

Table 4-3
Disposition of Sections from R12C59 HL- Piece 3
(See Figure 4-2)

Section	Area of Interest	Tests Performed
3	1st TSP	♦ OD Macro Photography ♦ Bobbin Coil and +Pt Inspection
3A	Freespan	None
3B	1st TSP	♦ SEM and EDS Examination ♦ OD Taped at 1st TSP ♦ 9,000 psi Pressurization ♦ SEM and EDS Examination

Table 4-4
Disposition of Sections from R12C59 HL - Piece 4
(See Figure 4-3)

Section	Area of Interest	Tests Performed
4	Freespan	♦ Visual inspection only
4A	Freespan	♦ Tensile test
4B	Freespan	♦ Split ring residual stress measurement
4C	Freespan	♦ Split ring residual stress measurement
4D	Freespan	♦ Huey test for sensitization
4E	Freespan	♦ Huey test for sensitization
4F	Freespan	♦ Metallography for grain size and carbide distribution (Met #2663)
4G	Freespan	♦ Bulk Chemistry
4H	Freespan	None

Table 4-5
Disposition of Sections from R11C60 HL - Piece 1

Section	Area of Interest	Tests Performed
1	None	♦ Visual examination only – Piece 1 contained lower portion of hydraulic expansion which was TIG relaxed.

Table 4-6
Disposition of Sections from R11C60 HL - Piece 2
(See Figure 4-4)

Sample	Support	Tests Performed
2	TTS	♦ OD Macro Photography ♦ Bobbin Coil and +Pt Inspection
2A	None	None
2B	TTS	♦ Ghent and Delta Coil Inspection ♦ UT Shear Wave Inspection ♦ UT Lamb Wave Inspection ♦ SEM and EDS Examination *Note: No destructive examination performed. Piece 2B (12inch in length) available for additional evaluations, if needed.*
2C	None	None

Table 4-7
Disposition of Samples from R11C60 HL - Piece 3
(See Figure 4-5)

Section	Area of Interest	Tests Performed
3	1st TSP	♦ OD Macro Photography ♦ Bobbin Coil and +Pt Inspection
3A	Freespan	None
3B	1st TSP	♦ SEM and EDS Examination
3C	Freespan	None

Table 4-8
Disposition of Samples from R11C60 HL - Piece 4
(See Figure 4-6)

Section	Area of Interest	Tests Performed
4	Freespan	♦ Visual inspection only
4A	Freespan	♦ Tensile test
4B	Freespan	♦ Split ring residual stress measurement
4C	Freespan	♦ Split ring residual stress measurement
4D	Freespan	♦ Huey test for sensitization
4E	Freespan	♦ Huey test for sensitization
4F	Freespan	♦ Metallography for grain size and carbide distribution (Met #2662)
4G	Freespan	♦ Bulk Chemistry
4H	Freespan	None

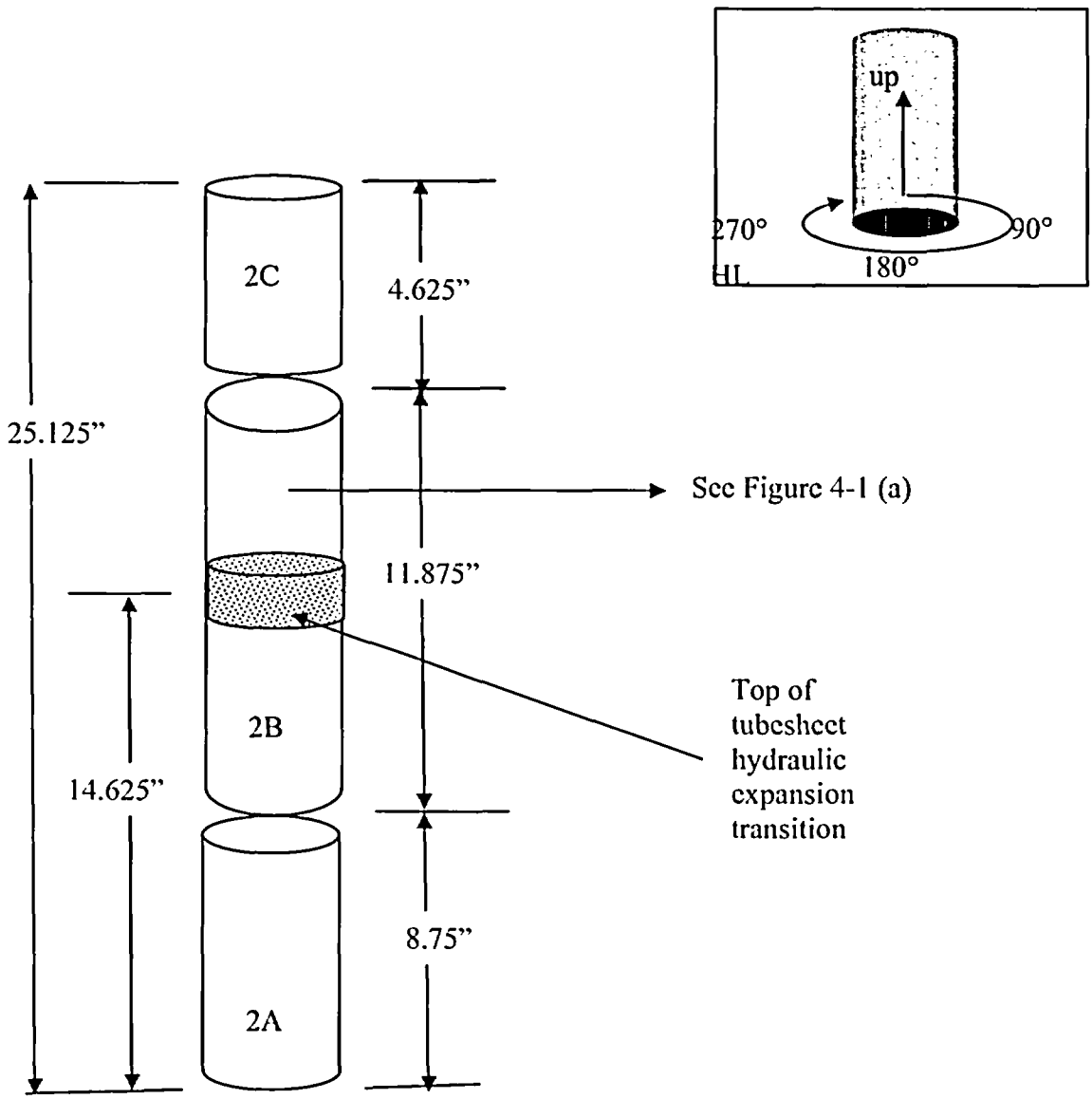

Figure 4-1 R12C59 HL - Piece 2 Sectioning Plan

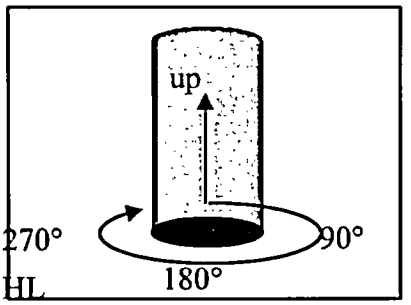

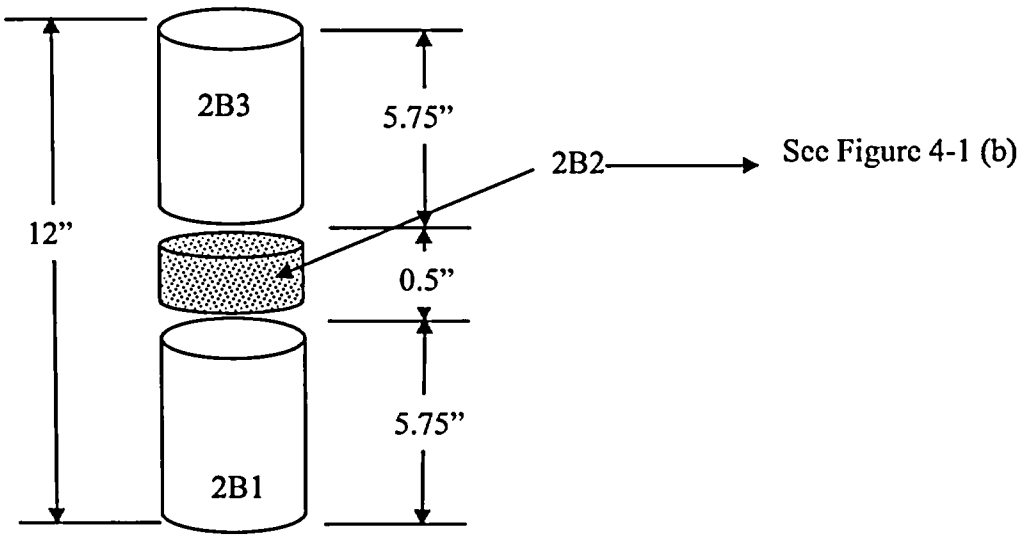

Figure 4-1 (a) R12C59 HL - Piece 2B Sectioning Plan

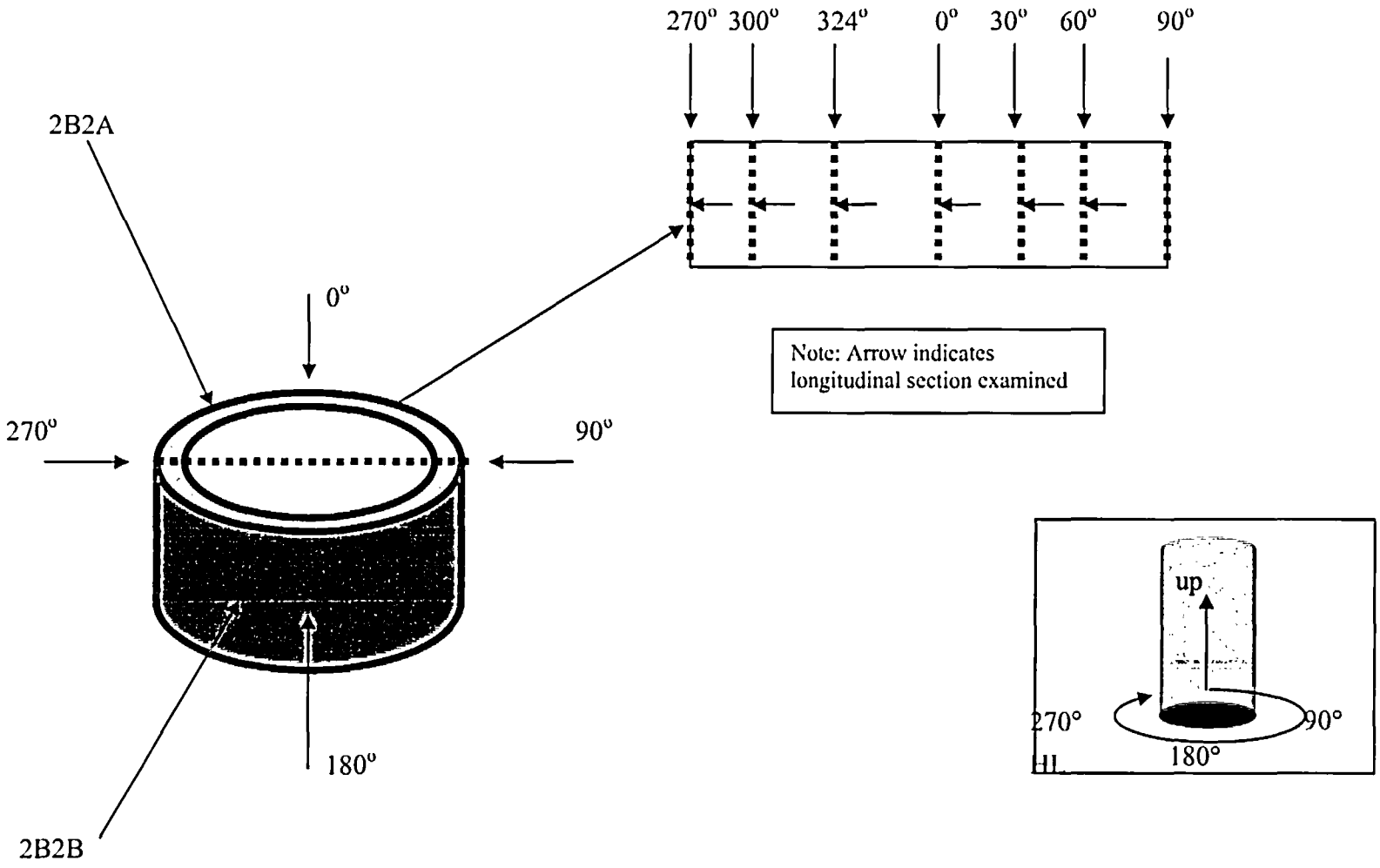

Figure 4-1 (b) Section Diagram of R12C59 HL - Piece 2B2 Sectioning Plan

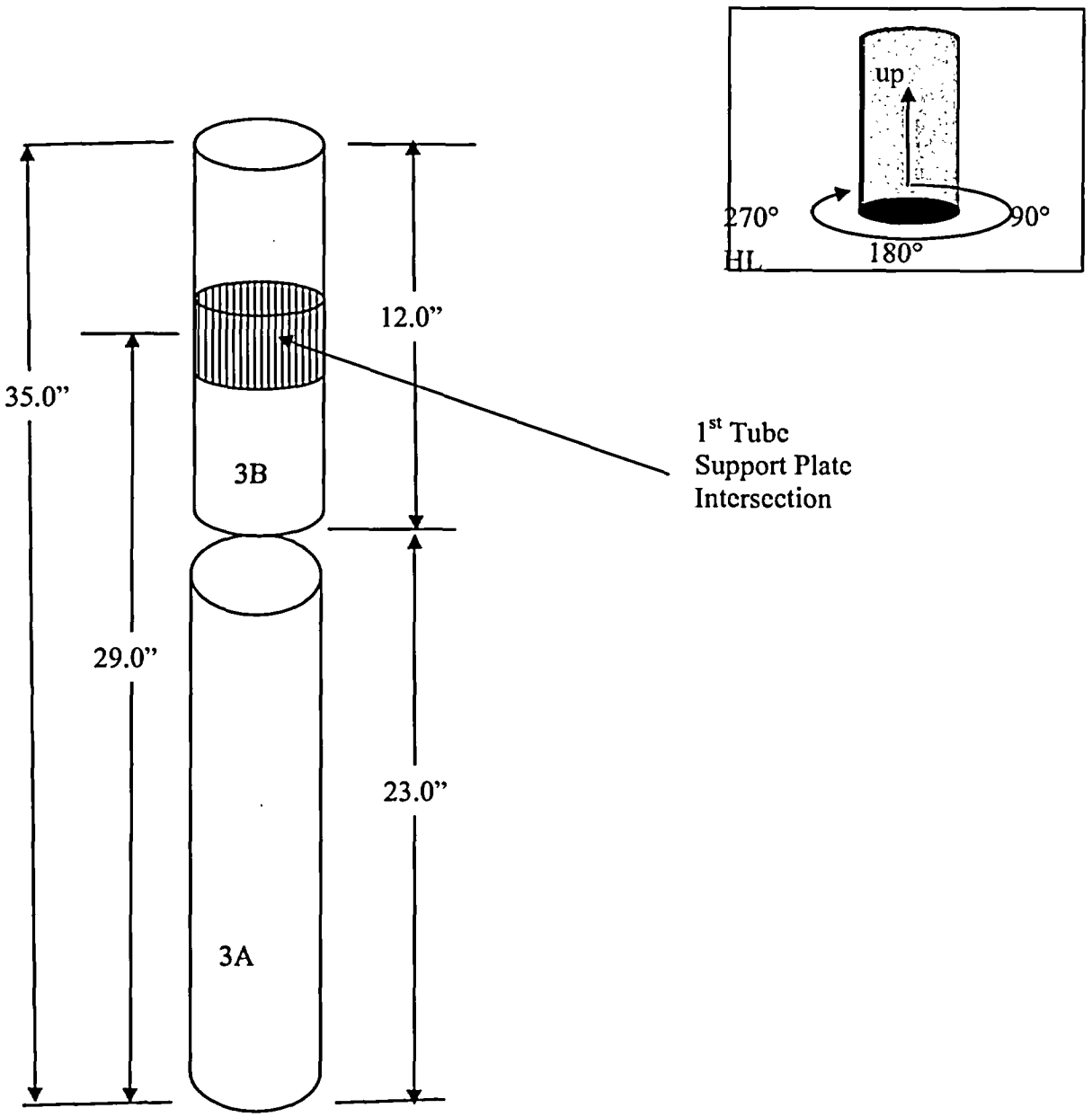

Figure 4-2 R12C59 HL - Piece 3 Sectioning Plan

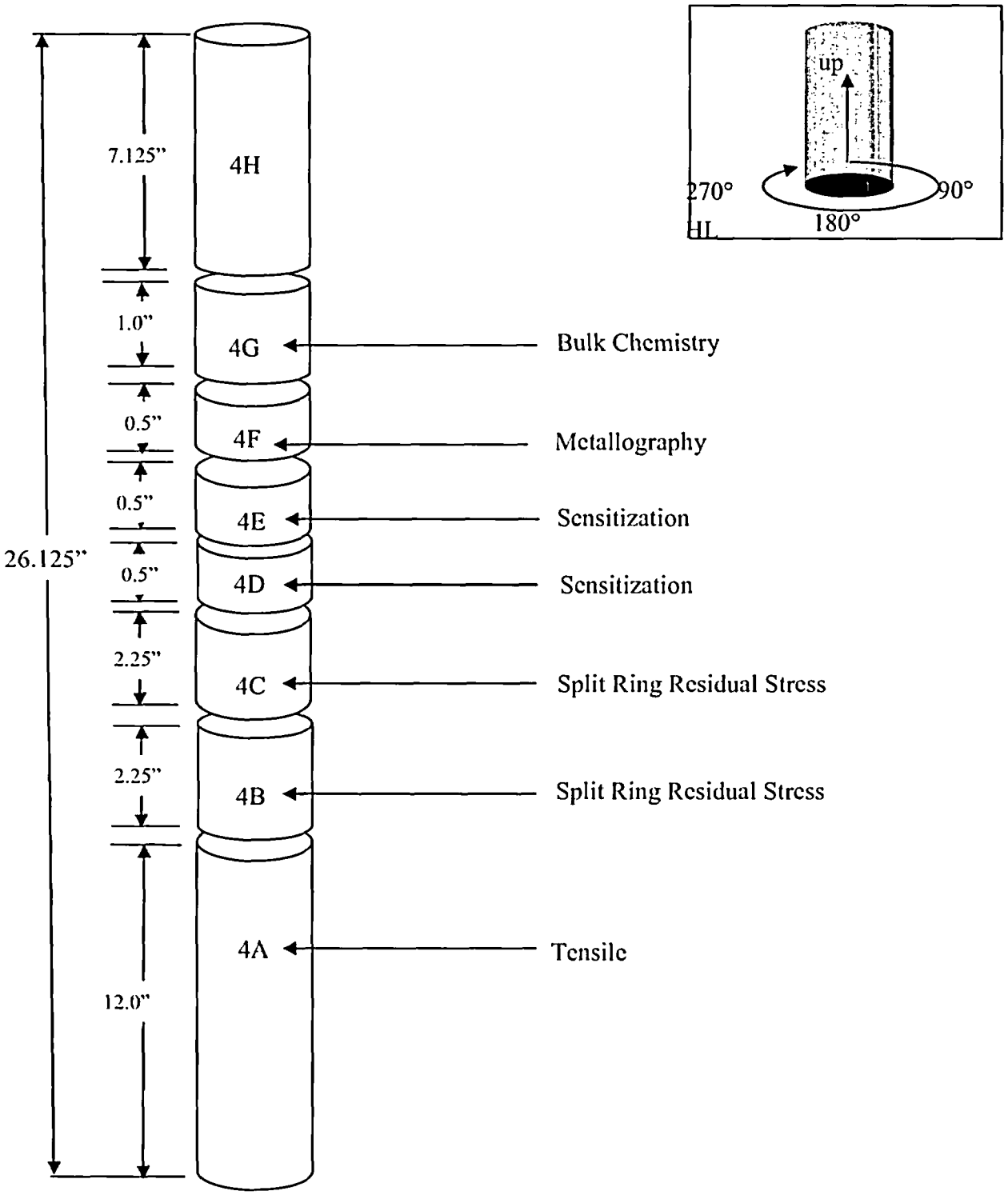

Figure 4-3 R12C59 HL - Piece 4 Sectioning Plan

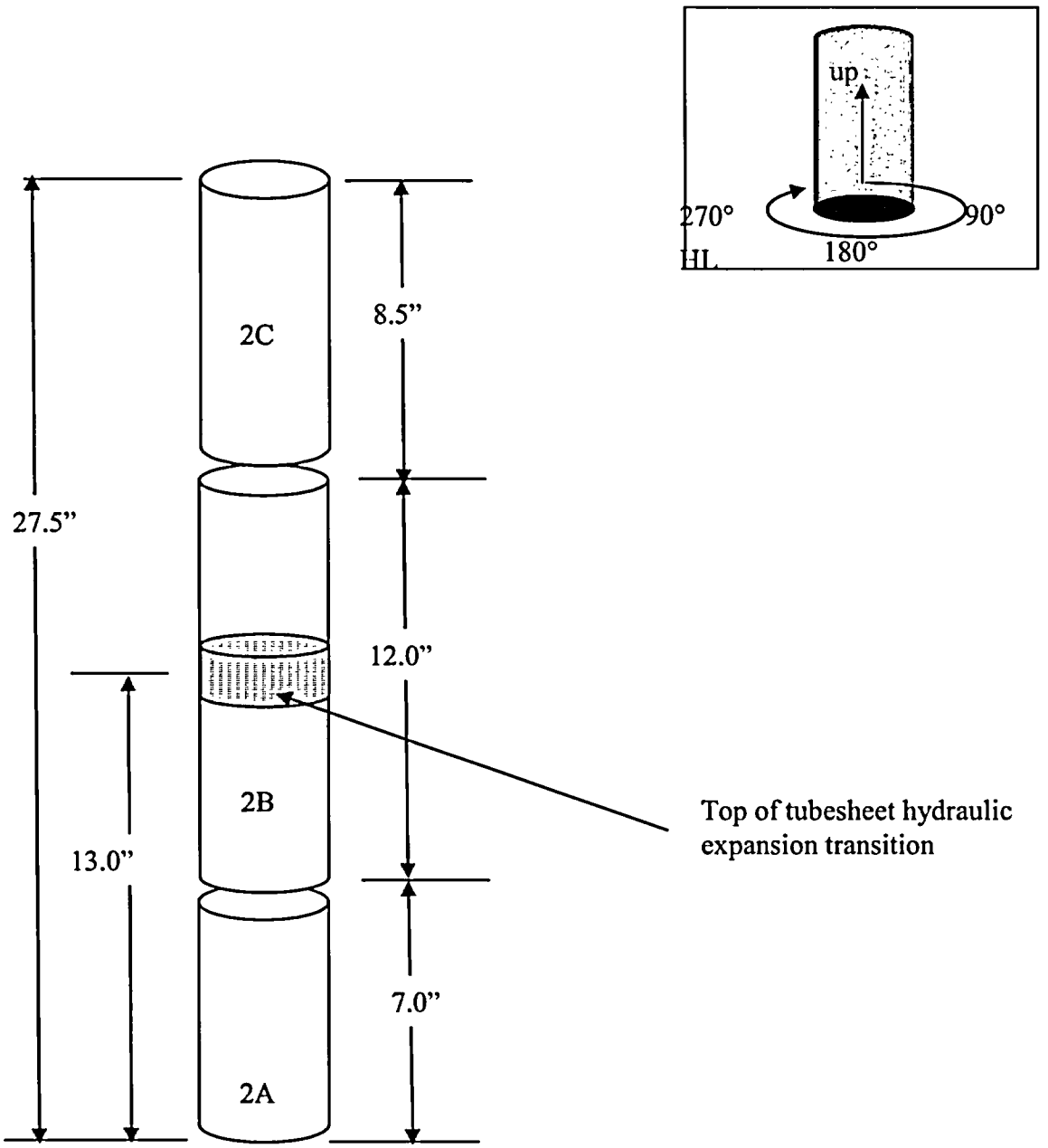

Figure 4-4 R11C60 HL - Piece 2 Sectioning Plan

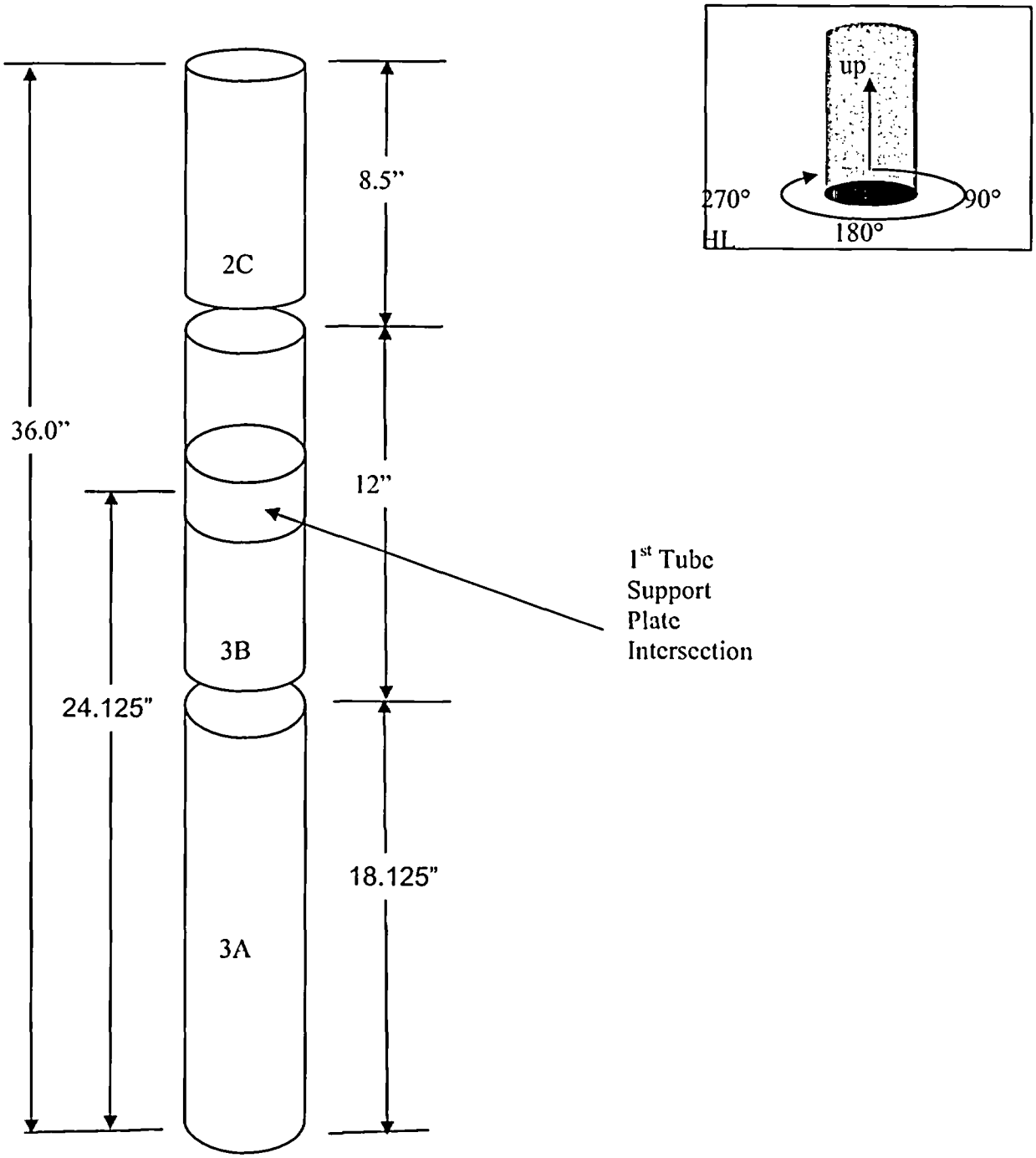

Figure 4-5 R11C60 HL - Piece 3 Sectioning Plan

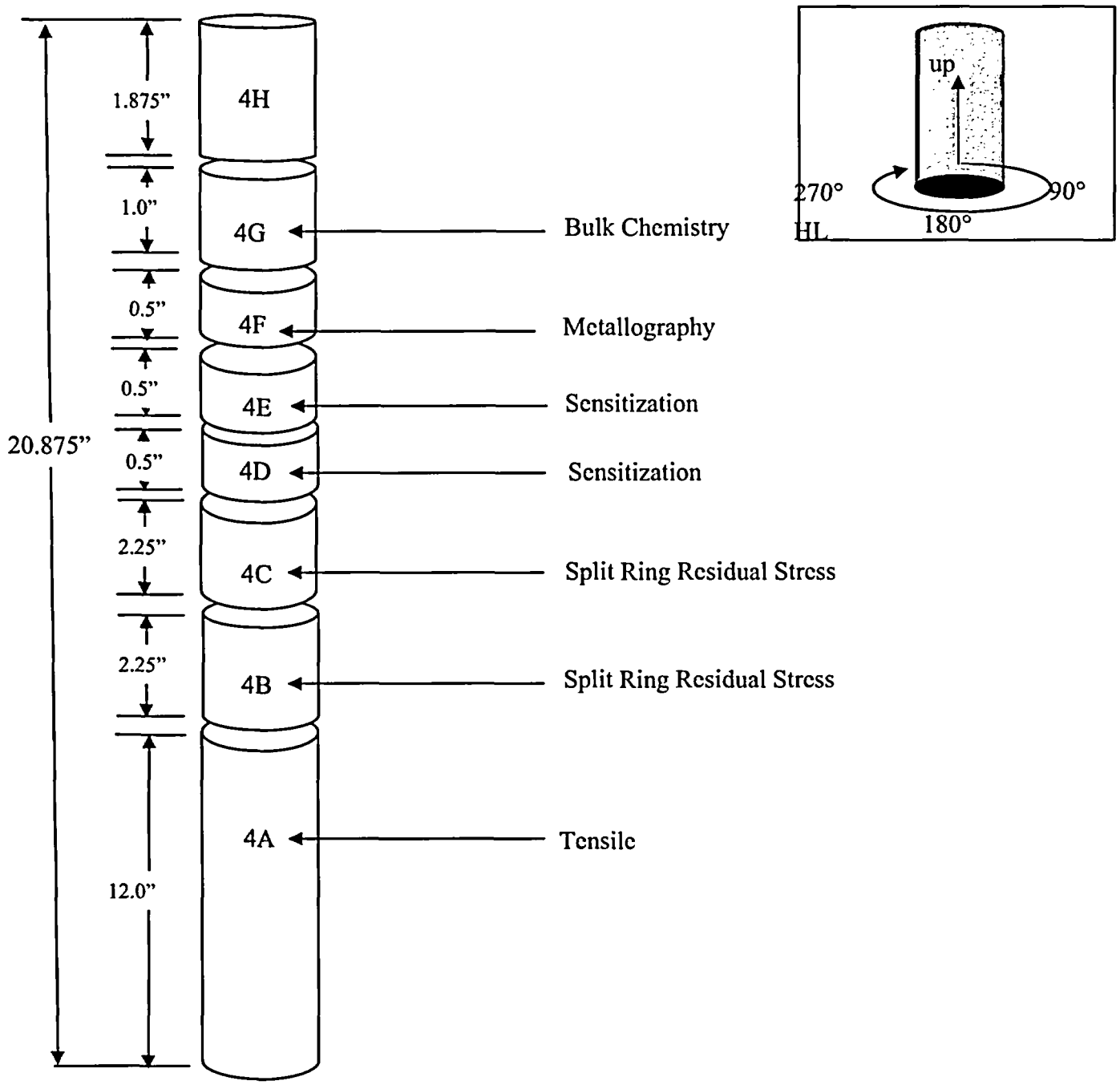

Figure 4-6 R11C60 HL - Piece 4 Sectioning Plan

SECTION 5

FIELD AND LABORATORY EDDY CURRENT DATA EVALUATION

5.1 Introduction

After initial visual inspection of the tube sections, the ends of the tube sections were squared–off and deburred to facilitate eddy current inspections. Two tasks were defined for the eddy current inspections:

- Review and reevaluation of field data for R12C59 HL and R11C60 HL
- Acquisition and analysis of bobbin coil, +Pt, 3-Coil, and Ghent probe laboratory data

Data are presented and discussed as appropriate to each of these tasks in the following sections.

In the following descriptions of the eddy current and ultrasonic inspections, the 0° locations of each specimen was a consistently maintained orientation related to a tube-pull grinding mark at the bottom of the tube piece; 90° et al. are expressed clockwise of 0° when looking in the direction of the primary flow.

5.2 Eddy Current (EC) Data - General Practices

Prior to the tube pull, the steam generator tubes were examined in the steam generator using eddy current (EC) inspection techniques. A 0.560-inch diameter bobbin probe was used as for the primary inspection and was supplemented by +Pt probes where indications were identified by the bobbin coil at the expansion transition at the TTS. For the two pulled tubes R12C59 HL and R11C60 HL the entire length of the tube from the tube end to above the second support (above where the tubes were cut) was inspected prior to the tube pulling processes with the +Pt probe. Data were collected at test frequencies of 10, 160, 320 and 630 kHz for bobbin probes and at 20, 100, 200, 300 and 600 kHz for +Pt probe. Furthermore, the field data were reevaluated as part of the tube examination. Bobbin calls were made using 160-630 kHz Mix data channel from the differential mode. The +Pt probe contains three coils: 1) a mid-frequency +Pt coil which forces directionality to any indication, 2) a mid-frequency 115 mil diameter pancake coil, and 3) a high frequency 80 mil diameter pancake coil. +Pt probe indications were usually identified with the +Pt coil using 300 kHz differential mode data.

The eddy current re-evaluation of the field data and the laboratory examinations were calibrated in a similar fashion. For the bobbin coil the voltage for all frequency channels except the 630 kHz, Mix and the 10 kHz channel was set to 4.0 volts for the 20% OD calibration holes and the phase to 40 degrees for the through hole. The 10 kHz channel was set to 4.0 volts on the support ring. The rotating probe data were adjusted such that all channels except the trigger and low frequency locator channels were set to 20 Volts on the through wall notch.

After the tubes were pulled and shipped to Westinghouse, eddy current inspections were conducted in the Hot Cell area of the Remote Hot Cell Metallographic Facility. The inspections were conducted with a bobbin and rotating +Pt probe configurations similar to the styles used in the field. All tube sections were inspected with the bobbin coil. The rotating probes were used only for tube sections containing the TTS or 1st TSP locations. In all cases the eddy current data were collected using the R/D Tech TC6700 tester and Westinghouse ANSER software. The laboratory bobbin probe and rotating probe inspections utilized calibration standards used during the field inspection FMST-10-03 and EP5-006-02 respectively. Prior to the +Pt examination of the tube sections containing the tube support (TSP) crevice regions and the top of tubesheet (TTS) conductive material was attached to the outside of the tubes to act as fuducial marks in the eddy current data. The conductive material was in the shape of a large "L" with the leg nominally located at 0 degrees and the bottom portion oriented toward 90 degrees. Thus the azimuthal location of the rotating eddy current probe indications can be determined allowing the destructive examinations to be focused to the precise areas of interest.

Table 5-1 presents a summary of field and laboratory eddy current data obtained for the TSP crevice and the TTS regions of the pulled tubes. The laboratory data presented are for the bobbin and +Pt probes used during the field inspection. Note that during the field inspection the TTS regions were inspected multiple times. The results reported in the Table 5-1 are for the final inspection results stored on Reel 169. The azimuthal locations of the indications shown on Table 5-1 are based on a detail review of the deposit signals seen during the laboratory review and comparing these signals with the field produced signals. A detailed discussion of this effort is included in Section 8. Included in Section 8, are Figures illustrating the location of both the +Pt and UT signals and the relationship of these signals with respect to the tubelane orientation.

In the field data analysis and laboratory review of the field data, circumferential indications were noted at the TTS of both R12C59 HL and R11C60 HL. None of the field indications were confirmed during the laboratory eddy current effort regardless of the rotating probe used.

The field eddy current response of the quatrefoil tube support / tube intersections (TSP1) of R12C59 HL and R11C60 HL showed no indications in the field data analysis or the laboratory data review. Further the laboratory examination found no indications in these tubing locations. During the laboratory examination the locations of the TSP1 region of R12C59 HL, its position on the tube was identified through the presence of OD deposits by both the pancake and bobbin coil examinations. No such deposits were present at TSP1 of R11C60 HL.

The following presents selected supporting eddy current data for the above observations.

5.3 Laboratory Reevaluation of Field Eddy Current Test Data

R12C59 HL at TTS

During the 2R10 field eddy current inspection program, the top of the tubesheet was inspected using the +Pt probe. Figure 5-1 shows a data display for the 300 kHz +Pt coil with the phase established such that circumferential indications produce a positive vertical defection. Figure 5-2 shows a data display of the +Pt Mix response for the indication and was used in the laboratory review of the field data to size the indications (Table 5-1). The extent of cracking was determined to be 40 degrees around the circumference.

R12C59 HL at TSP1

The original bobbin and +Pt probe field calls for the region of tube R12C59 HL at TSP1 was NDD. The laboratory review did not alter this conclusion, only a Mix residual was identified at the TSP location. No +Pt indications were identified.

R11C60 HL at TTS

During the 2R10 field eddy current inspection program, the TTS was inspected using the +Pt probe. Figure 5-3 shows a data display for the 300 kHz +Pt coil with the phase established such that circumferential indications produce a positive vertical deflection. Figure 5-4 shows a data display of the +Point Mix response for the indication and was used

in the Laboratory review of the field data to size the indications (Table 5-1). The extent of cracking was determined to be 38 degrees around the circumference.

R11C60 HL at TSP1

The original bobbin and +Pt probe field calls for the region of tube R12C59 HL at TSP1 was NDD. The laboratory review did not alter this conclusion, only a Mix residual was identified at the TSP location. No +Pt indications were identified.

5.4 Laboratory Bobbin and +Pt Probe Inspection and Analysis

The discussions that follow will center on the analysis of the laboratory eddy current results obtained with the +Pt and bobbin coil configurations used in the field. Note that all sections of tubing had artifacts of the tube removal. The responses from these artifacts presented no issues with the analysis of the data and are not highlighted below.

R12C59 HL - Piece 2B at TTS

Eddy current inspection of R12C59 HL – Piece 2B at the TTS in the laboratory did not reproduce the +Pt response seen during the field inspection. No flaw signals were seen. Figure 5-5 shows the circumferentially sensitive channel of the 300 kHz +Pt response. No circumferentially oriented indications were identified. Figure 5-6 shows the +Point response with the phase oriented so that axially oriented discontinuities respond in the positive direction. Short axial indications are found within the expanded portion of the tube adjacent to the expansion transition and were likely related to the tube pulling process and not indicative of operational degradation. Figure 5-7 shows the pancake coil response indicating the presence of deposits on the outside of the tube. No flaw signals were seen. The signal responses observed were indicative of OD deposits. The distribution of the deposits is similar to that seen in the field and was used to determine the azimuthal orientation of the field +Pt indication, see Section 8.

R12C59 HL - Piece 3B at TSP1

During the laboratory eddy current inspection of R12C59 HL – Piece 3B at the 1st TSP region, no bobbin coil or +Pt probe response suggestive of tubing discontinuities were identified. The bobbin coil, however did show tube removal artifacts and the presence of a deposit associated with the TSP1 location (Figure 5-8). A pattern was identified by the pancake coil inspection indicative of deposit formation in two of the quatrefoil region of

the tube support plate. Figure 5-9 shows the 100 kHz pancake coil response for this region of the tube.

Tube R11C60 HL - Piece 2B at TTS

Eddy current inspection of R11C60 HL – Piece 2B at the TTS region in the laboratory did not reproduce the +Pt response seen during the field inspections. Figure 5-10 shows the circumferentially sensitive channel of the 300 kHz +Pt response. Figure 5-11 shows the pancake coil response indicating the presence of deposits on the outside of the Tube. The distribution of the deposits is similar to that seen in the field and was used to determine the azimuthal orientation of the field +Pt indication, see Section 8.

Tube R11C60 HL - Piece 3B at TSP1

During the laboratory eddy current inspection of R11C60 HL – Piece 3B at the 1st TSP region, no bobbin coil or +Pt probe response indicative of tubing discontinuities were identified. No responses were identified that are suggestive of deposit formation quatrefoil region of the tube support plate. No graphics are presented since no discontinuities or deposit signal responses were seen.

5.5 Ghent and 3-Coil Probe Laboratory Data and Analysis

In addition to the +Pt probe two other rotating coil configurations were used to collect data on the TTS regions of R12C59 HL and R11C60 HL during the laboratory eddy current inspection efforts. The first was the Ghent probe which is a driver pick-up coil probe with two inspection volumes one sensitive to circmferentially oriented discontinuities and the other sensitive to axially oriented discontinuities. No indications were identified at any of the locations of interest. Figure 5-12 and 5-13 show the response of the probe in the vicinity of the TTS of R12C59 HL and R11C60 HL, respectively. Only responses from the deposits above the transition can be observed.

The second probe used in the laboratory inspection effort was a 3-Coil probe. This probe has a 115 mil diameter pancake coil and two coils which are stood on edge to yield preferential sensitivity to axially or circumferentially oriented discontinuities respectively. No indications were identified at any of the locations of interest. Figure 5-14 and 5-15 show the response of the probe in the vicinity of the TTS of R12C59 HL and R11C60 HL, respectively. Only responses from the deposits above the transition can be observed.

Since the results of these inspections with the Ghent and 3-Coil probes yielded no additional insight into the presence of the TTS indications beyond those of the +Pt probe, their results were not included in Table 5-1.

Table 5-1 Summary of Field and Laboratory Eddy Current and Ultrasonic Inspection Results

Location		Field Eddy Current		Field Data Review			Lab. Eddy Current		Ultrasonic		
		Bobbin Coil	+Pt^	Bobbin Coil	+Pt^		Bobbin Coil	+Point	Field		Lab
		Volts / % /	Volts / % / extent	Volts / % /	Volts / % / Extent	Loc.*	Volts / % /	Volts / % / Extent	% / Extent	Loc.*	
R12 C59											
	First Support	NDD	NDD	NDD	NDD	N/A	NDD	NDD	N/A	N/A	N/A
	Top of Tube sheet	N/A	.19/22/41° CSI	N/A	0.23/30/37°	324°	N/A	NDD	42/80°	0°-90°	NDD
[redacted]											
R11 C60	First Support	NDD	NDD	NDD	NDD	N/A	NDD	NDD	N/A	N/A	N/A
	Top of Tube sheet	N/A	.16/38/48° CSI	N/A	0.18/24/40°	327°	N/A	NDD	34/20°	130°	NDD

^ Final inspection Reel 169
* Location determined from laboratory reference and deposit pattern (See Section 8)
NDD - No Detectable Degradation CSI - Circumferential Single Indication
DI - Distorted Indication
PI - Possible Indication
N/A - Not Appropriate

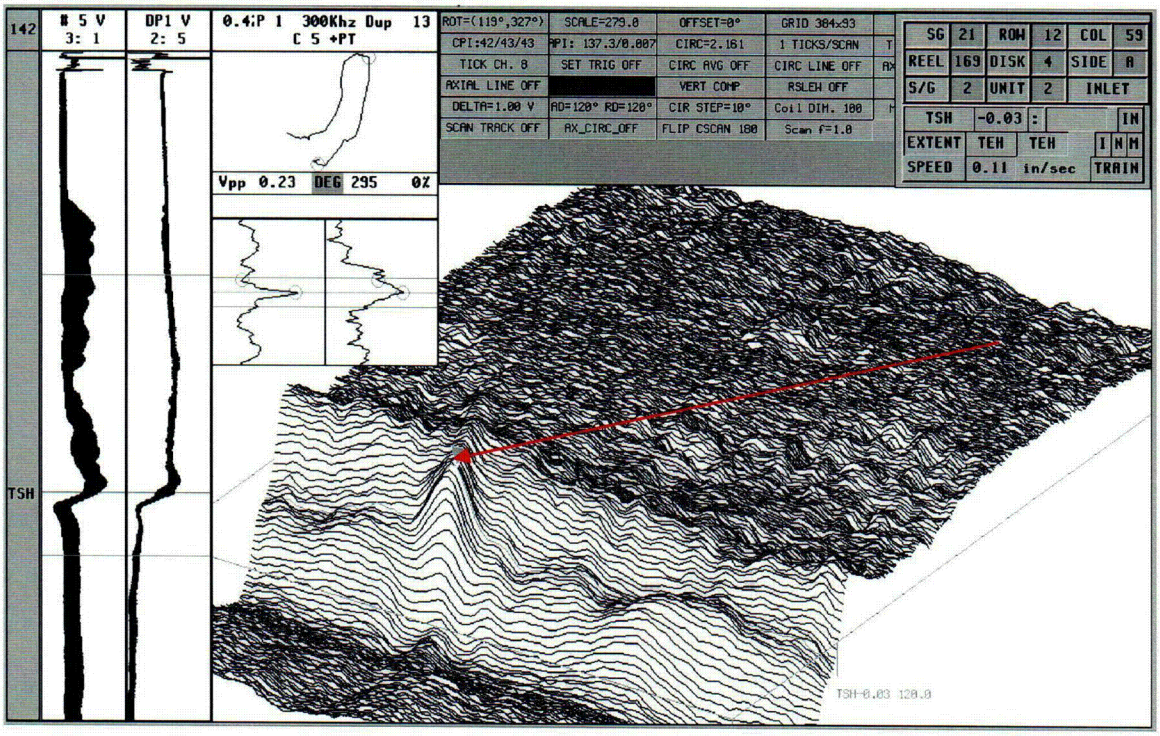

Figure 5-1 Plot of the 300 kHz +Pt coil field data from Vogtle Unit 2 S/G 2 of R12C59 HL showing an indication at the hot leg top of tube sheet (TTS). The +Pt response is adjusted so that response from a circumferentially oriented discontinuity is in the positive vertical direction. The indication is thus interpreted as originating from a circumferentially oriented discontinuity. Arrow denotes location of indication.

C08

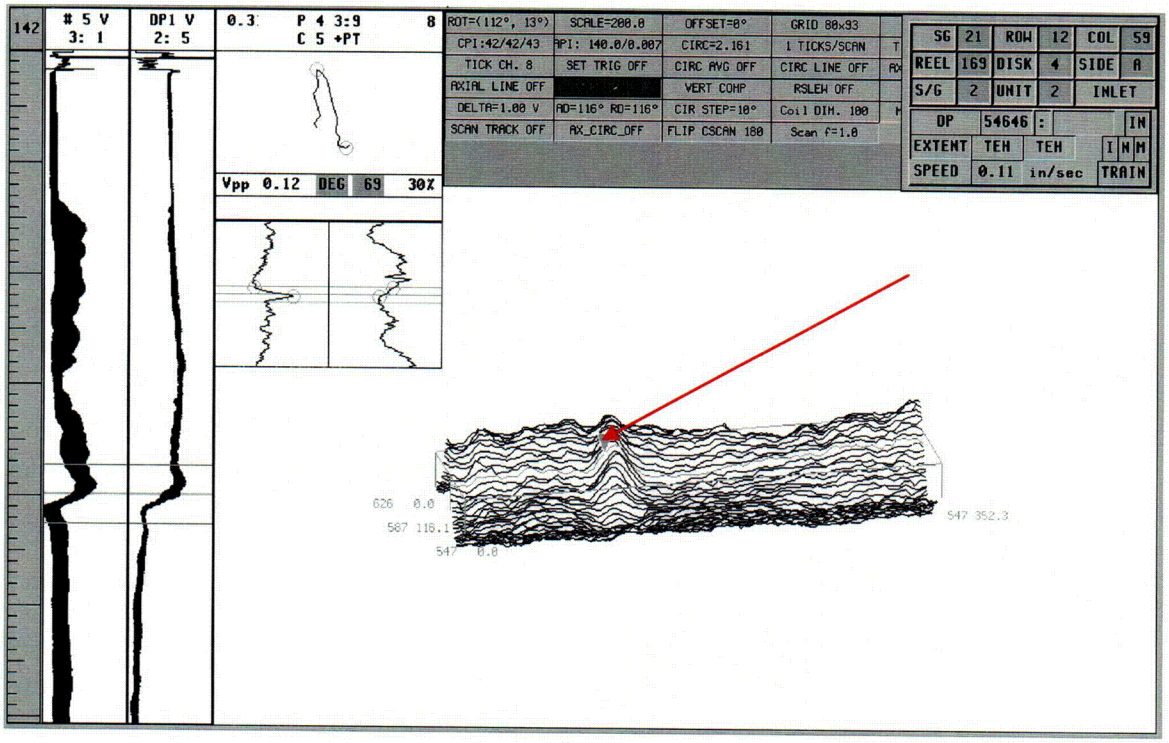

Figure 5-2 Plot of the Mix +Pt coil field data from Vogtle Unit 2 S/G 2 of R12C59 HL showing an indication at the hot leg top of tube sheet (TTS). The +Pt response is adjusted so that response from a circumferentially oriented discontinuity is in the positive vertical direction. Arrow denotes location of indication.

C09

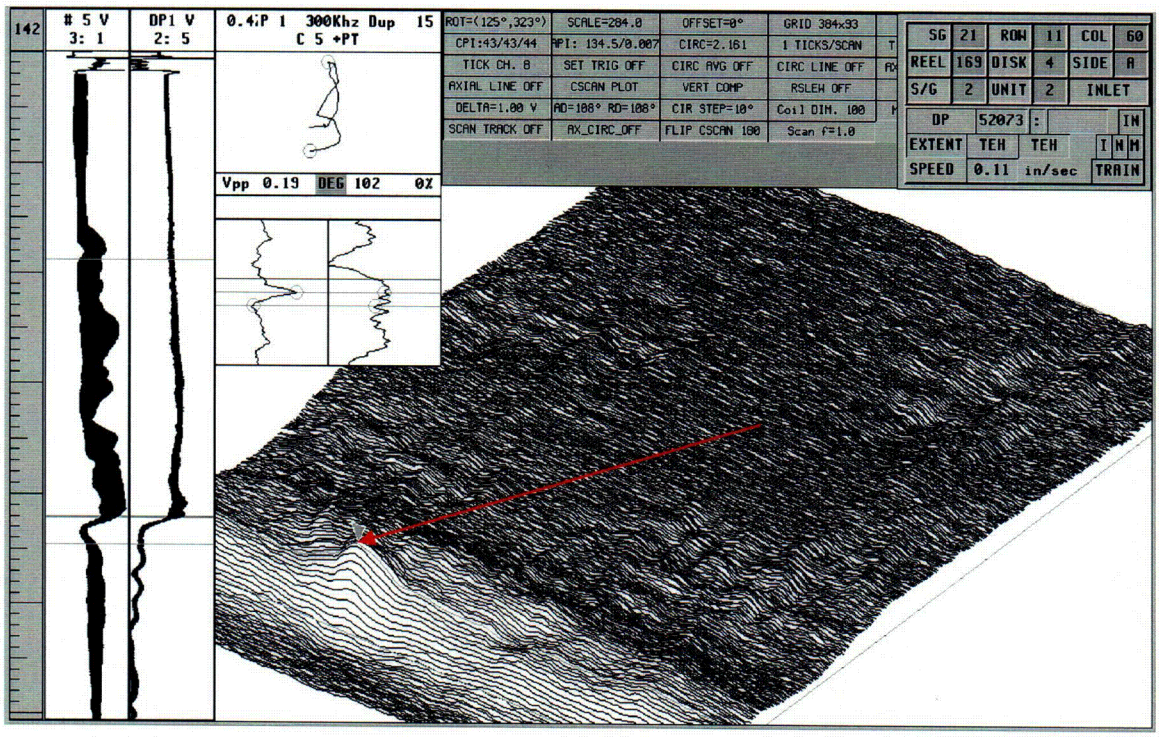

Figure 5-3 Plot of the 300 kHz +Pt coil field data from Vogtle Unit 2 S/G 2 of R11C60 HL showing an indication at the hot leg top of tube sheet (TTS). The +Pt response is adjusted so that response from a circumferentially oriented discontinuity is in the positive vertical direction. The indication is thus interpreted as originating from a circumferentially oriented discontinuity. Arrow denotes location of indication.

C10

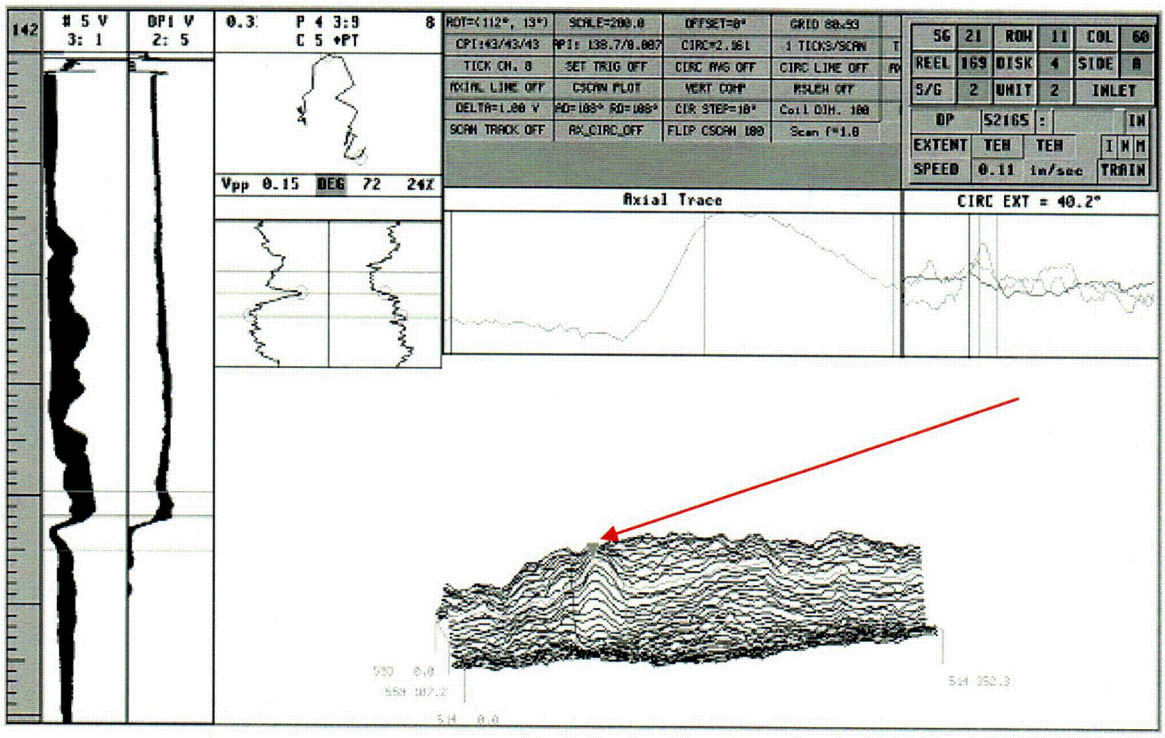

Figure 5-4 Plot of the Mix +Pt coil field data from Vogtle Unit 2 S/G 2 of R11C60 HL showing an indication at the hot leg top of tube sheet (TTS). The +Pt response is adjusted so that response from a circumferentially oriented discontinuity is in the positive vertical direction. Arrow denotes location of indication.

C11

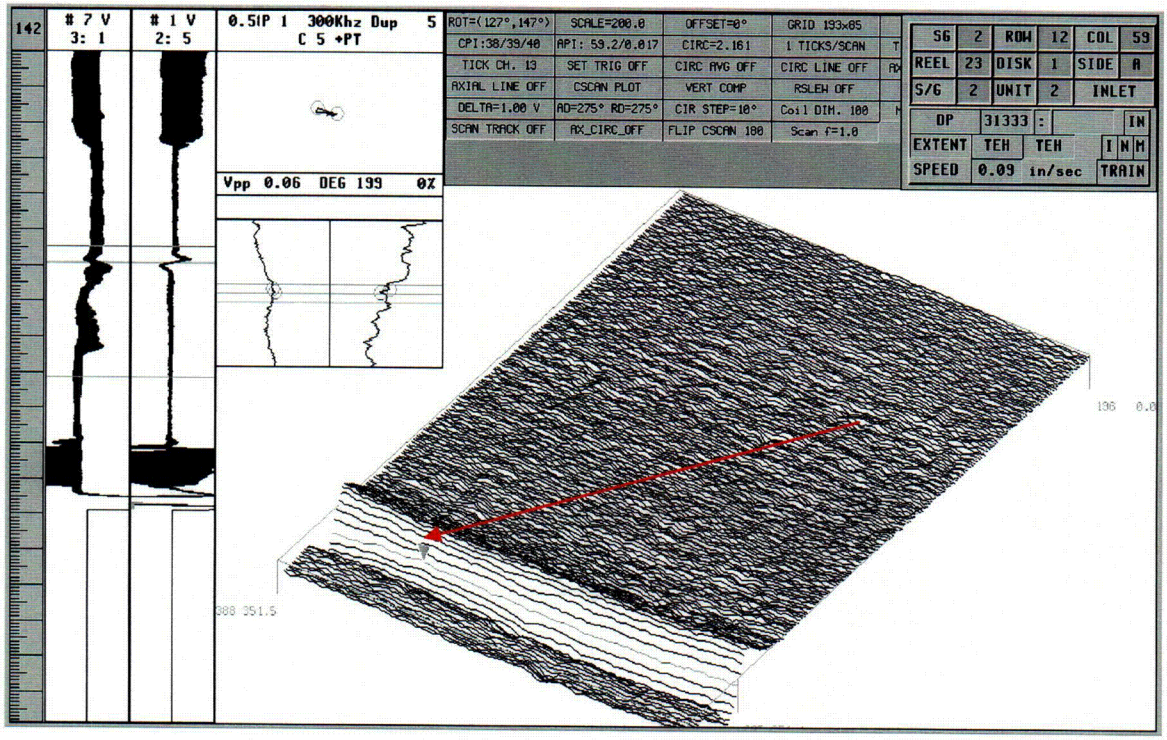

Figure 5-5 Laboratory +Pt coil response from the TTS region of R12C59 HL – Piece 2B. +Pt response adjusted so that circumferentially oriented discontinuities are positive). No indication seen. Arrow denotes location of field signal.

C12

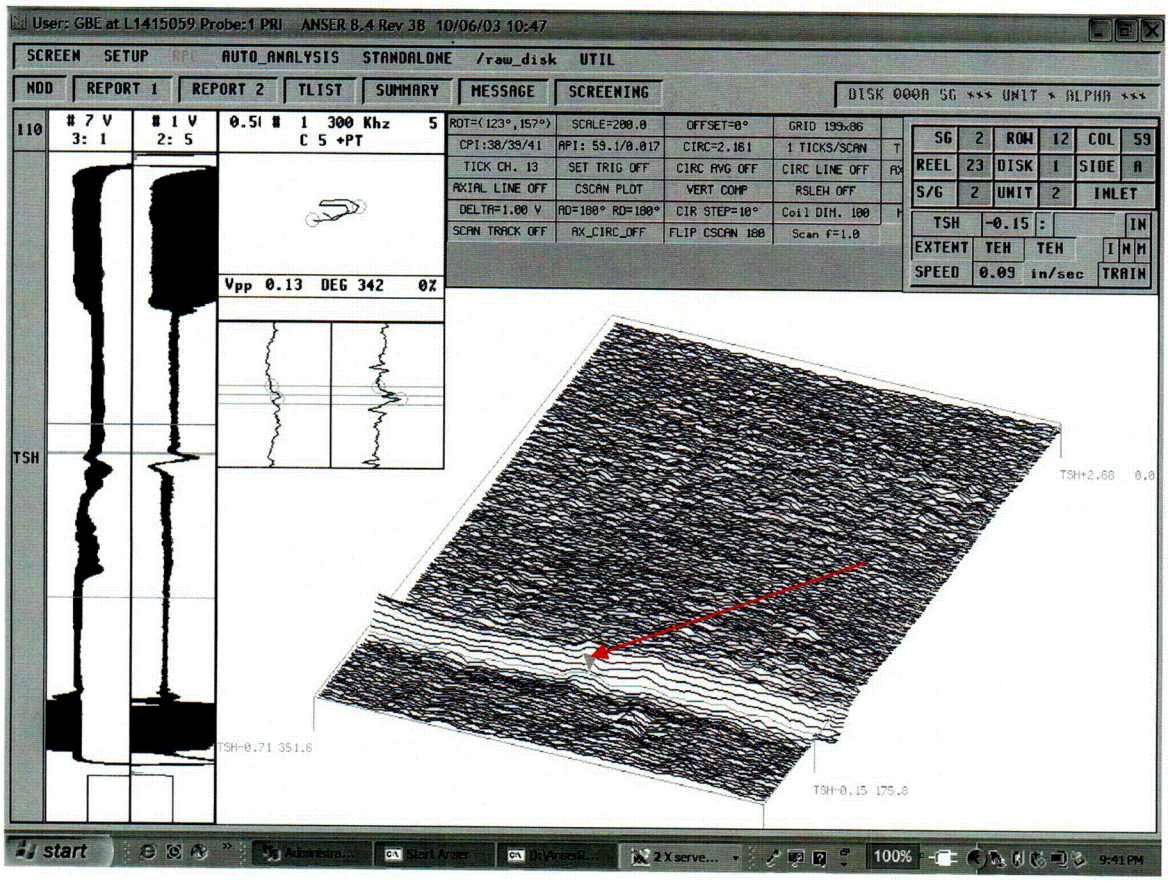

Figure 5-6 Laboratory +Pt coil response from the TTS region of R12C59 HL – Piece 2B. +Pt response adjusted so that axially oriented discontinuities are positive). Arrow shows the location of axial indication. Indication is believed to be associated with tube removal process. Note the indication is indicative of an axially oriented discontinuity located on the expanded side of the expansion response.

C13

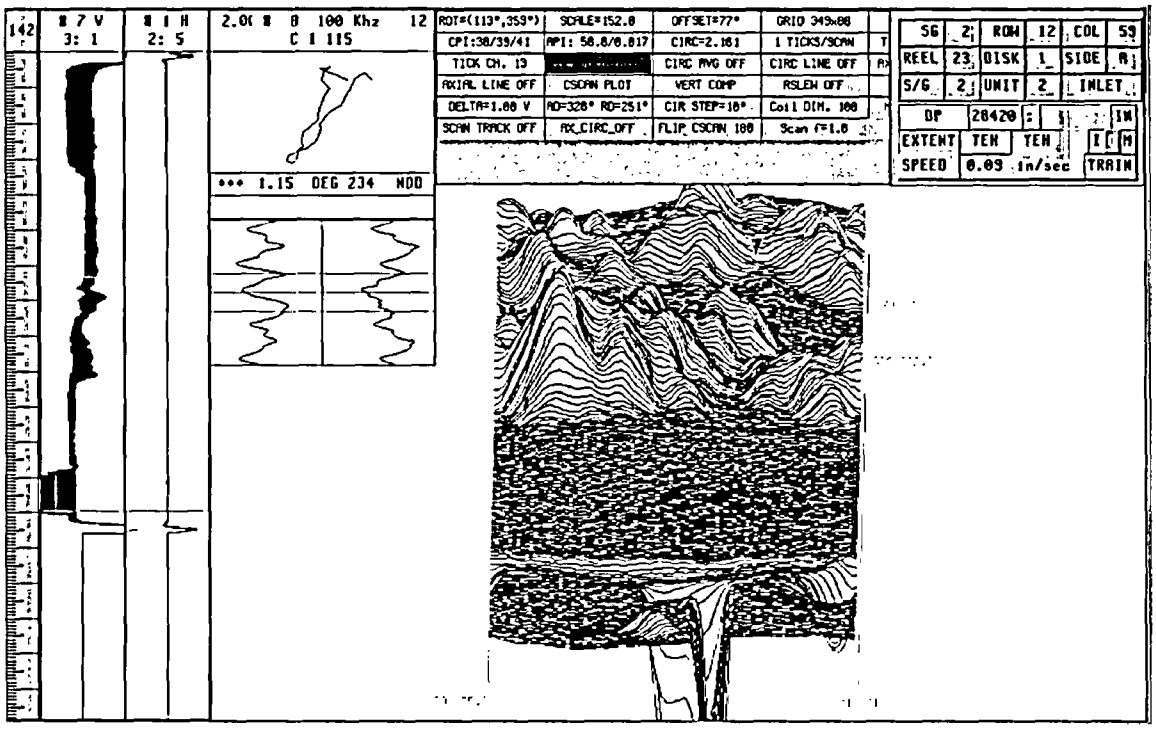

Figure 5-7 Laboratory 100 kHz Pancake coil response from the TTS region of R12C59 HL - Piece 2B. Signal response indicative of OD deposits. Pancake response adjusted so that circumferentially oriented discontinuities are positive.

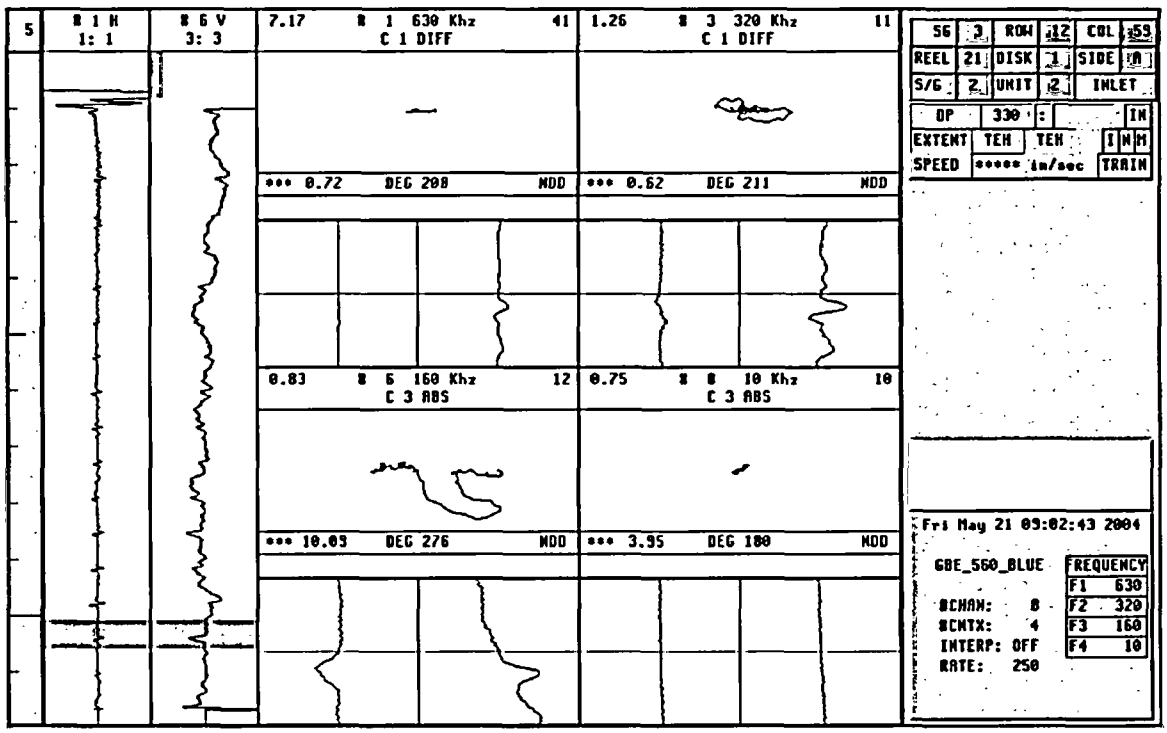

Figure 5-8 Laboratory bobbin coil response from the TSP1 region of R12C59 HL – Piece 3B. Periodic response in left most strip chart is an artifact of the tube removal. The Lissajous patterns are for the deposit associated with the TSP location.

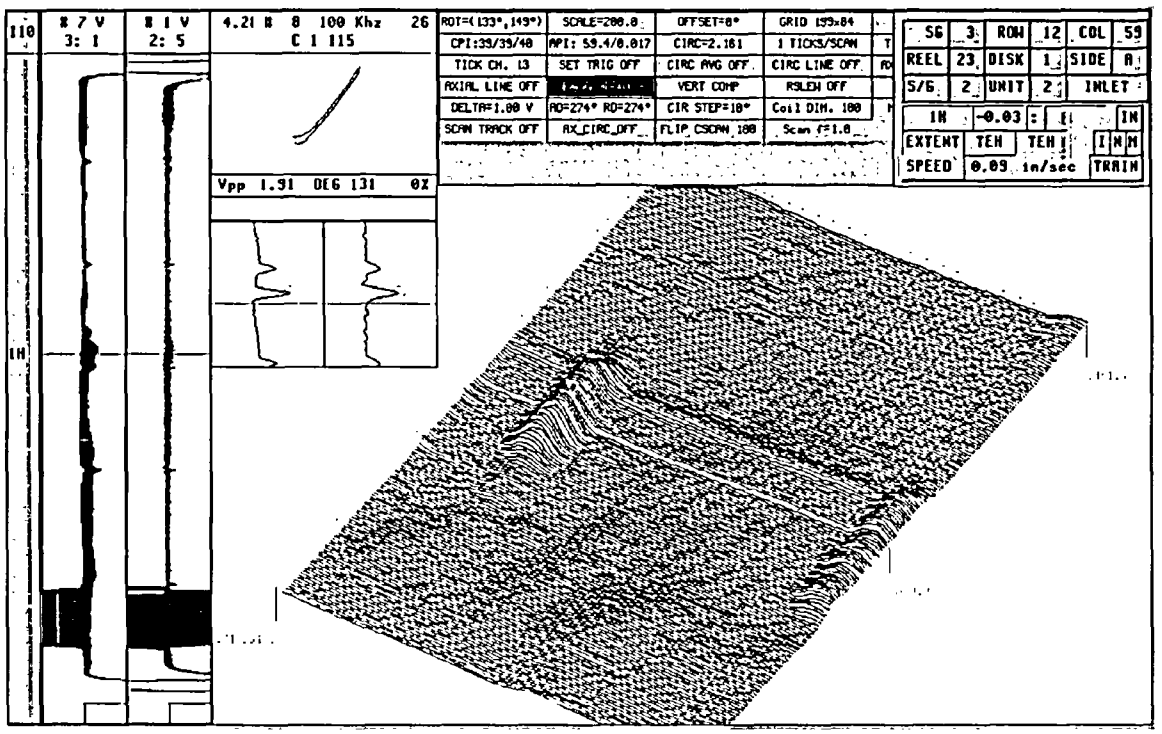

Figure 5-9 Laboratory 100 kHz response from the TSP1 region of R12C59 HL – Piece 3B. Note the two bands associated with the deposits within the quatrefoils.

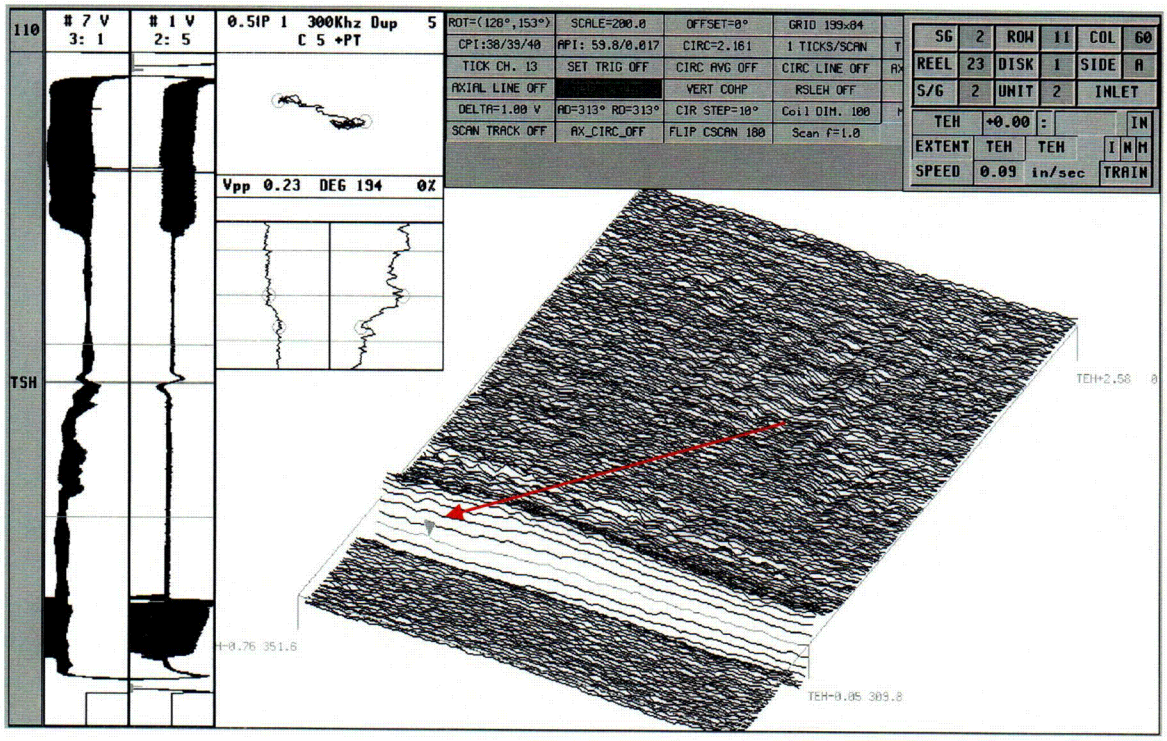

Figure 5-10 Laboratory 300 kHz +Point coil response from the TTS region of R11C60 HL – Piece 2B. +Pt response adjusted so that circumferentially oriented discontinuities are positive. No indication seen. Arrow denotes location of field signal.

C14

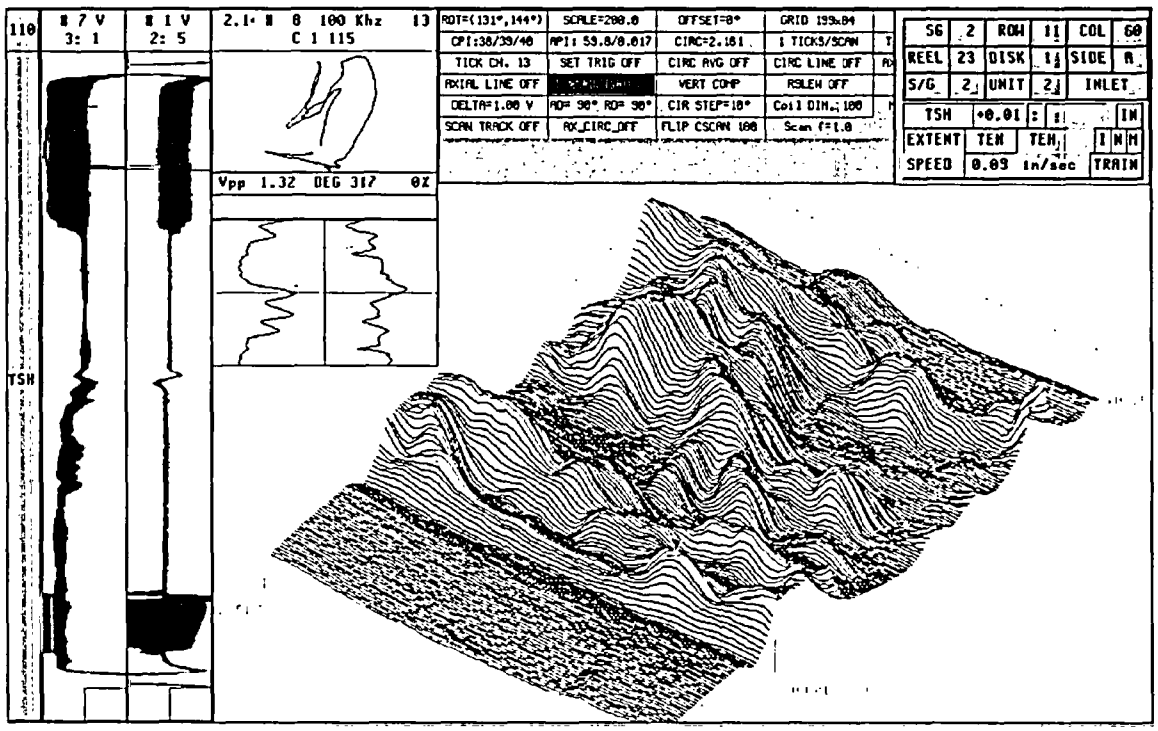

Figure 5-11 Laboratory 100 kHz Pancake coil response from the TTS region of R11C60 HL - Piece 2B. Signal response indicative of OD deposits. Pancake response adjusted so that circumferentially oriented discontinuities are positive.

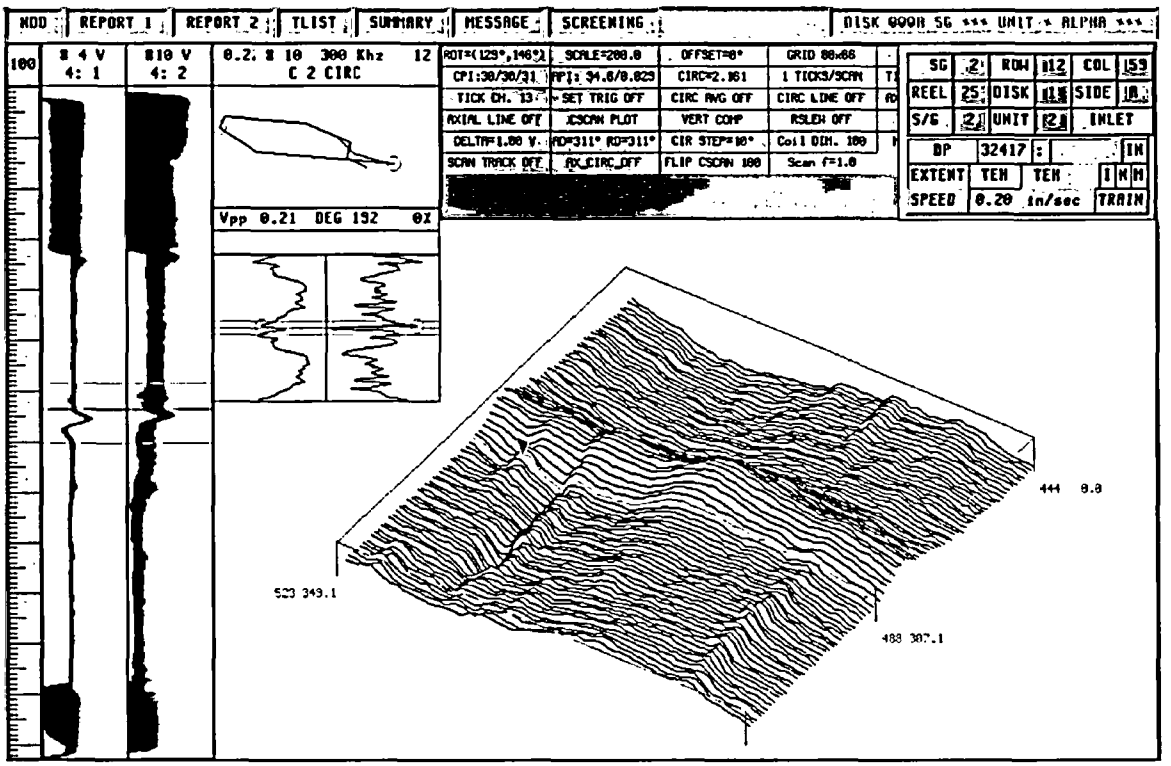

Figure 5-12 Laboratory 300 kHz Ghent probe response for the circumferentially sensitive coil configuration from the TTS region of R12C59 HL – Piece 2B. No indications noted.

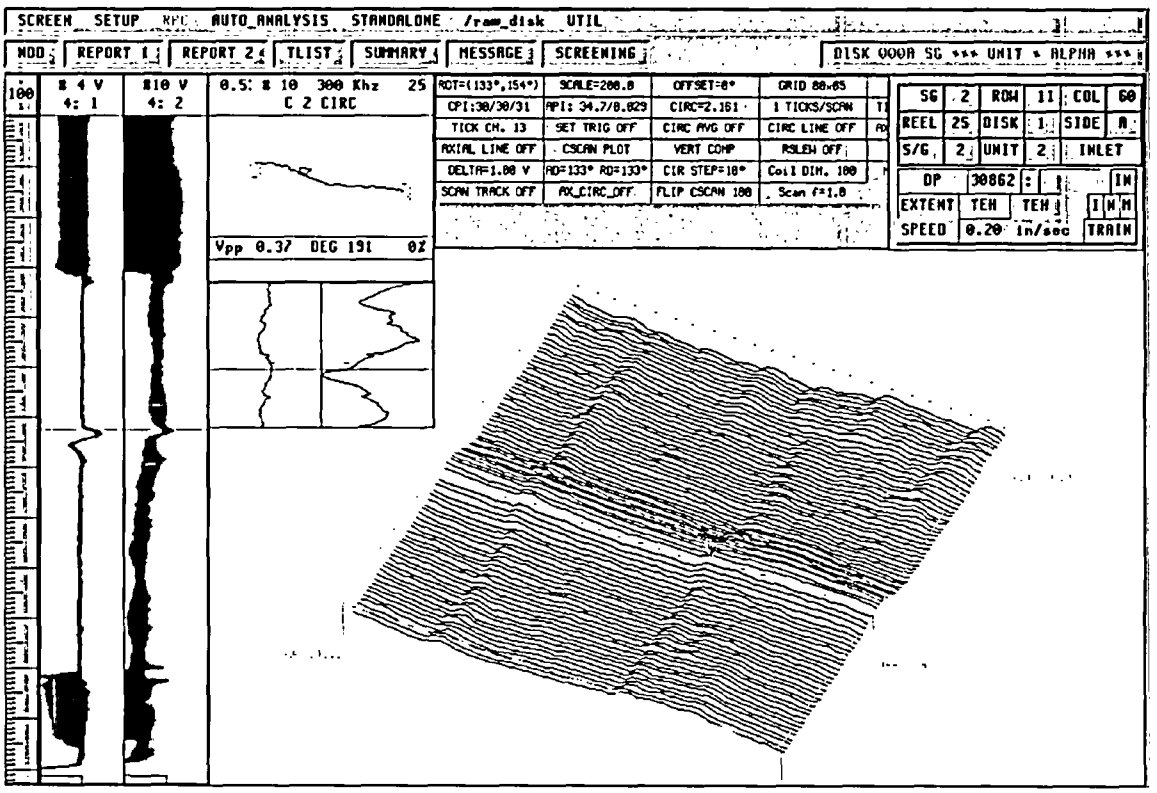

Figure 5-13 Laboratory 300 kHz Ghent probe response for the circumferentially sensitive coil configuration from the TTS region of R11C60 HL – Piece 2B. No indications noted.

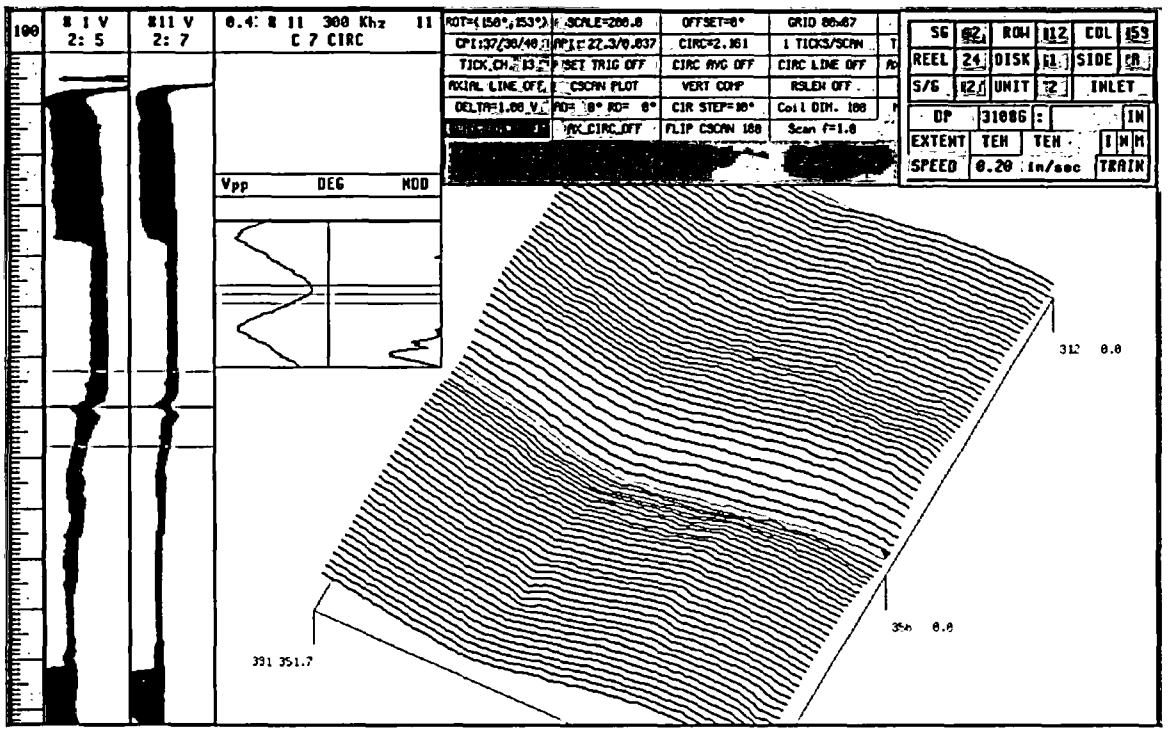

Figure 5-14 Laboratory 300 kHz 3 Coil probe response for the circumferentially sensitive coil configuration from the TTS region of R12C59 HL – Piece 2B. No indications noted.

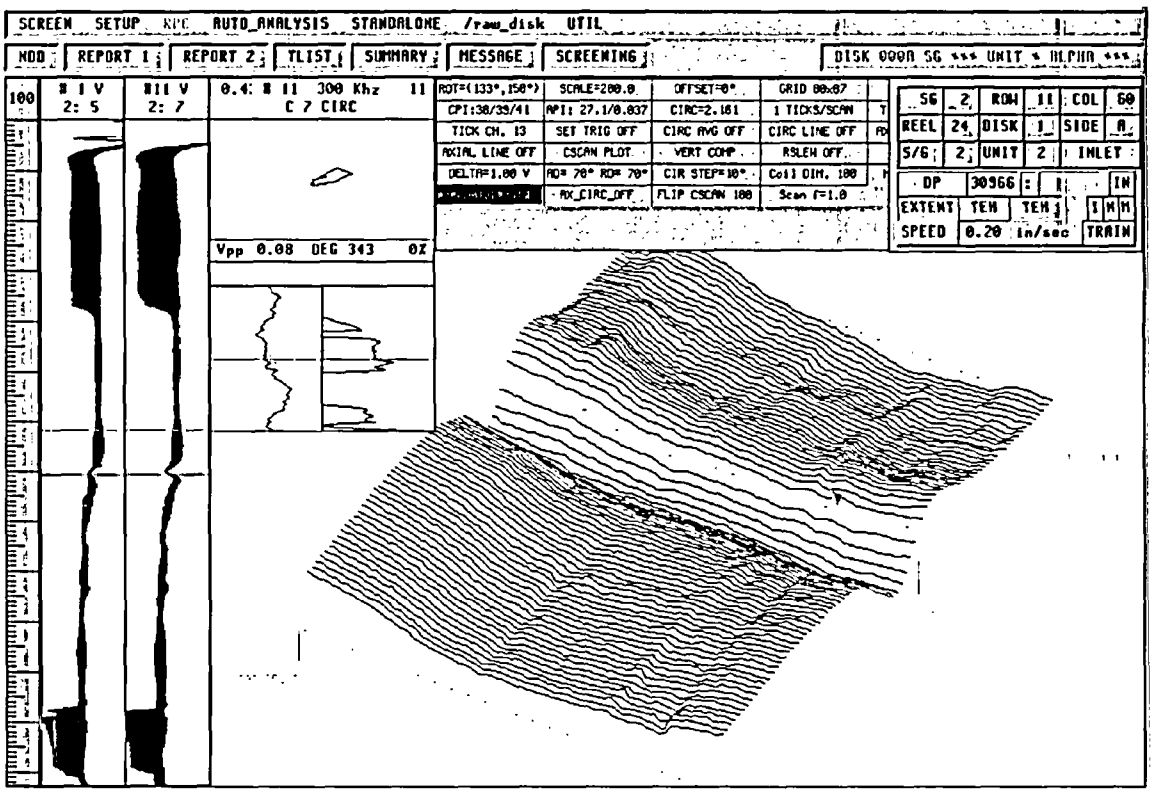

Figure 5-15 Laboratory 300 kHz 3 Coil probe response for the circumferentially sensitive coil configuration from the TTS region of R11C60 HL – Piece 2B. No indications were noted.

SECTION 6

ULTRASONIC (SHEAR WAVE) INSPECTION

6.1 Scope of Ultrasonic Inspections and Description of Techniques

After eddy current inspections two tasks were defined for the ultrasonic inspections:

- Review and reevaluation of field data for R12C59 HL and R11C60 HL
- Acquisition and analysis of ultrasonic data from the TTS regions of both tubes using a shear wave mode

The top of tubesheet region of both pulled tubes were examined with a rotating multiple-element style ultrasonic probe under hot cell conditions. The probe and calibration standard used to establish system sensitivity were the same as that used to perform the ultrasonic inspection in the field. The probe has three individual focused transducer elements mounted in a single probe body. The first transducer is a high frequency, spherical focused element that directs sound in the radial direction. This transducer is used for attenuation measurements and to detect thickness changes characteristic of pitting or wear damage. The second transducer is a spherically-focused search unit that directs sound around the circumference of the tube and is sensitive to radial-axial oriented discontinuities. The third transducer is spherically focused and directs sound energy along the tube axis at a 45° angle. This search unit is particularly sensitive to flaws oriented in a radial-circumferential direction. The ultrasonic transducers are interfaced to field style ultrasonic instrumentation. A Paragon (Wesdyne) ultrasonic/eddy current data acquisition system was used to collect the data. The ultrasonic portion of this system utilizes a R/D Tech 8-channel pulser-receiver and the eddy current instrument is a R/D Tech TC 6700. Based upon the encoder output from the positioning system, data were collected at 1-degree intervals around the circumference. The system is capable of acquiring either the ultrasonic RF or rectified RF data. For this inspection only the rectified data were acquired.

The hot cell probe delivery system consists of a mechanism to grip the UTEC probe to hold it in a fixed position. The tube sections were then mounted in a rotary table attached to a motor-driven lead screw. The rotation of the lead screw is monitored by a rotary encoder to provide axial position information of the tube section. The rotary table contains a motor and an encoder to give the azimuthal orientation of the tube section. The delivery

system is interfaced to a computer which is used to control the tube location. The tube is moved rotationally and axially in a controlled manner to produce a helical motion with a pitch of 0.004 inches with respect to the UTEC probe. The computer provides trigger pulses to the PARAGON data acquisition system so that the PARAGON acquisition software gathers UT and EC information every one-degree and 2 degrees respectively around the tube circumference. A rotational speed of about 20 revolutions per minute is used during the examination. Once the data is captured, it is graphically displayed showing angular position, axial position and signal amplitude. Data from each transducer element is displayed separately for evaluation. The PARAGON system allows the data to be displayed in a variety of formats. To enhance signal interpretation, color plots of where the signal amplitude determines the different colors are used in the analysis. The data is displayed showing axial and angular positions as well as signal strength for all indications.

A single reference tube standard was used to calibrate the UT system. The reference tube (UE-001-96) was used to calibrate the sytem in the field. This standard is used for setting the system sensitivity and the transducer offset, respectively.

In the UT analysis, a pseudo-color "C scan" plot of the data from each ultrasonic channel is presented on the computer screen and reviewed. In the discussions for the ultrasonic results that follow the data for the appropriate ultrasonic and/or eddy current channels are presented in the figures. As an example of the type of displays that are available for the three ultrasonic and eddy current channels are found in Figure 6-1. The displayed in this figure is for the calibration standard. Ultrasonic indications that are known to be from scratches as a result of the tube pull or loose debris are identified as spurious and may be identified in the graphic presentation. Ultrasonic indications believed to be relevant are further evaluated. The entire scan width represents 360° (the circumference unwrapped) while the spacing between scan lines represents pitch (axial) travel. The rotational pitch of the probe used during the examination was 0.004 inch.

Signals detected with the radial aim search unit (Channel 1) are measured for angular extent (ratio of the measured UT signal length to the measured length of a 360° scan multiplied by 360°). The axial UT length is obtained by counting the scan lines and multiplying by the inspection pitch. These functions are performed automatically by the PARAGON software. Data interpretation and flaw characterization is accomplished by reviewing the displays of each transducer. The displays are compared and conclusions drawn concerning the characteristics of the discontinuity detected. By which transducer a discontinuity is detected has a significant implication related to the orientation of the

discontinuity. The radial-aim search unit is designed to be sensitive to planar discontinuities such as wastage and pitting. Experience has shown that this search unit can also detect IGA (intergranular attack) and, in rare instances, measure the radial depth of cracks. The circumferential-aim search unit is sensitive to radial-axial discontinuities such as OD stress corrosion cracks and can be used to measure the axial extent of a wastage edge. The axial-aim is excellent for the detection of OD radial-circumferential cracking and can be used to measure the circumferential extent of a wastage edge.

6.2 Ultrasonic Inspection Data Evaluation - Field and Laboratory

For the field inspection, the UTEC probe was inserted into the tube from the tube sheet, while for the hot cell inspections, the probe was inserted from both ends of the tube. Table 5-1 in Section 5 presents a summary of key UT observations for the Vogtle tubing. The areas of interest were the TTS of R12C59 HL and R11C60 HL. Review of the field ultrasonic data from R12C59 HL and R11C60 HL confirmed possible tubing discontinuities, however, no such indications were found in the laboratory. The results of ultrasonic inspection data of the TTS region of both pulled tube will be discussed in the following paragraphs.

R12C59 HL – Piece 2B at TTS

During the laboratory UTEC inspection of R12C59 – Piece 2B at the TTS region, the ultrasonic data displayed numerous responses originating from both inside and outside of the tube. Figure 6-2 shows a display of the ultrasonic response from the 2B section in the laboratory and Figure 6-3 shows the field inspection results. The pattern of OD responses believed to originate from adherent deposits is quite similar between the two inspections. However, the field responses shown in Figure 6-3 that had been interpreted as originating from a discontinuity in the tube wall are absent from the Figure 6-2 data obtained in the laboratory. In Section 8 the deposit responses are used to identify the azimuthal location of the field UT indications.

R11C60 HL - Piece 2B at TTS

During the laboratory UTEC inspection of R12C59 – Piece 2B at the TTS region, the ultrasonic data displayed numerous responses originating from both inside and outside of the tube. Figure 6-4 shows a display of the ultrasonic response from the 2B section in the laboratory and Figure 6-5 shows the field inspection results. The pattern of OD responses

believed to originate from adherent deposits is quite similar between the two inspections although more is missing in the laboratory examination than was observed in the field. The response shown in Figure 6-4 does occur at the location where the Figure 6-5 field response had been interpreted as originating from a tube wall discontinuity. However the laboratory response is interpretable as originating from OD deposits rather than in the tube wall discontinuity. A discussion of the how the OD deposit response was used to identify the azimuthal location of the field UT indications is provided in Section 8 of this report.

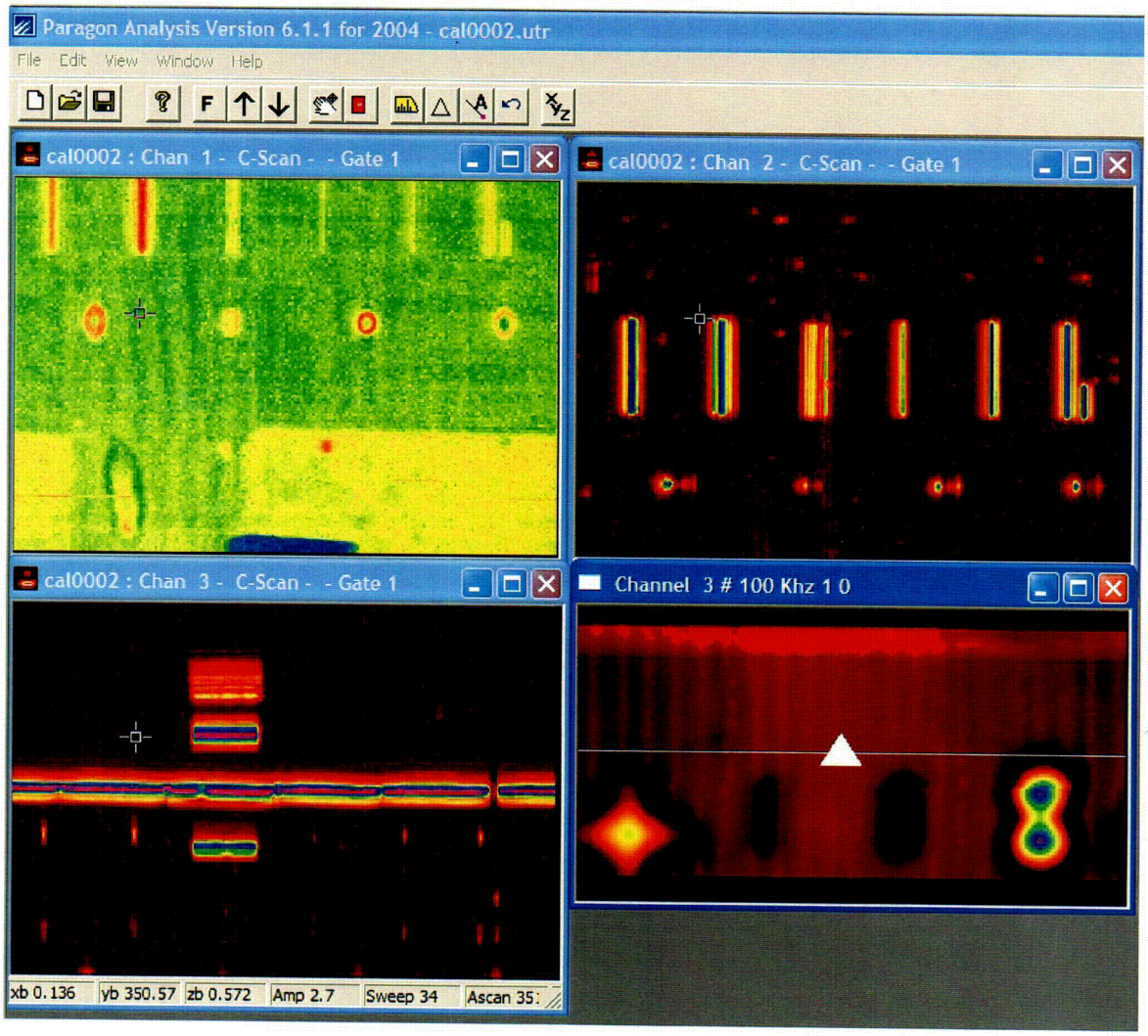

Figure 6-1 UTEC response to calibration standard UE-001-96. C-Scans are shown for all ultrasonic transducers and also the 100 kHz pancake eddy current coil.

C15

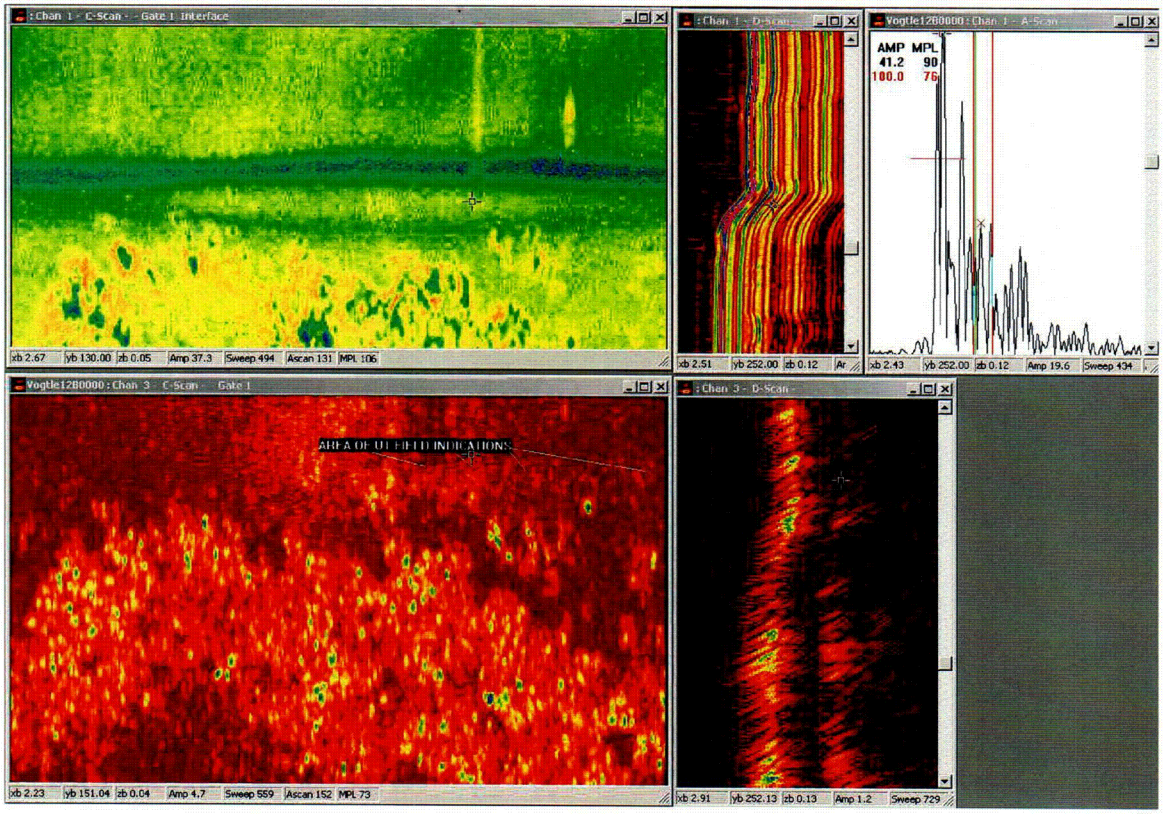

Figure 6-2 Laboratory UTEC ultrasonic results for the TTS of R12C59 HL – Piece 2B. Note the presence of the deposits on the tube OD are the prominent feature of the inspection.

C16

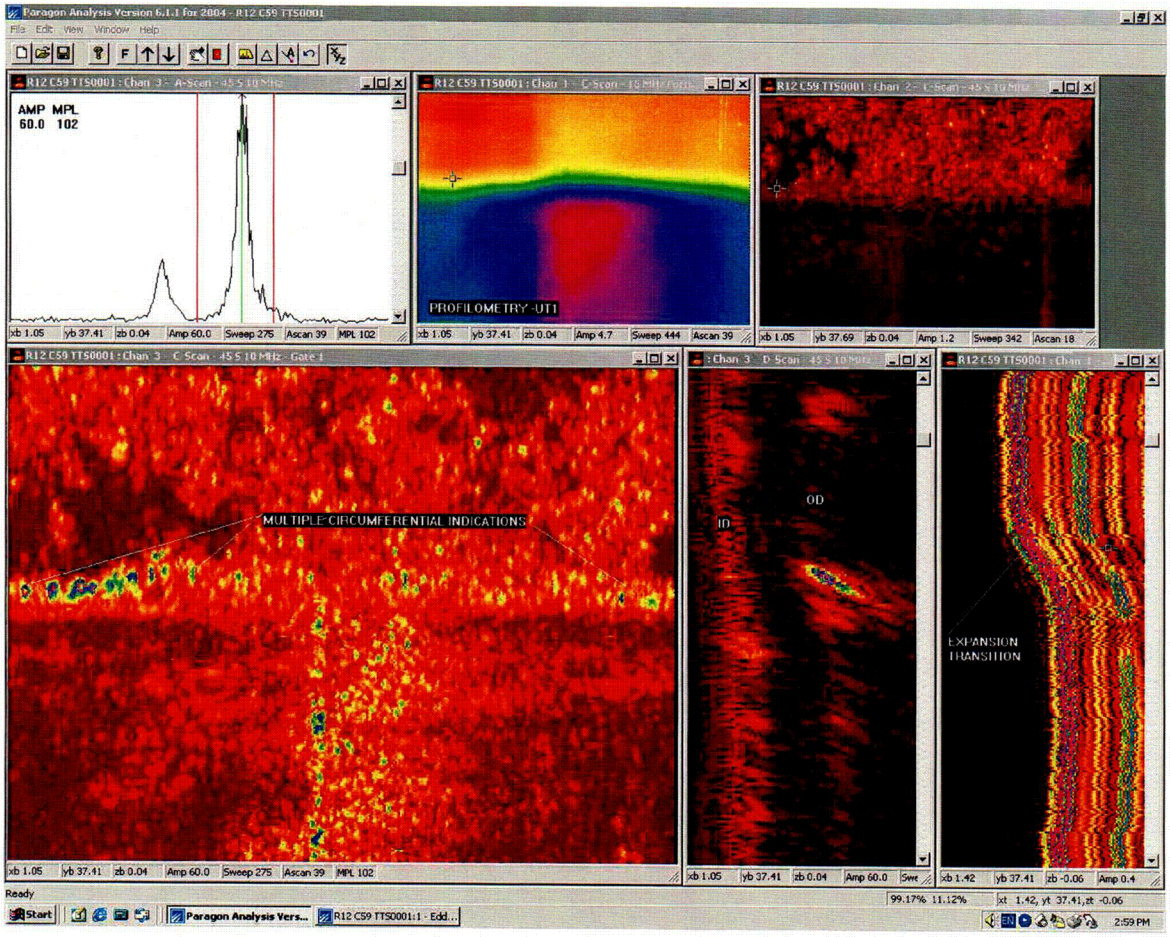

Figure 6-3 UTEC result from the field examination of the TTS region of R12C59. The locations of the indications are identified in the C-Scan.

Note that the images are inverted with respect to Figure 6-2 the overall pattern of the deposit response strongly correlates with that of Figure 6-2.

C17

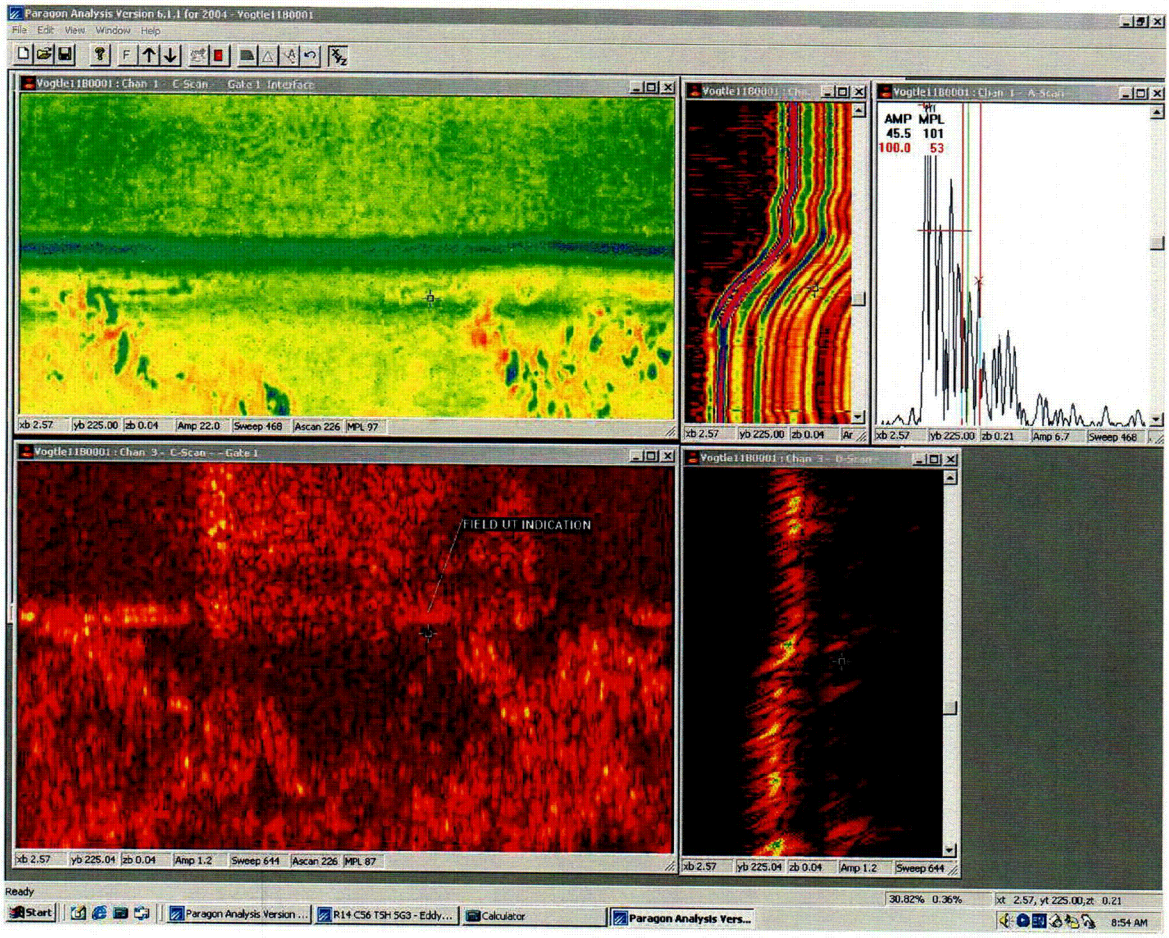

Figure 6-4 UTEC laboratory ultrasonic results for the TTS of R11C60 HL – Piece 2B. Note the presence of the deposits on the tube OD are the prominent feature of the inspection.

C18

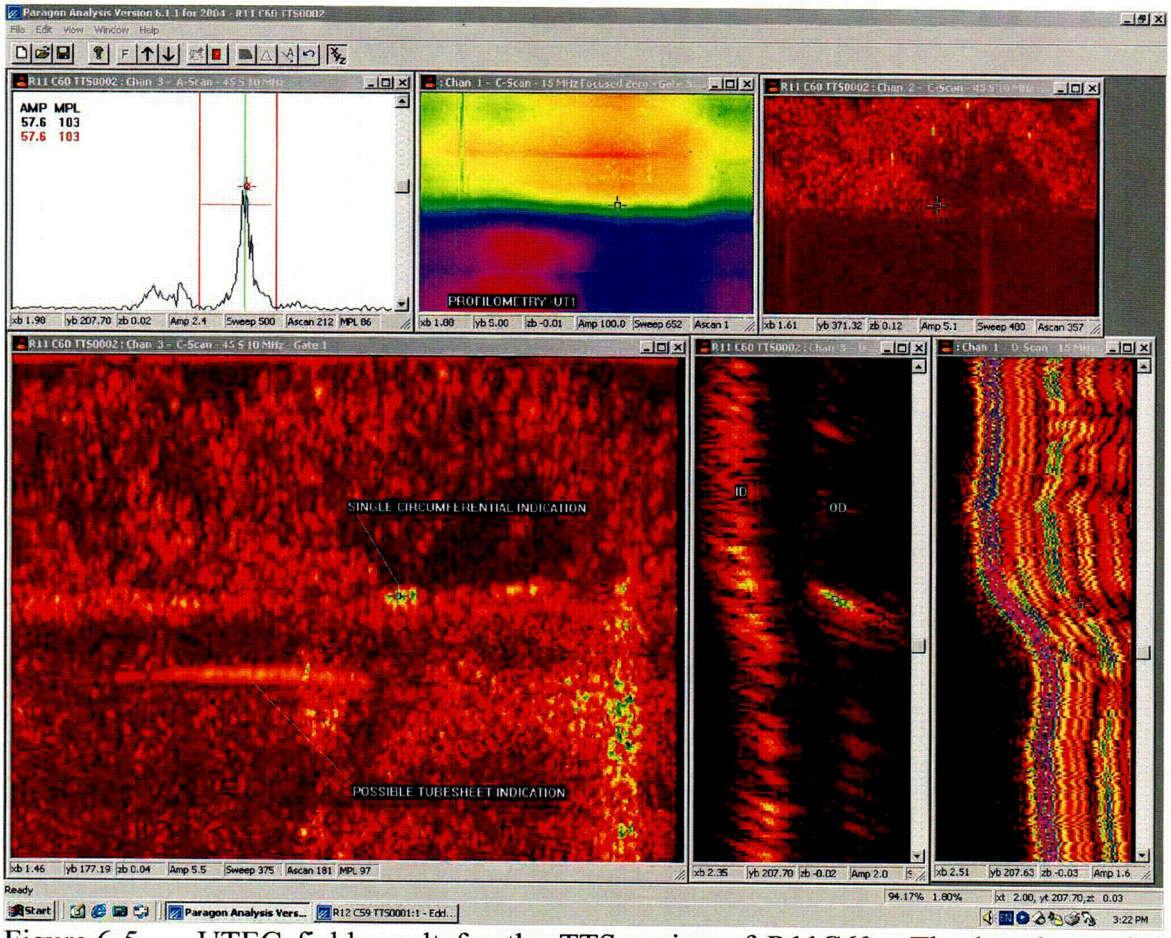

Figure 6-5 UTEC field result for the TTS region of R11C60. The locations of the indications are identified in the C-Scan.

Note that while the images are inverted with respect to Figure 6-4 the overall pattern of the deposit response strongly correlates with the deposit signals seen in Figure 6-4.

C19

SECTION 7

POST PRESSURIZATION EDDY CURRENT DATA

7.0 Results

As part of the destructive examination efforts of the pulled tube examination, Piece 2B and Piece 3B of Tube R12C59 HL were pressurized to approximately 9000 psi. During prior pulled tube examination efforts, ID pressurization has been employed to enhance the detection of tube degradation. It was anticipated that pressurization of the ID would result in sufficient tube expansion to cause adherent deposits to "spall-off" and / or the "opening-up" of any tube degradation. After the pressu rization, the tube sections were visually and eddy current inspected. The eddy current inspection was a repeat of the +Pt probe examination conducted initially. Little deposit "spalling" was observed and no degradation became apparent in either the visual or eddy current examinations. The following discussion is provided.

<u>Post Pressurization Eddy Current Test Data for the TTS Region of Tube R12C59 HL – Piece 2B</u>

The post pressurization eddy current +Pt response of the TTS region identified no indications. Figure 7-1 shows the 100 kHz Pancake Coil response. The deposit response mimicked that observed prior to the pressurization as shown in Figure 7-2. ID pressurization to 9000 PSI did not result in "spalling" or cracking of the OD deposits. Visual and SEM analyses showed no obvious change in the appearance of the TTS deposits.

<u>Post Pressurization Eddy Current Test Data for the TSP2 Region of Tube R12C59 HL - Piece 3B</u>

The post pressurization eddy current +Pt response of the TSP region identified no indications. Figure 7-3 shows the 100 kHz Pancake coil response. The line of deposit on the left side of the image, 10° azimuthal orientation, in Figure 7-3 is less pronounced than the response seen prior to pressurization, Figure 7-4, indicating that this region of the deposit had spalled off the tube during the pressurization. Backscatter Energy Mode montage images at the 10° azimuthal orientation are presented in Figure 7-5 comparing the OD deposit appearance before and after the pressurization effort. Evidence of "spalled" deposit can be seen. Results of the SEM and EDS analyses of both the OD tube surface and ID deposit are presented in Section 10.

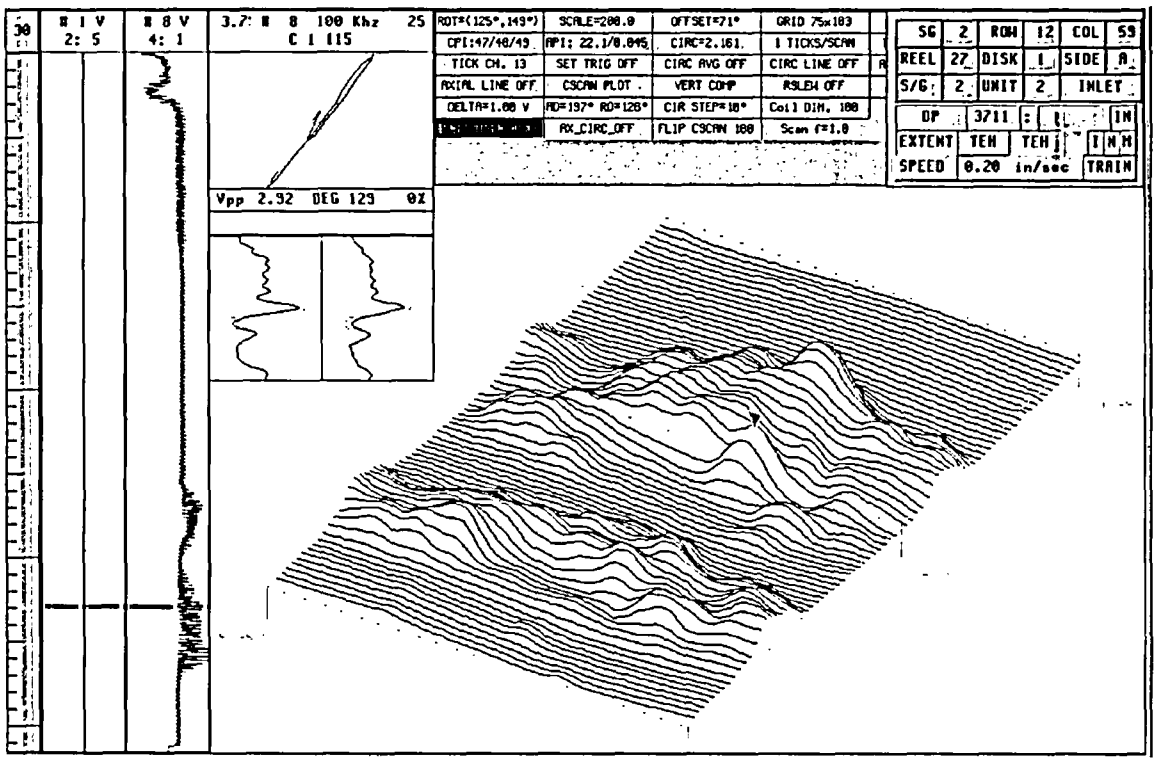

Figure 7-1 Post Pressurization 100 kHz Pancake Coil Eddy Current Response of the TTS Region for R12C59 HL - Piece 2B.

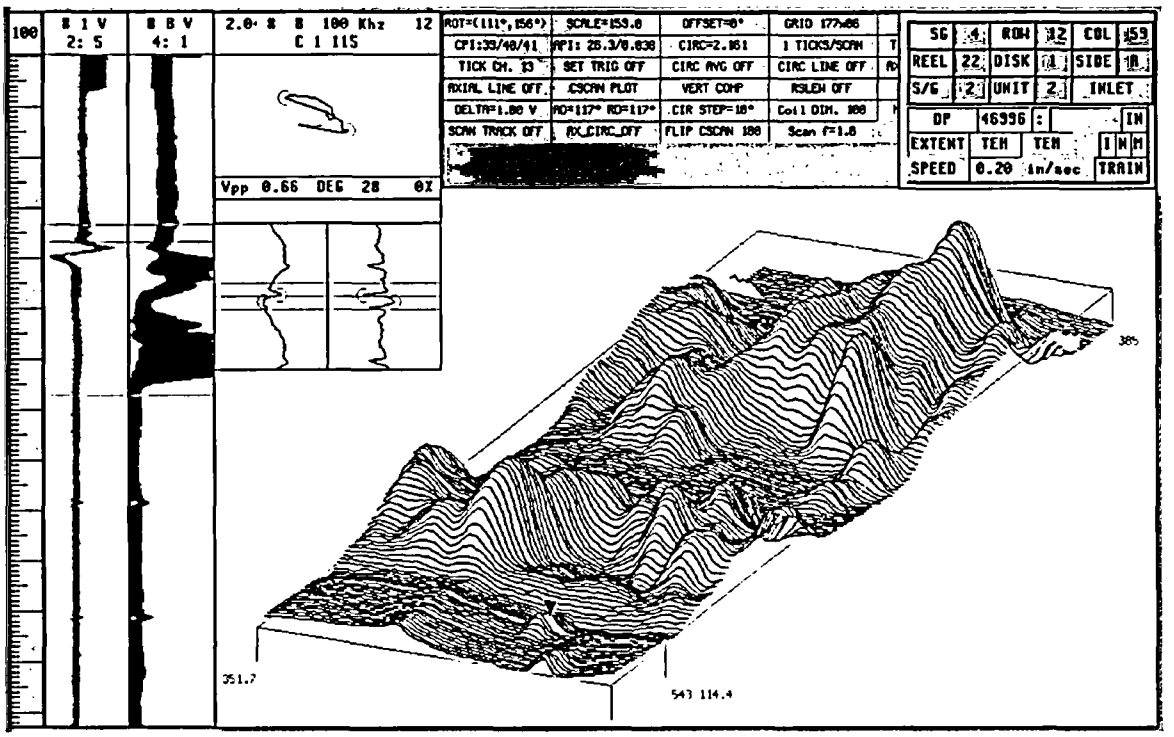

Figure 7-2 Laboratory 100 kHz Pancake Coil Eddy Current Response of the TTS Region of R12C59 HL - Piece 2B Prior to ID Pressurization.

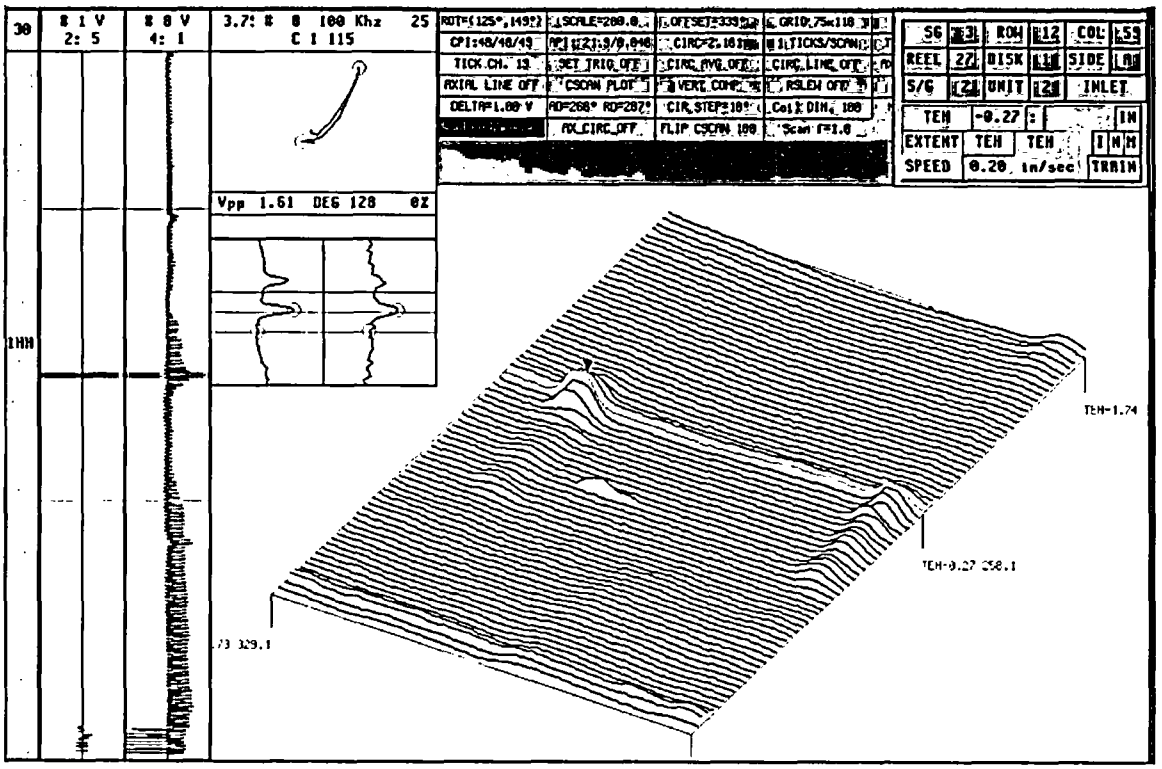

Figure 7-3 Post Pressurization 100 kHz Pancake Coil Eddy Current Response for the TSP1 Region of R12C59 HL – Piece 3B. Note the Deposit Response Seen on the Left Side of the Image is Less Pronounced When Compared to the Response Shown in Figure 7-4. This Response is Indicative of Less Deposit.

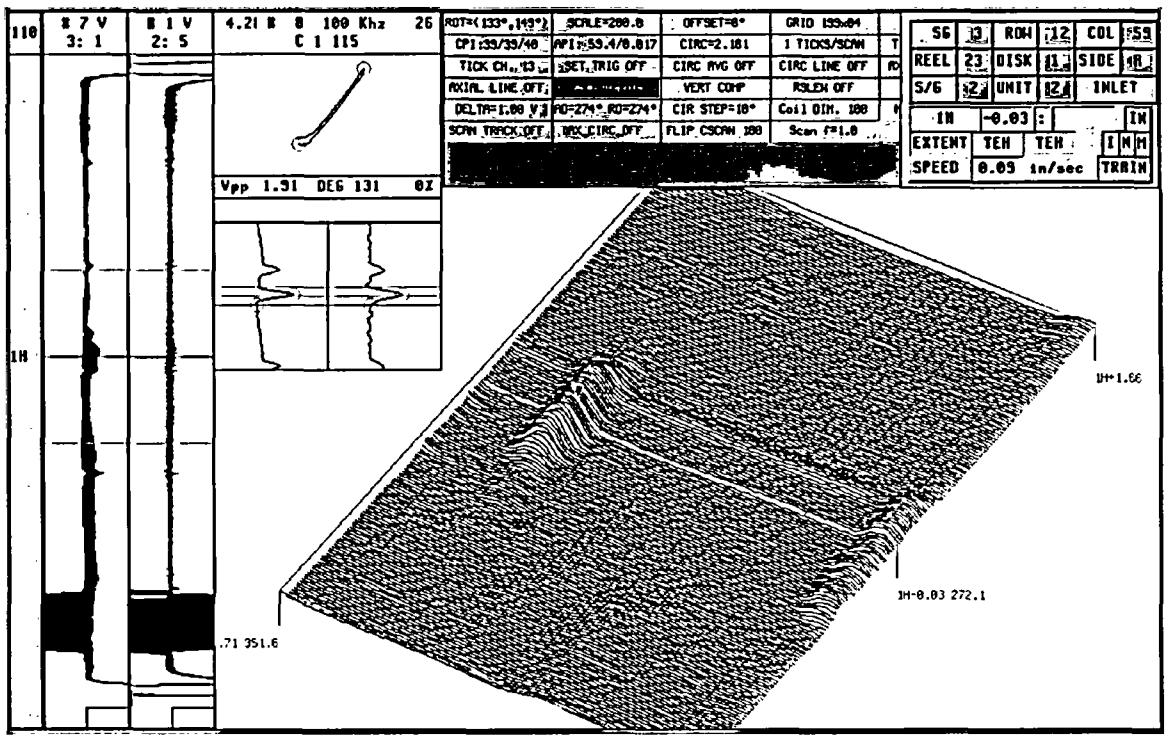

Figure 7-4 Laboratory 100 kHz response from the TSP1 region of R12C59 – Piece 3B prior to ID pressurization. Note the two bands associated with the deposits within the quatrefoils.

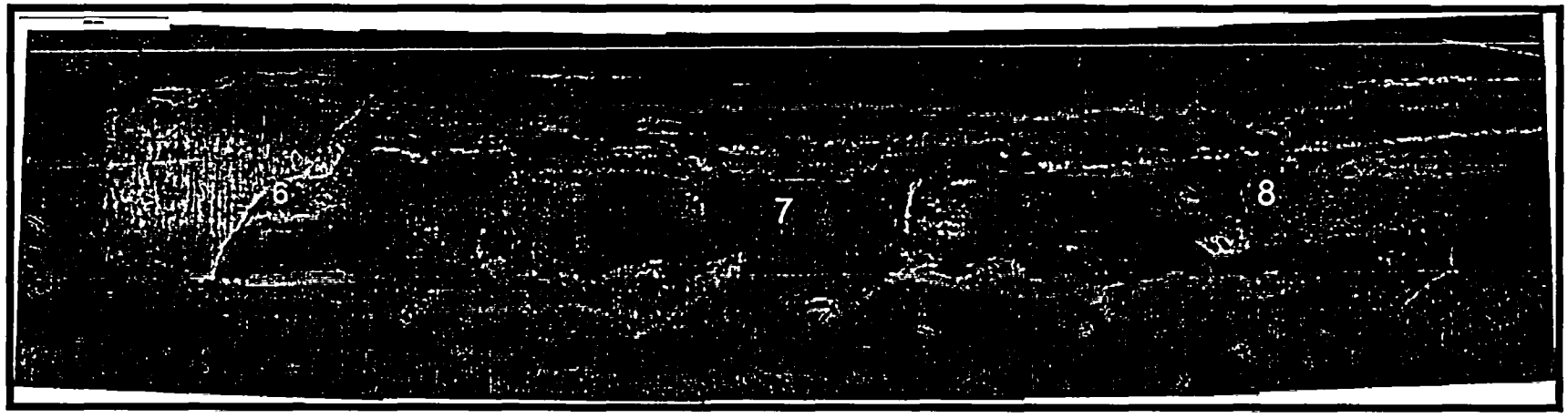

a) OD Deposit Prior to Pressurization

b) OD Deposit Following Pressurization

Figure 7-5 Backscatter Mc Mtage Showin g the Appearance of the OD Deposit at the Qatrefoil Land to Tube Intersection at the 10° Azimuthal Orientation For R12C59 – Piece 3B Before and After ID Pressurization. Note: The Change in Appearance of Deposit. Note: The areas identified as 6, 7, and 8 are regions selected for EDS analyses (Refer to Section 10).

SECTION 8

AZIMUTHAL ORIENTATION OF SIGNALS

One of the key issues associated with the Vogtle 2 pulled tube examination is the physical location of the field +Pt and UT signals. The axial location is easily determined by referencing the indication relative to the expansion transition. The azimuthal location is more difficult. In the laboratory, the metallic strips fastened to the OD of the tube sample serve as fuducial marks in the eddy current data allowing the circumferential position of an indication to be precisely located. The lack of eddy current or ultrasonic response seen during the laboratory efforts when compared to those in the field, presents particular difficulty in identifying the azimuthal location of the underlying discontinuity responsible for the eddy current or ultrasonic response. It was observed that the laboratory 100 kHz pancake coil eddy current response to deposits above the TTS yielded patterns similar to the field inspection results. A detailed comparison of the field and laboratory deposit distributions confirmed that there was sufficient similarity between the patterns that the physical orientation of the field responses could be determined in the laboratory. The location of the field +Pt indication was then carried out by determining the location of the +Pt indication relative to the deposit response found in the 100 kHz pancake coil response, and relating this response to the pattern found in the laboratory and ultimately to its orientation relative to the marks placed on the tube during laboratory NDE inspections.

The investigation began by reviewing the field eddy current data from Reel 169 for both R12C59 HL and R11C60 HL.

8.1 Orientation of TTS Signals in R12C59 HL

Initially the eddy current responses for both the +Pt and 115 mil diameter pancake coil were aligned so that when plotted the azimuthal location of the respective responses in the images corresponded. Figure 8-1 shows an eddy current plot for the 200 kHz +Point coil response for the region above the TTS of R12C59. Note the cursor has been placed on the indication. Figure 8-2 shows the 100 kHz pancake coil response for the same portion of the tube. The cursor is placed at the location where the pancake coil should have responded to the indication. The deposit pattern has a number of features that are potentially useful in locating this position in the laboratory. To begin the deposits occur in two bands one associated with the TTS and another slightly above the TTS. The edges of these bands have unique configurations. Specifically the deposit band at the TTS displays

a local minimum in its height at the location of the +Pt indication. This minimum can then be used to orient both the field UTEC inspection results and the data obtained in laboratory.

Figure 8-3 shows the laboratory 100 kHz pancake coil response for R12C59 section 2B in the laboratory. The cursor has been place at the minimum in the deposit width identified in the field. This orientation corresponds to approximately the 324 degree location.

To obtain the orientation of the UTEC indications, the field and laboratory eddy current data and the UT data for the deposit morphology are compared. Figure 8-4 shows the UTEC eddy current response for the field inspection presented a color C-scan. Further in Figure 8-5 the ultrasonic response to the deposits also identifies the minimum in the deposit width. Coupling theses results suggests that the field ultrasonic indications occurred at an orientation away from the +Pt indication at an azimuthal orientation of between 0 and 90 degrees.

8.2 Orientation of TTS Signals in R11C60 HL

The location of the +Pt indication in R11C60 HL is conducted in a similar fashion. The field data were reviewed for both the +Pt and 100 kHz pancake coil response (Figures 8-6 and 8-7 respectively). Features in the deposit response were then chosen to correlate with the laboratory and UTEC inspection results. The deposit pattern of R11C60 is qualitatively similar to that of R12C59 in that there are two bands of deposits at and above the TTS. For R11C60 there is an isolated deposit response in the space between the bands. This response occurs at almost the same azimuthal location as the +Pt indication and is easily recognized in the laboratory and UTEC data (Figures 8-8 and 8-9 respectively). The +Pt indication is then estimated to be located at an azimuthal orientation of 327 degrees. The ultrasonic response Figure 8-10 shows that the indication is not coincident with the +Pt indication but rather is at an orientation of 130 degrees.

8.3 Conclusion

A pictorial representation showing the orientation of the field +Pt and UT signals based on the results discussed above is presented in Figure 8-11. As discussed earlier, during the field tube pulling effort, a notch is based on each pulled section at the orientation corresponding to the divider plate. This orientation becomes the 0° orientation during the laboratory evaluation and is consistently maintained. As shown previously in Section 3,

and also in Figure 8-11, the 90° et al. are expressed clockwise of 0° when looking in the direction of the primary flow. As shown in this figure, both +Pt signals are located approximately at the same azimuthal orientation, i.e., 324° / 327° and are oriented towards the open columns. The UT signals are rotated 90° to 150° from the location of the +Pt signal. Although, once again, it appears that the azimuthal orientation of the UT signal corresponds to the open column between tubes.

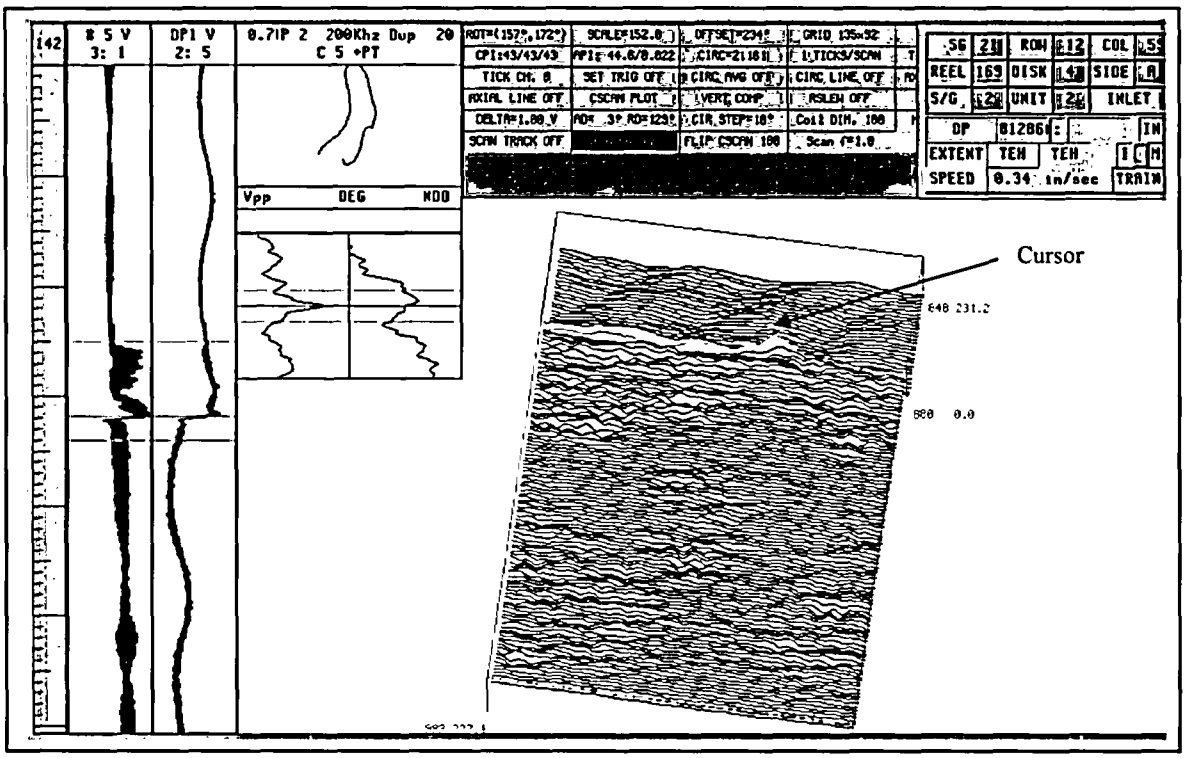

Figure 8-1 C –scan showing location of the field +Pt indication at the TTS in R12C59 HL. The cursor is located at the position of the reported field indication.

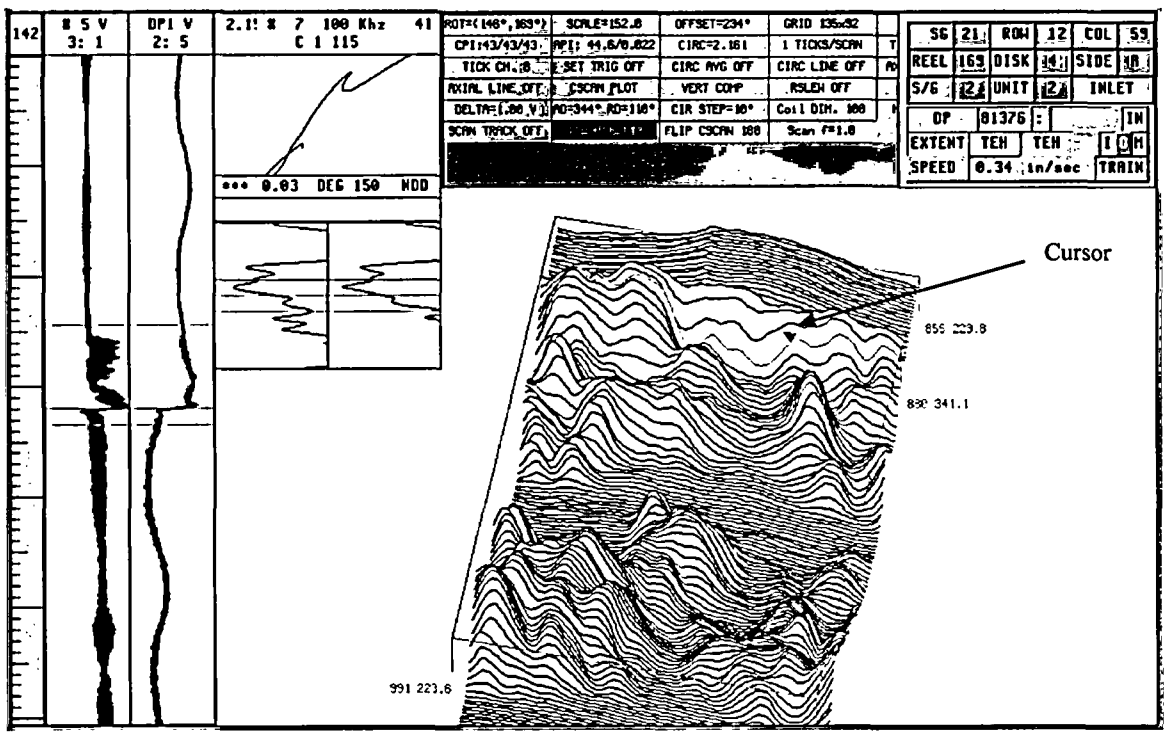

Figure 8-2 The field 100 kHz pancake coil response at the TTS of R12C59 HL with the coil display aligned with that of the +Pt (Figure 8-1). The cursor is located at the position of the +Pt indication. This location corresponds to the minimum in the width of the deposit band at the TTS.

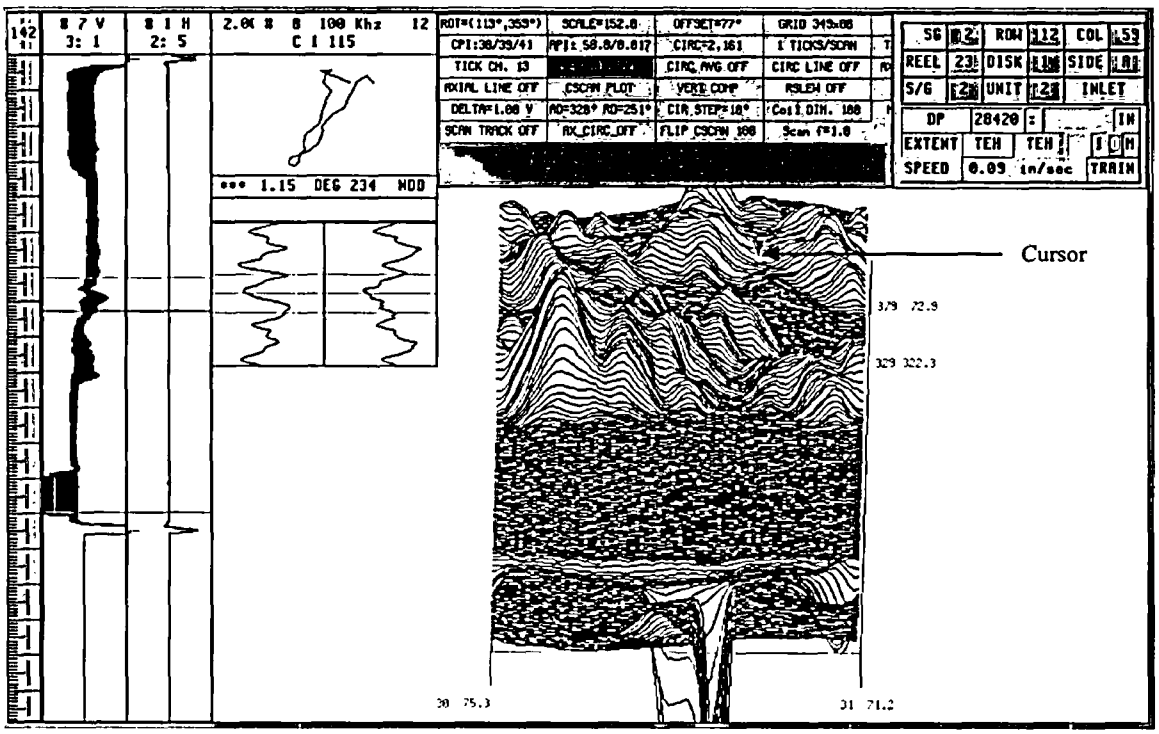

Figure 8-3 Laboratory 100 kHz pancake coil response of the TTS region of R12C59 HL – Piece B showing both the deposit pattern and the response of the metal foil. The cursor is placed at the approximate location of the minimum in the deposit width.

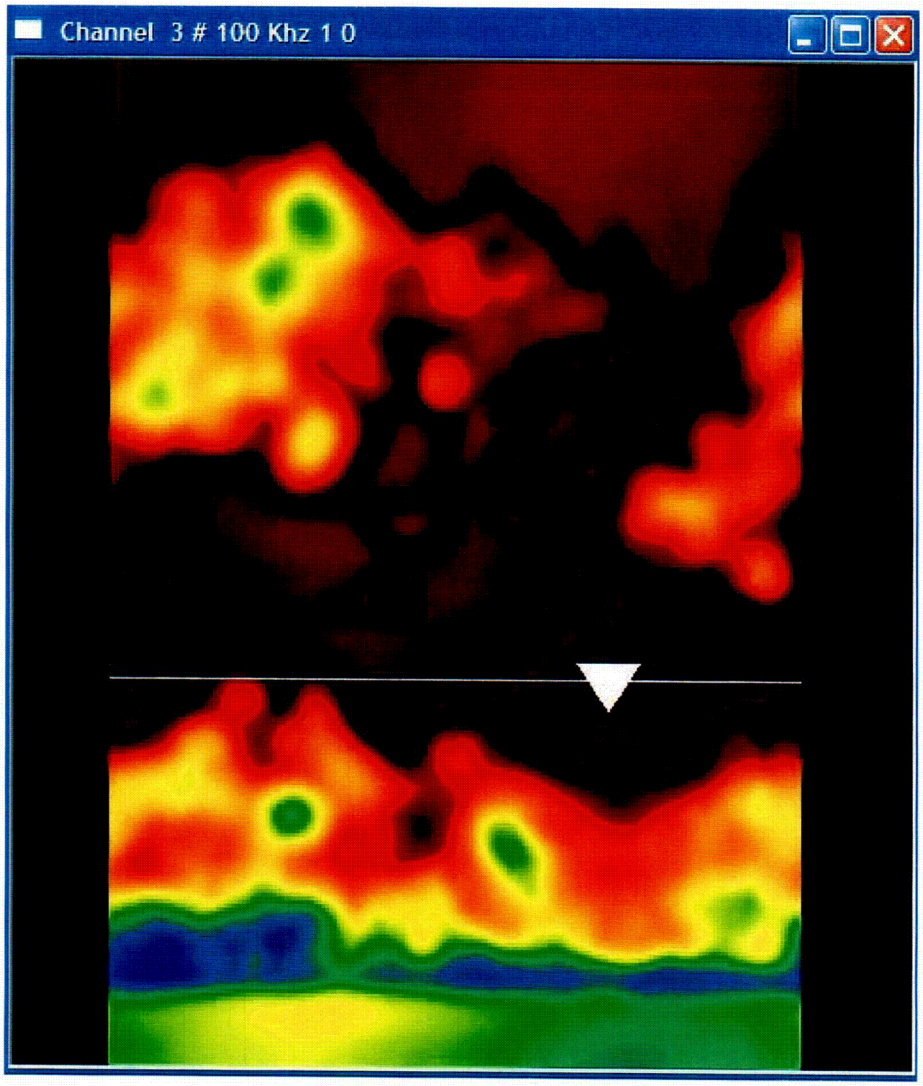

Figure 8-4 Field 100 kHz response of the UTEC the pancake probe near the TTS of R12C59 HL plotted as a color C-san. The cursor indicates the approximate location of the minimum in the deposit width.

C20

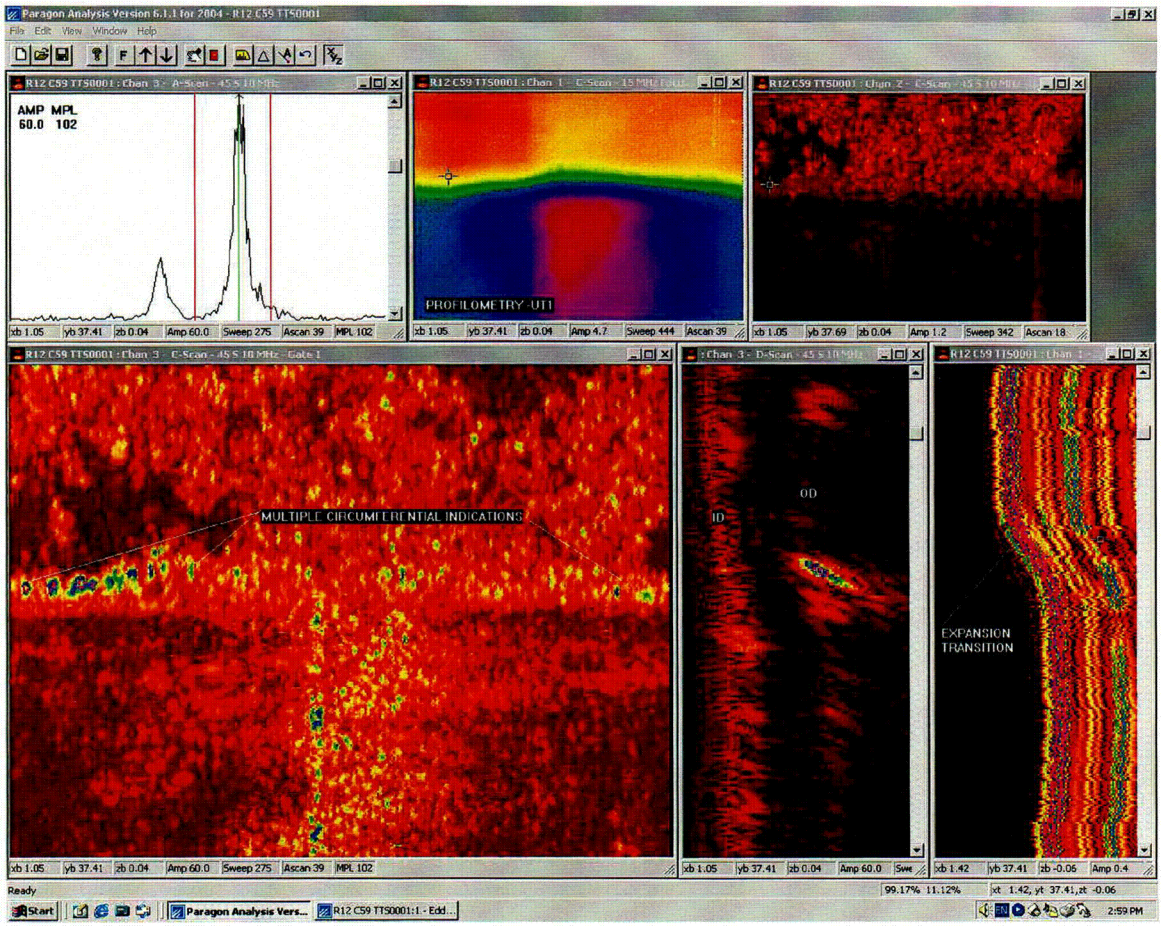

Figure 8-5 UTEC field result for the TTS region of R12C59 HL. Note the locations of the indications are identified in the C-Scan. Note also the lack of deposit response in the upper right region of the C-scan which corresponds to the minimum width highlighted in Figure 8-4. Since the minimum width location corresponds to the field +Pt indication, the UT indications are not coincident.

CZ1

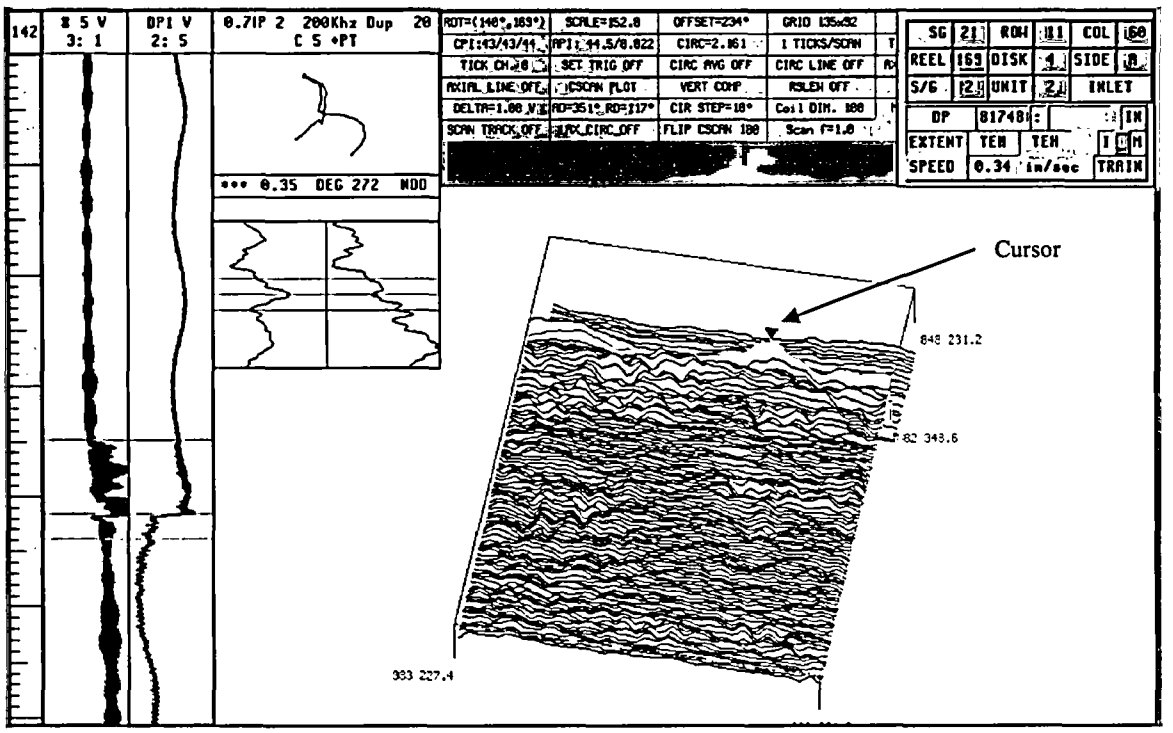

Figure 8-6 Location of the field +Pt indication reported at the TTS in R11C60 HL. The cursor is located at the position of the reported field indication.

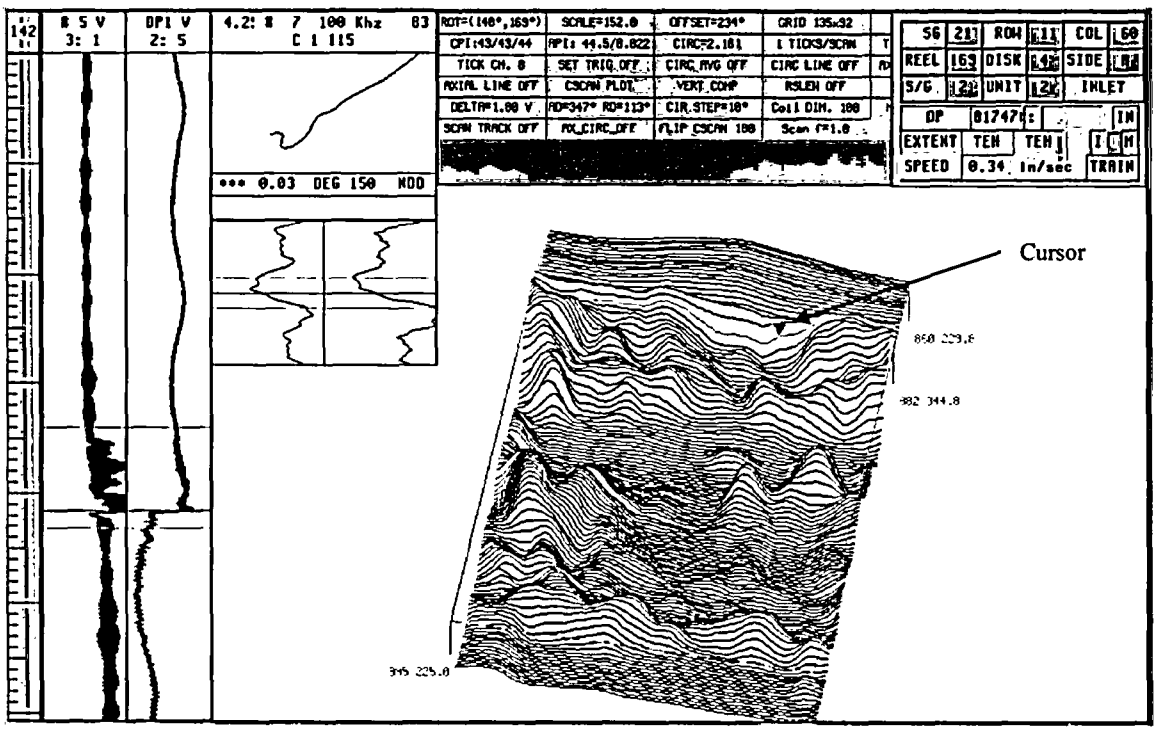

Figure 8-7 The field 100 kHz pancake coil response at the TTS of R11C60 HL with the coil display aligned with that of the +Pt (Figure 8-6). The cursor is located at the position of the +Pt indication. This location corresponds to the isolated response between the deposit bands above the TTS.

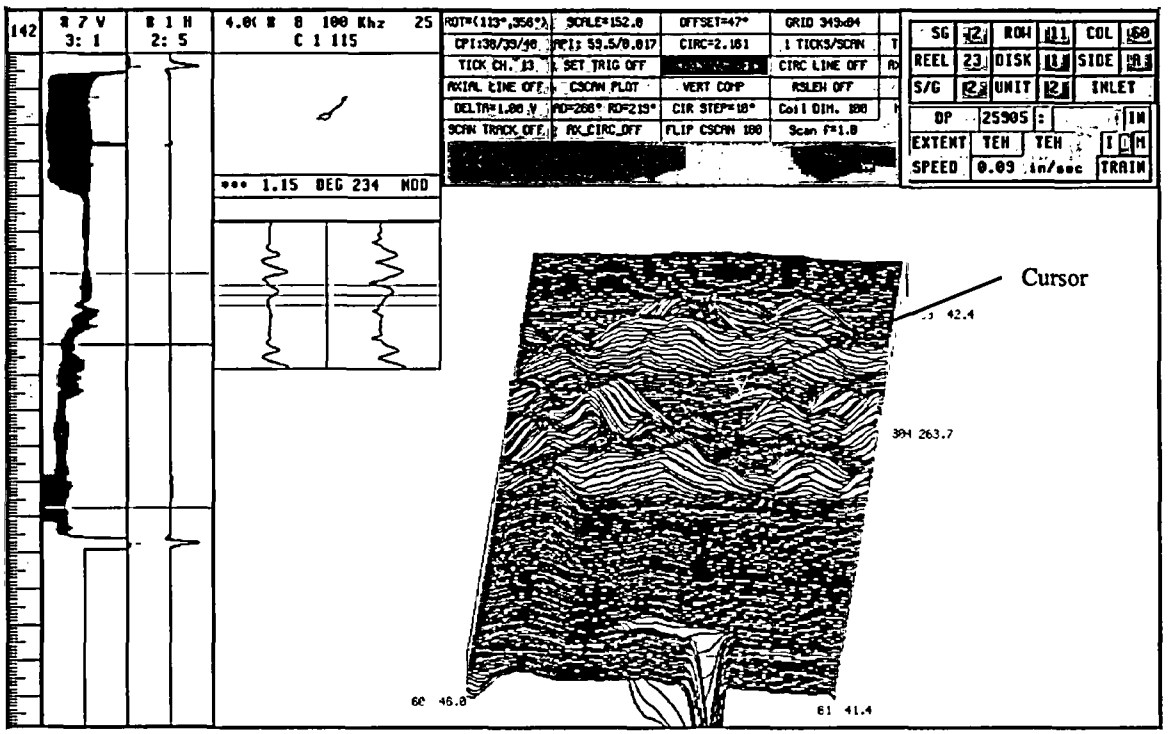

Figure 8-8 Laboratory 100 kHz pancake coil response of the TTS region of R11C60 HL – Piece 2B showing both the deposit pattern and the response of the metal foil. The cursor is placed at the approximate location of the isolated response between the deposit bands.

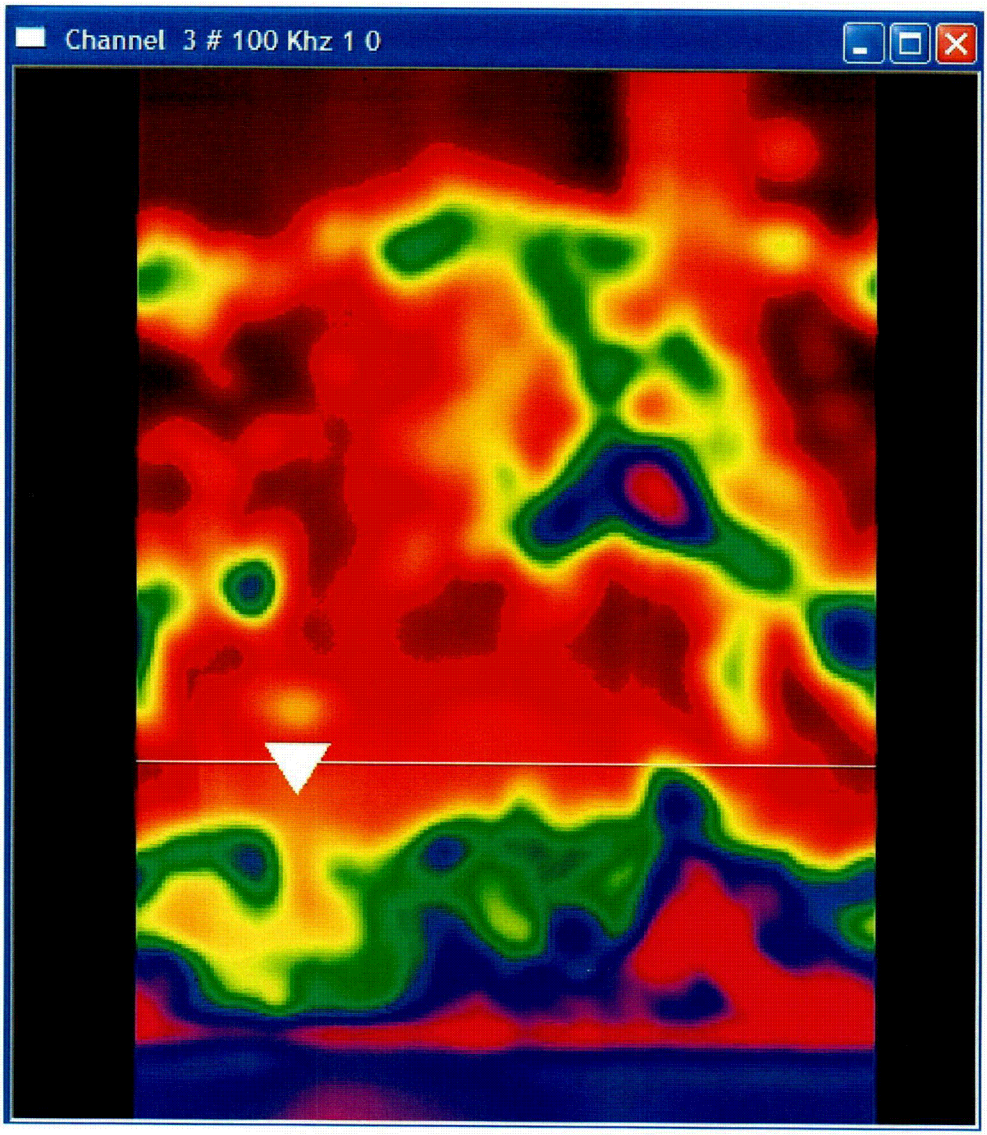

Figure 8-9 Field 100 kHz response of the pancake coil on the UTEC probe plotted as a color C-scan plot for R11C60 HL. The cursor indicates the approximate azimuthal location of the isolated response between deposit bands.

C22

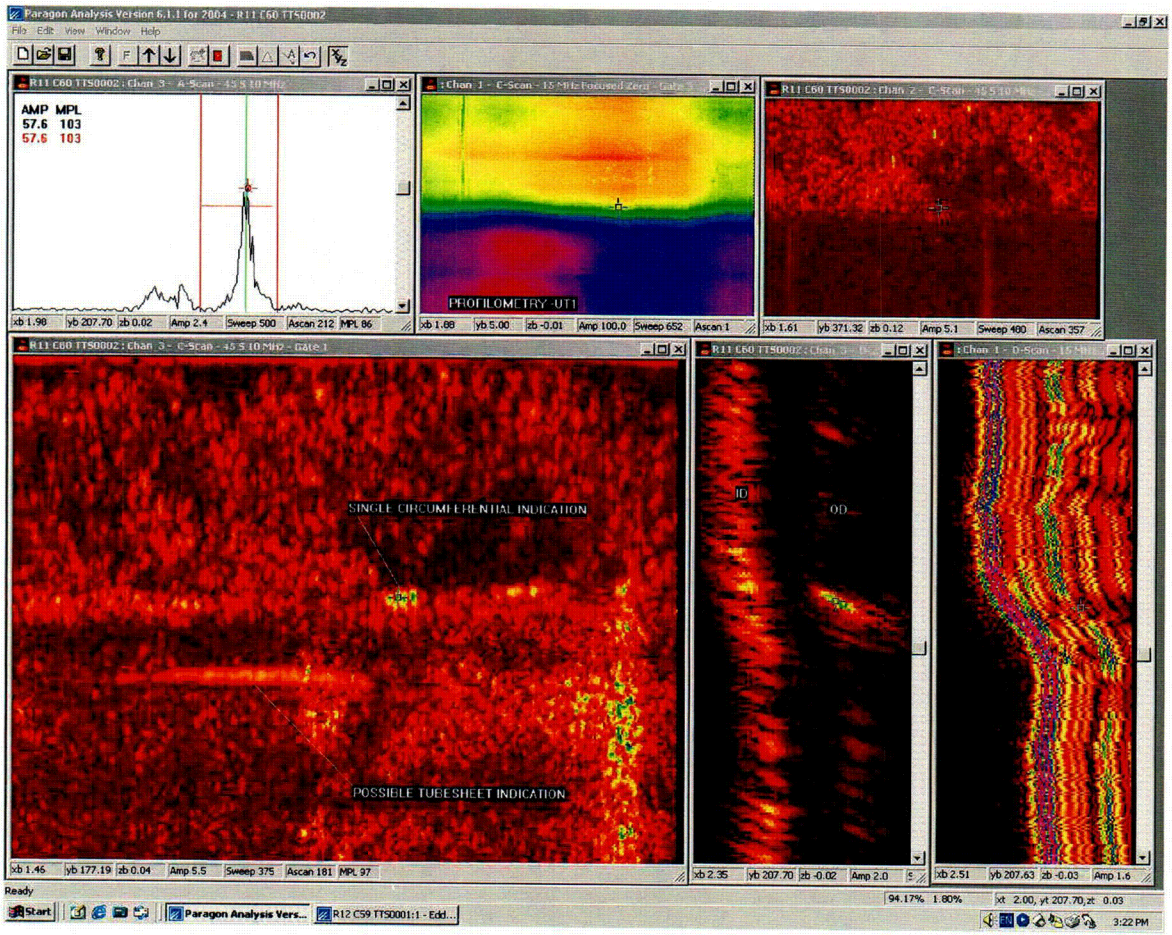

Figure 8-10 UTEC field result for the TTS region of R11C60 HL. Note the locations of the indications are identified in the C-Scan. Since the isolated indication of Figure 8-9 corresponds to the field +Pt indication, the UT indications are not coincident.

C23

Figure 8-11 Pictorial Representation of the Azimuthal Orientation of the Field +Pt and UT Signals. As Discussed in Section 8, the Azimuthal Orientations of the Signals Were Based on the Topography of the OD Deposit. The Location of the +Pt Signals are Shown in Red. The UT Signals are Shown in Green.

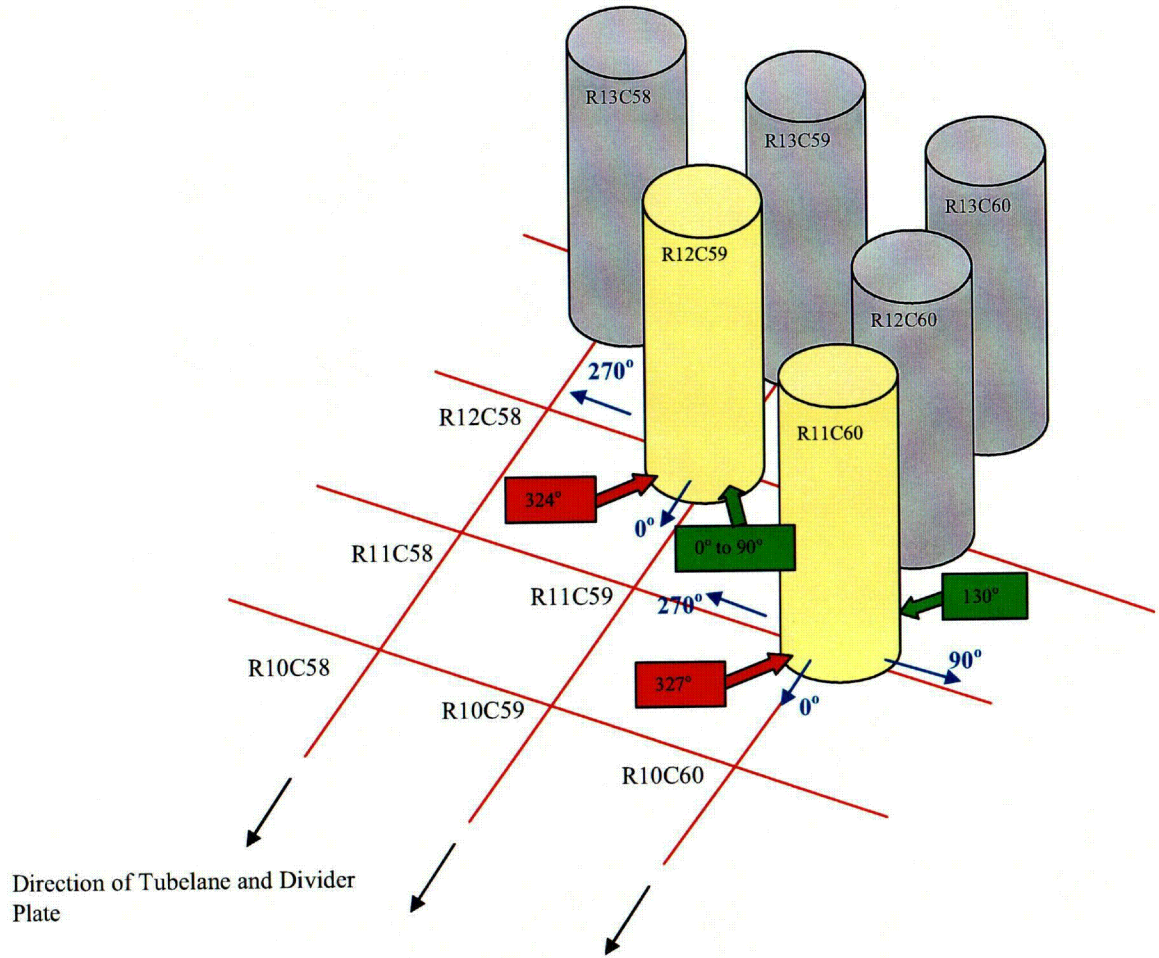

C24

SECTION 9

LAMB WAVE MODE ULTRASONIC EXAMINATION

9.0 Introduction

The lack of degradation and NDE responses experienced during the laboratory examinations in the vicinity of where both ultrasonic and eddy current inspection yielded field indications gave impetus to identifying options for discriminating indications of the type found with those of true degradation. The assumption is that since both the eddy current and ultrasonic indications disappeared after the tube was removed from the steam generator, the reported field indications were tied to the deposit morphology. This is supported by the observation that the ultrasonic indications correspond to edges of adherent deposits situated within the expansion transition. Ultrasonic response from deposits is routinely observed in field inspection; however, response characteristics normally allow these signals to be discriminated from degradation responses. The unique feature of the Vogtle tubes is that indications occurred in the geometry change associated with the expansion transition and this exasperated the signal discrimination. The coupling of the phenomenon formed a unique circumstance that allowed the resulting field signals to be misinterpreted as degradation.

The assumption is that the primary inspection will continue to be eddy current based, with those indications displaying the characteristic of the TTS of R12C59 HL and R11C60 HL being ultrasonically examined to determine whether the indications originate from degradation. While the analysis (Section 8) showed that the UT and EC indication originated from different azimuthal orientations, the fact that the ultrasonic examination identified an indication suggests in the future the two phenomena could overlap and a tube be incorrectly removed from service. As an adjunct to the ultrasonic examination using the shear wave mode, an alternate modality involving the use of plate modes was examined. From an implementation standpoint the plate mode techniques strongly resemble the existing techniques in that an ultrasonic transducer launches a wave into the tube wall though a coupling media. The difference is that the frequency of the wave and its incident angle on the tube surface is chosen so that the entire tube wall is excited. The particular mode intended for this application goes under name of Lamb waves for infinite plates. The attractive feature of some of these modes is that the energy is confined within the tube wall such that the wave has little interaction with what might be adherent to the tube surface. Since the assumption is that the adherent deposits are the origin of the unwanted ultrasonic responses the use of an inspection modality that does not interact

with this phenomenon could provide a means of verifying the origin of the ultrasonic response.

9.1 Lamb Wave Implementation

Ideally the plate mode inspection would have been carried out using a probe similar to the UTEC probe but with the axially oriented transducer aimed at an angle to yield the appropriate plate mode. However, due to scheduling considerations such a probe could not be built in the time allotted. Consequently a probe was used that launched the wave from the outside of the tube. Figure 9-1 shows the probe mounted on the outside of the calibration tube. The probe consists of a wedge with a transducer mounted on a carriage whose orientation can be adjusted with respect to the tube surface allowing optimization of the incident angle of the sound for the desired inspection mode. Once adjusted, the carriage was locked into place on the wedge and the inspection conducted. In this position the ultrasonic wave should interact strongly with discontinuities and weakly with deposits. For the guided mode inspection to be a viable discrimination tool there should be little or no response originating from the adherent tube deposits.

9.2 Results

The probe was slid onto the calibration tube which contained two circumferentially oriented notches. The notches were 20% and 50% of the wall thickness and approximately 1/2 inch in length. The sensitivity of the instrumentation was adjusted such that the 50% notch yielded a response of approximately 3/4 the display sensitivity. Figures 9-2 and 9-3 show the response for the 20% and 50% notches respectively.

After recording the notch responses the probe was slid onto the unexpanded end of the TTS sections of R12C59 HL –Piece 2B and R11C60 HL – Piece 2B until it reached the deposit bands noted in the eddy current examinations. Figures 9-4 and 9-5 show the response of these tubes section. No response consistent with degradation was observed on either tube section.

Based on the lack of response from the adherent deposits associated with the TTS tube sections supports further investigation into the use of Lamb waves (guided wave modes) as a viable tool for separating deposit response from degradation.

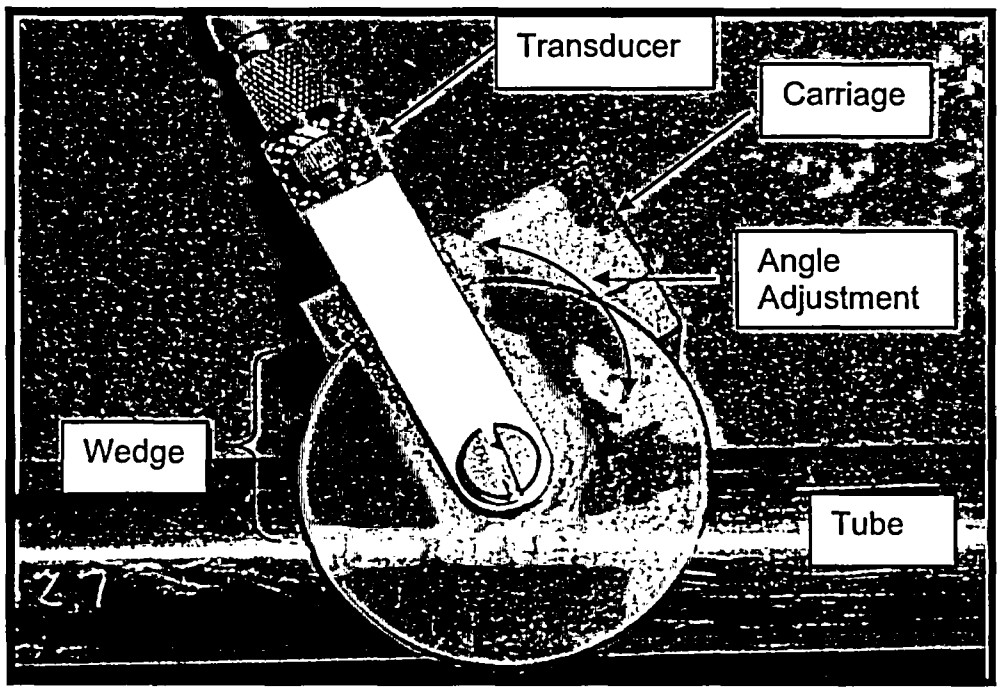

Figure 9-1 Ultrasonic probe used to perform the "Lamb wave" inspection shown on calibration tube.

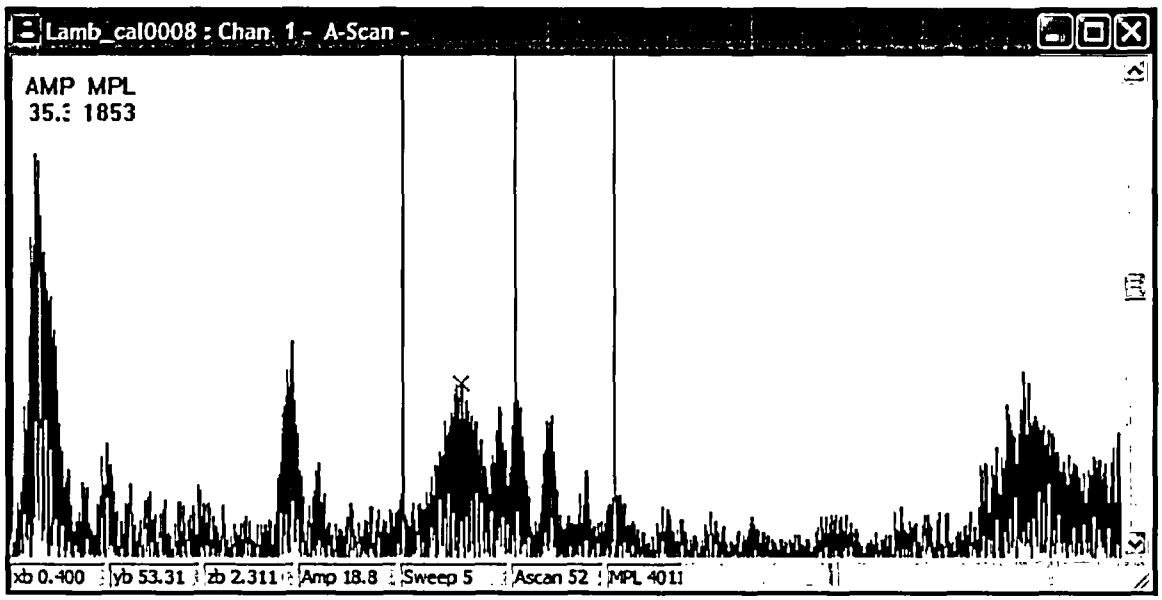

Figure 9-2 Lamb wave mode UT data showing response from 20% calibration notch. Note the response from the end of tube on the right side of the image.

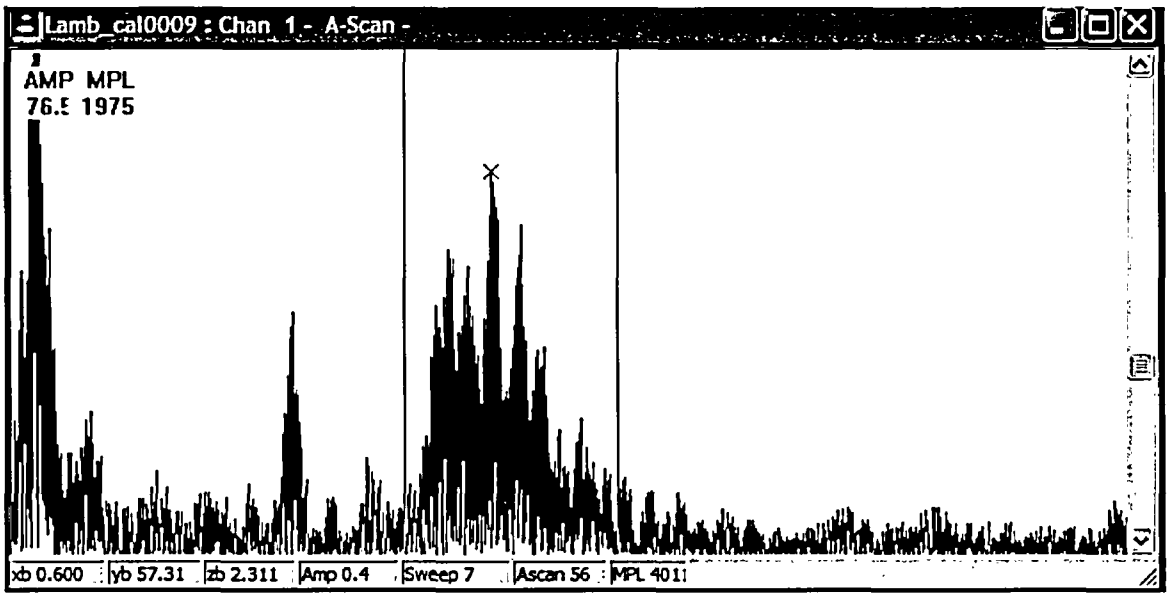

Figure 9-3 Lamb wave mode UT data showing response from the 50% calibration notch. Note that the end of tube response has been shadowed by the presence of the notch.

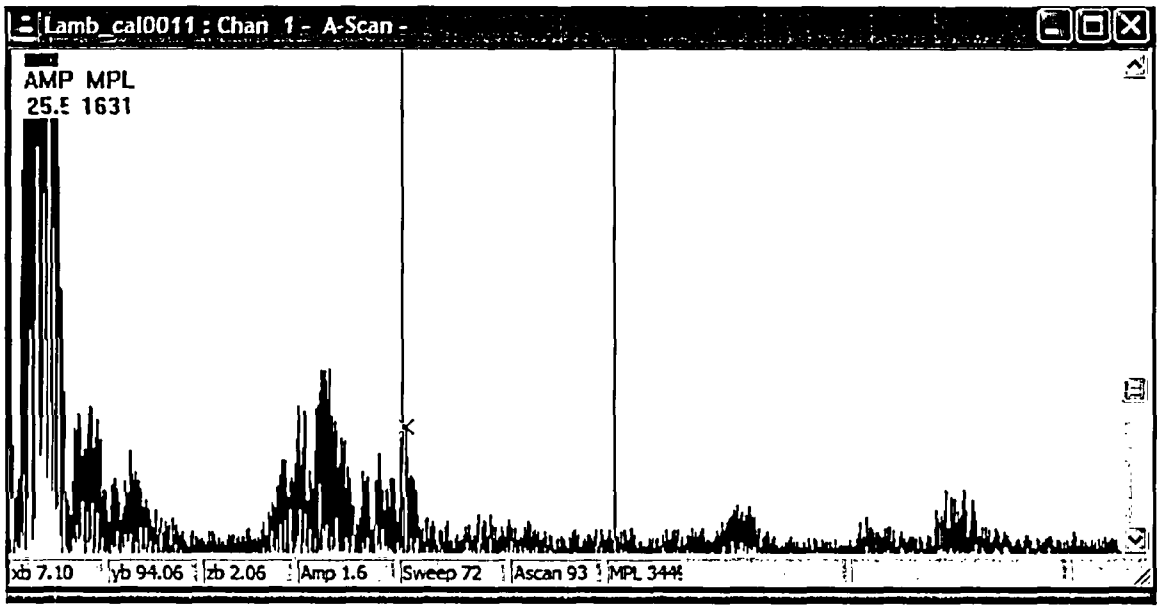

Figure 9-4 Lamb wave mode UT data showing response from R12C59 – Piece 2B. The observed response does not suggest the presence of degradation.

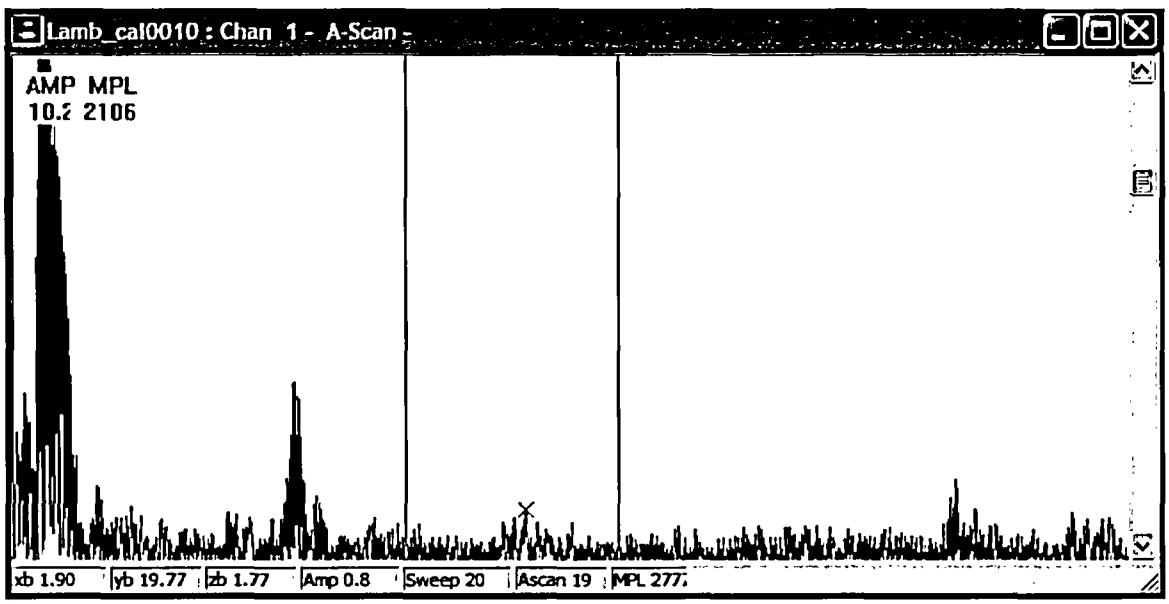

Figure 9-5 Lamb wave mode UT data showing response from R11C60 – Piece 2B. The observed response does not suggest the presence of degradation.

SECTION 10

DEPOSIT AND SURFACE ANALYSIS

In an effort to characterize the physical appearance and to identify the various elements or chemical compounds present on the surfaces of steam generators tubes removed from Vogtle Unit 2, analyses were performed on the deposits by Scanning Electron Microscopy (SEM), Energy Dispersive Spectroscopy (EDS) and X-ray Diffraction (XRD). The results of each of these efforts are presented in this section.

10.1 Scanning Electron Microscopy (SEM) and Energy Dispersive Spectroscopy (EDS)

The physical appearance and chemistry of the deposits found on the OD surface of the Vogtle Unit 2 tubes R12C59 HL and R11C60 HL were determined using surface sensitive analytical techniques, i.e., Scanning Electron Microscopy (SEM) and Energy Dispersive Spectroscopy (EDS). The SEM utilizes a focused beam of electrons that is scanned across the specimen surface under high vacuum. The benefit of the SEM over stereo or optical microscopy is its depth of field at high magnification which allows high resolution examination of rough surfaces. EDS is the most common method for local chemical analysis. EDS is based on x-ray fluorescence resulting from the bombardment of the surface with an electron beam. EDS is usually performed in a SEM where examination of the topography is being performed. EDS analysis determines the composition over a depth of 1.5 to 2 μm with a spatial resolution on the order of 1 μm. The technique will detect Na and heavier elements present in concentrations greater than approximately 0.1 atom %. EDS has relatively poor energy resolution, and therefore, some difficulties can be encountered in separating elements with closely spaced characteristic x-ray lines, e.g., Pb, S, and Mo. The analysis is usually semi-quantitative and is routinely utilized to identify the chemical constituents of scales and deposits. The EDS method is useful in identifying deposit or tube surface contamination if such is present and can analyze for elements down to atomic number 11. Data obtained from the various deposit and tube surface analyses are presented in tabular form, as well as, SEM images with EDS spectra's.

10.1.1 Scanning Electron Microscopy (SEM)

R12C59 HL - Piece 2B - Top of Tubesheet OD Surface

Scanning electron microscopy (SEM) and energy dispersive spectroscopy (EDS) were performed on surface deposits at selected top of tubesheet locations of R12C59 HL Piece 2B. The areas selected for the examination were the azimuthal orientation corresponding to the reported +Pt and UTEC indications identified during the field inspection effort. The character of the OD deposit is illustrated in the reflected electron images and in the backscattered images. A reflected electron image presents a better view of the physical topography of the examined surface with an almost three-dimensional quality. A backscattered electron image differentiates between areas of different composition, because elements with higher atomic numbers appear brighter in this image. Furthermore, cracks are often better visible in the backscattered electron image.

SEM micrographs of the TTS region of R12C59 HL - Piece 2B at the 324° azimuthal orientation are presented in Figure 10-1. This orientation corresponds to the position where the +Pt indication was identified during the field inspection. Both a backscatter energy mode and a reflective energy mode montage are shown in this figure. The montage shown in Figure 10-1 represents approximately 1 inch of the OD surface. The approximate location of the expansion transition as noted on Figure 10-1 is based on the results of the laser profiling of the ID silastic mold discussed in Section 3. The light colored areas or "rub marks" seen in the backscatter energy mode display are related to handling the tube sections in the Hot Cell glove box and are not considered representative of the as pulled OD surface. Figures 10-2 and 10-3 are additional SEM micrographs showing specific topography features of the deposit. Also shown on Figure 10-2, are areas where EDS analyses where performed. Additional discussion of the EDS analyses are presented in Section 10.1.2. As can be seen from these figures, the OD deposit seen in this area appeared relatively uniform with no evidence of cracking. The only difference noted from the SEM micrographs is the topography of the deposit at and slightly above the TTS expansion. The deposit near the expansion transition appeared to be composed of small crystallites and exhibit an amorphous structure. The deposit one inch or so above the transition did not exhibit the amorphous appearance, but rather a smoother and more dense surface. Figures 10-2 and 10-3 illustrate the deposit topography. No unusual physical features were seen at the 324° azimuthal orientation.

Figures 10-4, 10-5, and 10-6 are SEM micrographs of the TTS region at the 45° azimuthal orientation. This orientation corresponds to the position where the field UT signal was reported. Both a backscatter energy mode and a reflected energy mode montage are presented these figures. Figures 10-5 and 10-6 are additional SEM micrographs showing specific topography features of the deposit. As discussed earlier, the light colored areas or "rub marks" seen in the backscatter energy mode display are related to handling the tube sections in the Hot Cell glove box and are not considered representative of the as pulled OD surface. The montages shown in Figure 10-4 represents approximately 1 inch of axial length along the tube above the TTS expansion transition. The deposit seen in this area appeared relatively uniform with no evidence of cracking. The general appearance of the deposit at the 45° azimuthal orientation is similar to that seen at the 324° location. That is the deposit near the expansion transition appeared to be composed of small crystallites and exhibit an amorphous structure (Figures 10-5 and 10-6). The deposit one inch or so above the transition did not exhibit the amorphous appearance, but rather a smoother and more dense surface. Area 6B in Figure 10-5 and area 6R in Figure 10-6 illustrates this observation. Close examination of the Reflected Energy Mode montage (Figure 10-6) identified small areas near the top of the tubesheet, where it appeared that the OD deposit was thin or non-existent. The polishing marks on the tube OD surface can be seen through the deposit. Area 3R, shown in Figure 10-6, illustrates this condition.

R11C60 HL - Piece 2B - Top of Tubesheet OD Surface

Scanning electron microscopy (SEM) and energy dispersive spectroscopy (EDS) were performed on surface deposits at selected top of tubesheet locations of R11C60 HL - Piece 2B. Similar to R12C59 HL- Piece 2B, the areas selected for the examination were the azimuthal locations corresponding to the reported +Pt and UT indications identified during the field inspection effort. The character of the OD deposit is illustrated in the reflected electron images and in the backscattered images. Figures 10-7 and 10-8 are SEM micrographs of the TTS region at the 327° azimuthal orientation. This azimuthal orientation corresponds to the position where the field +Pt signal was reported. The montage shown in Figure 10-7 represents approximately 1 inch of axial length along the tube above the TTS expansion transition and exhibits a similar topography as seen on R12C59 HL at this location. No unusual physical features were seen at the 327° azimuthal orientation. The white colored areas or "rub marks" seen in the backscatter energy mode display are related to handling the tube sections in the Hot Cell glove box and are not considered representative of the as pulled OD surface. Figures 10-8 and 10-9 are additional SEM micrographs of selected areas shown in Figure 10-7. Shown on Figure 10-

8 are areas where EDS analyses were performed. Additional discussion of the EDS analyses are presented in Section 10.1.2.

Figures 10-10, 10-11, and 10-12 are SEM micrographs of the TTS region at the 130° azimuthal orientation. This orientation corresponds to the position where the UT indication was identified during the field inspection. Both a backscatter energy mode and a reflected energy mode montage are presented these figures. As discussed earlier the light colored areas or "rub marks" seen in the backscatter energy mode display are related to handling the tube sections in the Hot Cell glove box and are not considered representative of the as pulled OD surface. The montages shown in Figure 10-10 represents approximately 1 inch of axial length along the tube above the TTS expansion transition and exhibits a similar topography as seen on R12C59 HL at this location. Figures 10-11 and 10-12 are SEM micrographs of selected areas shown in Figure 10-10. The general appearance of the deposit at the 130° azimuthal orientation is similar to that seen at the 327° location. That is, the deposit near the expansion transition appeared to be composed of small crystallites and exhibit an amorphous structure. The deposit one inch or so above the transition did not exhibit the amorphous appearance, but rather a smoother and more dense surface. Close examination of the Reflected Energy Mode montage identified small areas near the top of the tubesheet, where it appeared that the OD deposit was thin or non-existent. Figure 10-13 is a Reflective Energy Mode SEM micrograph showing a local region within the expansion transition which is apparently void of deposit. The polishing marks on the tube OD surface can be seen in this area. This condition is similar to that seen on R12C59 HL – Piece 2B at the 45° azimuthal orientation where the field UTEC call was reported.

<u>R12C59 HL – Piece 3B – 1st Tube Support Plate</u>

Montages of the OD deposit at the 1st TSP of R12C59 Piece 3B at the 10° azimuthal orientation is presented in Figure 10-14. Both a Backscatter and a Reflective Energy mode montages are displayed. Additional SEM micrographs are presented in Figures 10-15 and 10-16 to further illustrate the appearance of the deposit. Figures 10-17 and 10-18 are similar SEM micrographs at the 100° azimuthal orientation, although limited Reflective Energy mode SEM micrographs are presented. Included in these figures are areas where EDS analyses were performed. The results of these analyses are discussed later in this section. It is evident from these figures that deposit buildup has occurred between the quatrefoil land and the OD tube surface, while little to no deposit buildup was seen at the other two quatrefoil land to tube intersections. During the laboratory eddy current

evaluation (Section 5), buildup of deposit was identified for two of the four quatrefoil land to tube intersections.

R11C60 HL – Piece 3B – 1st Tube Support Plate

Montages of the OD deposit at the 1st TSP of R11C60 Piece 3B at the 10° azimuthal orientation is presented in Figure 10-19. Both a Backscatter and a Reflective Energy Mode montages are displayed. Additional SEM micrographs are presented in Figures 10-20 and 10-21 to further illustrate the appearance of the deposit. Included in these figures are areas where EDS analyses were performed. The results of these analyses are discussed later in this section. It is evident from these figures that little to no deposit buildup has occurred at the 1st TSP of the R11C60 HL tube. During the laboratory eddy current evaluation (Section 5), the lack of deposit buildup was also noted.

10.1.2 Energy Dispersive Spectroscopy (EDS)

The OD deposit areas selected from the TTS region of the R12C59 HL and R11C60 HL for the EDS analyses were the azimuthal locations where +Pt and UT indications were reported during the field inspection. A limited EDS evaluation was also performed on the deposits associated with the quatrefoil land to tube intersections. The objective of the analyses was to determine if there was any unique deposit chemistry in these areas when compared to the TSP intersection deposits. Detailed tabulations of the results of the EDS analyses of the OD tube deposits are presented in Tables 10-1 through 10-7, while the actual areas analyzed are presented in Figures 10-22 through 10-35. The first group of elements listed in each table (Ni, Cr, Fe, and Ti) is associated with Alloy 600 and feed water iron transport. When the nickel concentration is high, little deposit is usually present. When the iron concentration is high significant amounts of externally born deposits are present. The second group of elements (Mg, Si, Al, Ca, and Mn) listed can contribute to cohesiveness and morphology of the tube deposits. The elements in this group do not directly contribute to corrosion degradation but help to provide a more dense deposit structure for the concentration of deleterious elements. The next group of seven elements (S, P, Na, K, Cu, Cl, and Pb) found on the OD surface of the deposit is the group in which each element can possibly contribute to corrosion degradation under unfavorable circumstances. The last group of elements, carbon and oxygen, are likely evidence that the majority of the elements, except for copper and lead, are present as oxides or oxygen / carbon containing compounds.

R12C59 HL - Piece 2B - Top of Tubesheet OD Surface

EDS analyses for the TTS region of R12C59 HL at the 324° orientation (field +Pt signal) and 45° (field UT signal) are presented in Tables 10-1 and 10-2, respectively. The analyses showed that "bulk" or average composition of the surface deposit was a mix of iron, chromium, and nickel oxides. Low to trace amounts of zinc, magnesium, aluminum, silicon, titanium, copper, lead, and manganese were detected. No significant differences in the elements identified or the levels detected were seen between the two azimuthal locations evaluated. Figure 10-22 present SEM photographs and EDS traces of the OD surface deposits analyzed at the 324° orientation, while Figure 10-24 present results at the 45° orientation. The results summarized in Tables 10-1 and 10-2 can be related to the various figures by the numerical number assigned to the EDS result for each analysis location. The figure captions provide further details regarding the location and deposit description.

Figures 10-23 and 10-25 are backscatter EDS area maps showing the distribution of various elements. This analysis technique is often utilized to identify non-uniform distribution of chemical species within a given region. The results for the 324° azimuthal orientation is presented in Figure 10-23, while Figure 10-25 presents the results at the 45° azimuthal orientation. For all of the EDS area map displays, the top left image is the area analyzed, while the remaining images represent the distribution of various elements within the area analyzed. A higher concentration of a given element within the area analyzed is represented by the less black or "lighter" regions. No appreciable difference is noted in the results presented in Figures 10-23 and 10-25. The local region of apparent higher Pb, S, P, and Cl seen at the 45° azimuthal position (Figure 10-25) is likely related to the pulled tube section contacting "lead" shielding during remote handling in the Hot Cell glove box.

R11C60 HL - Piece 2B – TTS

EDS analyses for the TTS region of R11C60 HL at the 327° orientation (field +Pt signal) and 130° (field UT signal) are presented in Tables 10-3 and 10-4. The analyses showed that "bulk" or average composition of the surface deposit was a mix of iron, chromium, and nickel oxides. Low to trace amounts of zinc, magnesium, aluminum, silicon, titanium, copper, lead, and manganese were detected. No significant differences in the elements identified or the levels detected were seen between the two azimuthal locations evaluated. Figure 10-26 present SEM photographs and EDS traces of the OD surface deposits analyzed at the 327° orientation, while Figure 10-28 present results at the 130° orientation.

The results summarized in Tables 10-3 and 10-4 can be related to the various figures by the numerical number assigned to the EDS result for each analysis location. The figure captions provide further details regarding the location and deposit description.

Figures 10-27 and 10-29 are backscatter EDS area maps showing the distribution of various elements. This analysis technique is often utilized to identify non-uniform distribution of chemical species within a given region. The results for the 327° azimuthal orientation is presented in Figure 10-27, while Figure 10-29 presents the results at the 130° azimuthal orientation. As noted earlier, the top left image of the EDS area map display represents the area analyzed while the remaining images represent the distribution of various elements within the area analyzed. A higher concentration of a given element within the area analyzed is represented by the less black or "lighter" regions. No appreciable difference is noted in the results presented in Figures 10-27 and 10-29, except for the apparent higher concentration of Cu and Ni seen at an area corresponding to the azimuthal orientation where the field +Pt signal was reported. This is shown in the Cu and Ni image displays presented in Figure 10-27.

R12C59 HL – Piece 3B – 1st TSP

EDS analyses for the 1st TSP region of R12C59 HL at the 10° orientation and 100° orientation are presented in Tables 10-5 and 10-6. The analyses showed that "bulk" or average composition of the surface deposit was a mix of iron, chromium, and nickel oxides. Low to trace amounts of zinc, magnesium, aluminum, silicon, titanium, copper, and manganese were detected. No significant differences in the elements identified or the levels detected were seen between the two azimuthal locations evaluated. Figure 10-30 present SEM photographs and EDS traces of the OD surface deposits analyzed at the 10° orientation, while Figure 10-32 present results at the 100° orientation. The results summarized in Tables 10-5 and 10-6 can be related to the various figures by the numerical number assigned to the EDS result for each analysis location. The figure captions provide further details regarding the location and deposit description. The results summarized in Tables 10-3 and 10-4 can be related to the various figures by the numerical number assigned to the EDS result for each analysis location. The figure captions provide further details regarding the location and deposit description.

Figures 10-31 and 10-33 are backscatter EDS area maps showing the distribution of various elements. This analysis technique is often utilized to identify non-uniform distribution of chemical species within a given region. The results for the 10° azimuthal

orientation is presented in Figure 10-31, while Figure 10-33 presents the results at the 100° azimuthal orientation. As noted earlier, the top left image of the EDS area map display represents the area analyzed while the remaining images represent the distribution of various elements within the area analyzed. A higher concentration of a given element within the area analyzed is represented by the less black or "lighter" regions. No appreciable difference is noted in the results presented in Figures 10-31 and 10-33. For both locations, the deposit seen at the quatrefoil land to tube intersection is predominantly an iron oxide with low levels of nickel and chromium.

R11C60 HL – Piece 3B – 1st TSP

EDS analyses for the 1st TSP region of R11C60 HL at the 10° orientation is presented in Table 10-7. The analyses showed that "bulk" or average composition of the surface deposit was a mix of iron, chromium, and nickel oxides. Low to trace amounts of zinc, magnesium, aluminum, silicon, titanium, copper, and manganese were detected. Figure 10-34 present SEM photographs and EDS traces of the OD surface deposits analyzed at the 10° orientation. The results summarized in Table 10-7 can be related to the various figures by the numerical number assigned to the EDS result for each analysis location. The figure captions provide further details regarding the location and deposit description.

Backscatter EDS area maps showing the distribution of various elements at the 10° azimuthal orientation are presented in Figure 10-35. This analysis technique is often utilized to identify non-uniform distribution of chemical species within a given region. As noted earlier, the top left image of the EDS area map display represents the area analyzed while the remaining images represent the distribution of various elements within the area analyzed. A higher concentration of a given element within the area analyzed is represented by the less black or "lighter" regions. As shown in the Figure 10-35 images, the deposit seen at the quatrefoil land to tube intersection is predominantly an iron oxide with low levels of nickel and chromium.

SEM and EDS Analyses of After ID Pressurization of R12C59 HL Piece 2B (TTS) and Piece 3B (1st TSP)

In an attempt to enhance the ability to detect the presence of any tube degradation and to remove OD deposits for subsequent chemistry evaluations attempt Piece 2B and 3B from R12C59 HL were pressurized to 9,000 psi. As discussed earlier, there was no obvious change in the appearance of the deposit at the top of the tubesheet based on light optical

and eddy current evaluations. In addition, only loose deposit was removed via the carbon tape during the pressurization of the TTS region. SEM micrographs of the TTS area of R12C59 HL-Piece 2B following pressurization to 9,000 psi is shown in Figure 10-36. No evidence of cracking or "spalling" of the deposit was seen. The loose deposit collected on the carbon tape is shown in Figure 10-37. Shown on Figure 10-37 are the regions where EDS analyses were performed. SEM micrographs and EDS traces for the areas analyzed are presented in Figure 10-38. The analyses showed that "bulk" composition of the surface deposit was predominantly iron with low levels of chromium and nickel. Low to trace amounts of zinc, magnesium, silicon, titanium, lead, and manganese were detected. Local regions of higher levels of copper and aluminum were also noted.

In addition to pressurizing the TTS region of R12C59 - Piece 2B, the 1st TSP region (Piece 3B) was also pressurized. Backscatter Energy Mode montages showing the pre-pressurized and post pressurized appearance of the deposit at the quatrefoil land to tube intersection (10° orientation) are shown in Figure 10-39. Shown in the post pressurized montage, are areas where the deposit had "spalled" and collected on the carbon tape. EDS analyses of the deposit collected on the tape are shown in Figure 10-39. The results are similar to the EDS analyses reported in Table 10-5. Backscatter EDS area map analyses are presented in Figure 10-41. The "spalled" oxide deposit was predominantly an iron/nickel/chromium oxide based on the elements identified during the EDS analyses. The apparent Cd ,Cl, and S concentration seen in Figure 10-41 is likely due to remote handling in the glove box.

SEM and EDS Analyses of Ring Section Removed from R12C59 HL Piece 2B2A (TTS)

In order to further evaluate the TTS region of R12C59 HL at the azimuthal locations where field indications were reported a ½" ring was cut from Piece 2B for further evaluation. The ½" ring was cut at the 90° and 270° azimuthal locations. The section containing the reported field indications was flattened. In order to collect the OD deposit for EDS and XRD analyses, Piece 2B2A was wrapped with carbon tape prior to flattening. A light optical micrograph of the OD surface of Piece 2B2A after flattening is shown in Figure 10-42, while the oxide collected on the carbon tape is shown in Figure 10-43. Detailed surface SEM analyses were performed at azimuthal positions representing the regions were the field +Pt and UTEC signals were reported. Figure 10-44 is a montage of the OD surface of R12C59 – Piece 2B2A at 324° azimuthal orientation following the removal of the oxide deposit. The area shown is the expansion transition region. Figure 10-45 are higher magnification SEM micrographs of selected areas shown in Figure 10-44. No

unusual surface conditions were noted. Results of EDS analyses of selected areas shown in Figure 10-45 are presented in Figure 10-46. The predominant elements detected were iron, nickel, and chromium. Low to trace amounts of zinc, magnesium, silicon, titanium, lead, and manganese were detected. Local regions of higher levels of copper and aluminum were also noted on the tube surface. Backscatter EDS area map analyses are presented in Figure 10-47. No unusual conditions were noted.

Figure 10-48 is a montage of the OD surface of R12C59 – Piece 2B2A at 0° azimuthal orientation following the removal of the oxide deposit. The area shown is the expansion transition region. Figure 10-49 are higher magnification SEM micrographs of selected areas shown in Figure 10-48. No unusual surface conditions were noted. Results of EDS analyses of selected areas shown in Figure 10-49 are presented in Figure 10-50. The predominant elements detected were iron, nickel and chromium. Low to trace amounts of aluminum, zinc, magnesium, silicon, titanium, lead, and manganese were detected. A local region of higher copper concentration was also noted on the tube surface.

10. 2 X-Ray Diffraction

In an effort to identify the various elements or chemical compounds present on the OD deposits removed from the top of tubesheet expansion region of R12C59 HL – Piece 2B2A, analyses were performed on the deposits by X-ray Diffraction (XRD). A deposit sample was removed from the surface of Piece 2B2A by attaching tape to the tube segment while the tube segment was bent. The tape was inverted and an X-ray diffraction analysis was performed on the exposed deposit. The exposed deposit surface separated at the tube surface, and the topography of the tube surface was replicated on the exposed deposit. Prior to removal of the OD deposit from Piece 2B2A scanning electron microscopy with energy dispersive x-ray spectroscopy (SEM/EDS) was performed. The results of the SEM/EDS analyses are used to supplement the XRD analysis to more completely characterize the deposits and are discussed later in this section.

The composition and the crystal structure of deposits formed on steam generator tubes reflect the solution environment in which the deposits resided. Knowledge about the solution environment will in some cases help elucidate the local corrosion processes that occurred in the vicinity of the deposits.

The XRD system used in this work was a Scintag XDS 2000 equipped with a high purity germanium detector. A scan range from 5° to 110° 2θ at a step size of 0.02 degrees and a

scan rate of 0.33 degrees per minute were used for data acquisition. Cu Kα radiation was used. The X-ray energy window on the detector was set to exclude Cu K□ radiation and X-ray fluorescence from iron in each sample.

The tape used to remove deposits for XRD analysis was Scotch 2090 manufactured by 3M. Portions of the tape were cut to fit into the standard 0.75-inch diameter sample holders and mounted on glass slides.

The experimental patterns were subsequently analyzed using the Scintag program, DMSNT SEARCHMATCH that determined the best matches between the experimental patterns and known phases in the JCPDS X-ray Diffraction Library. Possible matches identified by the computer were then examined manually for match quality. Furthermore, additional phases suspected of being present in the deposits, although not identified by SEARCHMATCH, were also examined to determine their possible presence.

The X-ray diffraction pattern is shown in Figure 10-51 and a summary of the weight percent of each phase detected is presented in Table 10-8. A background pattern from the tape with no deposits is also shown in the Figure 10-51. Detection limits for the analyses that were done were estimated to be in the 1 to 3 percent range for typical well-crystallized material.

Magnetite was one of the primary constituents of the deposits. The peak positions in the x-ray diffraction pattern suggest that there was also some nickel substitution in the magnetite inverse spinel structure. Nickel substituted magnetite is commonly found as the major component of most secondary deposit samples.

As shown in Table 10-8, bohmite, calcium sulfate, and calcite were detected on the deposit removed from the TTS region of R12C59 HL. Bohmite (aluminum oxide hydroxide) was also a major component of the deposit at the tube interface. Bohmite has been observed in past sludge analyses at the Vogtle units and at other plants. The relative intensity different bohmite peaks indicated that the bohmite crystals were most likely thin and oriented in a preferred direction within the deposit.

A peak was observed at 3.04 angstroms (between 29 and 30 degrees) that is possibly due to a mixture of calcium phosphate phases. A great number of calcium phosphate phases have a major peak at this location, but a definitive match was not found for any calcium phosphate library phase. This is also the main peak for lead oxide, Pb_2O_3. Either phase is

consistent with the SEM/EDS analyses of the deposits on this tube. Metallic copper was identified, as well as a peak at approximately 44 degrees indicated the presence of Alloy 600 or another similar nickel-alloy phase. The identification of Pb_2O_3 is not believed to represent a compound that was present during plant operation. As noted throughout this report, the pulled tube sections inadvertently came into contact with "lead" blocks which are utilized in the Hot Cell remote handling glove box for shielding purposes.

Table 10-1 EDS Analyses of TTS OD Deposits for R12C59 Piece 2B at 324° Azimuthal Orientation (Field +Pt Signal)

	Area Scanned (Refer to Figures 10-2, 10-22, and 10-23)								
Element	**7B-EDS1**	**7B-EDS2**	**7B-EDS3**	**7B-EDS4**	**8B-EDS1**	**8B-EDS7**	**8B-EDS8**	**8B-EDS9**	**Average**
Ni	6.04	0.56	0.92	5.20	-	-	-	-	1.59
Cr	2.70	0.61	1.08	0.79	-	-	-	-	0.65
Fe	19.72	3.76	4.86	18.79	4.59	75.15	-	0.93	15.98
Ti	3.44	-	-	-	-	-	-	-	0.43
Mg	1.67	-	-	1.31	-	-	3.49	0.48	0.43
Si	5.34	2.26	1.85	9.66	-	-	11.98	-	3.89
Al	6.86	3.14	32.32	12.34	-	-	7.54	0.42	7.83
Ca	1.73	0.32	3.02	0.24	-	-	0.48	12.77	2.32
P	0.94	-	1.74	-	-	-	-	-	0.34
Mn	2.68	0.79	2.31	6.07	-	-	14.83	1.65	3.54
Cu	5.04	67.32	0.06	-	94.70	1.47	0.53	-	21.13
Pb	-	-	-	-	-	-	-	-	-
Cl	-	-	-	-	-	-	-	-	-
S	-	-	-	-	-	-	-	-	-
O	40.24	19.97	48.42	43.16	0.21	22.92	54.84	55.91	35.71
C	3.60	1.27	3.41	2.44	0.50	0.45	6.31	8.28	3.28

Table 10-2 EDS Analyses of TTS OD Deposit for R12C59 Piece 2B 45° Azimuthal Orientation (Field UT Signal)

	Area Scanned (Refer to Figures 10-5, 10-24, and 10-25)							
Element	7B-EDS2	7B-EDS3	7B-EDS4	7B-EDS5	7B-EDS6	8B-EDS1	8B-EDS2	Average
Ni	-	25.31	20.21	0.30	12.57	0.28	-	8.38
Cr	-	16.90	1.94	-	4.72	-	-	3.37
Fe	2.93	12.29	3.41	4.58	17.68	7.92	8.13	8.14
Ti	-	-	-	-	-	13.63	0.69	2.05
Mg	-	-	1.31	-	-	1.20	-	0.36
Si	18.61	1.30	0.49	-	4.66	3.08	-	4.02
Al	13.35	2.18	0.54	-	6.64	3.37	1.58	3.95
Ca	8.46	0.27	-	-	-	6.91	-	2.23
P	-	-	-	-	1.45	4.00	-	0.78
Mn	-	0.72	0.04	-	1.25	3.18	-	0.74
Cu	-	4.86	52.14	94.43	7.25	0.26	70.95	32.84
Pb	-	-	-	-	-	-	-	-
Cl	-	-	-	-	-	-	-	-
S	-	-	-	-	-	-	-	-
O	51.36	34.73	19.78	0.41	39.15	49.01	17.14	30.23
C	5.28	1.44	1.45	0.28	4.63	7.16	1.51	3.11

Table 10-3 EDS Analyses of TTS OD Deposit for R11C60 Piece 2B at 327° Azimuthal Orientation (Field +Pt Signal)

	Area Scanned (Refer to Figures 10-8, 10-26, and 10-27)							
Element	7B-EDS1	7B-EDS2	7B-EDS3	7B-EDS4	7B-EDS6	7B-EDS7	7B-EDS8	Average
Ni	47.62	11.84	46.50	3.34	1.42	1.79	0.91	16.2
Cr	9.74	2.05	3.22	0.40	0.58	0.43	-	2.35
Fe	11.62	50.89	7.46	10.49	11.01	9.76	22.55	17.68
Ti	-	-	-	-	-	-	-	-
Mg	-	-	-	1.31	3.46	-	3.70	1.21
Si	0.79	1.89	0.27	7.13	8.68	1.45	4.29	3.50
Al	0.58	1.85	-	27.15	12.89	2.88	9.91	7.89
Ca	-	0.64	-	2.03	1.86	0.31	7.88	1.82
P	-	-	-	-	0.52	-	4.28	.69
Mn	-	-	-	-	9.70	1.37	1.17	1.75
Cu	-	-	1.99	-	-	55.43	0.98	8.34
Pb	-	-	-	-	-	-	-	-
Cl	-	-	-	-	-	-	-	-
S	-	0.38	1.11	-	0.17	0.38	0.25	0.33
O	28.85	28.78	33.24	46.17	46.86	23.23	41.11	35.46
C	0.80	1.67	3.15	3.31	2.85	1.46	2.97	2.32

Table 10-4 EDS Analyses of TTS OD Deposit for R11C60 Piece 2B at 130° Azimuthal Orientation (Field UT Signal)

	Area Scanned (Refer to Figures 10-11, 10-28, and 10-29)		
Element	**6B-EDS2**	**6B-EDS3**	**Average**
Ni	5.82	0.12	2.97
Cr	-	-	-
Fe	50.52	1.36	25.94
Ti	-	-	-
Mg	-	-	-
Si	3.02	-	1.51
Al	1.61	26.91	14.26
Ca	1.05	3.18	2.12
P	-	1.3	0.65
Mn	-	-	-
Cu	-	-	-
Pb	-	-	-
Cl	-	-	-
S	-	-	-
O	33.45	56.26	44.86
C	4.54	10.87	7.71

Table 10-5 EDS Analyses of 1st TSP OD Deposit for R12C59 Piece 3B at Quatrefoil Land / Tube Intersection (10° Azimuthal Orientation)]

	Area Scanned (Refer to Figures 10-15, 10-30, and 10-31)										
Element	6B-EDS1	6B-EDS2	6B-EDS3	6B-EDS4	6B-EDS5	6B-EDS6	7B-EDS1	8B-EDS1	8B-EDS2	8B-EDS3	Average
Ni	14.98	43.12	-	0.29	7.17	-	2.73	9.95	42.47	-	12.07
Cr	7.16	12.53	-	-	13.97	-	0.06	0.60	7.42	-	4.17
Fe	42.90	10.58	5.85	74.61	74.08	0.61	68.64	20.43	20.61	1.16	31.95
Ti	-	-	-	-	-	-	-	-	-	-	-
Mg	-	-	-	-	-	-	-	-		-	-
Si	-	-	-	-	0.94	-	-	0.56	-	-	0.15
Al	1.34	0.37	-	-	-	86.53	0.56	0.33	-	-	8.91
Ca	-	-	0.80	-	-	-	-	-	-	-	0.08
P	-	-	-	-	-	-	-	-	-	13.17	1.32
Mn	0.35	0.38	0.47	0.90	0.69	-	0.18	0.02	-	1.92	3.96
Cu	-	-	90.93	-	-	4.09	0.61	45.27	-	-	14.09
Pb	-	-	-	-	-	-	-	-	-	-	-
Cl	-	-	-	-	-	-	-	-	-	-	-
S	-	-	-	-	-	-	-	-	-	-	-
O	30.88	31.39	1.01	23.7	1.29	6.27	25.59	20.92	28.08	52.05	22.12
C	2.38	1.62	0.95	0.5	1.85	2.50	1.64	1.94	1.41	8.88	2.37

Table 10-6 EDS Analyses of 1st TSP OD Deposit for R12C59 Piece 3B at Quatrefoil Land / Tube Intersection (100° Azimuthal Orientation)

	Area Scanned (Refer to Figures 10-18, 10-32, and 10-33)							
Element	**7B-EDS1**	**7B-EDS2**	**8B-EDS2**	**9B-EDS1**	**9B-EDS2**	**9B-EDS3**	**10B-EDS4**	**Average**
Ni	2.24	89.23	9.97	2.99	0.94	1.06	17.77	17.74
Cr	0.05	-	-	-	0.61	0.56	14.64	2.27
Fe	69.99	8.69	88.30	56.72	55.28	48.25	28.36	50.80
Ti	-	-	-	-	-	-	-	-
Mg	-	-	-	-	-	1.23	-	0.12
Si	-	0.79	-	-	1.49	1.49	-	0.54
Al	-	-	-	-	2.81	3.00	0.53	0.91
Ca	-	-	-	8.78	0.71	0.65	-	1.45
P	-	-	-	-	-	0.23	-	0.02
Mn	0.45	-	-	-	3.12	4.24	0.95	1.25
Cu	-	-	-	-	1.60	4.07	0.4	0.87
Pb	-	-	-	-	-	-	-	-
Cl	-	-	-	-	-	-	-	-
S	-	-	-	-	-	-	-	-
Cd	-	-	-	-	-	-	-	-
O	25.60	0.70	1.28	28.53	31.01	32.49	34.49	22.01
C	1.67	0.58	0.45	2.99	2.44	2.74	2.31	1.88

Table 10-7 EDS Analyses of 1st TSP OD Deposit for R11C60 - Piece 3B at Quatrefoil Land / Tube Intersection (10° Azimuthal Orientation)

	Area Scanned (Refer to Figures 10-20, 10-34, and 10-35)							
Element	**4B-EDS1**	**4B-EDS2**	**4B-EDS3**	**4B-EDS5**	**5B-EDS1**	**6B-EDS1**	**7B-EDS1**	**Average**
Ni	16.14	47.56	14.04	6.31	16.83	17.69	10.65	18.46
Cr	14.13	11.29	7.35	1.66	12.69	11.31	7.74	9.45
Fe	28.23	7.34	39.64	42.02	28.73	31.19	11.58	26.96
Ti	0.74	-	0.74	-	0.60	0.70	0.36	0.45
Mg	-	-	-	-	-	-	-	-
Si	0.39	0.49	0.20	0.54	0.56	0.31	0.23	0.39
Al	0.54	0.37	0.42	0.78	0.50	0.53	12.96	2.30
Ca	-	-	-	1.15	-	-	0.24	0.20
P	-		-	-	-	-	-	-
Mn	1.03	0.28	0.60	0.29	1.07	0.99	0.54	0.69
Cu	-	-	-	-	-	-	1.96	0.28
Pb	-	-	-	-	-	-	-	-
Cl	-	-	-	-	-	-	-	-
S	-	-	-	-	-	-	-	-
Cd	-	-	-	-	-	-	-	-
O	35.85	31.03	33.37	38.98	35.76	34.33	45.60	36.42
C	2.94	1.64	3.64	7.89	3.25	2.94	5.99	4.04

Table 10-8 Semi-Quantitative XRD Phase Compositions of Deposit Removed from the TTS Region of R12C59 HL – Piece 2B2A.

Phase	Weight %
Magnetite Fe_3O_4 PDF 19-629	35.6
Tenorite CuO PDF 41-254	0.0
Cuprite Cu_2O PDF 5-667	0.0
Copper Cu PDF 4-836	12.2
Kaolinite $Al_2Si_2O_5(OH)_4$ PDF 29-1488	0.0
Nickel Ni PDF 4-850 or Alloy 600	8.0
Lead Oxide Pb_2O_3 PDF 23-331	8.7
Hematite Fe_2O_3 PDF 33-664	0.0
Quartz SiO_2 PDF 33-1161	0.0
Bohmite ALOOH PDF 21-1307	22.5
Calcium Sulfate $CaSO_4$ PDF 45-0157	7.9
Calcite $CaCO_3$ PDF 5-586	5.1

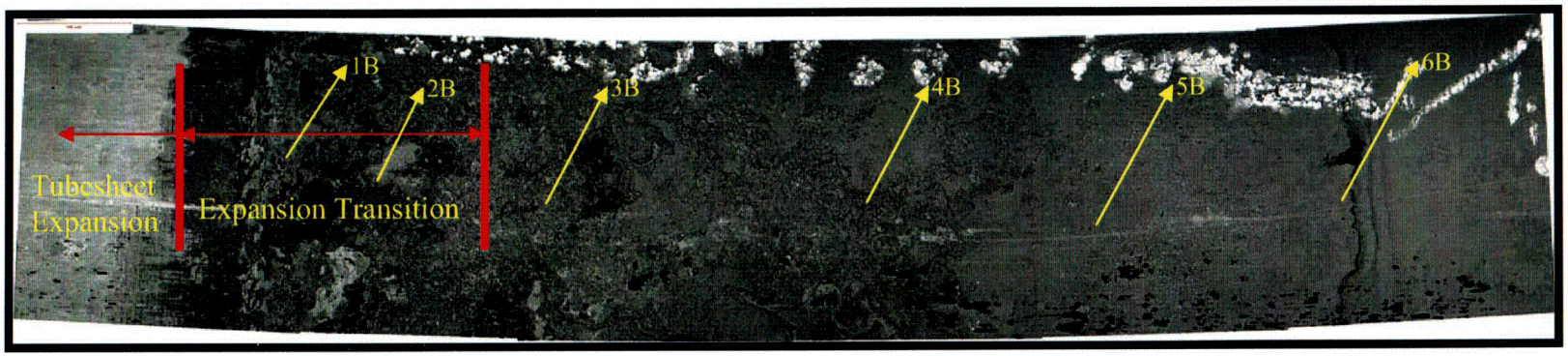

a) Backscatter Energy Mode

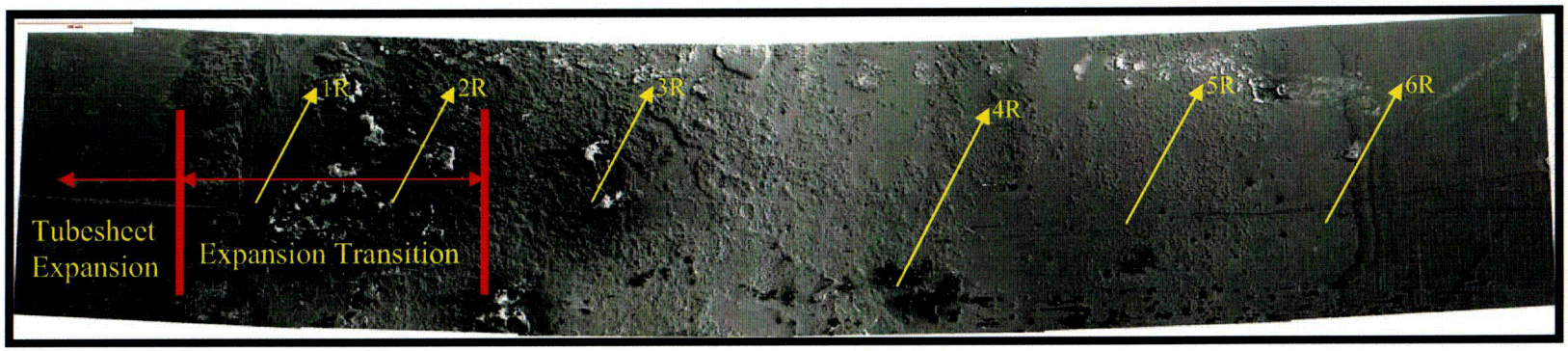

b) Reflected Energy Mode

Figure 10-1 Montage of OD deposit from TTS region of R12C59 Piece 2B at 324° azimuthal orientation (field +Pt signal location). The location of the expansion transition is based on the results of laser profiling of the ID silastic mold. Additional SEM micrographs of the areas noted are shown in Figures 10-2 and 10-3. The white areas seen on the above SEM micrographs are the result of remote handling in the glove box.

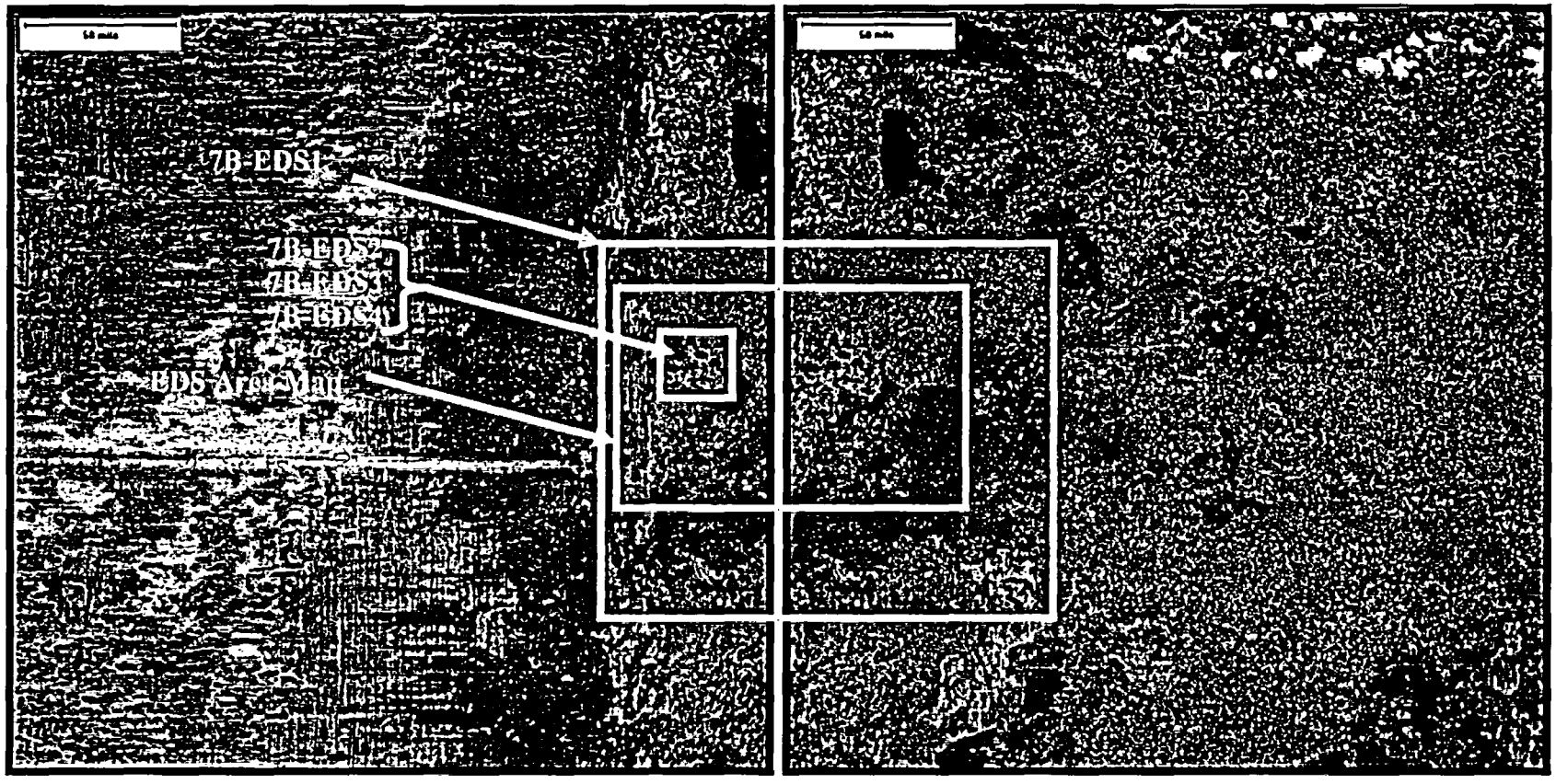

a) Area 1B

b) Area 2B

Figure 10-2 Backscatter Energy Mode SEM micrographs showing OD deposit on R12C59 HL Piece 2B at areas noted in Figure 10-1. The areas outlined represent regions where EDS analyses were performed. The results of the EDS analyses are provided in Table 10-1 and Figures 10-22 and 10-23. The white areas seen on the above SEM micrographs are the result of remote handling in the glove box.

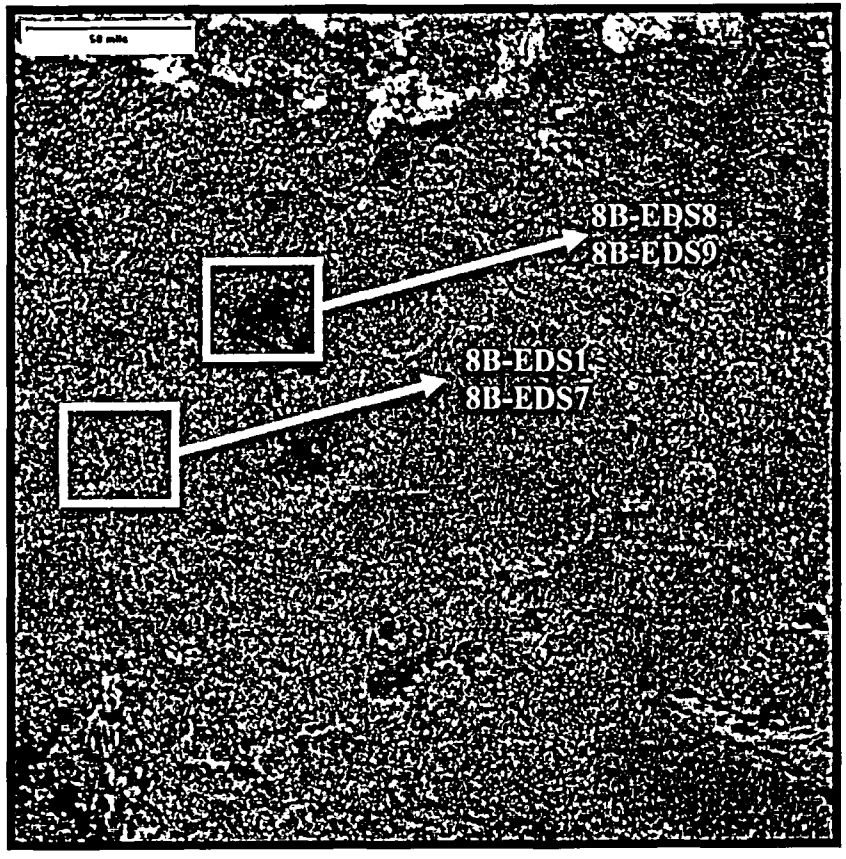

c) Area 3B

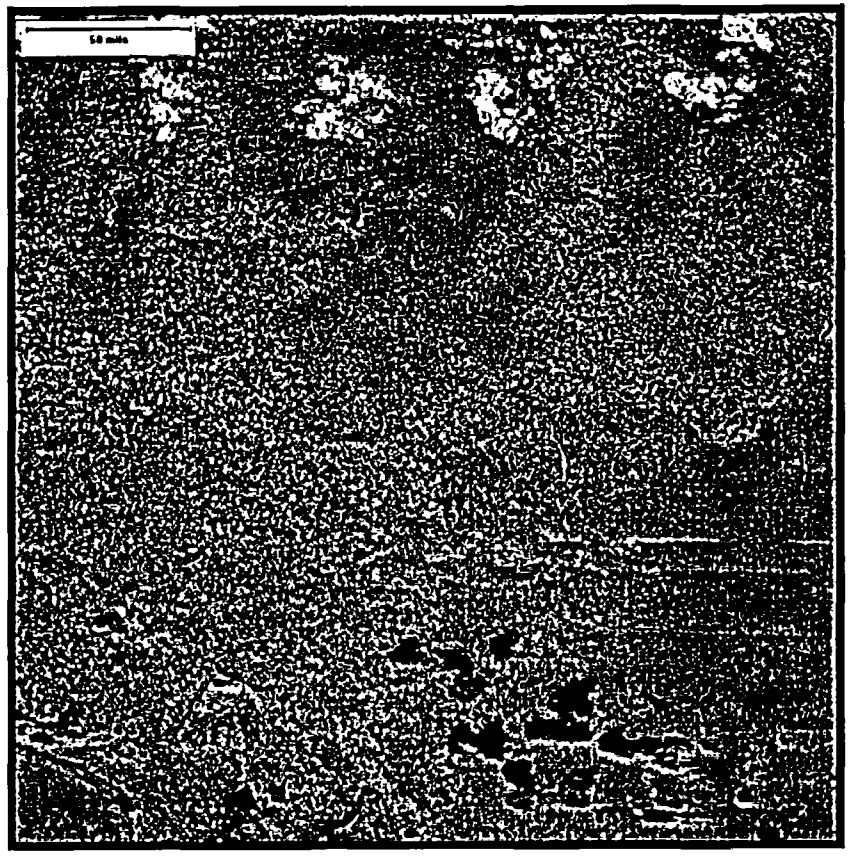

d) Area 4B

Figure 10-2 (Cont'd) Backscatter Energy Mode SEM micrographs showing OD deposit on R12C59 HL Piece 2B at areas designated on Figure 10-1. The results of the EDS analyses are provided in Table 10-1 and Figures 10-22 and 10-23. The white areas seen on the above SEM micrographs are the result of remote handling in the glove box.

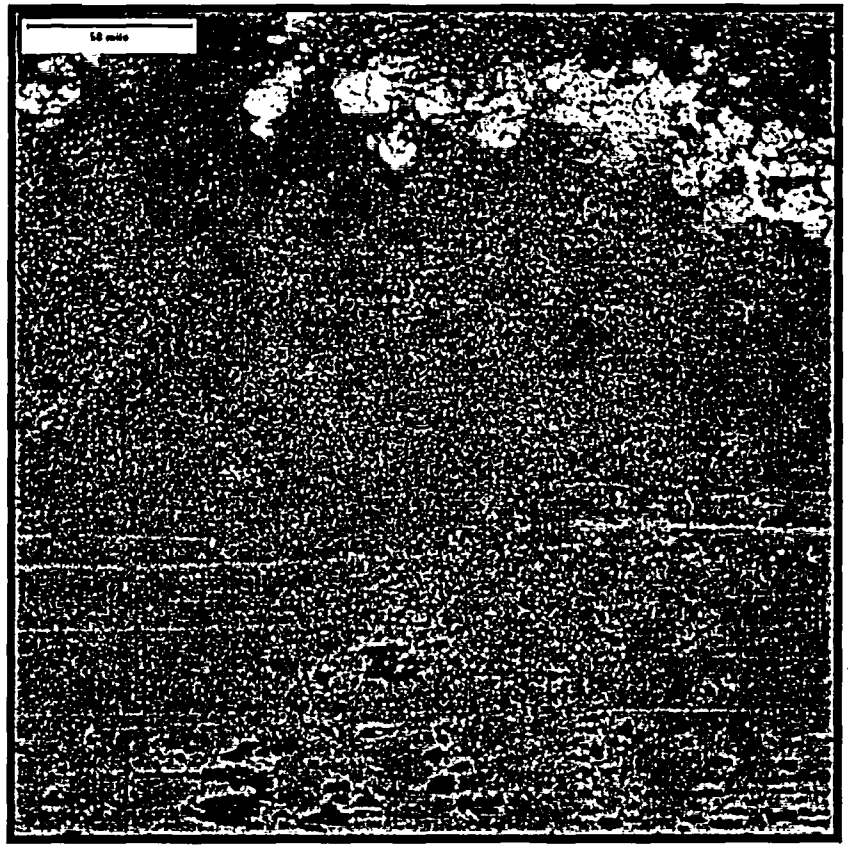

e) Area 5B

f) Area 6B

Figure 10-2 (Cont'd) Backscatter Energy Mode SEM micrographs showing OD deposit on R12C59 HL Piece 2B at areas designated on Figure 10-1. The white areas seen on the above SEM micrographs are the result of remote handling in the glove box.

a) Area 1R

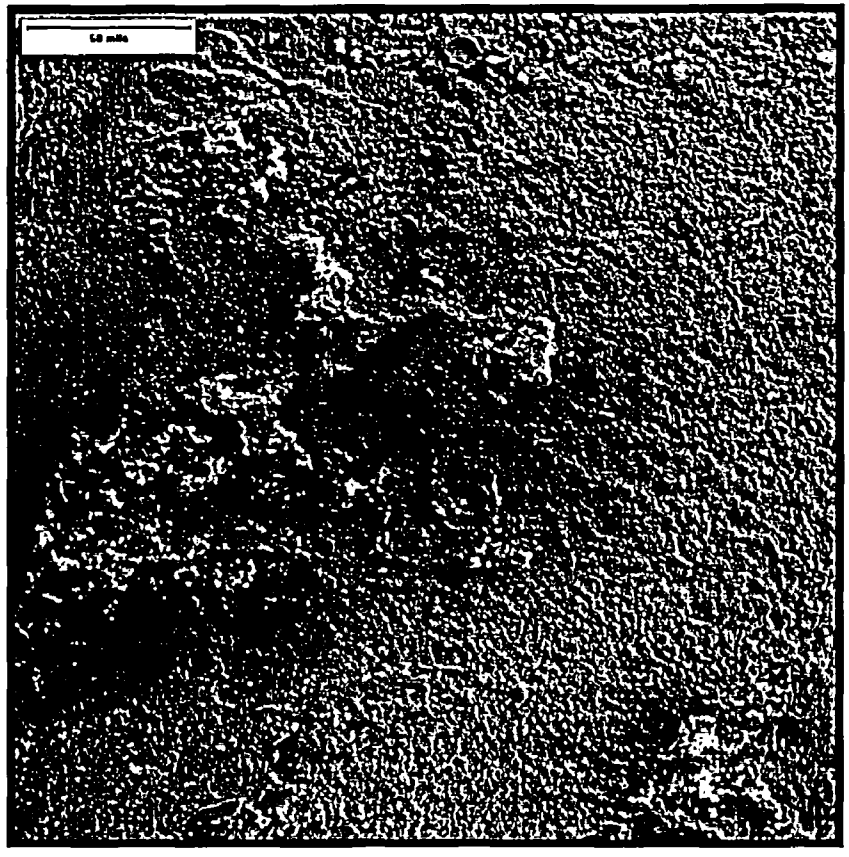

b) Area 2R

Figure 10-3 Reflected Energy Mode SEM micrographs showing OD deposit on R12C59 HL Piece 2B at areas designated on Figure 10-1.

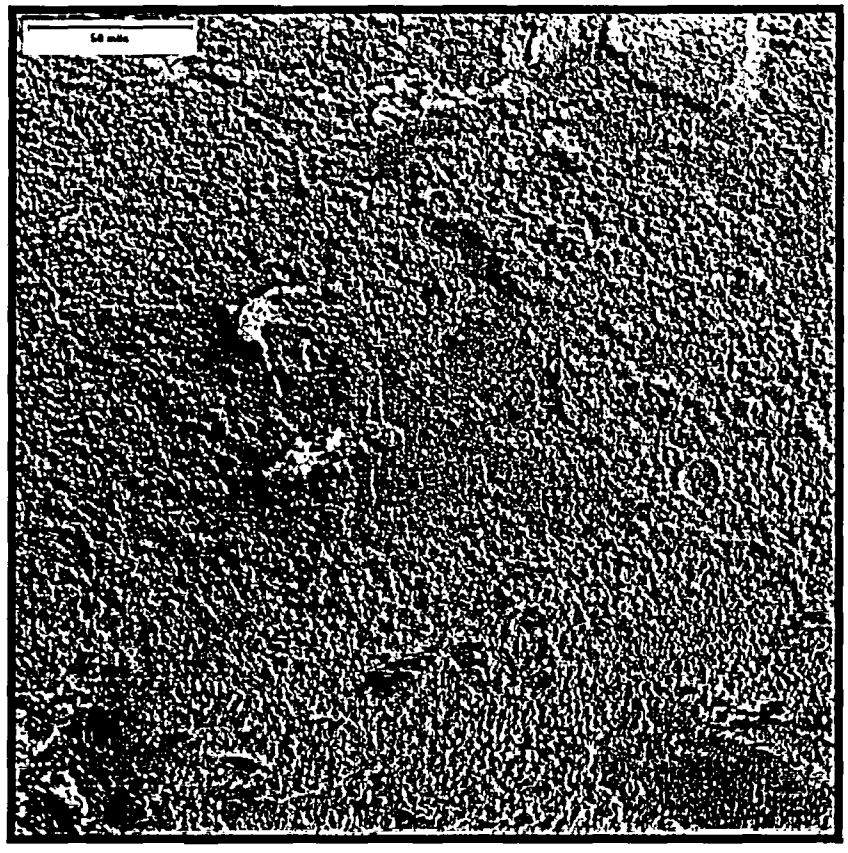

c) Area 3R

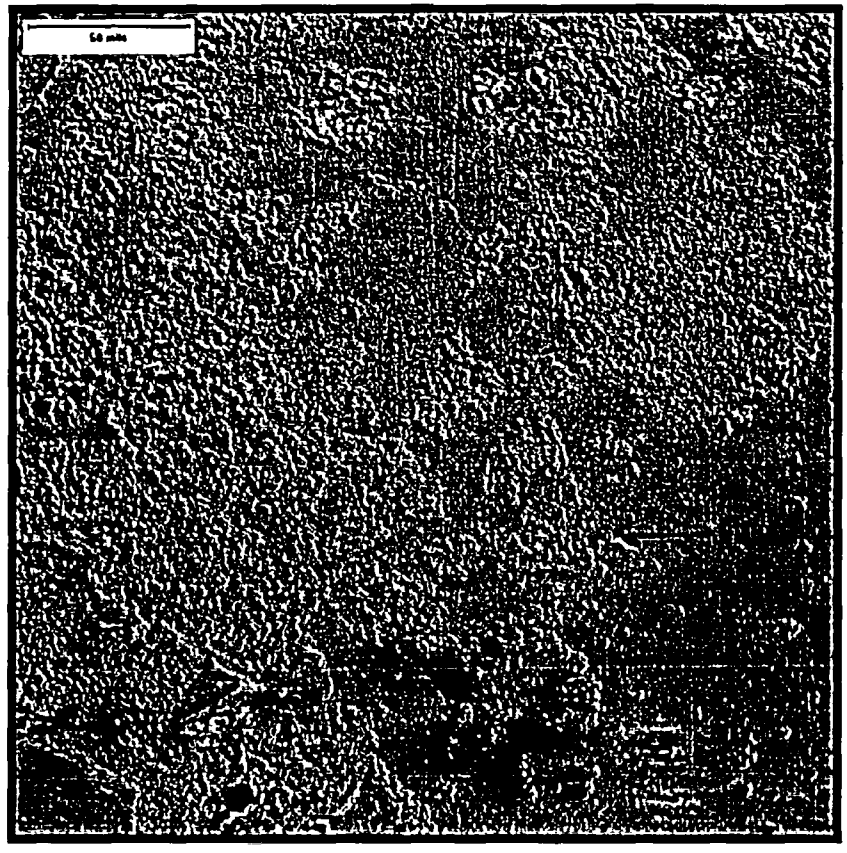

d) Area 4R

Figure 10-3 (Cont'd) Reflected Energy Mode SEM micrographs showing OD deposit on R12C59 HL Piece 2B at areas designated on Figure 10-1.

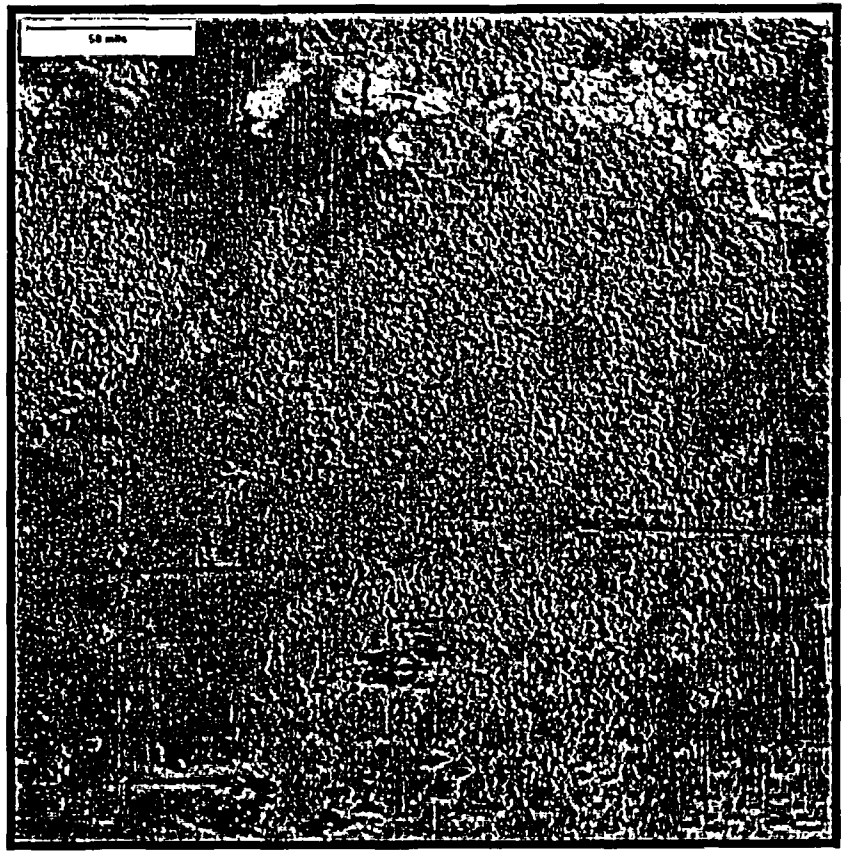

c) Area 5R

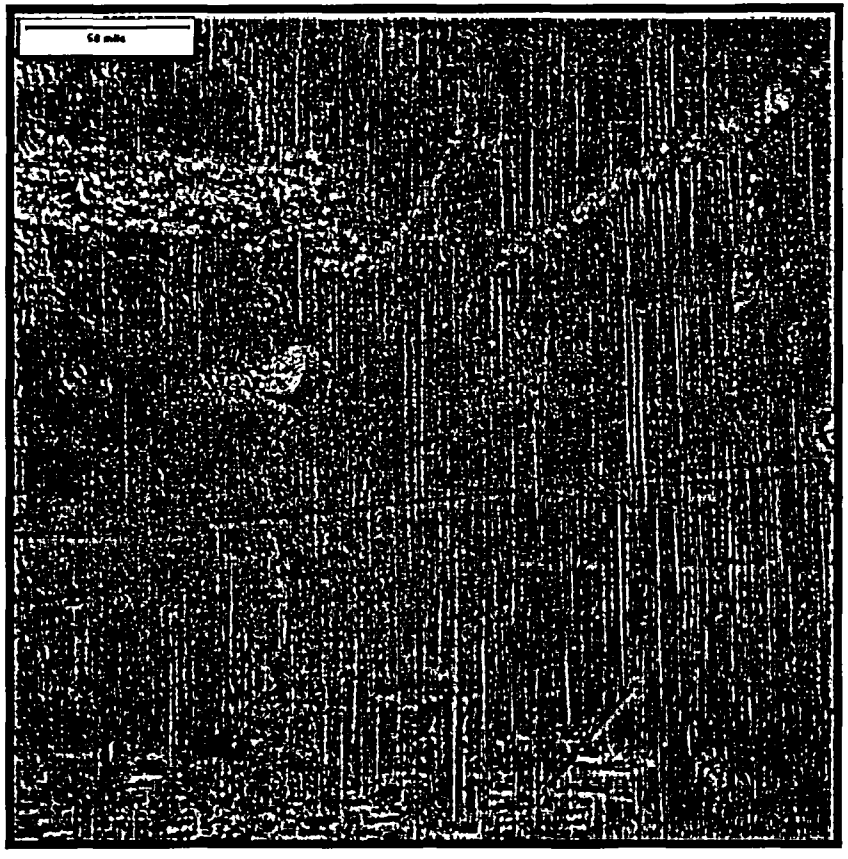

d) Area 6R

Figure 10-3 (Cont'd) Reflected Energy Mode SEM micrographs showing OD deposit on R12C59 HL Piece 2B at areas designated on Figure 10-1. The white areas seen on the above SEM micrographs are the result of remote handling in the glove box.

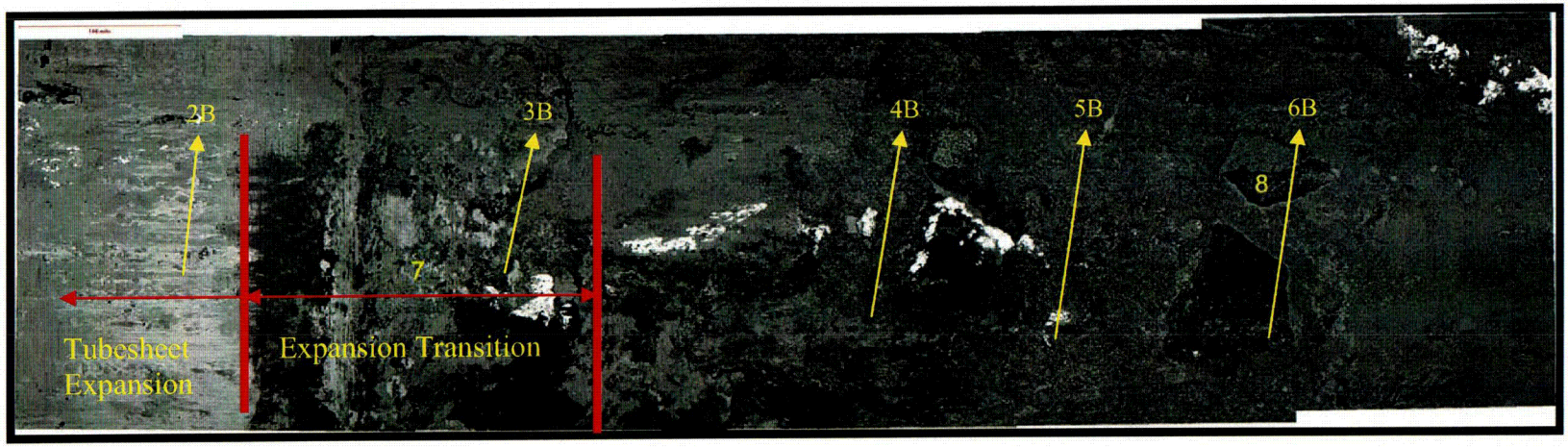

a) Backscatter Energy Mode

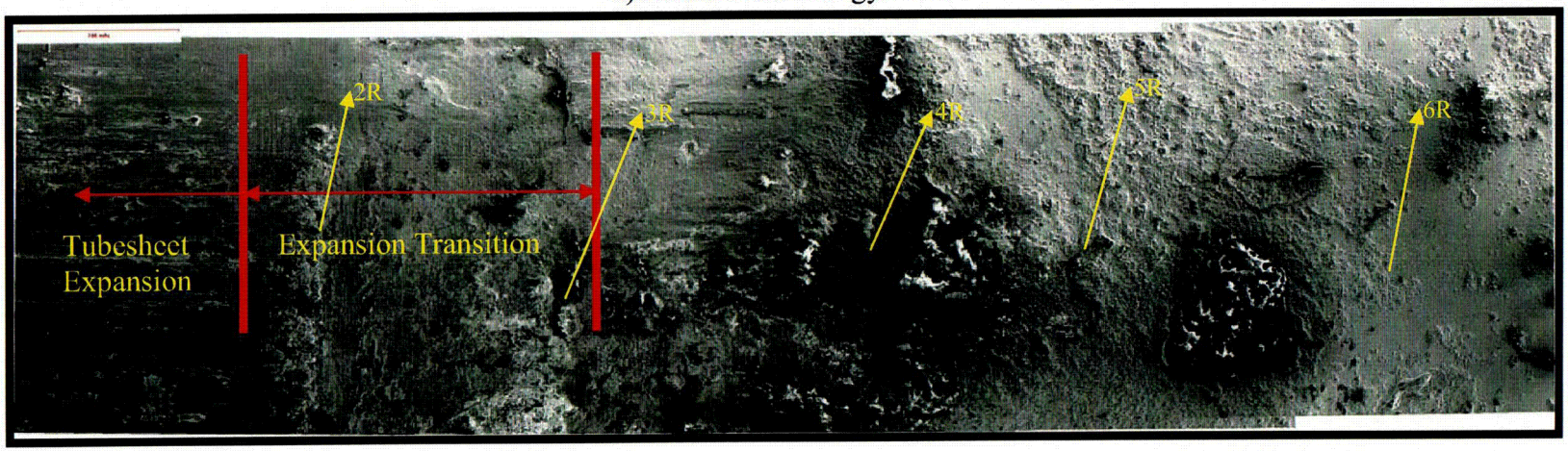

b) Reflected Energy Mode

Figure 10-4 Montage of OD Deposit from TTS Region of R12C59 Piece 2B at 45° Azimuthal Orientation (Field UT signal location). The location of the expansion transition is based on the results of laser profiling of the ID silastic mold. Additional SEM micrographs of the areas noted are shown in Figures 10-5 and 10-6. Areas identified as (7) and (8) on the Backscatter Energy Mode montage are regions were EDS analyses were performed.

a) Area 2B

b) Area 3B

Figure 10-5 Backscatter Energy Mode SEM micrographs showing OD deposit on R12C59 HL Piece 2B at 45° azimuthal orientation and at areas designated in Figure 10-4. Results of EDS analyses are shown in Table 10-2 and Figures 10-24 and 10-25. The white areas seen on the above SEM micrographs are the result of remote handling in the glove box.

c) Area 4B

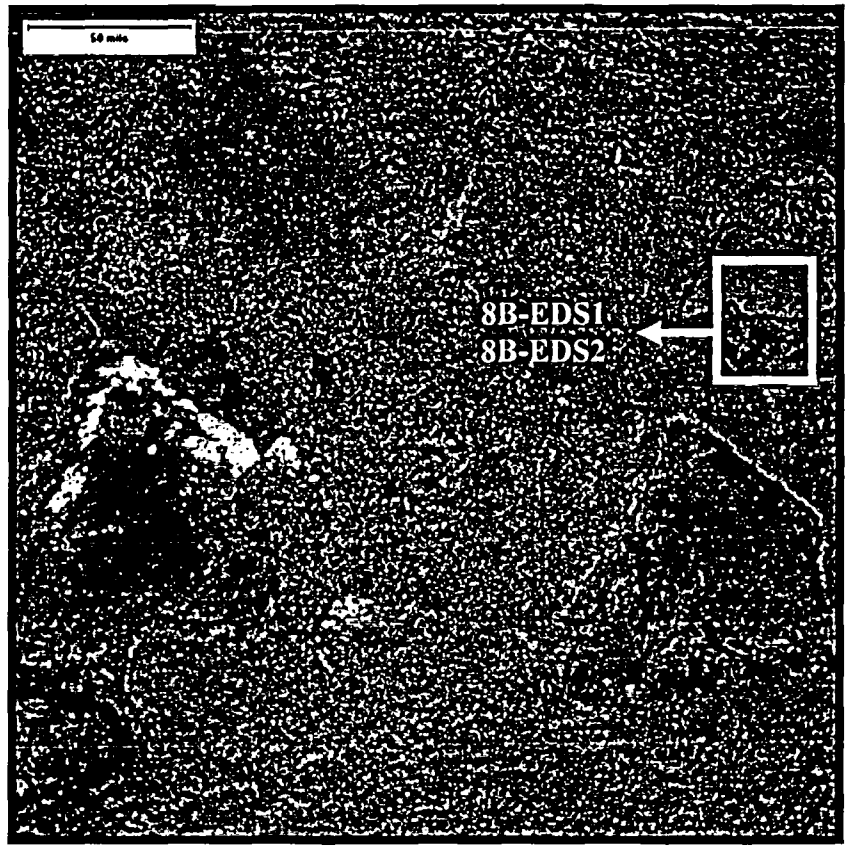

d) Area 5B

Figure 10-5(Cont'd) Backscatter Energy Mode SEM micrographs showing OD deposit on R12C59 HL Piece 2B at the 45° azimuthal orientation and at areas designated in Figure 10-4. Results of EDS analyses are shown in Table 10-2 and Figure 10-24. The white areas seen on the above SEM micrographs are the result of remote handling in the glove box.

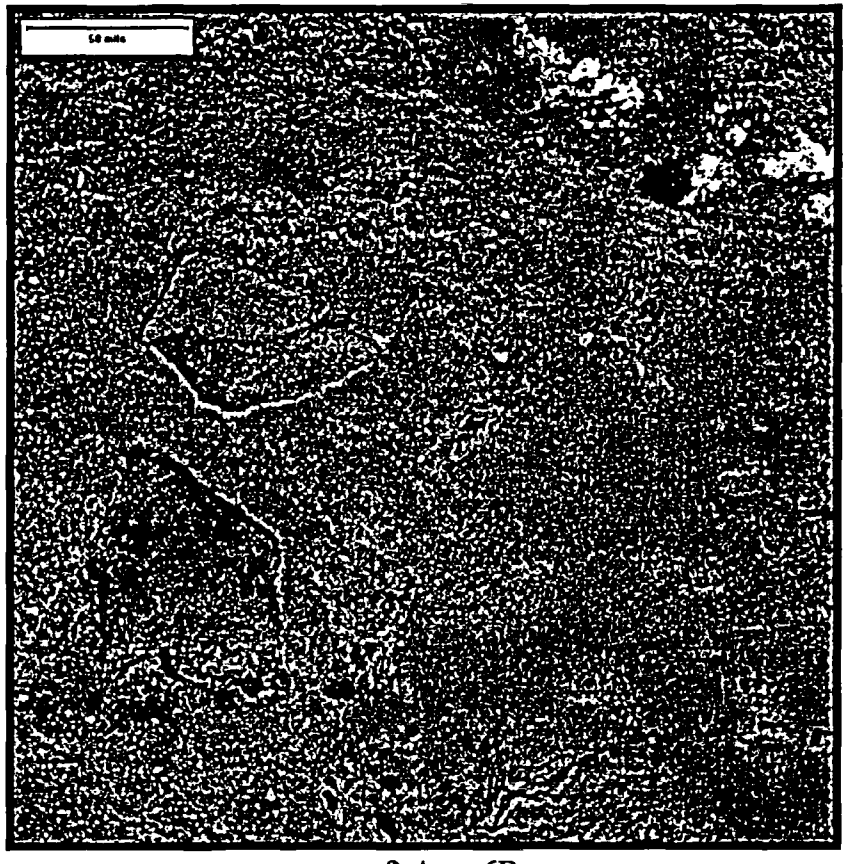

f) Area 6B

Figure 10-5 (Cont'd) Backscatter Energy Mode SEM micrographs showing OD deposit on R12C59 HL Piece 2B at the 45° azimuthal orientation and at areas designated in Figure 10-4. The white areas seen on the above SEM micrograph are the result of remote handling in the glove box.

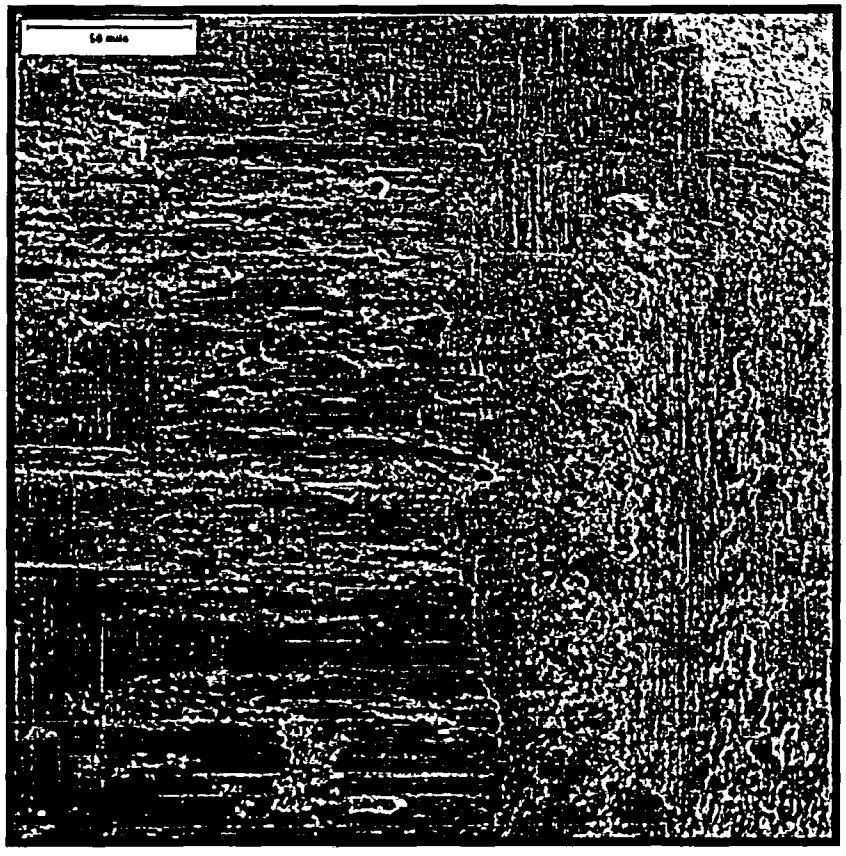

a) Area 2R

Figure 10-6 Reflected Energy Mode SEM micrographs showing OD deposit on R12C59 HL Piece 2B at the 45° azimuthal orientation and at areas designated on Figure 10-4.

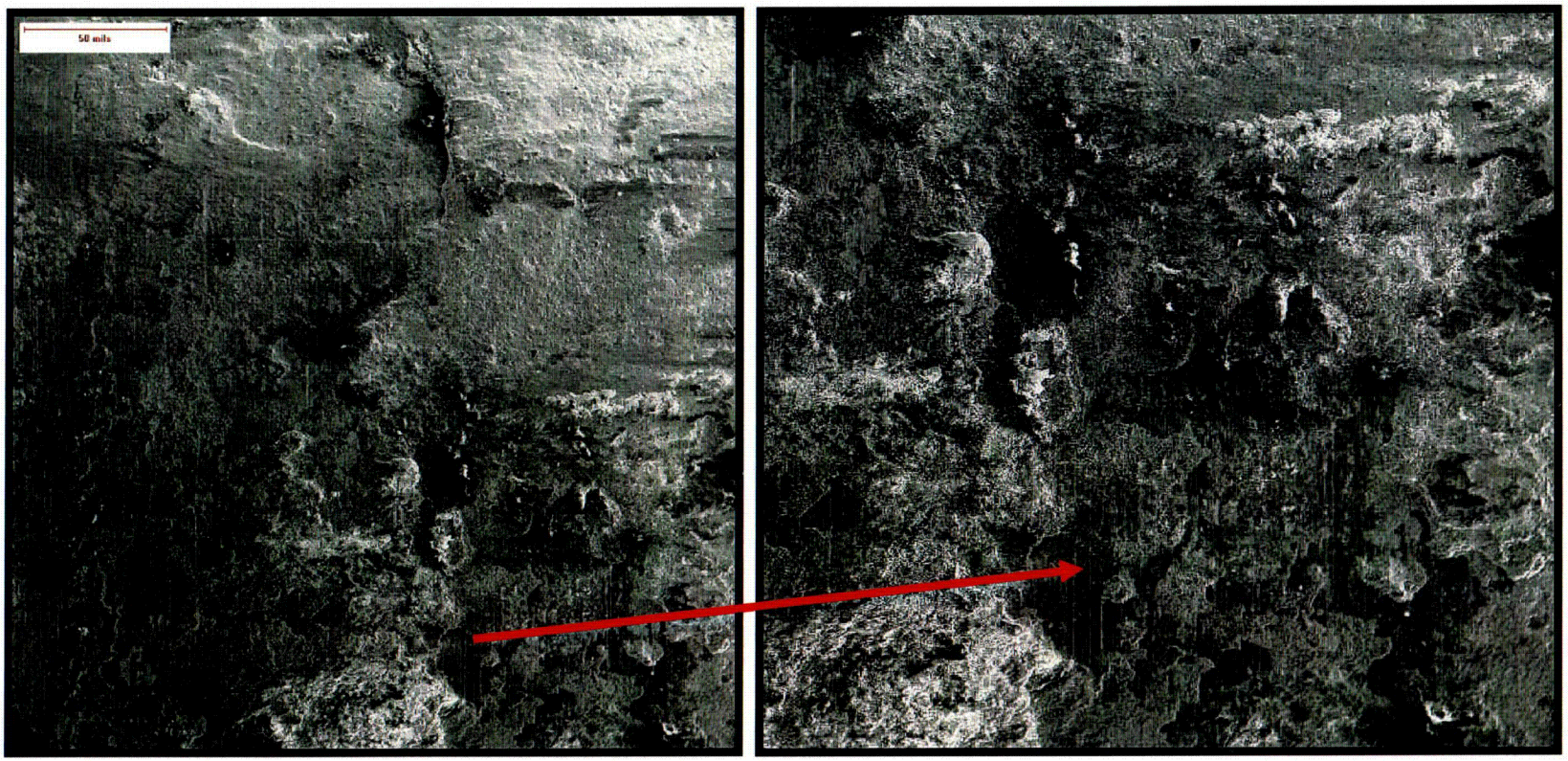

b) Area 3R

Figure 10-6 (Cont'd) Reflected Energy Mode SEM Micrograph Showing OD Deposit Appearance at TTS Region of R12C59 - Piece 2B at 45° Azimuthal Orientation (Field UT signal location) at Area 3R shown in Figure 10-4.
Note: Local area at tube expansion transition showing an apparent lack of OD surface deposit

c) Area 4R

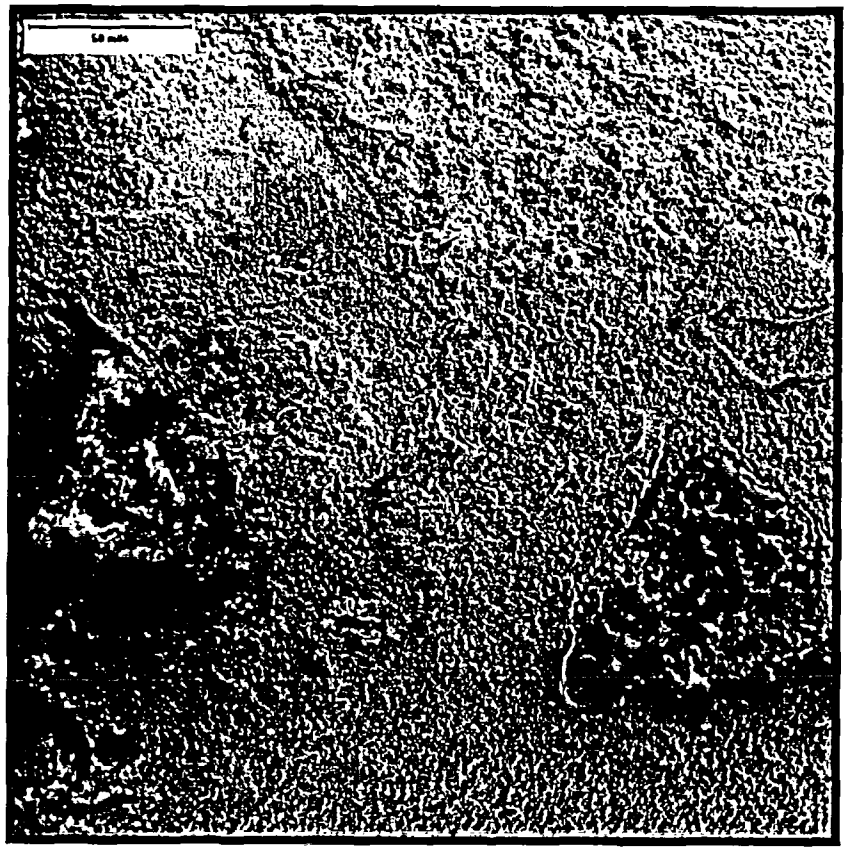

d) Area 5R

Figure 10-6 (Cont'd) Reflected Energy Mode SEM micrographs showing OD deposit on R12C59 HL Piece 2B at the 45° azimuthal orientation and at areas designated on Figure 10-4.

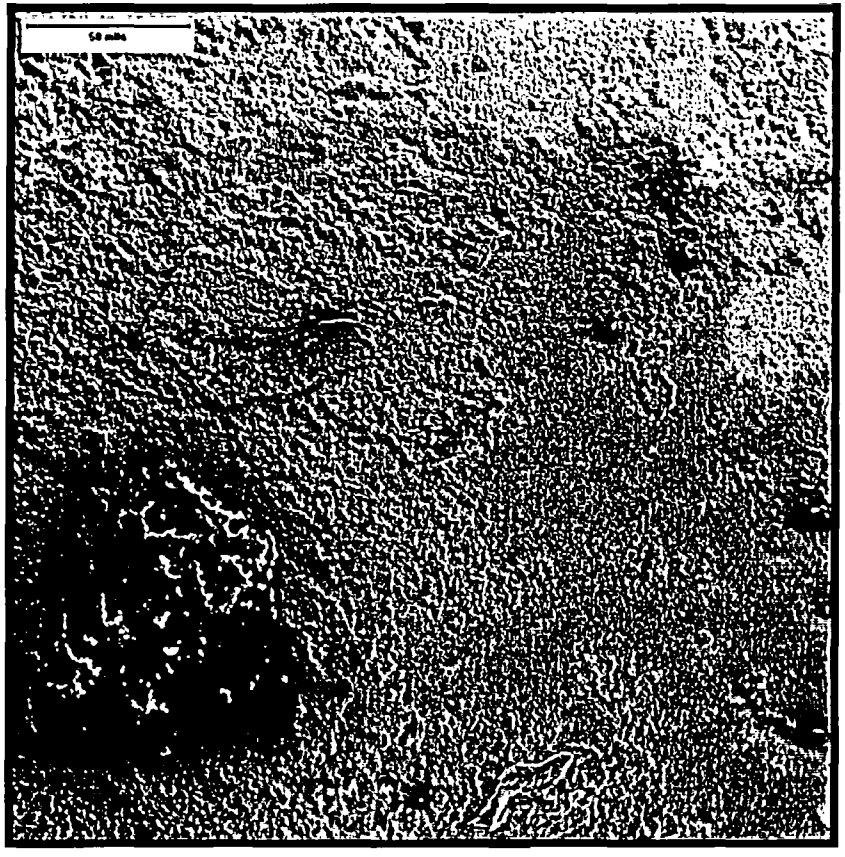

c) Area 6R

Figure 10-6 (Cont'd) Reflected Energy Mode SEM micrographs showing OD deposit on R12C59 HL Piece 2B at the 45° azimuthal orientation and at areas designated on Figure 10-4.

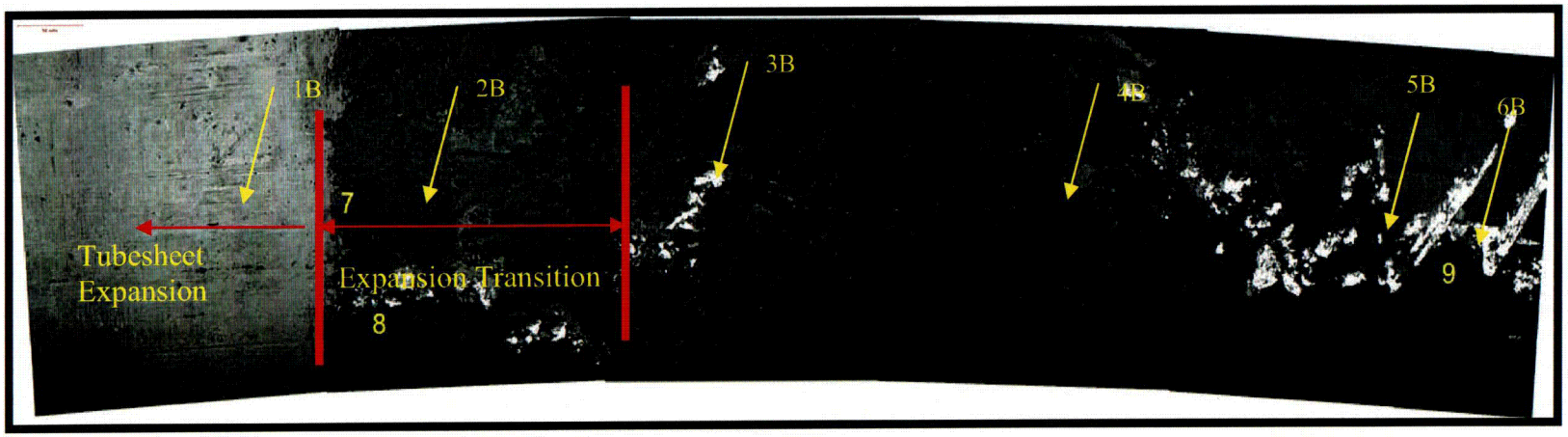

a) Backscatter Energy Mode

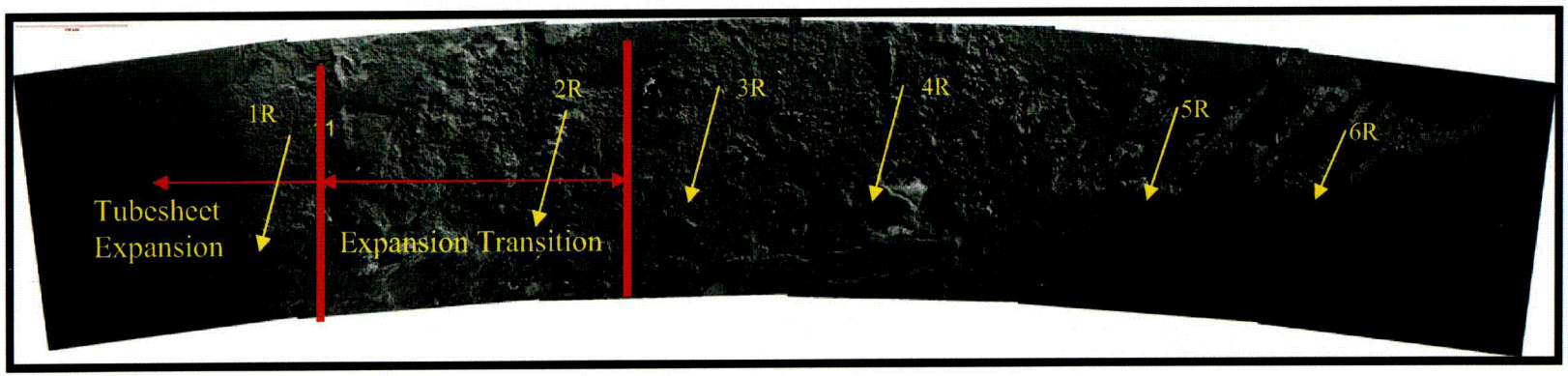

b) Reflected Energy Mode

Figure 10-7 Montage of OD Deposit from TTS Region of R11C60 Piece 2B at 327° Azimuthal Orientation (+Pt signal location). The location of the expansion transition is based on the results of laser profiling of the ID silastic mold. Additional SEM micrographs of the areas noted are shown in Figures 10-8 and 10-9. Areas identified as (7), (8), (9), and (11) are regions were EDS analyses were performed. White areas shown are related to handling in the Hot Cell glove box.

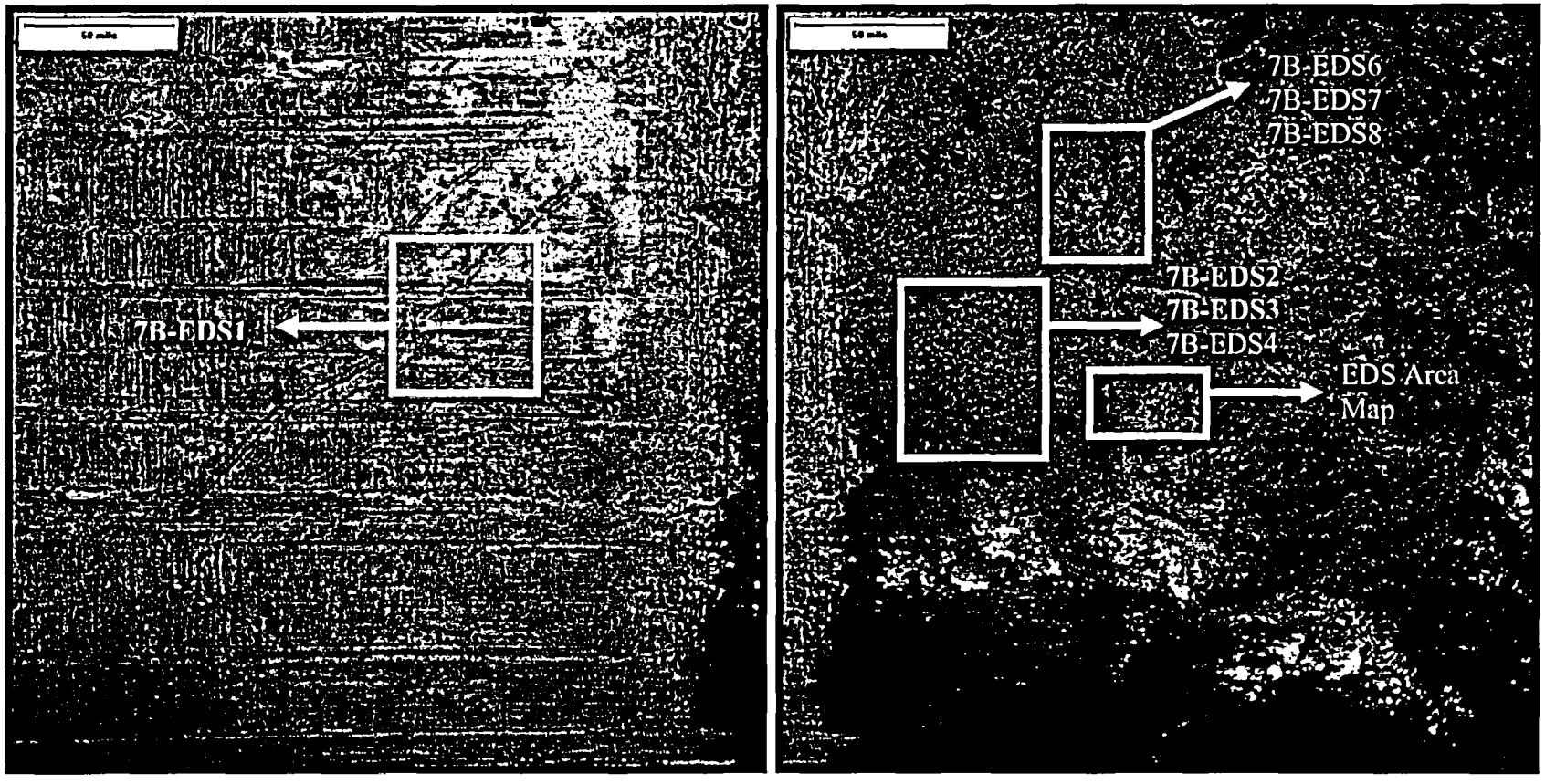

a) Area 1B

b) Area 2B

Figure 10-8 Backscatter Energy Mode SEM micrographs showing OD deposit on R11C60 HL - Piece 2B at 327° azimuthal orientation and at areas designated in Figure 7. Results of EDS analyses are shown in Table 10-3 and Figures 10-26 and 10-27. White areas shown are related to handling in the Hot Cell glove box.

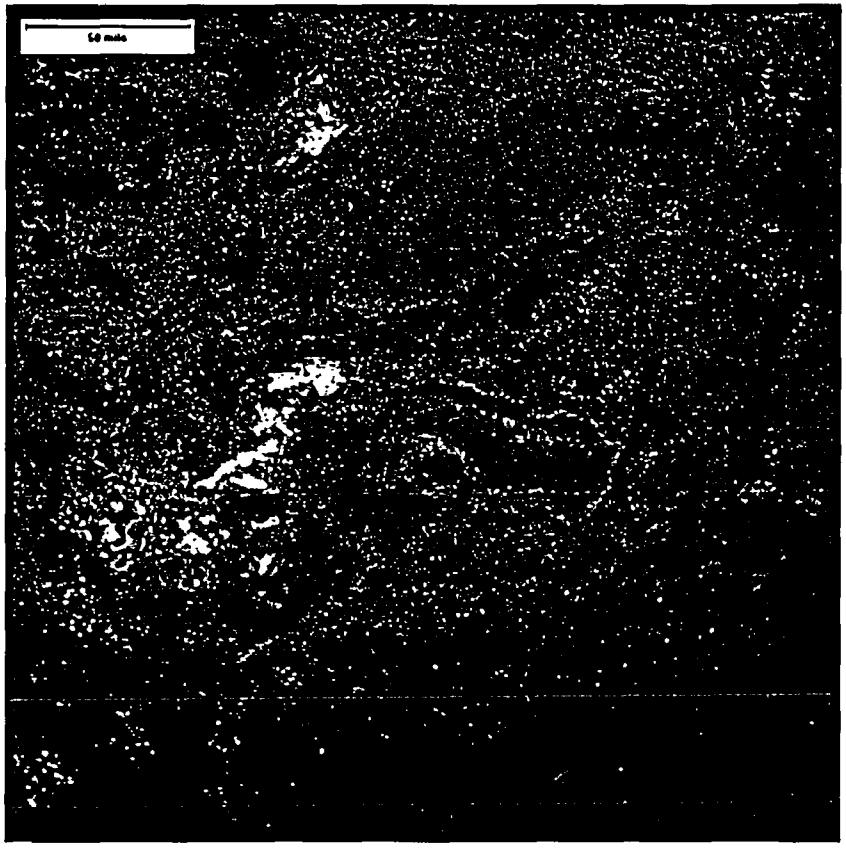

c) Area 3B

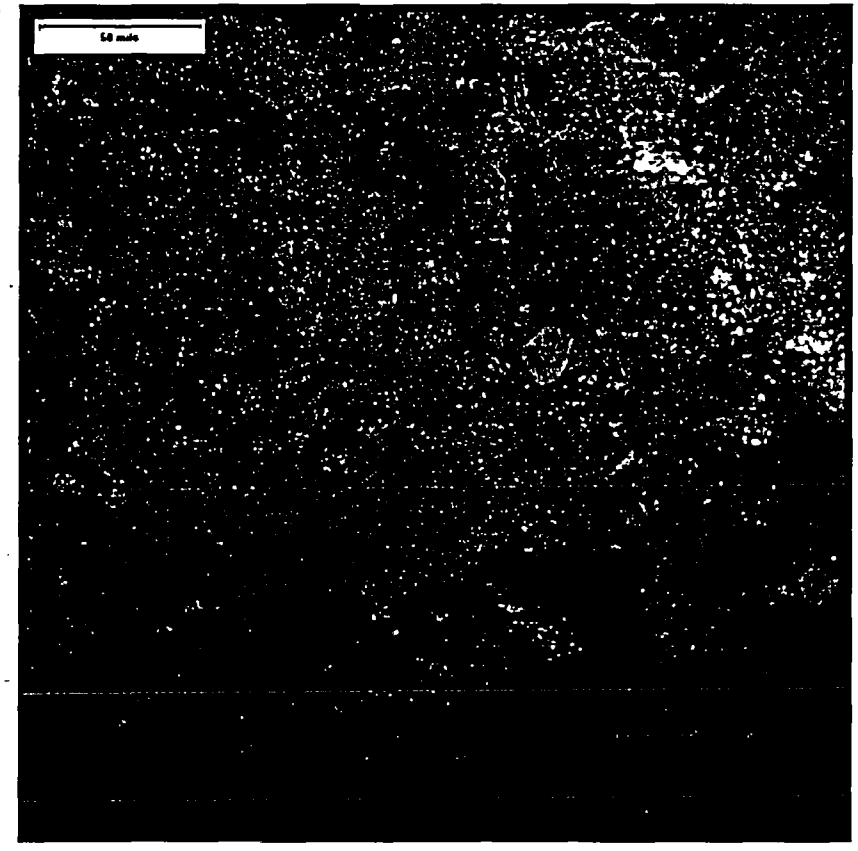

d) Area 4B

Figure 10-8(Cont'd) Backscatter Energy Mode SEM micrographs showing OD deposit on R11C60 HL Piece 2B at 327° azimuthal orientation and at areas designated in Figure 10-7. White areas shown are related to handling in the Hot Cell glove box.

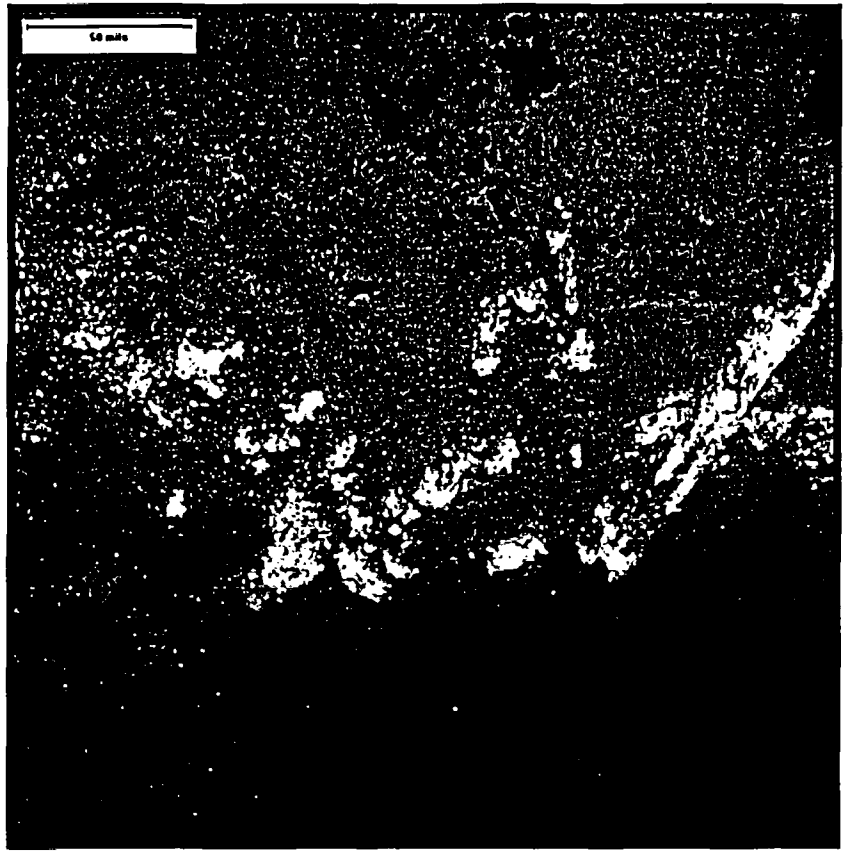

c) Area 5B

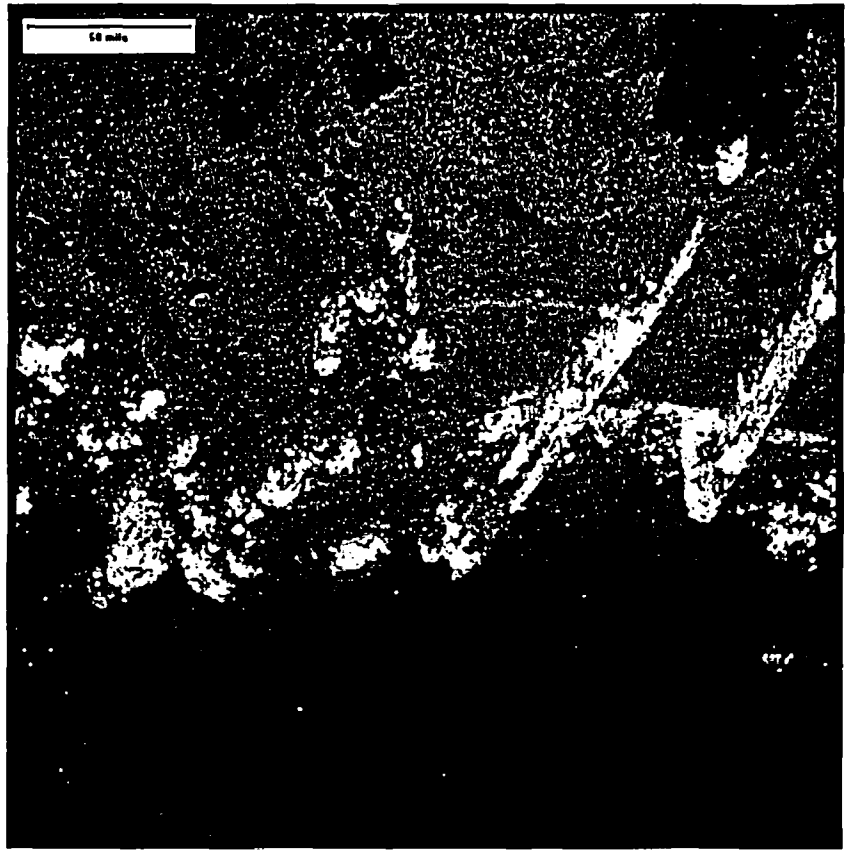

f) Area 6B

Figure 10-8(Cont'd) Backscatter Energy Mode SEM micrographs showing OD deposit on R11C60 HL Piece 2B at 327° azimuthal orientation and at areas designated in Figure 10-7. The white areas seen in the above micrographs are related to handling of the pulled tube sections in the Remote Handling Hot Cell Glove Box.

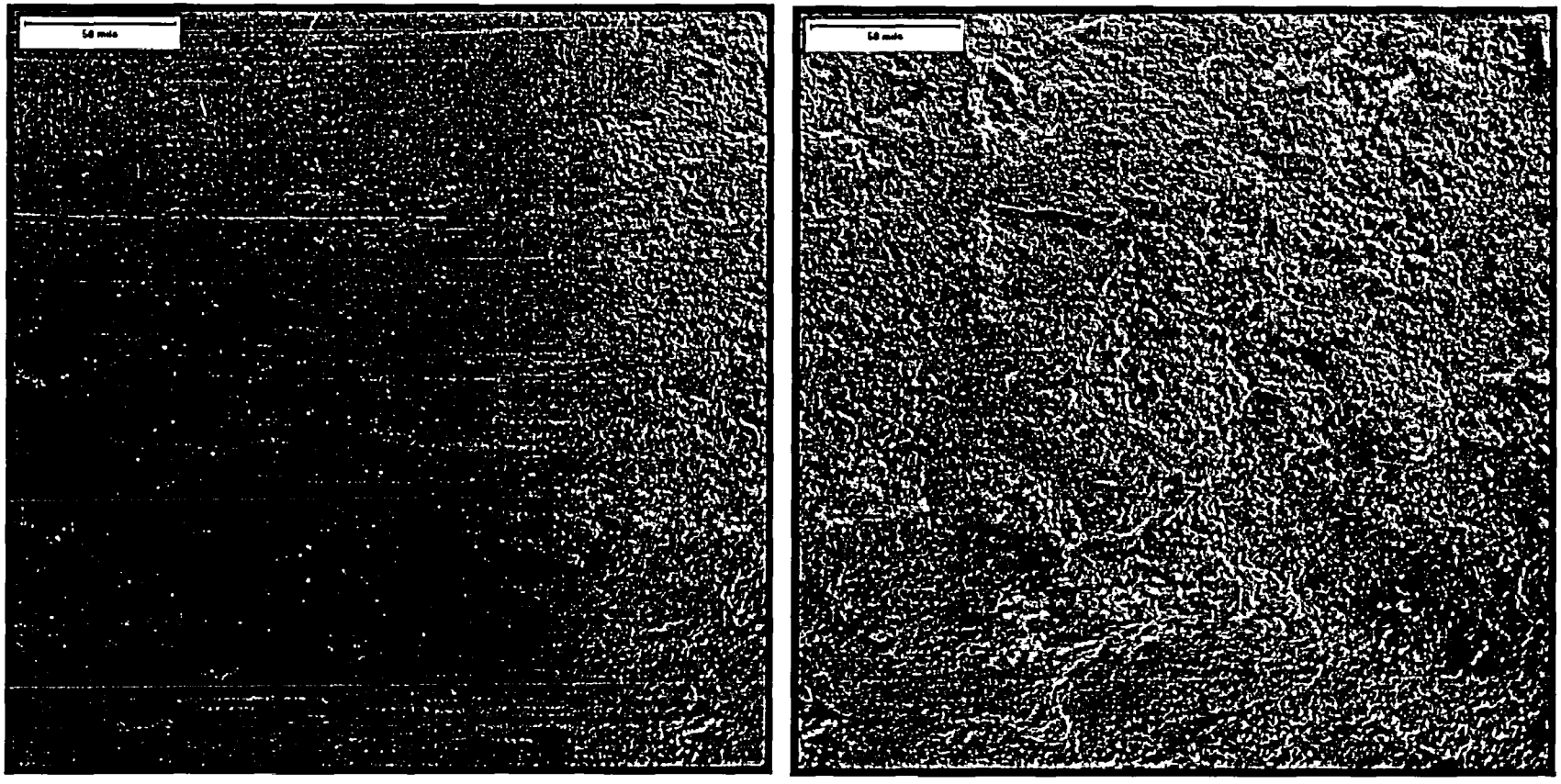

a) Area 1R b) Area 2R

Figure 10-9 Reflective Energy Mode SEM micrographs showing OD deposit on R11C60 HL Piece 2B at 327° azimuthal orientation and at areas designated in Figure 10-7.

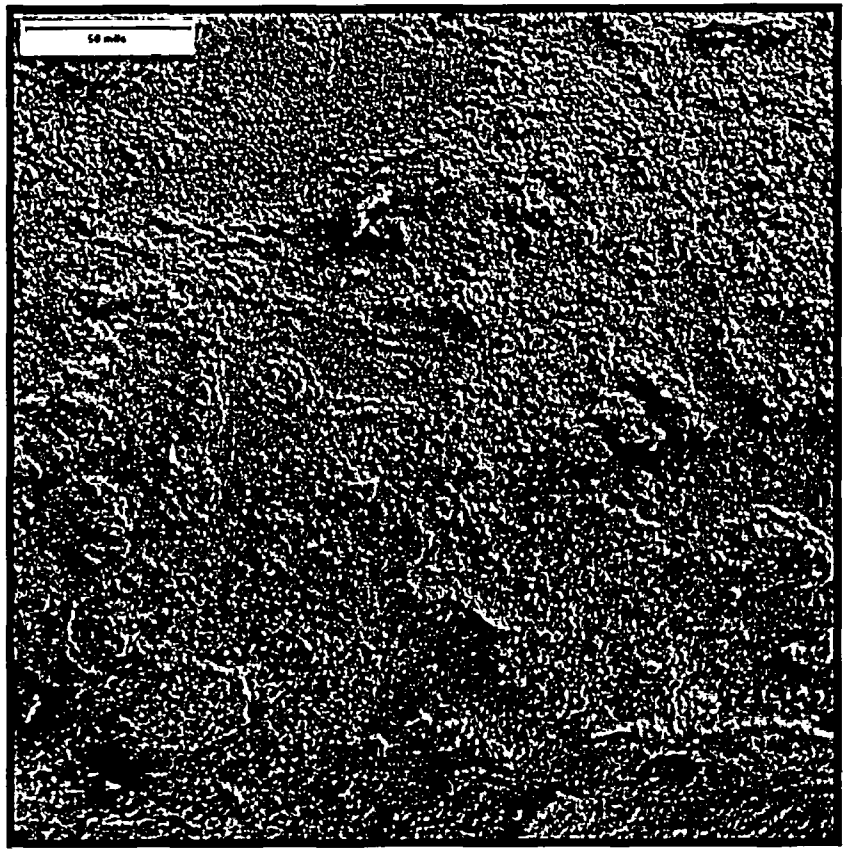

c) Area 3R

d) Area 4R

Figure 10-9 (Cont'd) Reflective Energy Mode SEM micrographs showing OD deposit on R11C60 HL Piece 2B at 327° azimuthal orientation and at areas designated in Figure 10-7.

e) Area 5R

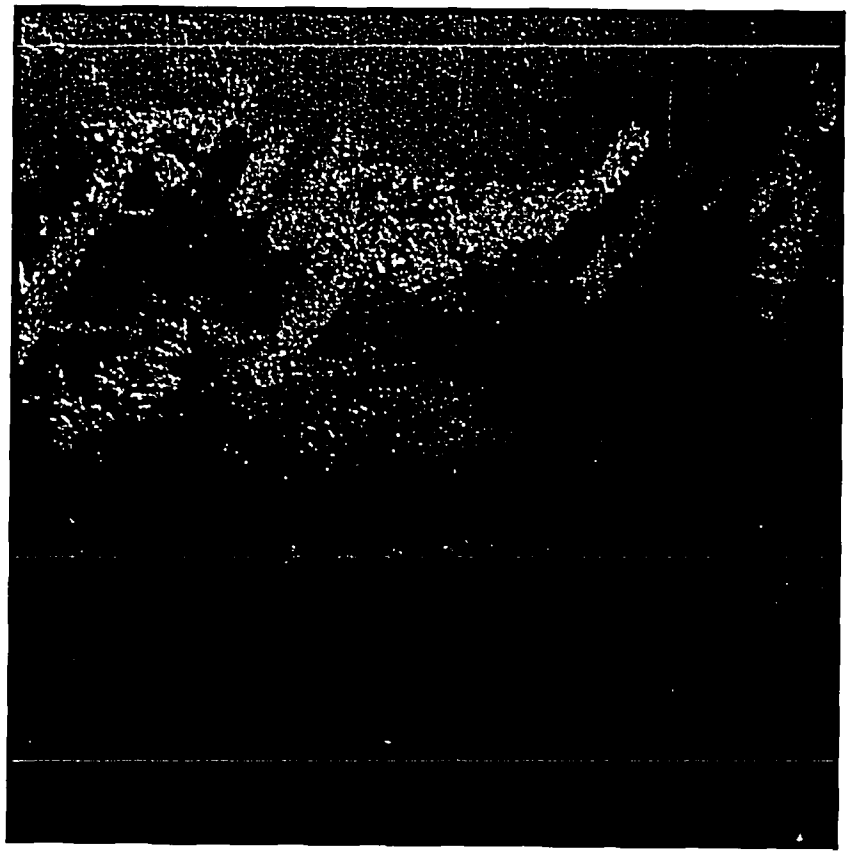

f) Area 6R

Figure 10-9 (Cont'd) Reflective Energy Mode SEM micrographs showing OD deposit on R11C60 HL Piece 2B at 327° azimuthal orientation and at areas designated in Figure 10-7.

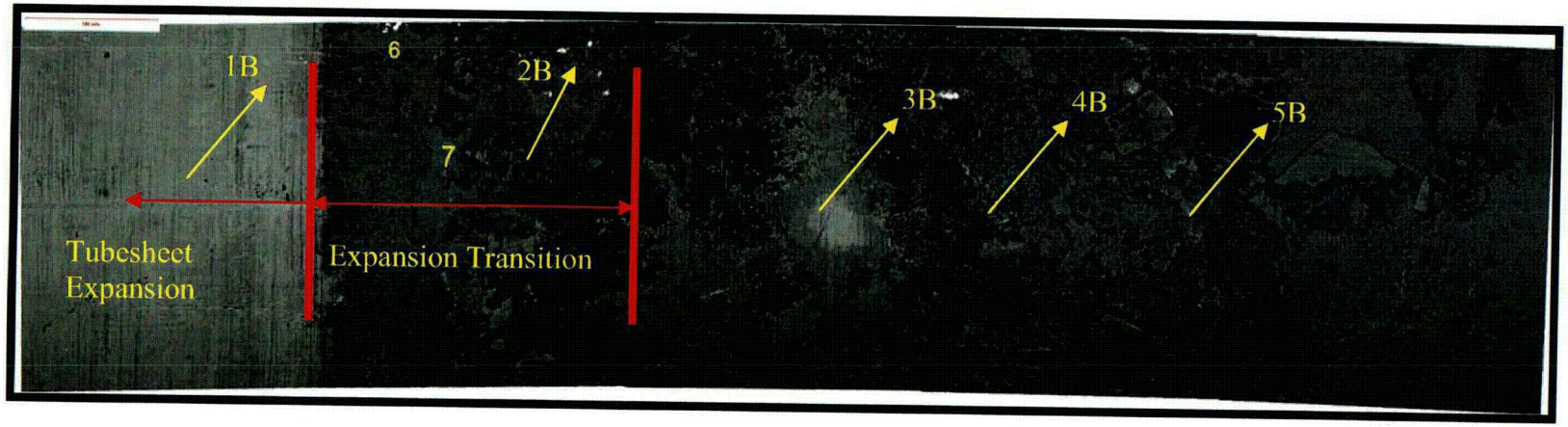

a) Backscatter Energy Mode

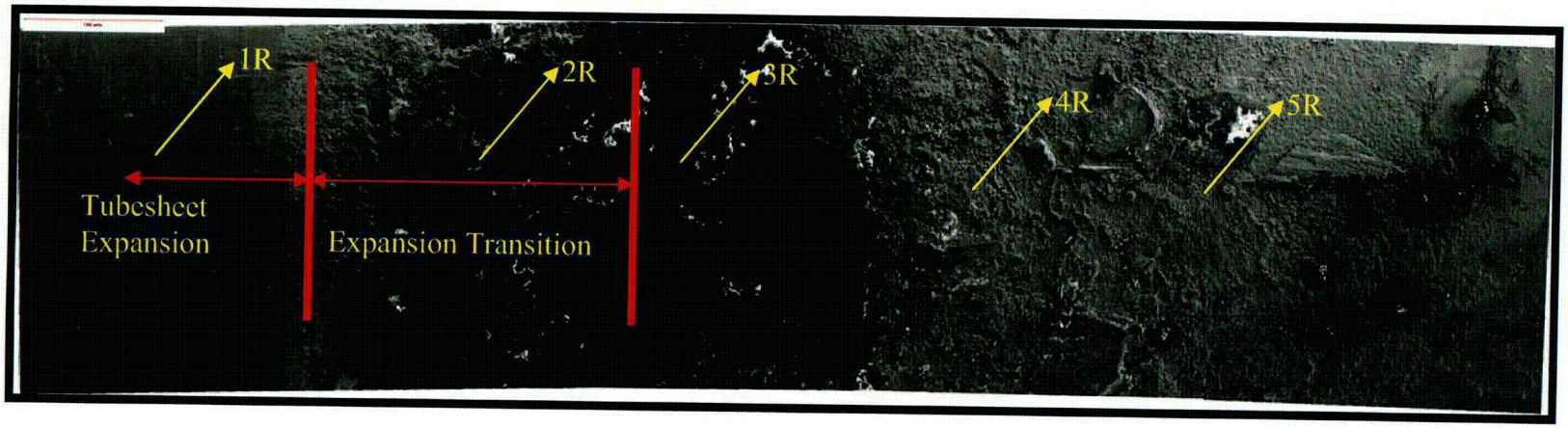

b) Reflective Energy Mode

Figure 10-10 Montage of OD Deposit from TTS Region of R11C60 Piece 2B at 130° Azimuthal Orientation (+UT signal location). The location of the expansion transition is based on the results of laser profiling of the ID silastic mold. Additional SEM micrographs of the areas noted are shown in Figures 10-11 and 10-12. Areas identified as (6) and (7) are regions were EDS analyses were performed.

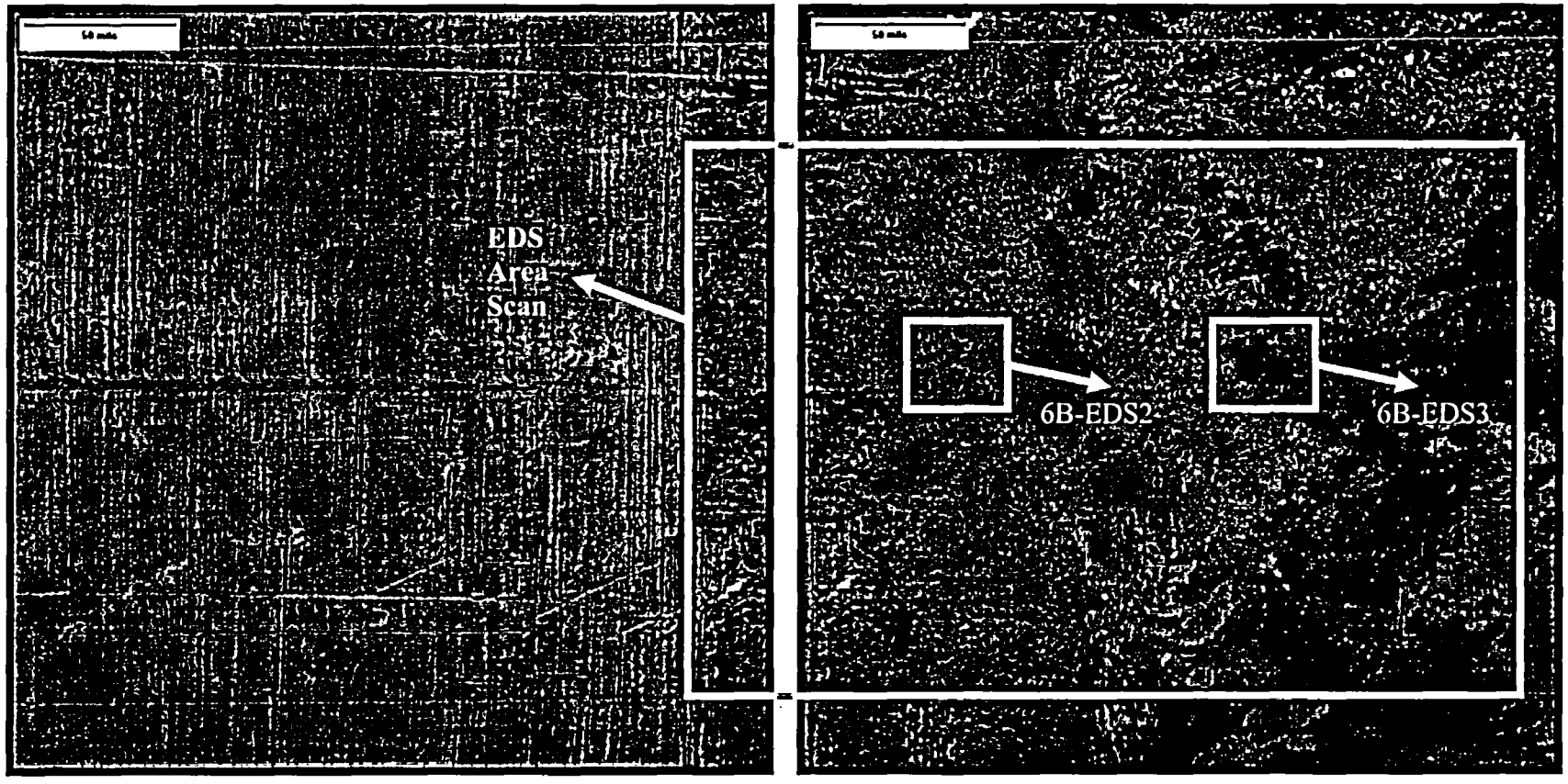

a) Area 1B

b) Area 2B

Figure 10-11 Backscatter Energy Mode SEM micrographs showing OD deposit on R11C60 HL Piece 2B at 130° azimuthal orientation and at areas designated in Figure 10-10. Results of EDS analyses are shown in Table 10-4 and Figures 10-28 and 10-29.

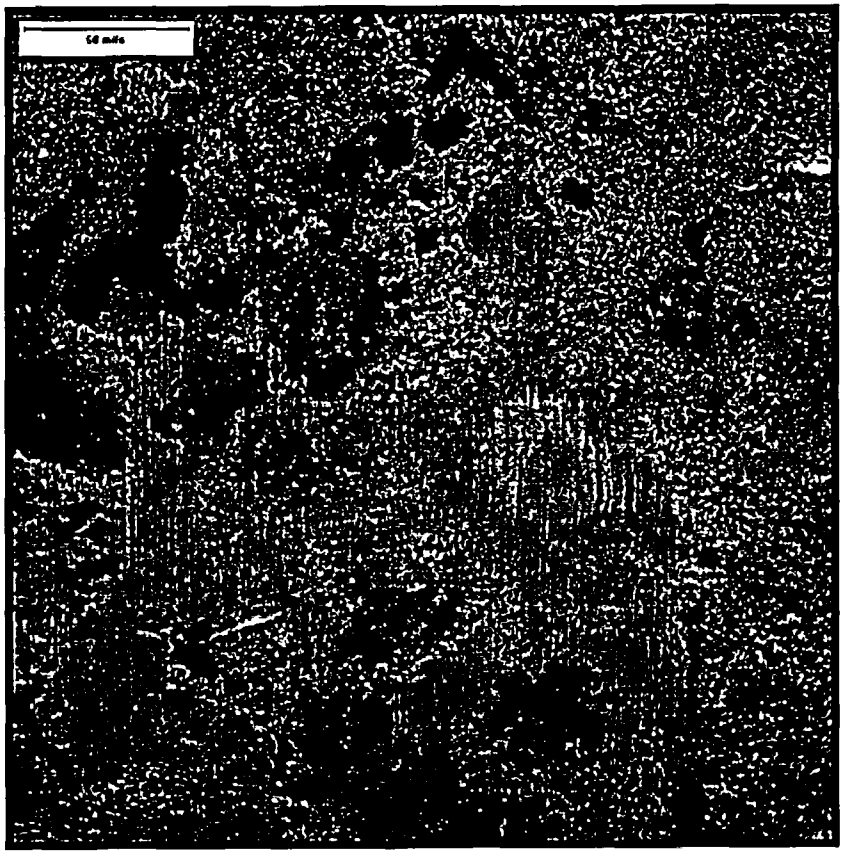

c) Area 3B

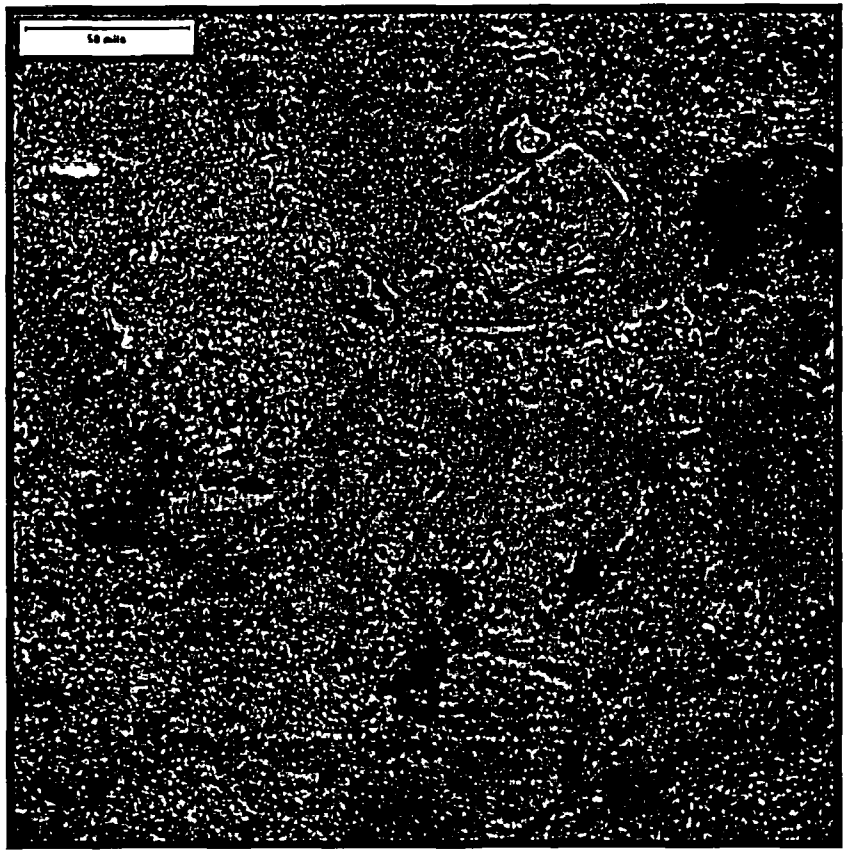

d) Area 4B

Figure 10-11 (Cont'd) Backscatter Energy Mode SEM micrographs showing OD deposit on R11C60 HL Piece 2B at 130° azimuthal orientation and at areas designated in Figure 10-10.

e) Area 5B

Figure 10-11 (Cont'd) Backscatter Energy Mode SEM micrographs showing OD deposit on R11C60 HL Piece 2B at 130° azimuthal orientation and at areas designated in Figure 10-10.

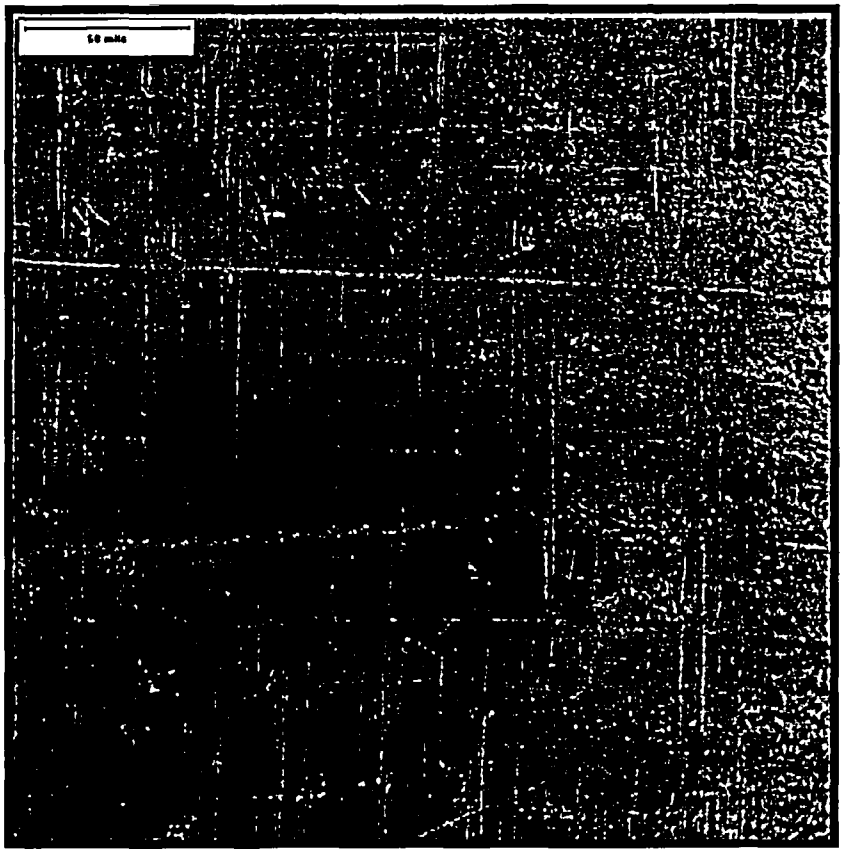

a) Area 1R

b) Area 2R

Figure 10-12 Reflective Energy Mode SEM micrographs showing OD deposit on R11C60 HL Piece 2B at 130° azimuthal orientation and at areas designated in Figure 10-10. Refer to Figure 10-13 for additional SEM micrograph of point identified as (7) in right micrograph (b) Area 2R.

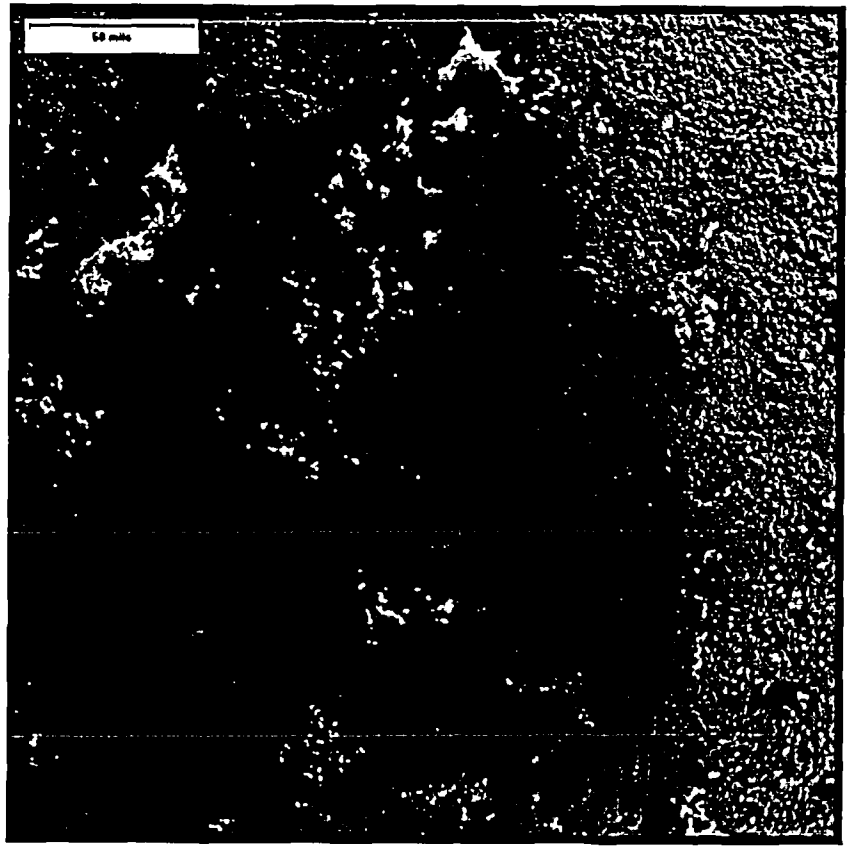

c) Area 3R

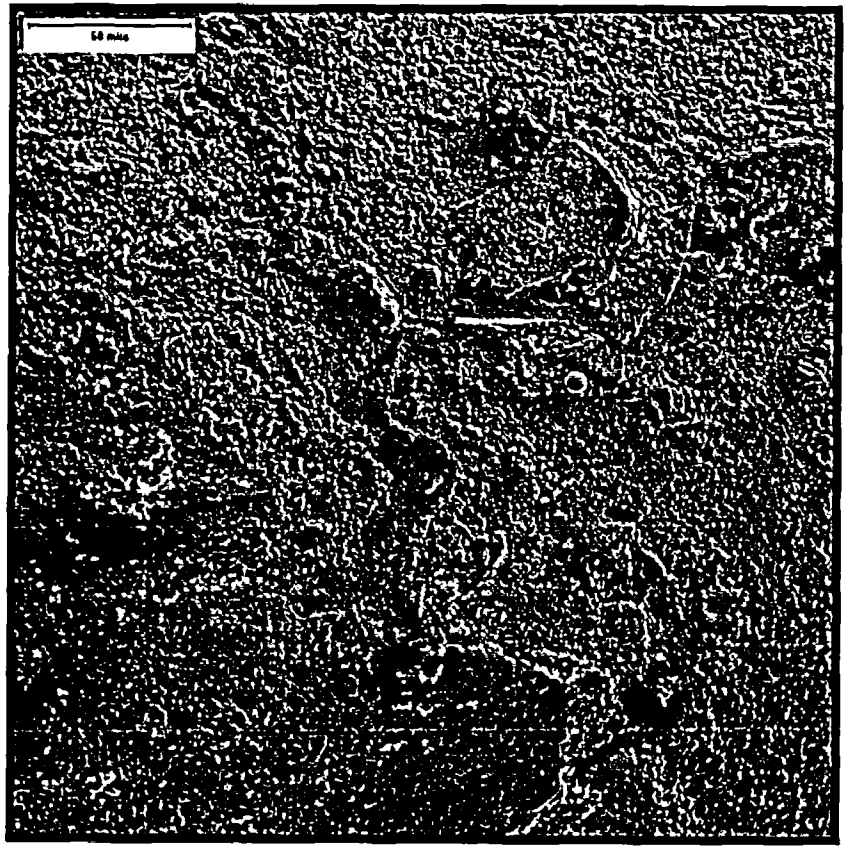

d) Area 4R

Figure 10-12(Cont'd) Reflective Energy Mode SEM micrographs showing OD deposit on R11C60 HL Piece 2B at 130° azimuthal orientation and at areas designated in Figure 10-10.

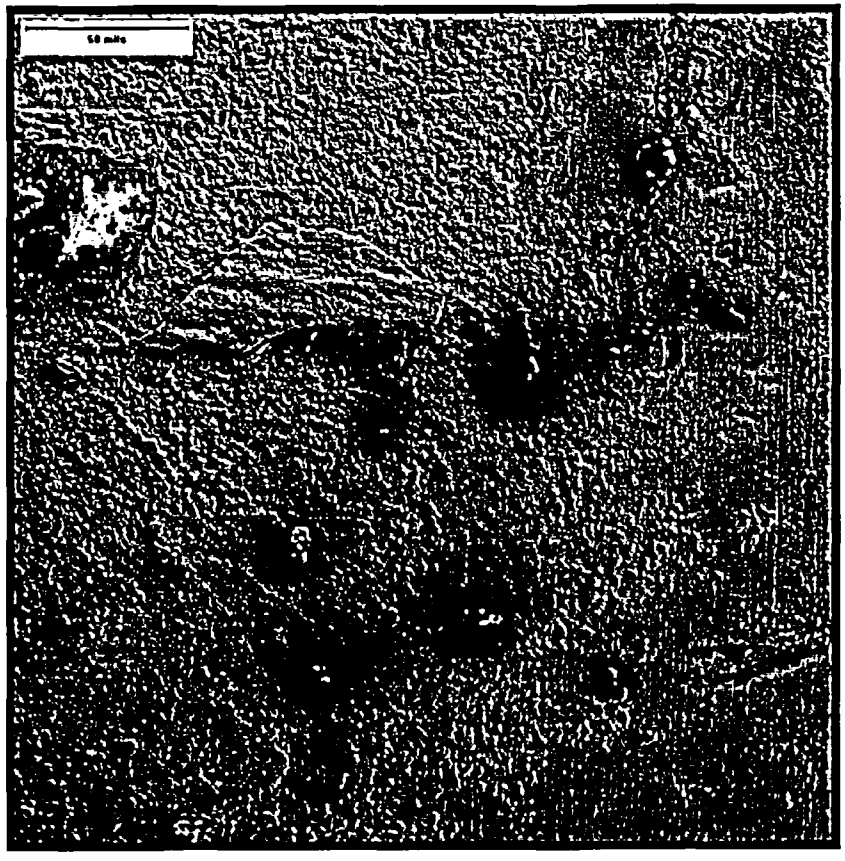

c) Area 5R

Figure 10-12(Cont'd) Reflective Energy Mode SEM micrographs showing OD deposit on R11C60 HL Piece 2B at 130° azimuthal orientation and at areas designated in Figure 10-10.

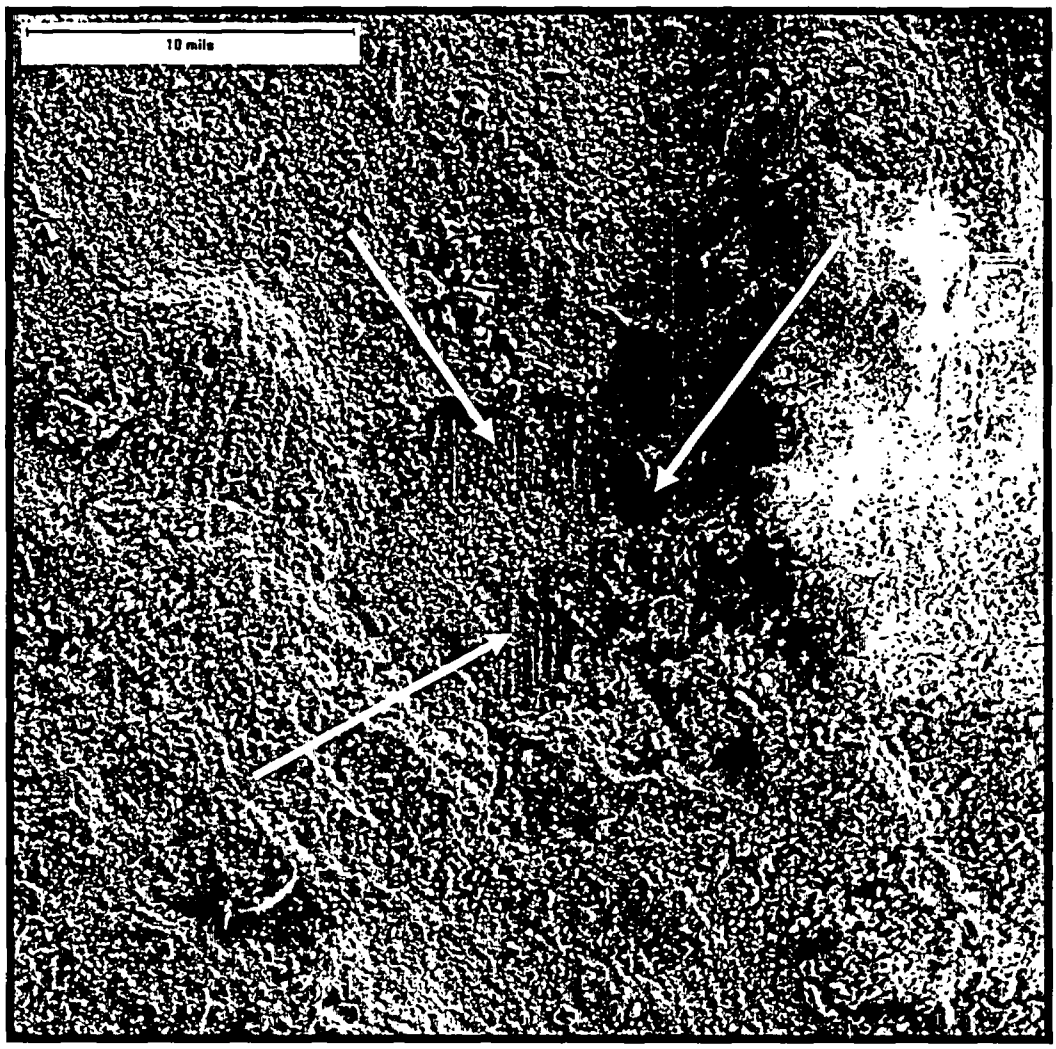

Figure 10-13 Reflective Energy Mode SEM micrograph showing local region of "missing deposit" on R11C60 HL Piece 2B at 130° azimuthal orientation. Area shown is identified as (7) in Figure 10-4.

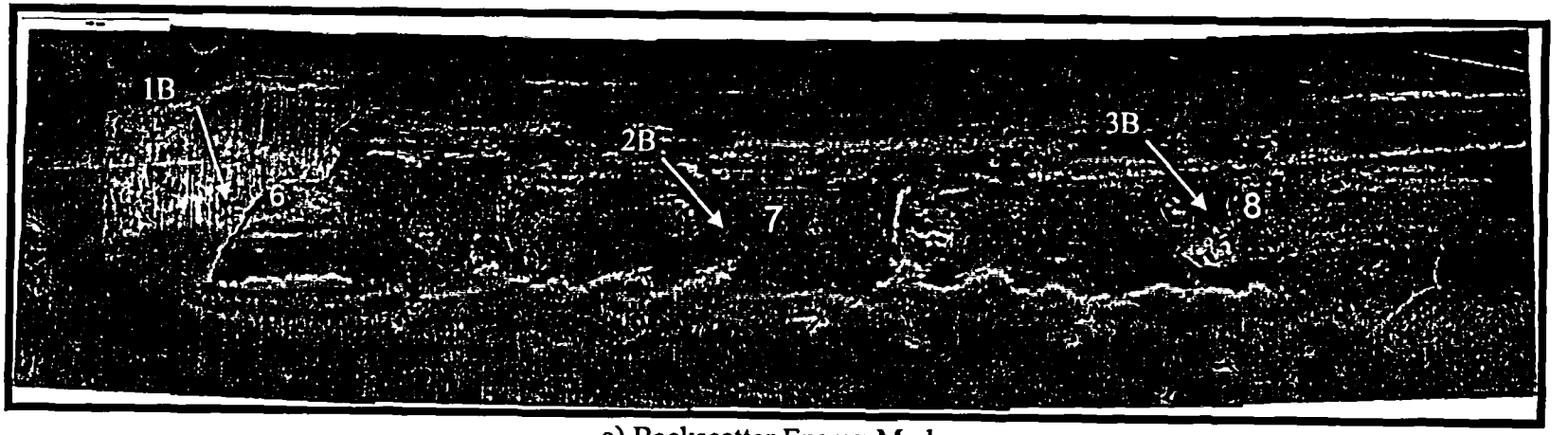

a) Backscatter Energy Mode

b) Reflective Energy Mode

Figure 10-14 Montage of OD deposit from 1st TSP of R12C59 HL Piece 3B at 10° azimuthal orientation. Refer to Figure 10-15 for additional SEM micrographs of areas shown. Areas identified as 6, 7, and 8 are regions where EDS analyses were performed.

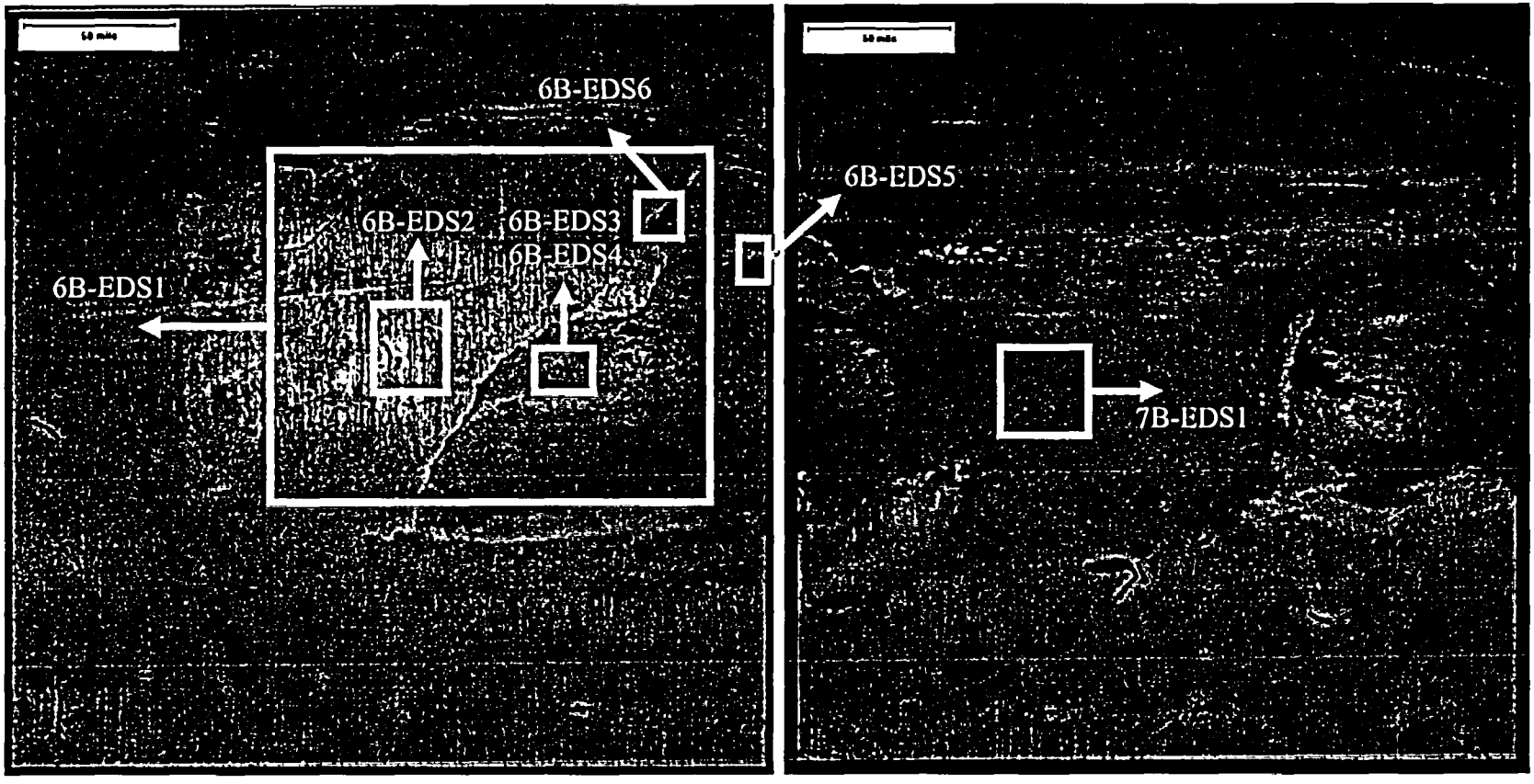

a) Area 1B

b) Area 2B

Figure 10-15 Backscatter Energy Mode SEM micrograph showing OD deposit appearance at 1st TSP of R12C59 HL Piece 3B at 10° azimuthal orientation. Refer to Figure 10-14 for area location. Results of EDS analyses are presented in Table 10-5 and Figures 10-30 and 10-31.

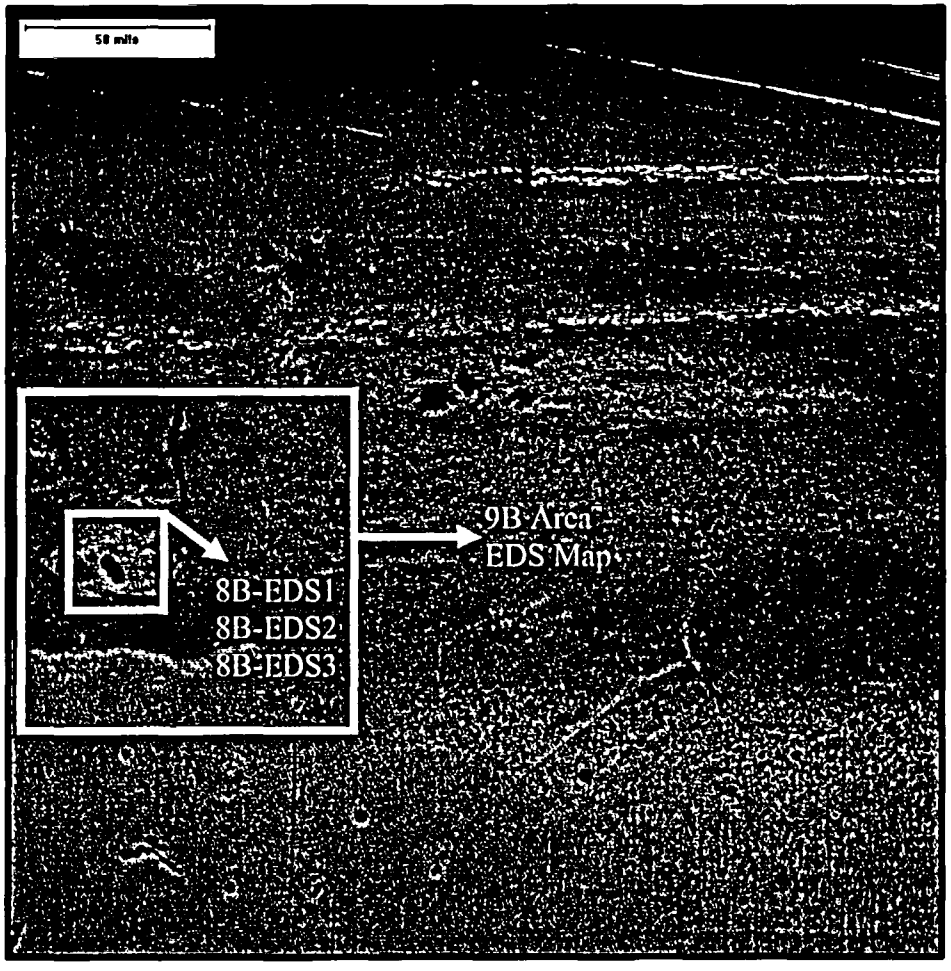

c) Area 3B

Figure 10-15 (Cont'd) Backscatter Energy Mode SEM micrograph showing OD deposit appearance at 1st TSP of R12C59 HL Piece 3B at 10° azimuthal orientation. Refer to Figure 10-13 for area location. Results of EDS analyses are presented in Table 10-5 and Figures 10-30 and 10-31.

a) Area 1R

b) Area 2R

Figure 10-16 Reflective energy mode SEM micrograph showing OD deposit appearance at 1st TSP of R12C59 HL Piece 3B at 0° azimuthal orientation. Refer to Figure 10-14 for area location.

c) Area 3R

Figure 10-16(cont'd) Reflective energy mode SEM micrograph showing OD deposit appearance at 1st TSP of R12C59 HL Piece 3B at 0° azimuthal orientation. Refer to Figure 10-14 for area location.

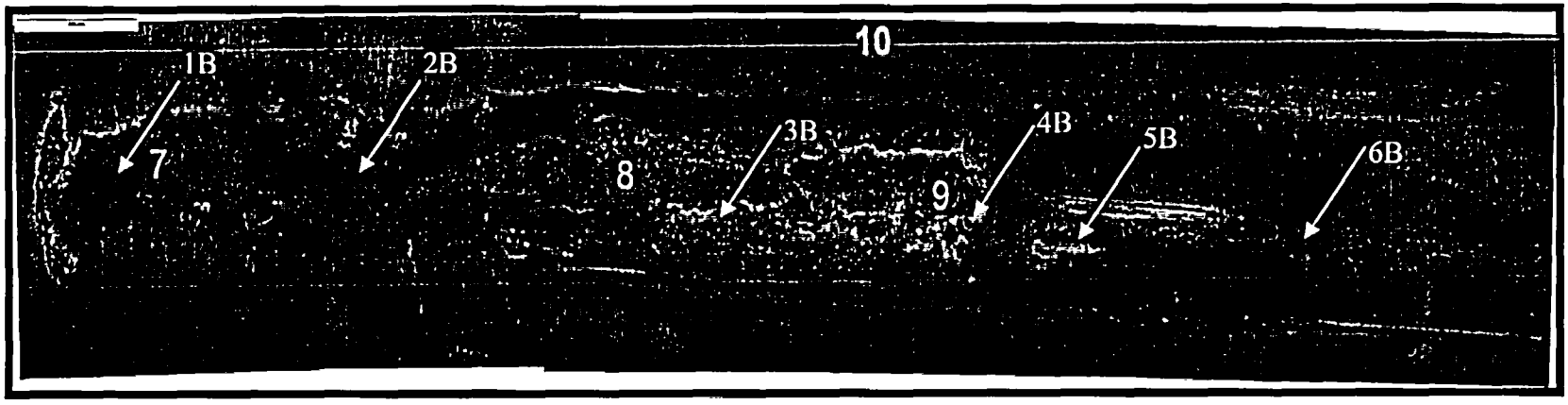

a) Backscatter Energy Mode

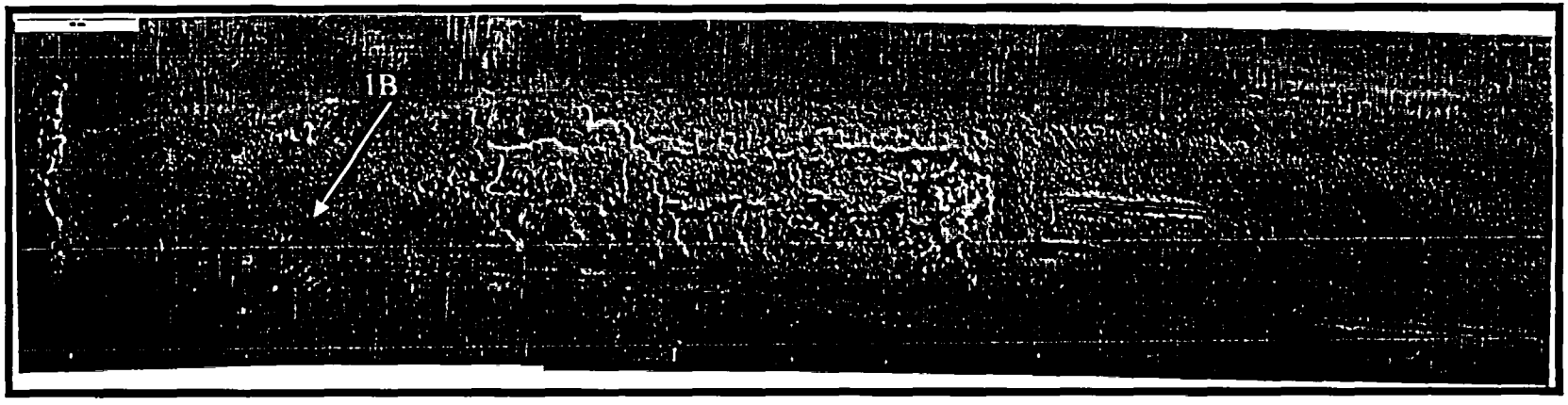

b) Reflective Energy Mode

Figure 10-17 Montage of OD deposit from 1st TSP of R12C59 HL Piece 3B at 100° azimuthal orientation. Refer to Figure 10-18 for additional SEM micrographs of areas shown. Areas identified as 7, 8, 9, and 10 are regions where EDS analyses were performed.

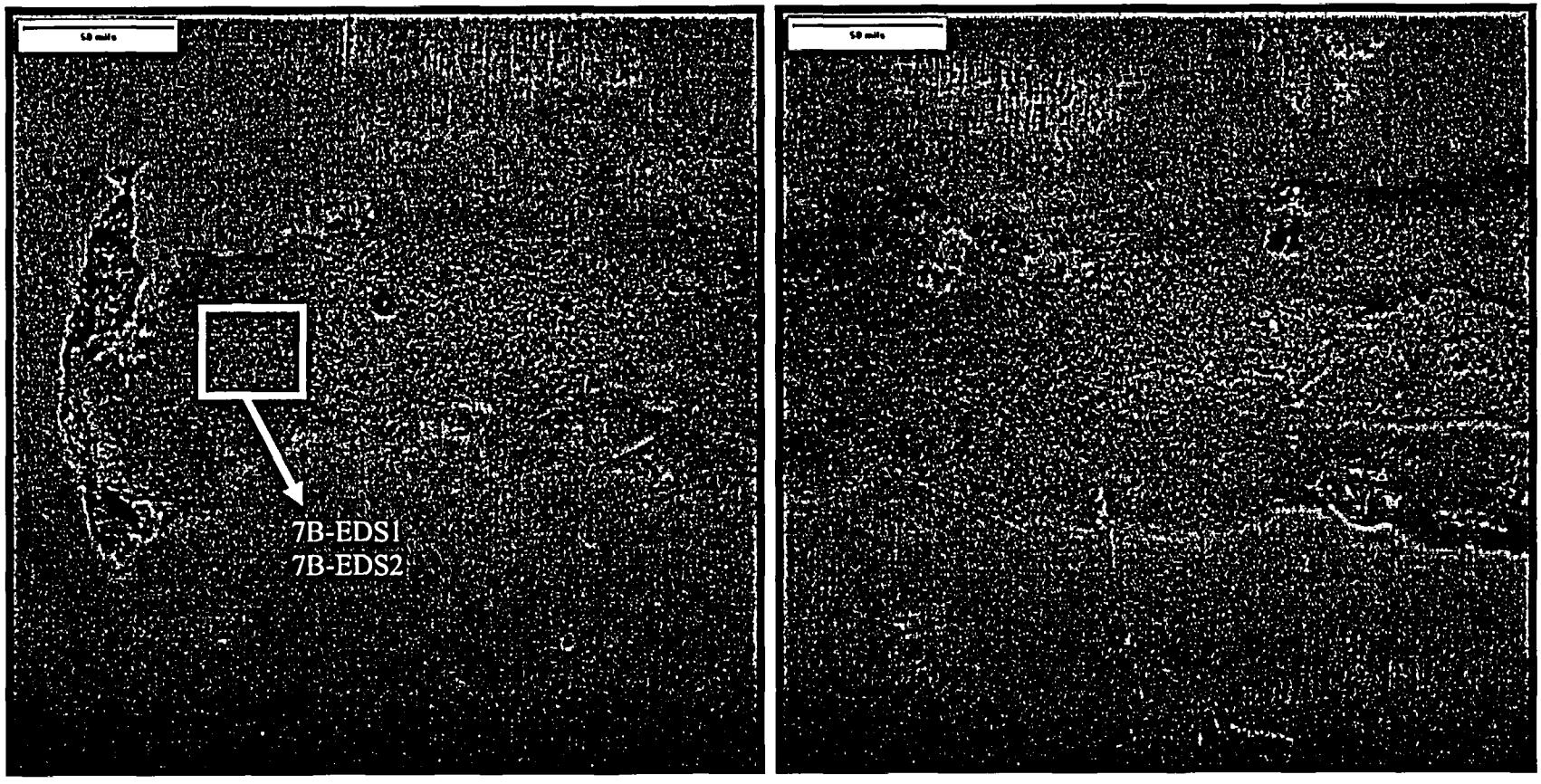

a) Area 1B

b) Area 2B

Figure 10-18 Backscatter Energy Mode SEM micrograph showing OD deposit appearance at 1st TSP of R12C59 HL Piece 3B at 100° azimuthal orientation. Refer to Figure 10-17 for area location. Results of EDS analyses are presented in Table 10-6 and Figures 10-32 and 10-33.

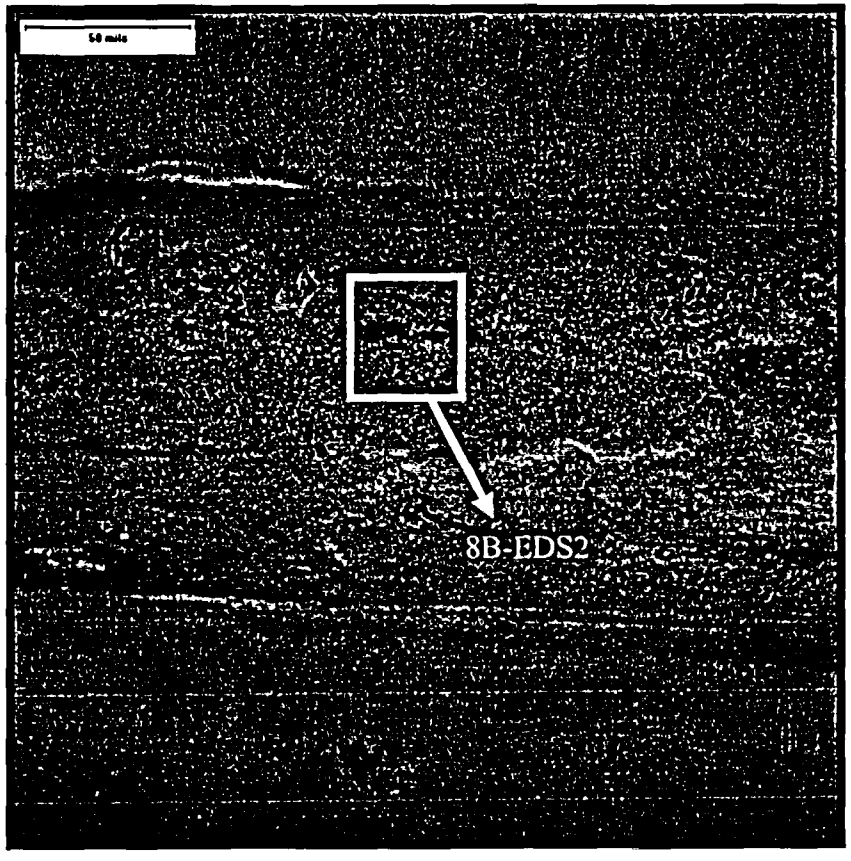

c) Area 3B

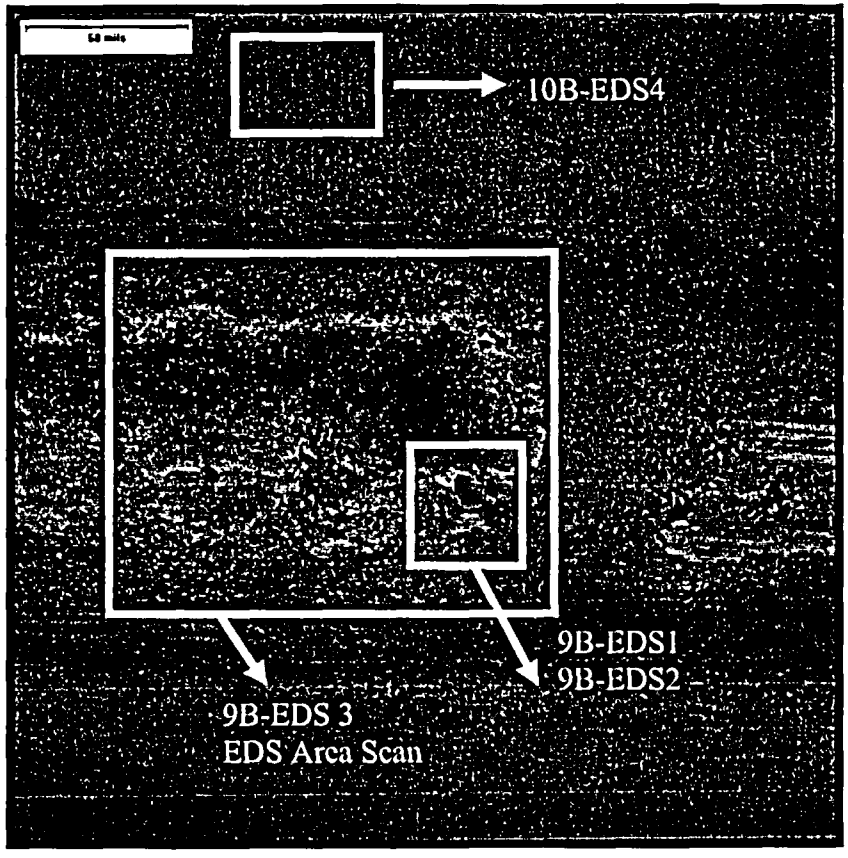

d) Area 4B

Figure 10-18 (cont'd) Backscatter Energy Mode SEM micrograph showing OD deposit appearance at 1st TSP of R12C59 HL Piece 3B at 100° azimuthal orientation. Refer to Figure 10-16 for area location. Results of EDS analyses are presented in Table 10-6 and Figures 10-32 and 10-33.

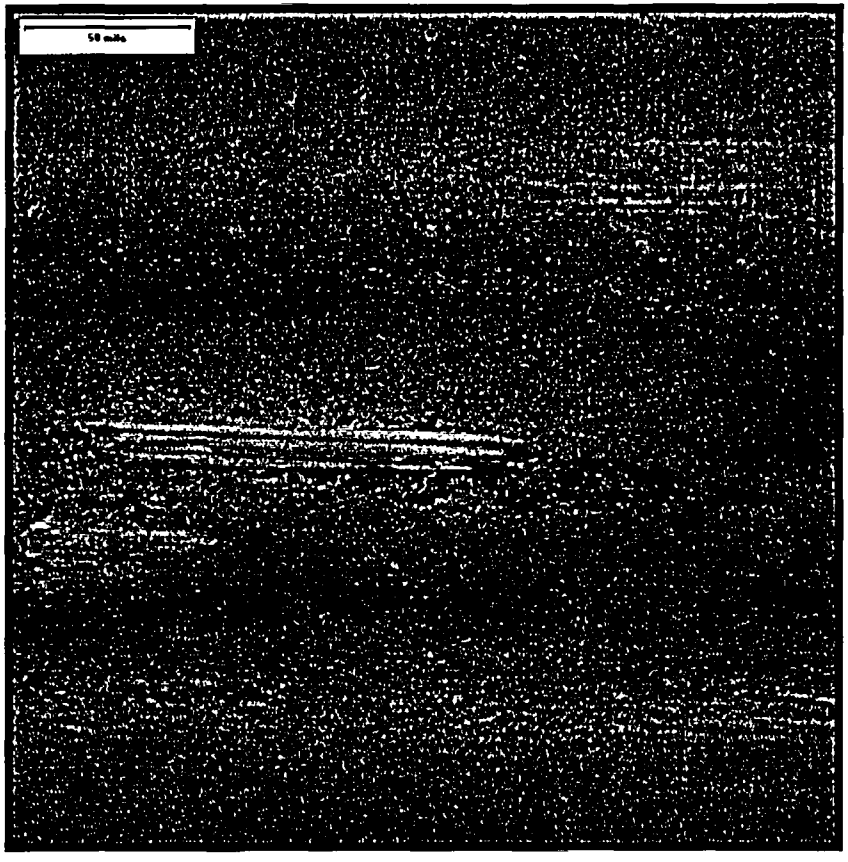

c) Area 5B

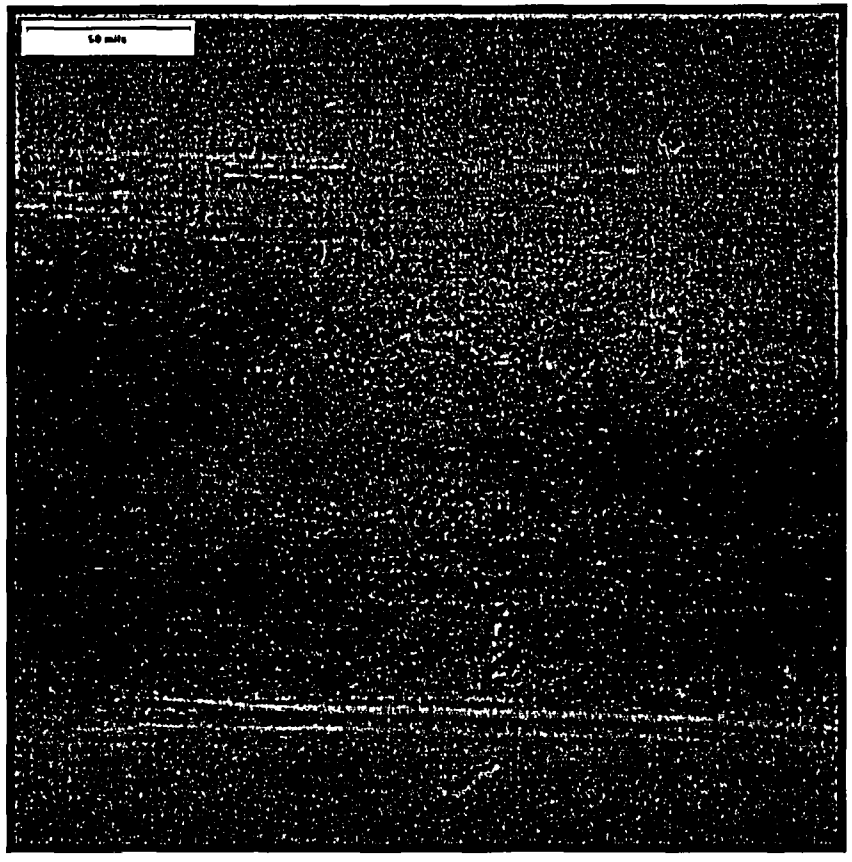

f) Area 6B

Figure 10-18 (cont'd) Backscatter Energy Mode SEM micrograph showing OD deposit appearance at 1st TSP of R12C59 HL Piece 3B at 100° azimuthal orientation. Refer to Figure 10-17 for area location.

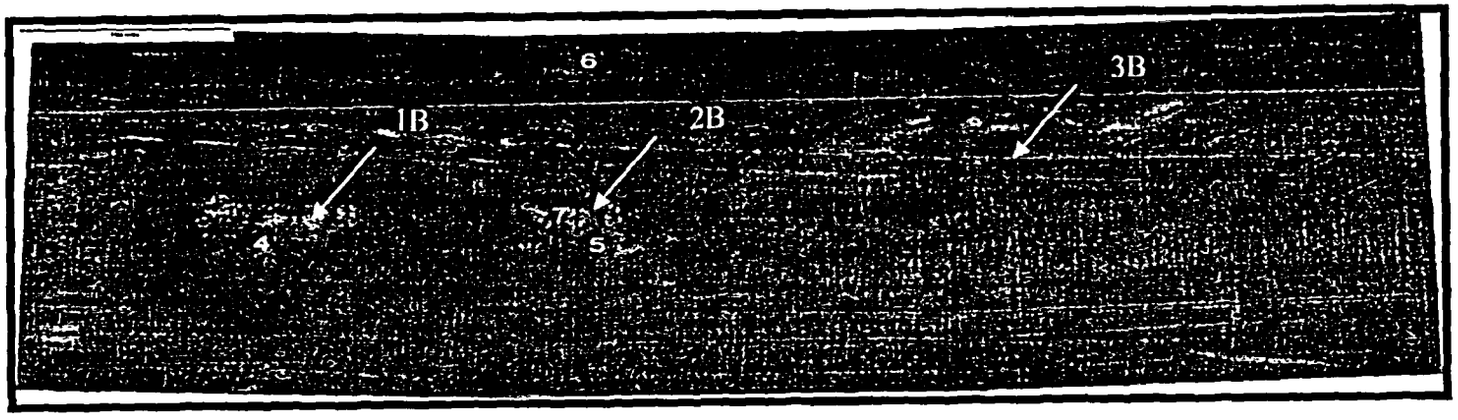

a) Backscatter Energy Mode

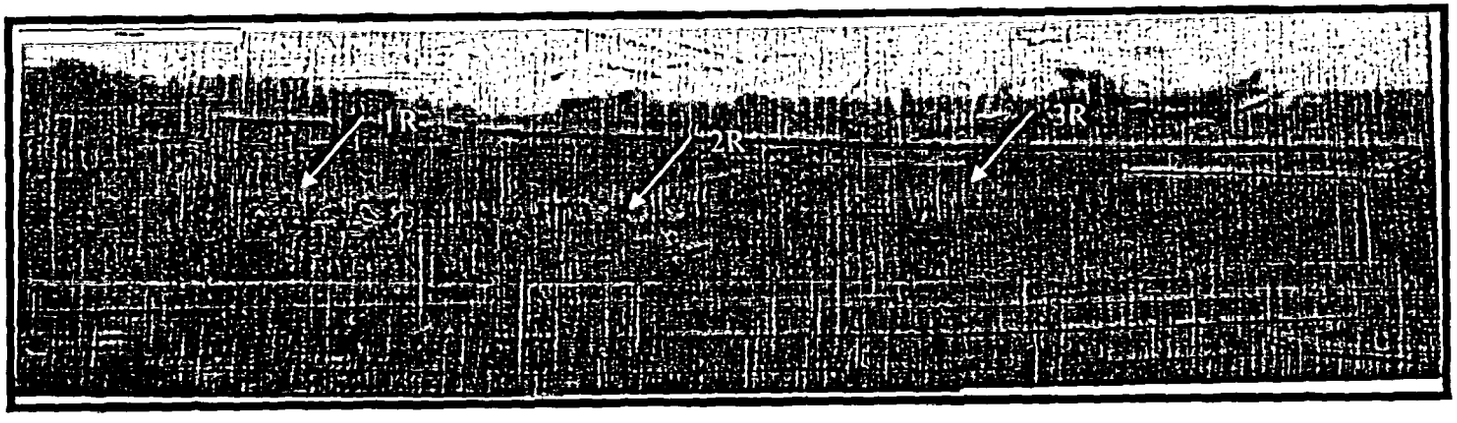

b) Reflective Energy Mode

Figure 10-19 Montage of OD deposit from 1st TSP of R11C60 HL Piece 3B at 10° azimuthal orientation. Refer to Figure 10-20 for additional SEM micrographs of areas shown. Areas identified as 4, 5, 6, and 7 are regions where EDS analyses were performed.

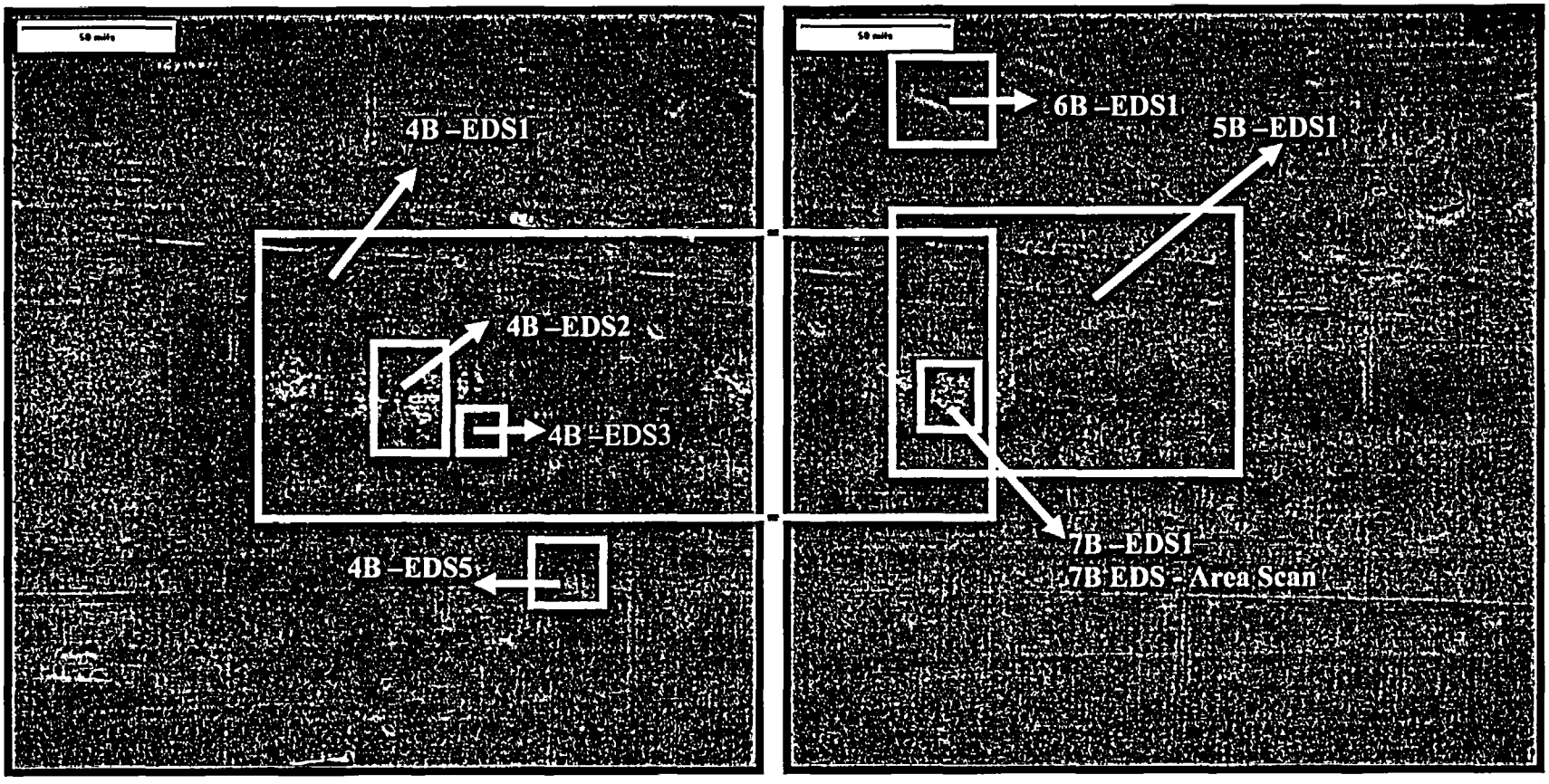

a) Area 1B

b) Area 2B

Figure 10-20 Backscatter Energy Mode SEM micrograph showing OD deposit appearance at 1st TSP of R11C60 HL Piece 3B at 10° azimuthal orientation. Refer to Figure 10-19 for area location. Results of EDS analyses are presented in Table 10-7 and Figures 10-34 and 10-35.

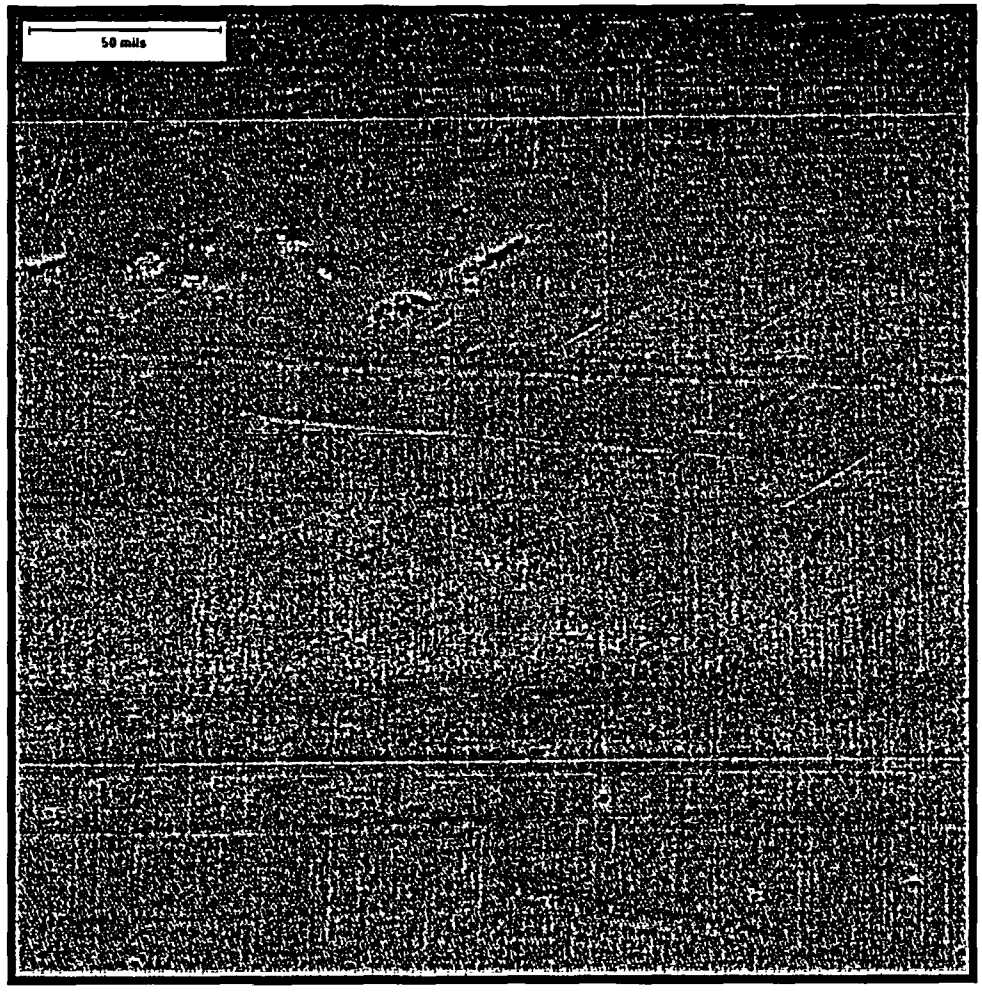

c) Area 3B

Figure 10-20 (Cont'd) Backscatter Energy Mode SEM micrograph showing OD deposit appearance at 1st TSP of R11C60 HL Piece 3B at 10° azimuthal orientation. Refer to Figure 10-19 for area location.

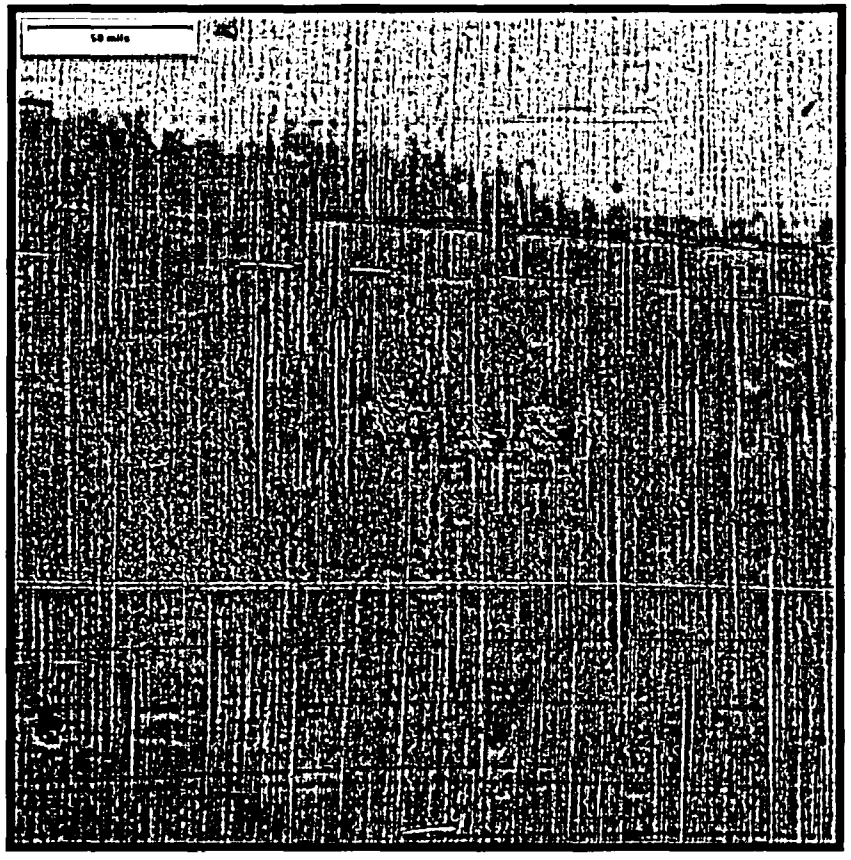

a) Area 1R

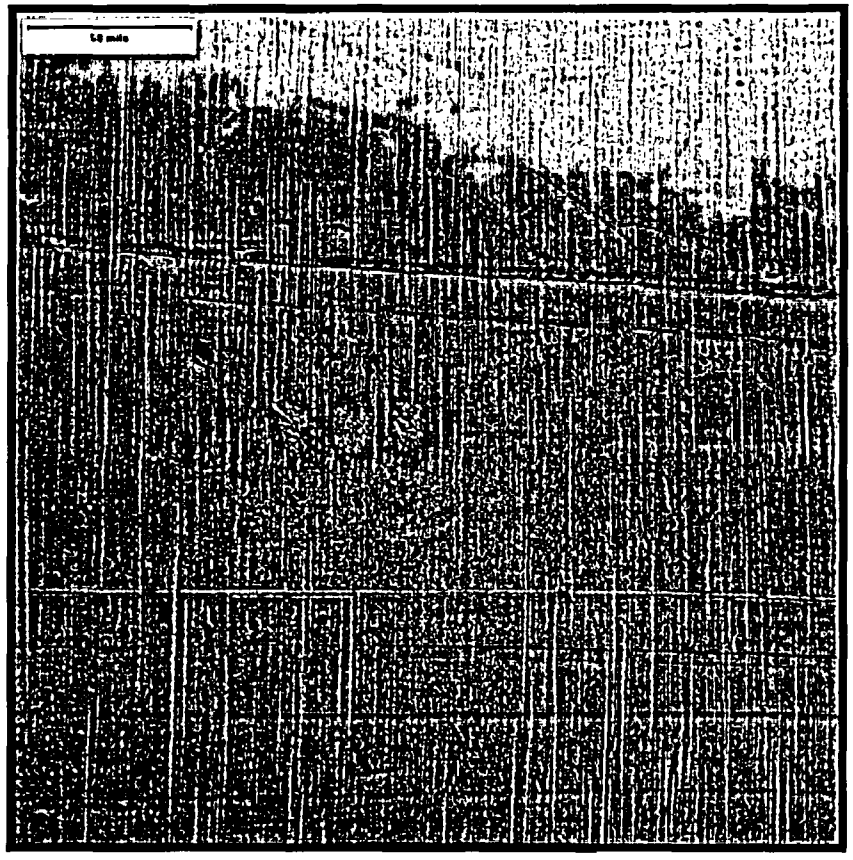

b) Area 2R

Figure 10-21 Reflective Energy Mode SEM micrograph showing OD deposit appearance at 1st TSP of R11C60 HL Piece 3B at 10° azimuthal orientation. Refer to Figure 10-19 for area location.

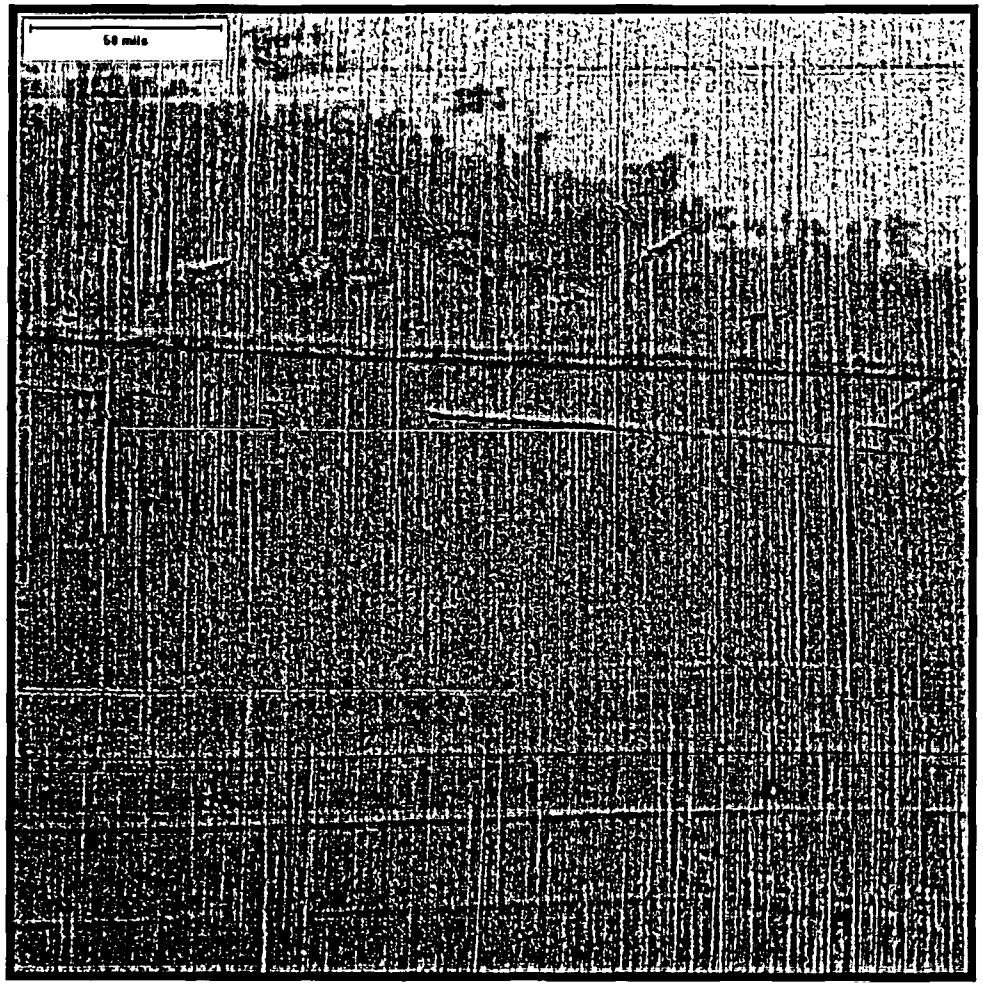

c) Area 3R

Figure 10-21 (cont'd) Reflective Energy Mode SEM micrograph showing OD deposit appearance at 1st TSP of R11C60 HL Piece 3B at 10° azimuthal orientation. Refer to Figure 10-19 for area location.

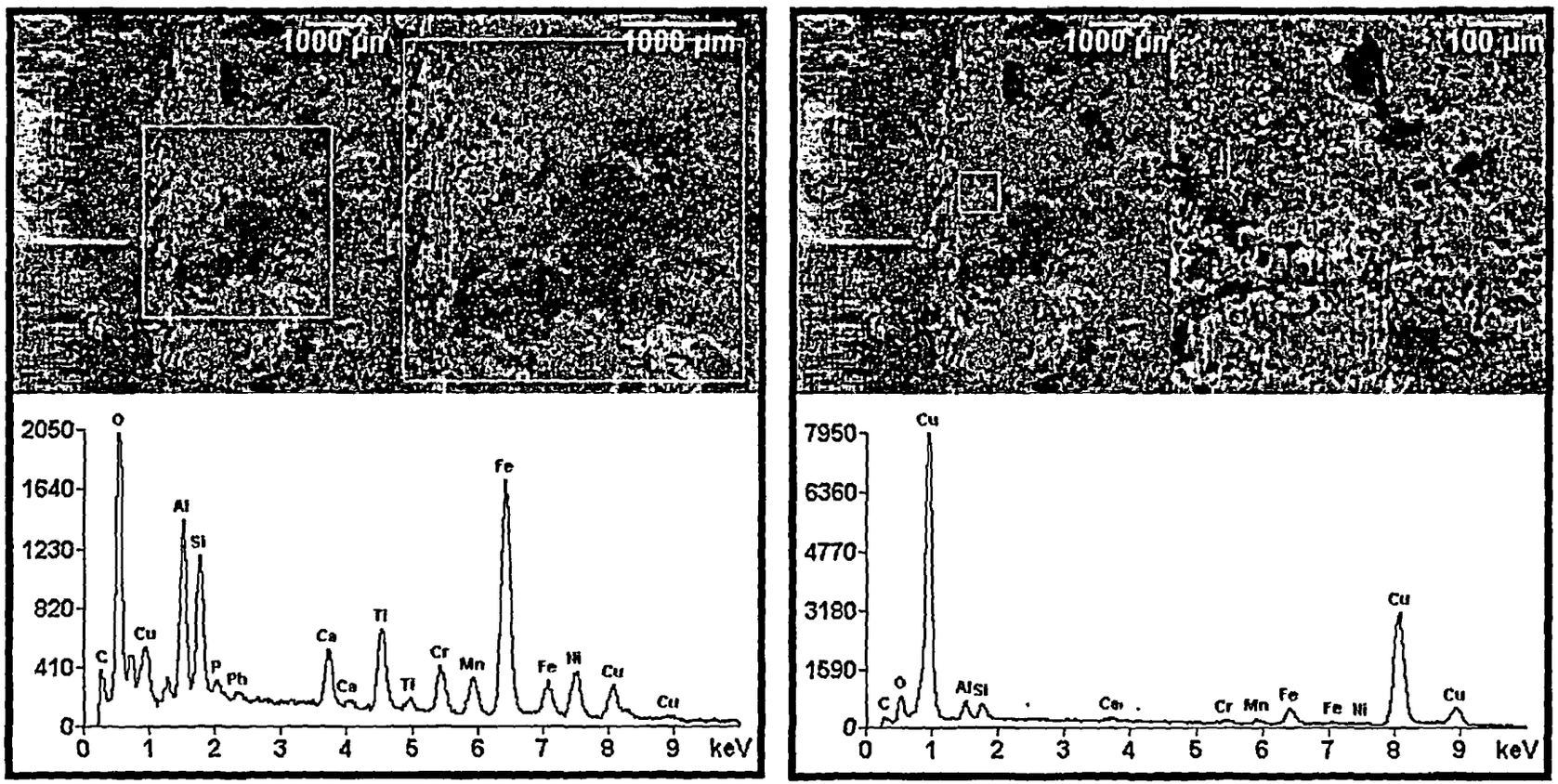

a) 7B-EDS1

b) 7B-EDS2

Figure 10-22 SEM Photography and EDS Elemental Trace of OD Deposit from TTS Region of R12C59 Piece 2B at 324° Azimuthal Orientation (Field +Pt signal location)

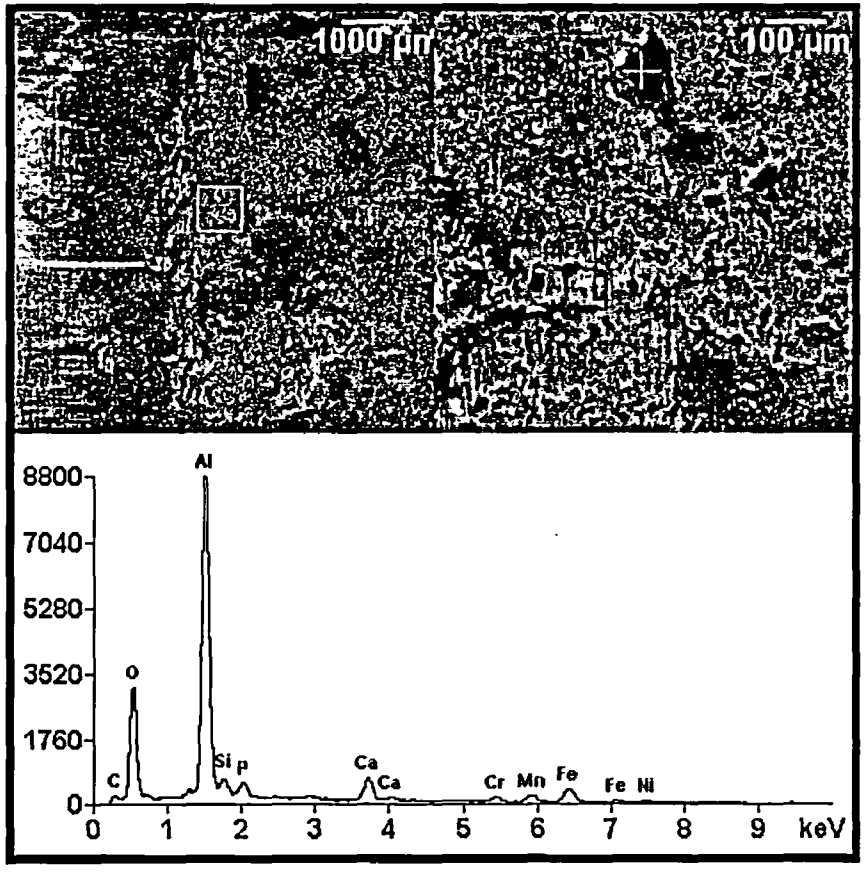

c) 7B-EDS3

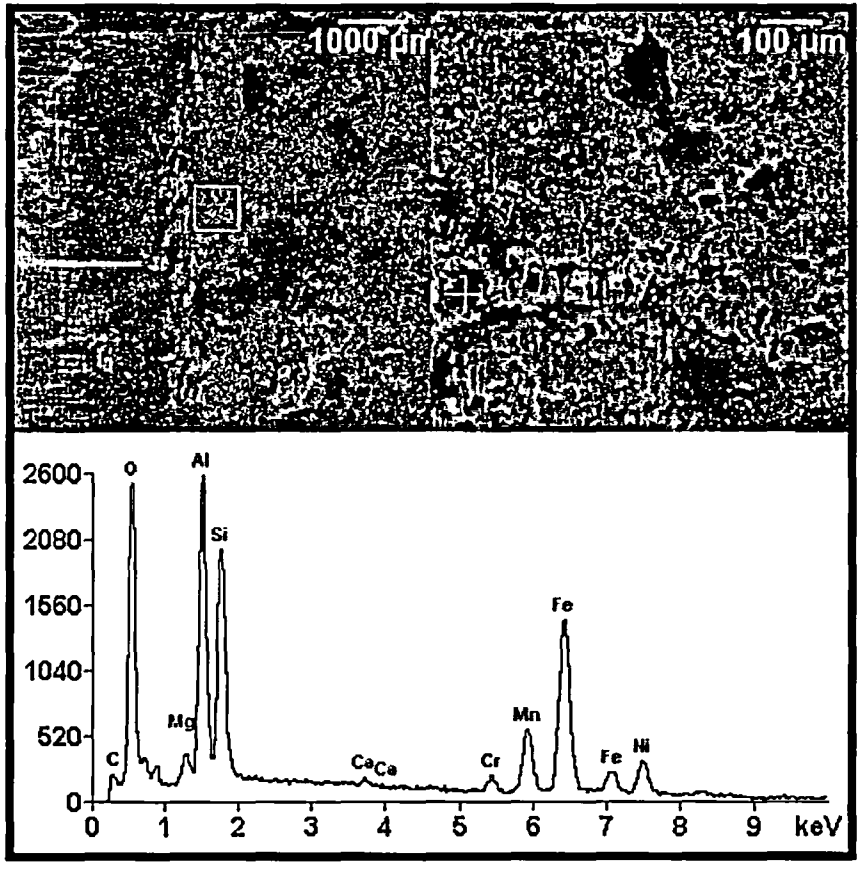

d) 7B-EDS4

Figure 10-22 (Cont'd) SEM Photography and EDS Elemental Trace of OD Deposit from TTS Region of R12C59 Piece 2B at 324° Azimuthal Orientation (Field +Pt signal location).

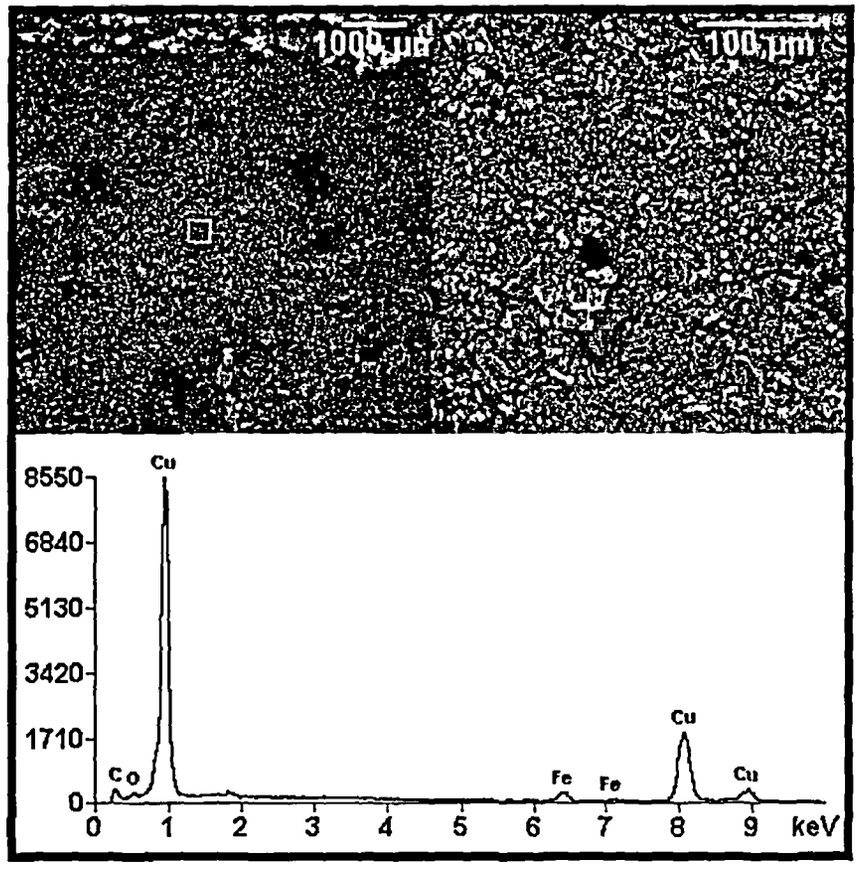

e) 8B-EDS1

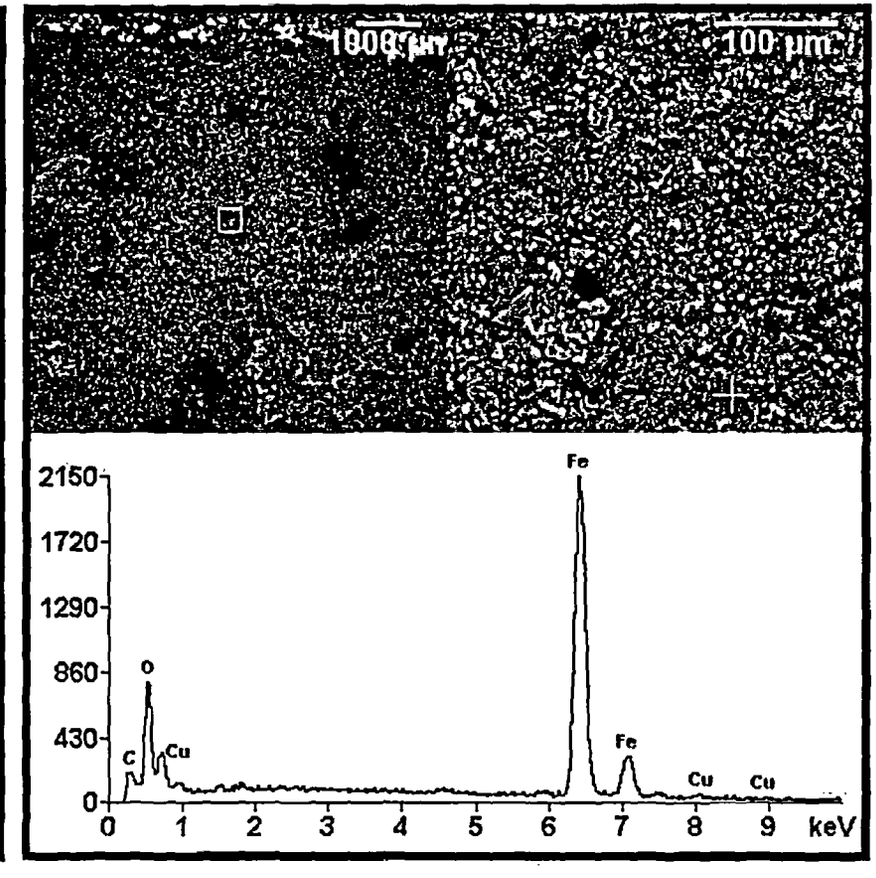

f) 8B-EDS7

Figure 10-22 (Cont'd) SEM Photography and EDS Elemental Trace of OD Deposit from TTS Region of R12C59 Piece 2B at 324° Azimuthal Orientation (Field +Pt signal location).

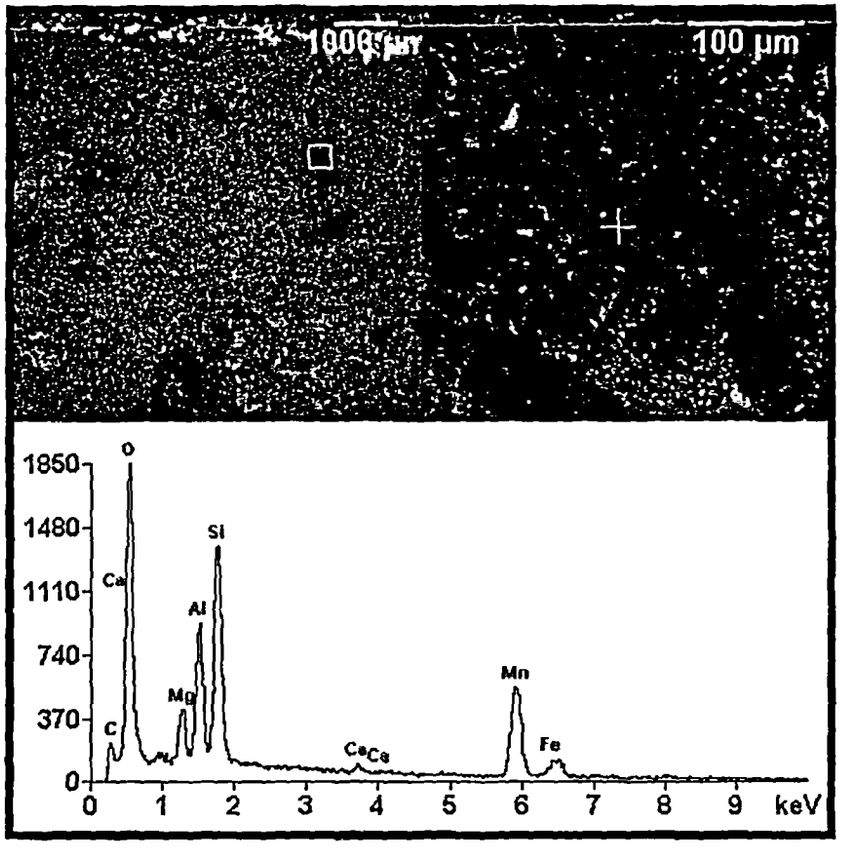

g) 8B-EDS8

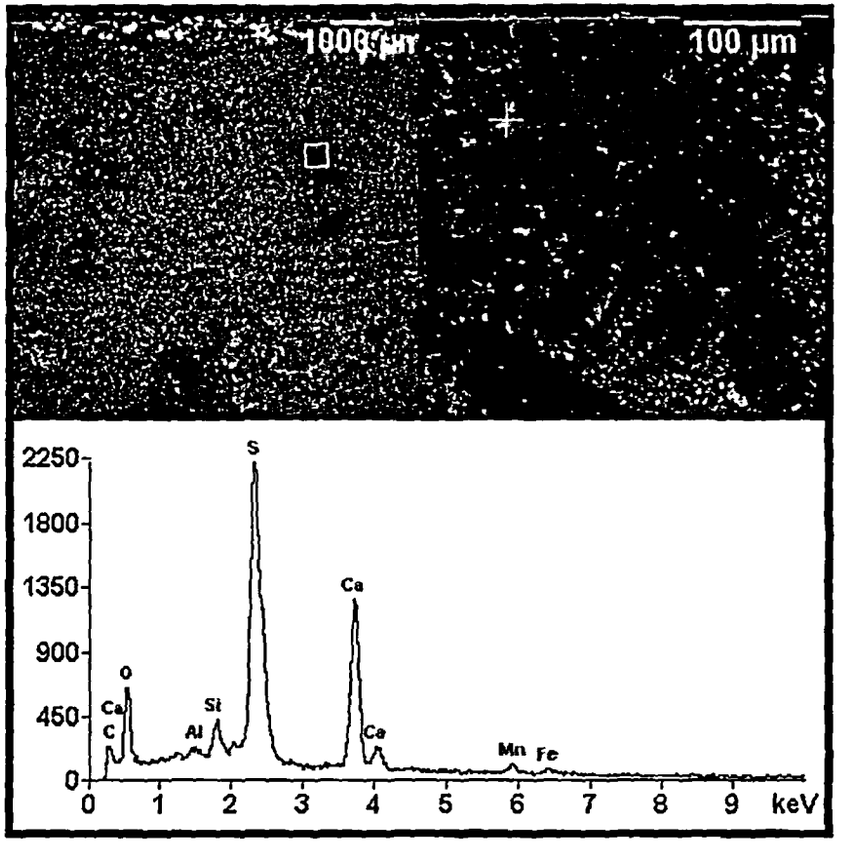

h) 8B-EDS9

Figure 10-22(Cont'd) SEM Photography and EDS Elemental Trace of OD Deposit from TTS Region of R12C59 Piece 2B at 324° Azimuthal Orientation (Field +Pt signal location).

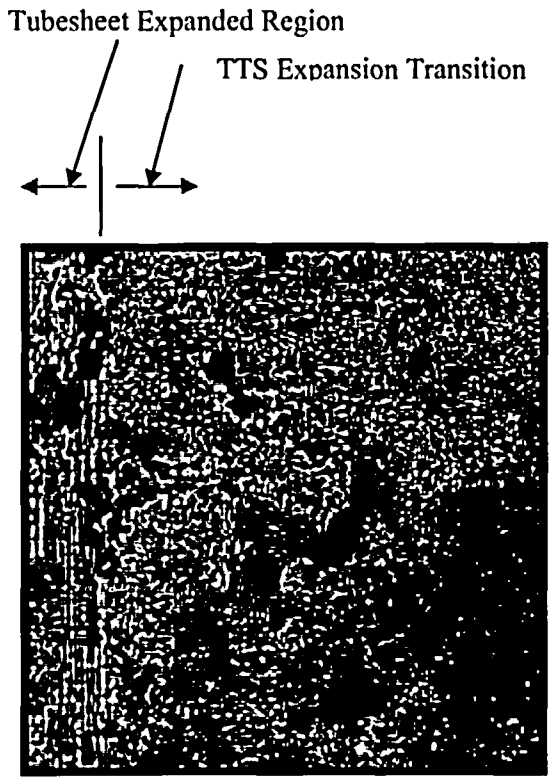

SEM Micrograph Showing
OD Deposit Area Analyzed

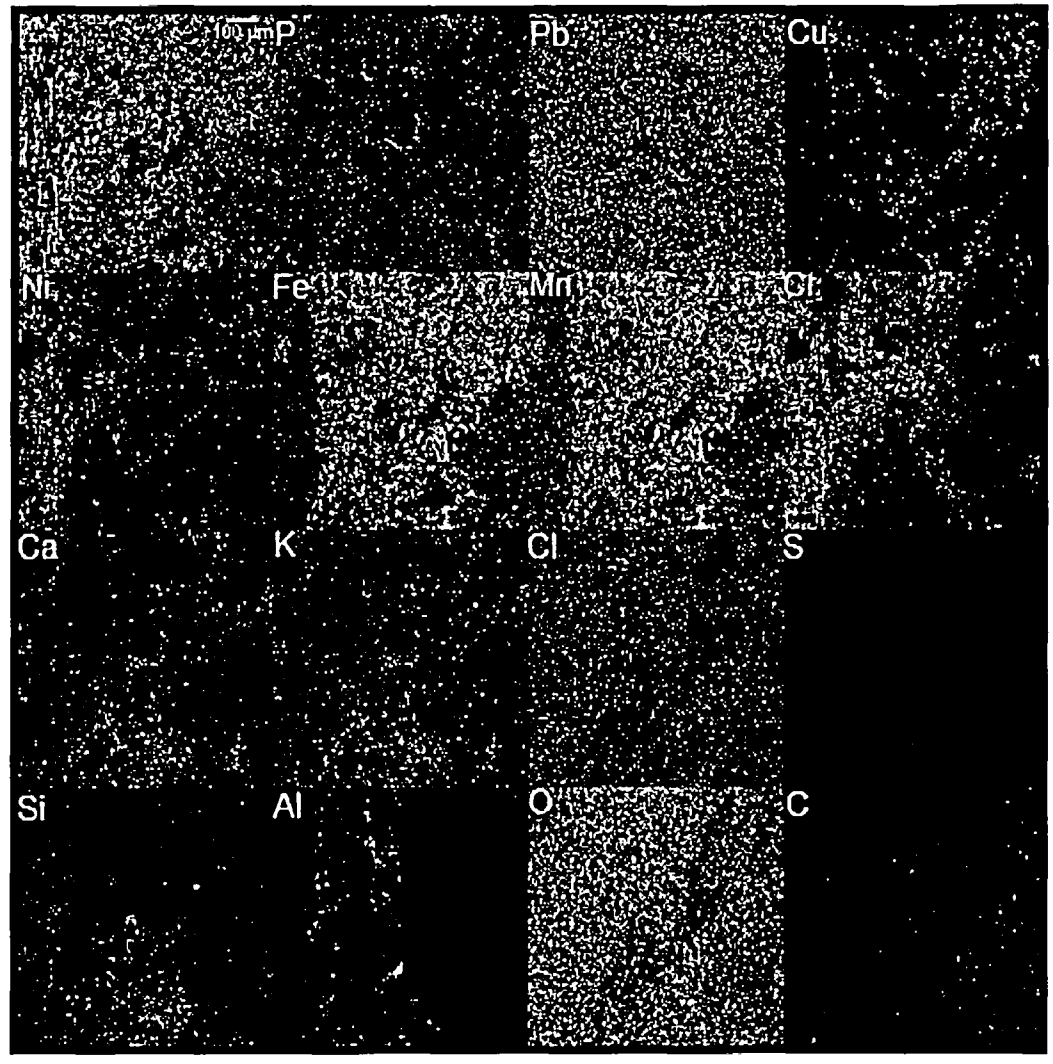

Figure 10-23 Backscatter EDS Area Maps Showing Concentration of Various Elements Identified on the OD Surface at TTS of R12C59 - Piece 2B at 324° Azimuthal Orientation (Field +Pt signal location).

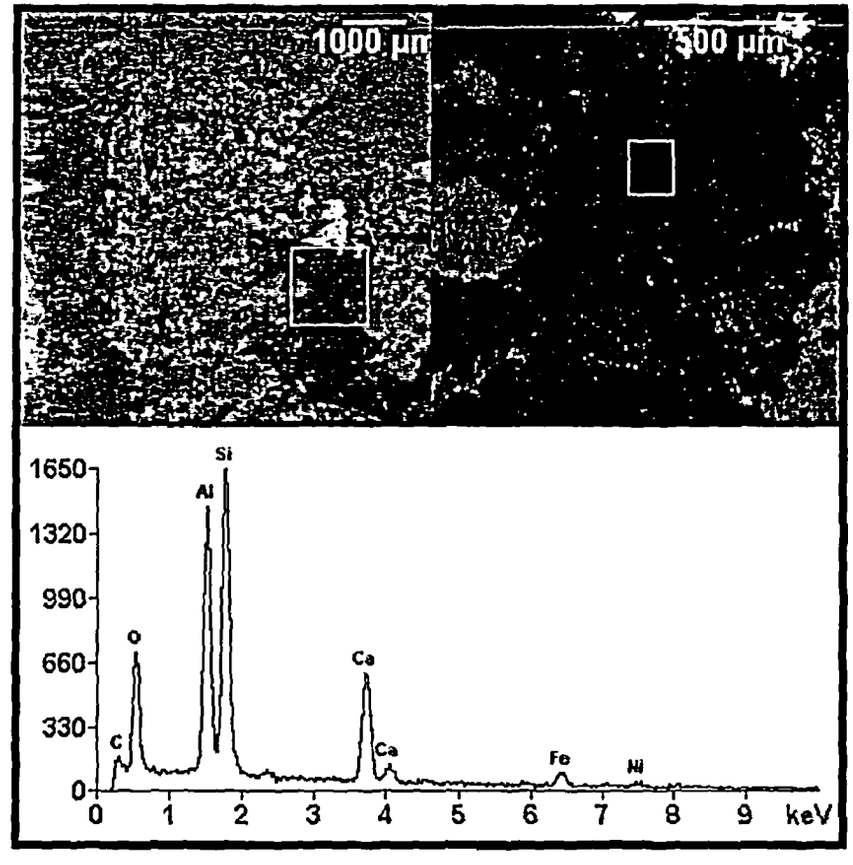

a) 7B-EDS2

Figure 10-24 SEM Photography and EDS Elemental Trace of OD Deposit from TTS Region of R12C59 Piece 2B at 45° Azimuthal Orientation (Field UT Signal Location).

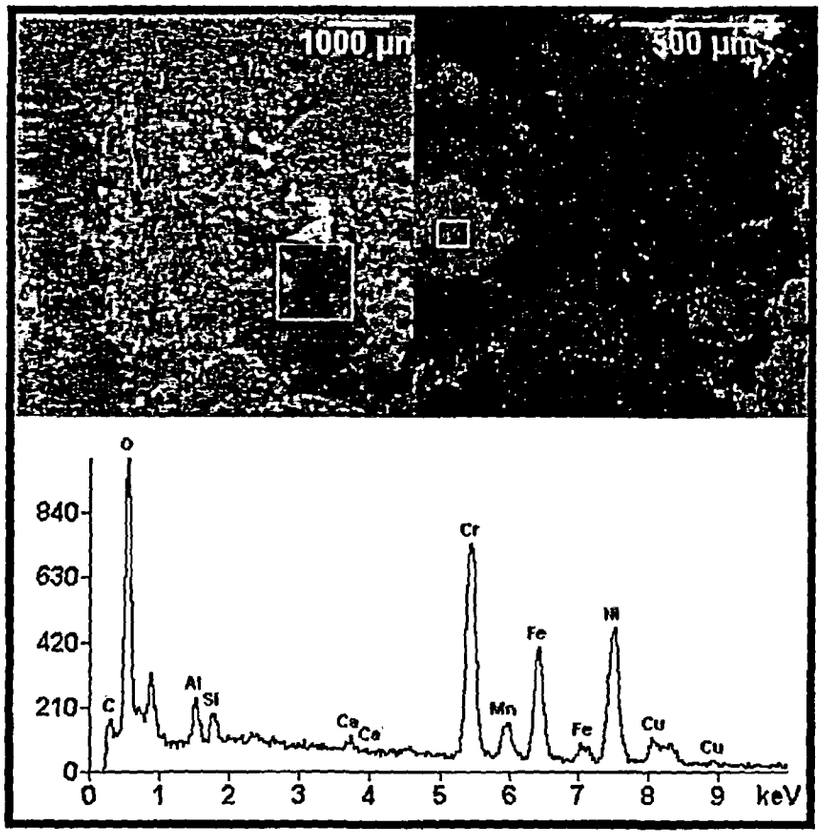

b) 7B-EDS3

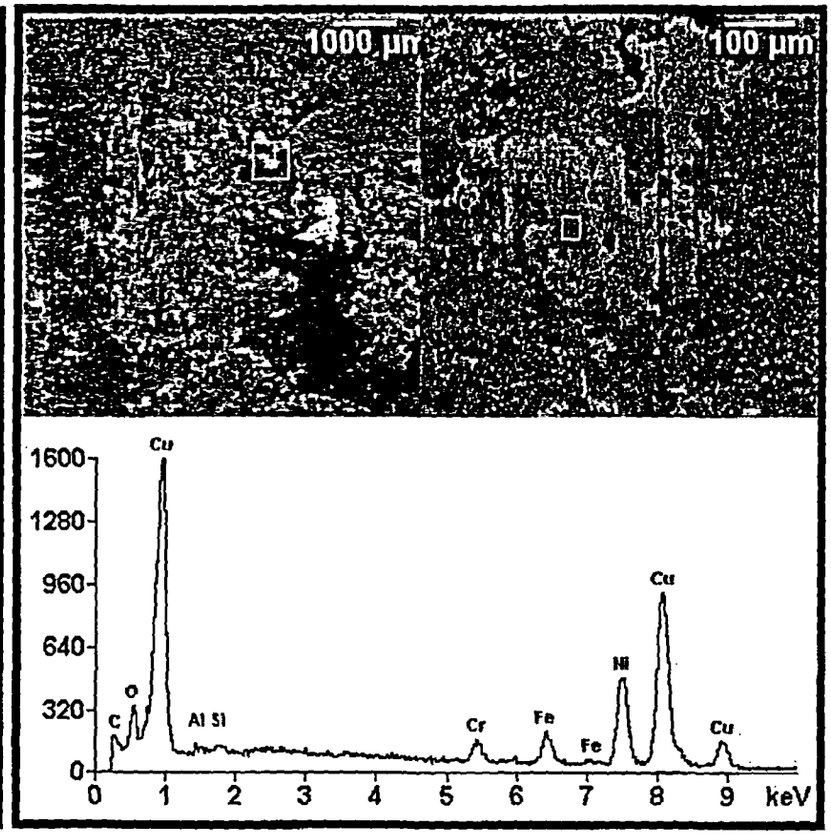

c) 7B-EDS4

Figure 10-24(Cont'd) SEM Photography and EDS Elemental Trace of OD Deposit from TTS Region of R12C59 Piece 2B at 45°Azimuthal Orientation (Field UT Signal Location).

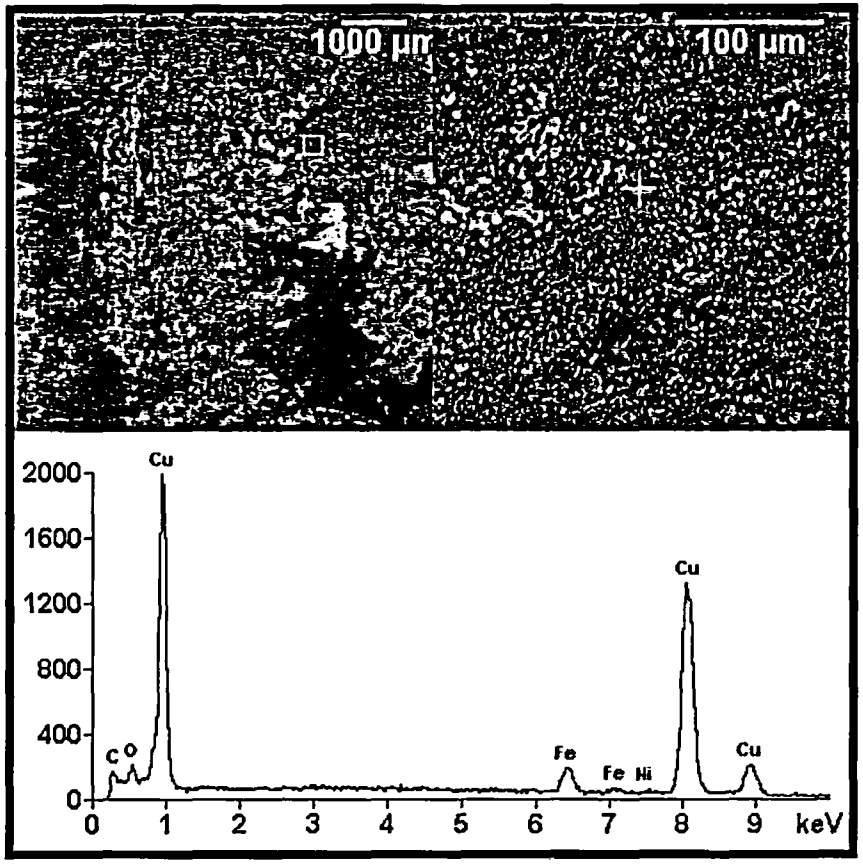

d) 7B-EDS5

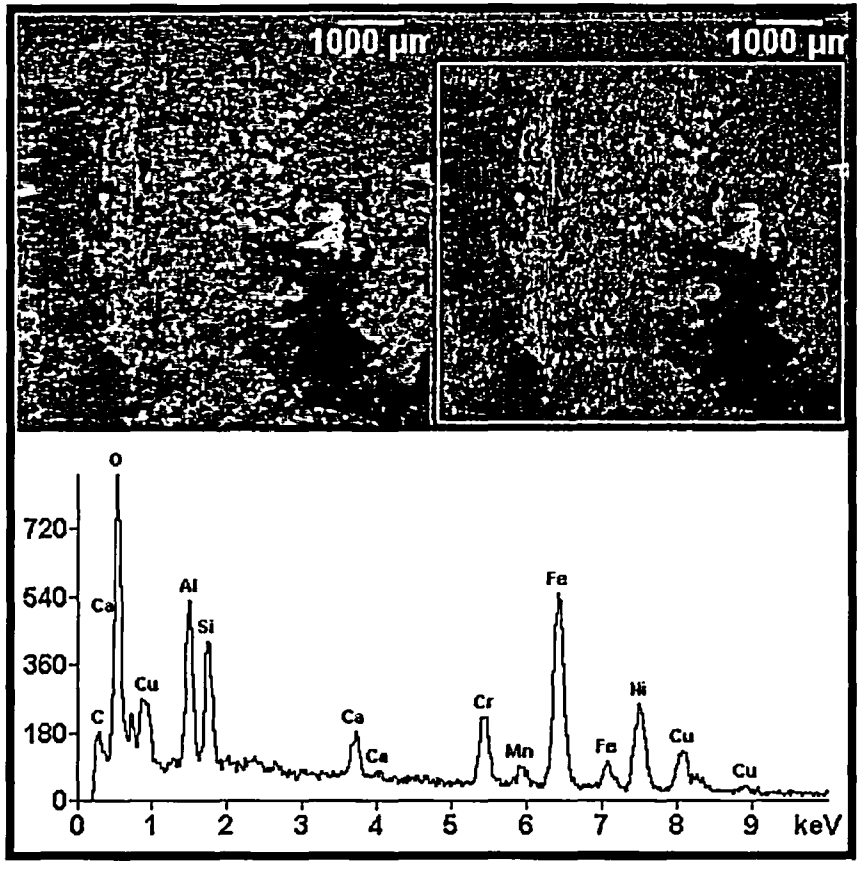

e) 7B-EDS6

Figure 10-24 (Cont'd) SEM Photography and EDS Elemental Trace of OD Deposit from TTS Region of R12C59 Piece 2B at 45° Azimuthal Orientation (Field UT Signal Location).

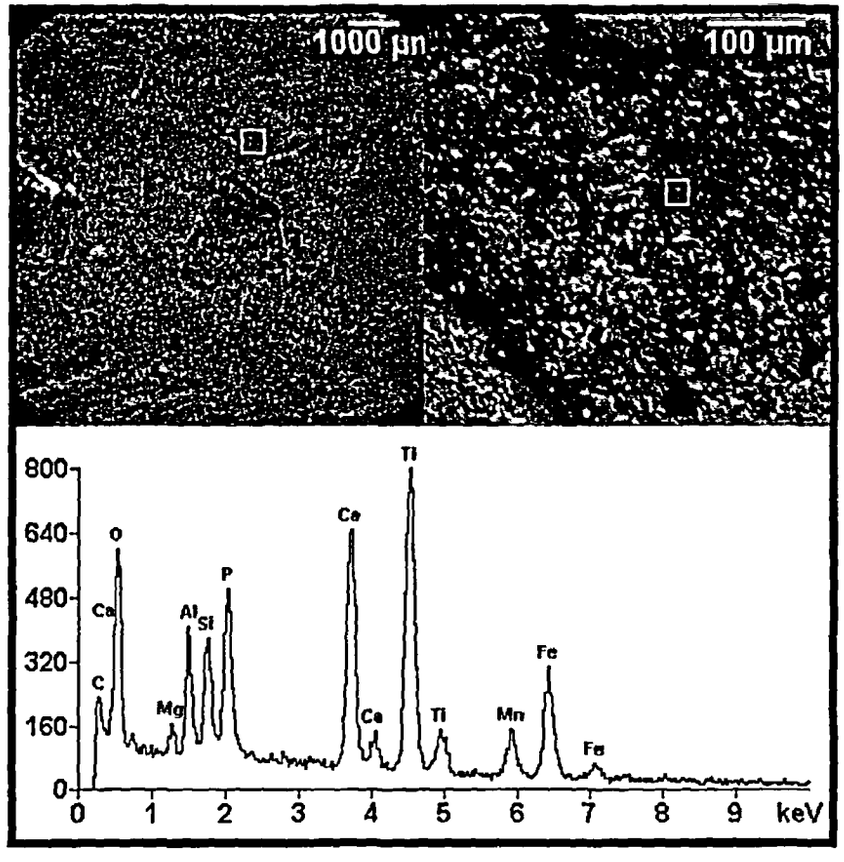

f) 8B-EDS1

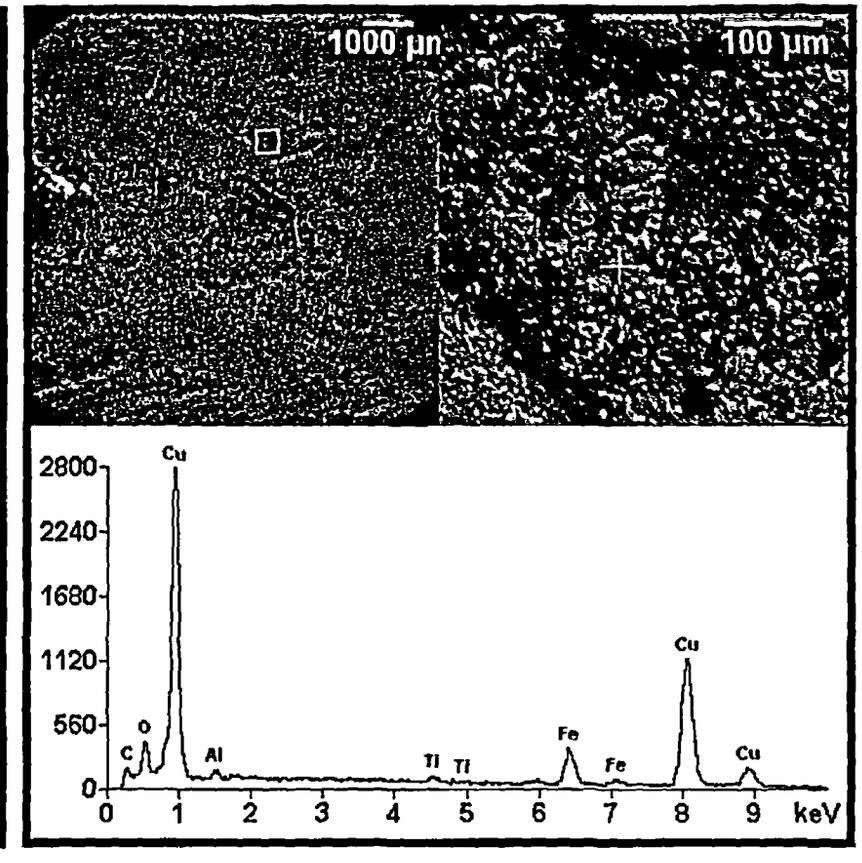

g) 8B-EDS2

Figure 10-24 (Cont'd) SEM Photography and EDS Elemental Trace of OD Deposit from TTS Region of R12C59 Piece 2B at 45° Azimuthal Orientation (Field UT Signal Location).

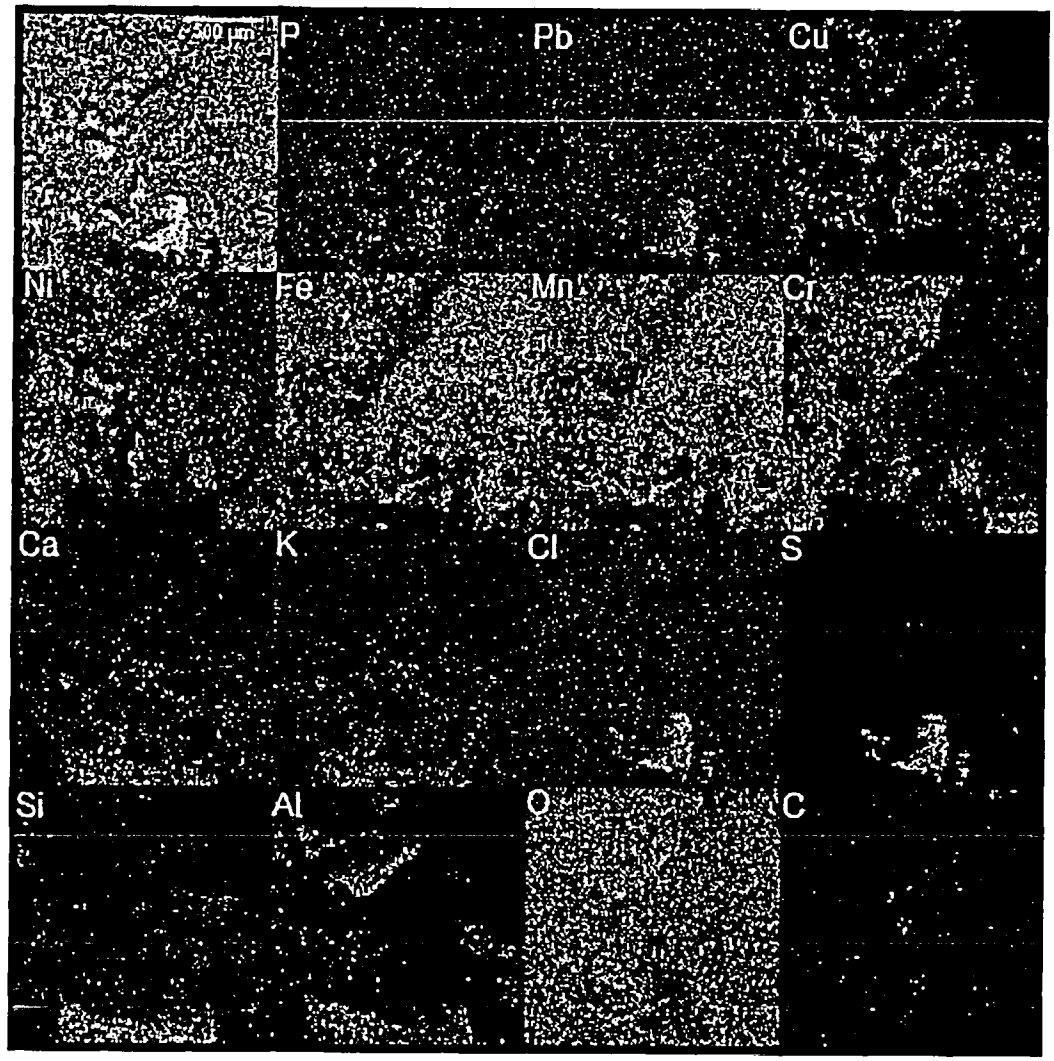

Figure 10-25 Backscatter EDS Area Maps Showing Concentration of Various Elements Identified on the OD Deposit at TTS of R12C59 Piece 2B at 45° Azimuthal Orientation (Field UT Signal Location).

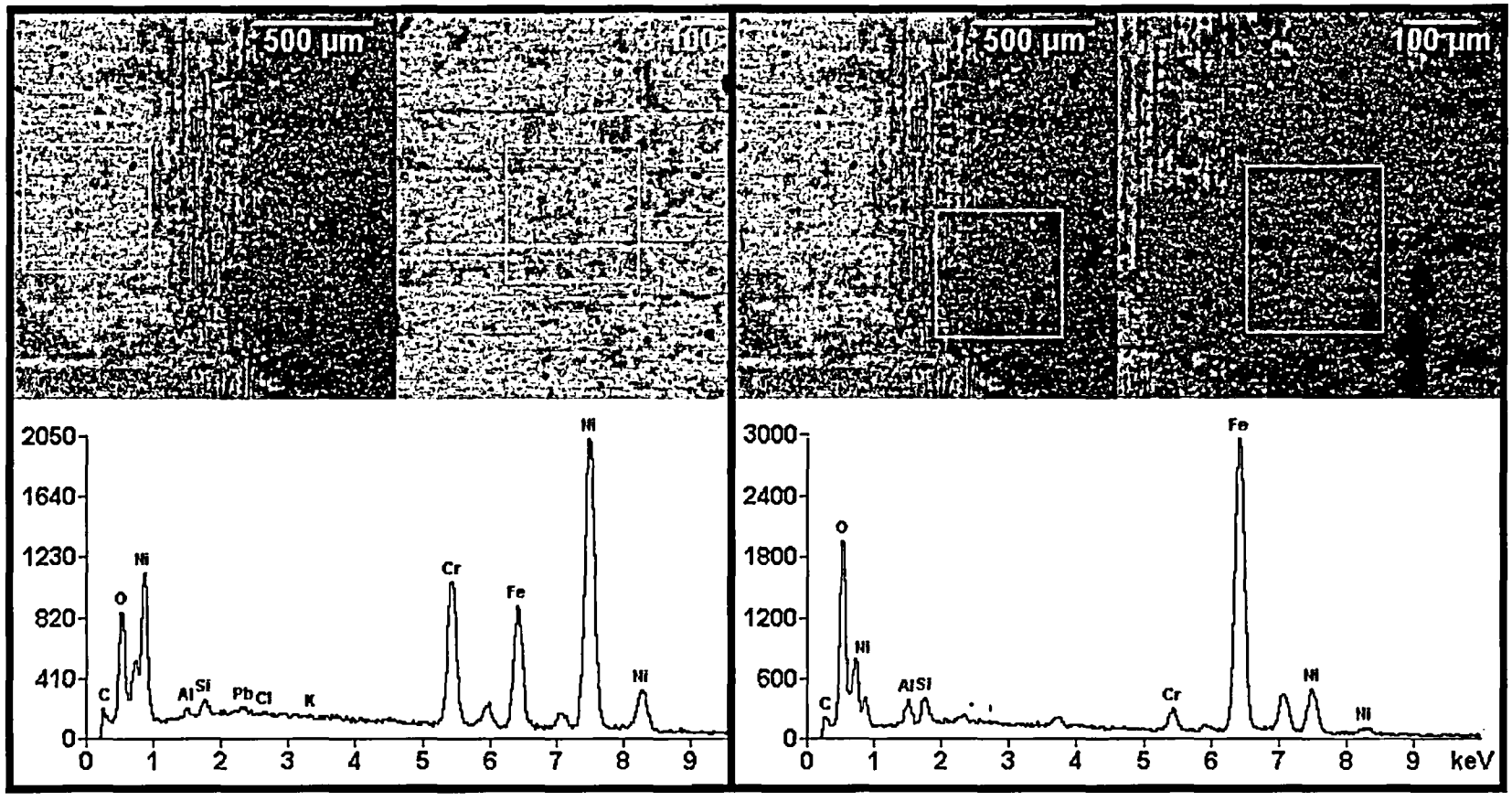

a) 7B-EDS1

b) 7B-EDS2

Figure 10-26 SEM Photography and EDS Elemental Trace of OD Deposit from TTS Region of R11C60 Piece 2B at 327° Azimuthal Orientation (Field +Pt signal location).

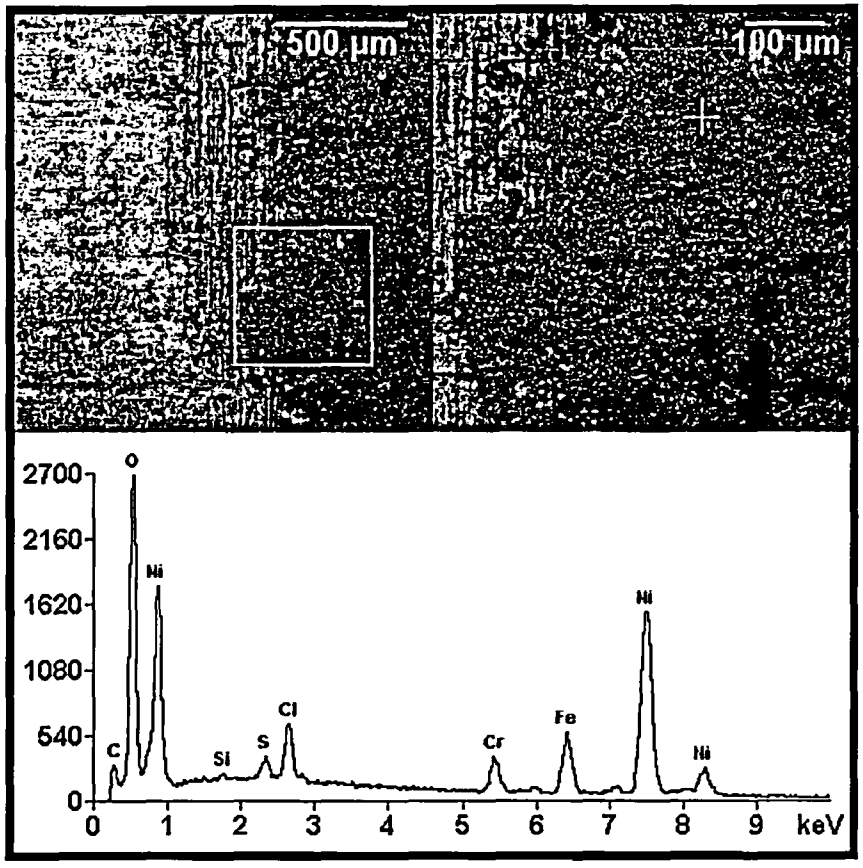

c) 7B-EDS3

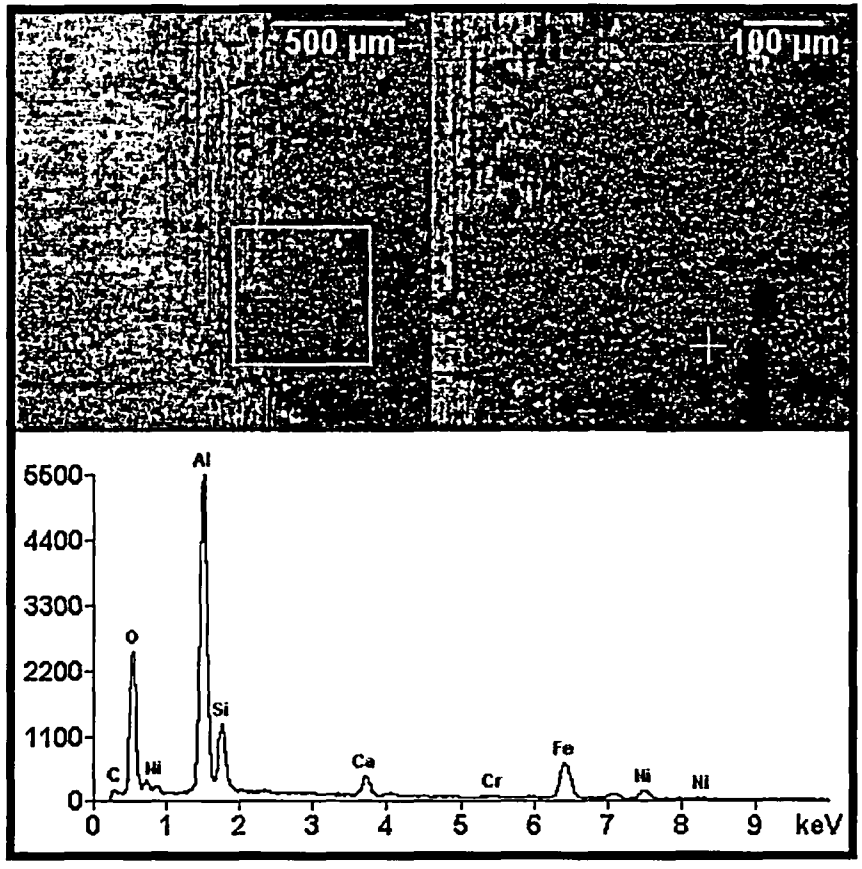

d) 7B-EDS4

Figure 10-26 (Cont'd) SEM Photography and EDS Elemental Trace of OD Deposit from TTS Region of R11C60 Piece 2B at 327° Azimuthal Orientation (Field +Pt signal location).

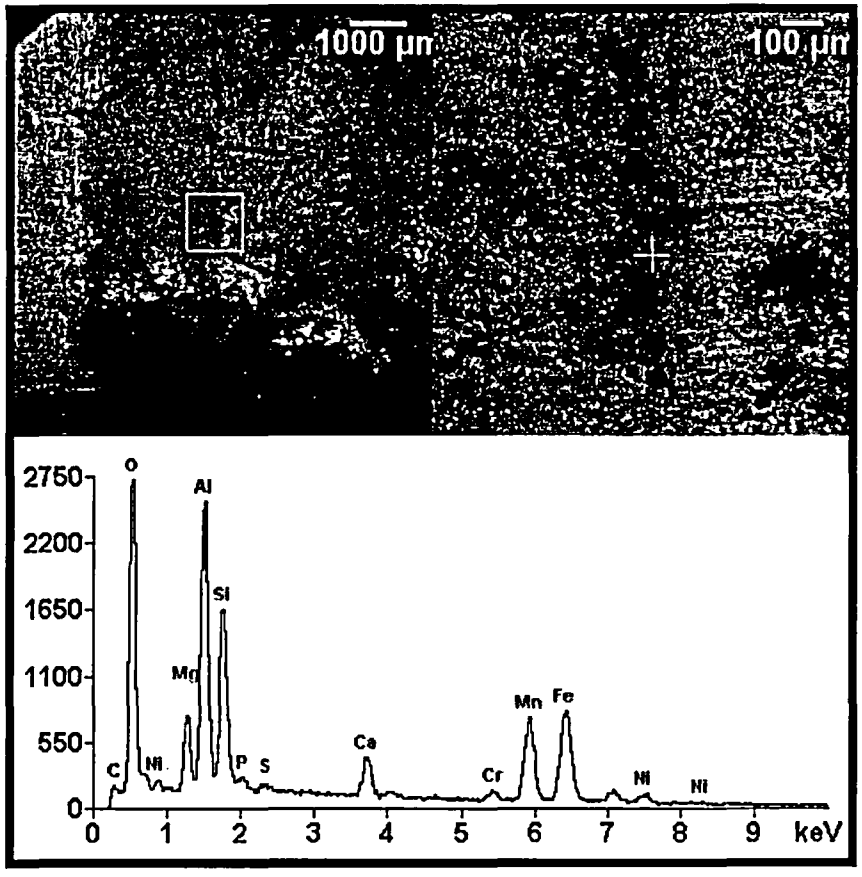

c) 7B-EDS6

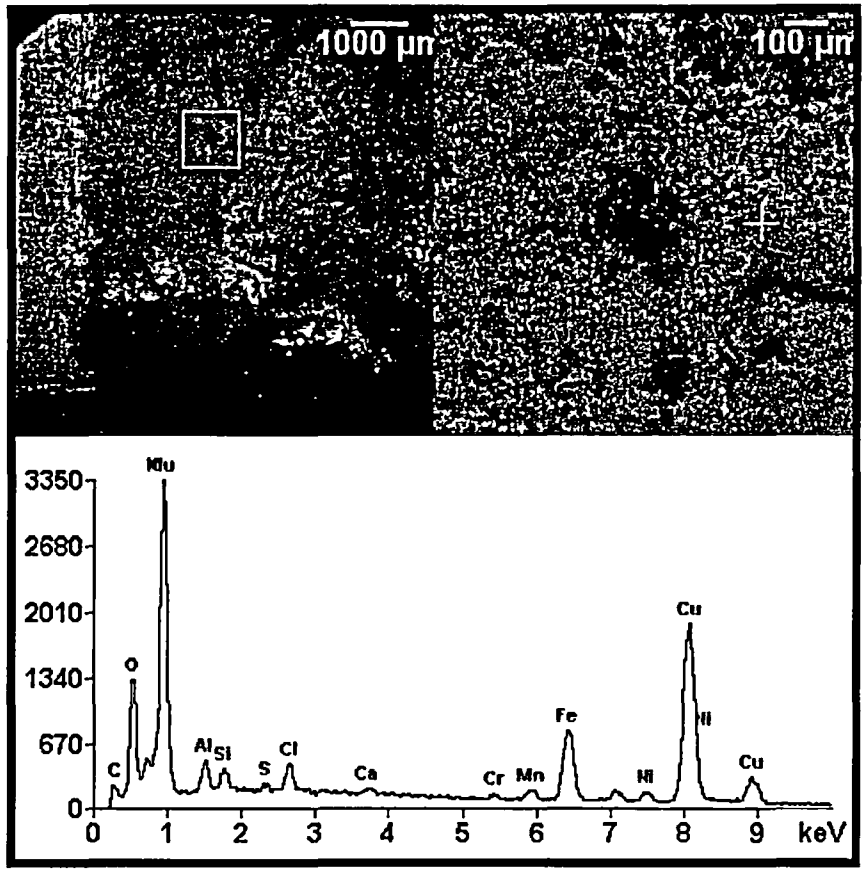

f) 7B-EDS7

Figure 10-26 (Cont'd) SEM Photography and EDS Elemental Trace of OD Deposit from TTS Region of R11C60 Piece 2B at 327° Azimuthal Orientation (Field +Pt signal location).

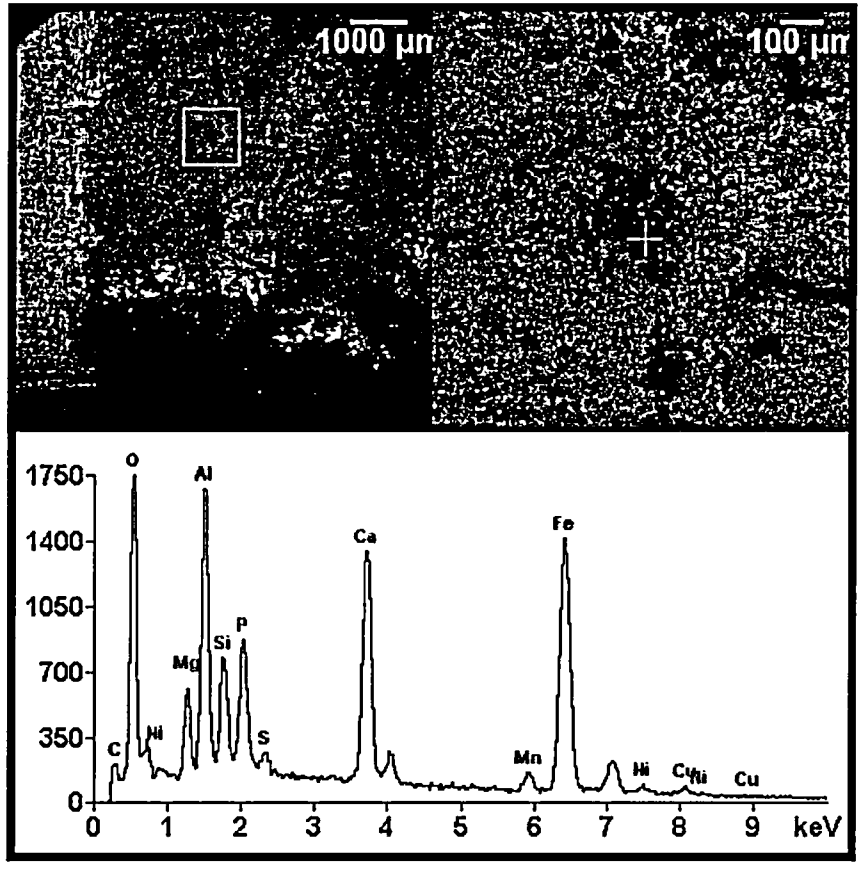

g) 7B-EDS8

Figure 10-26 (Cont'd) SEM Photography and EDS Elemental Trace of OD Deposit from TTS Region of R11C60 Piece 2B at 327° Azimuthal Orientation (Field +Pt signal location).

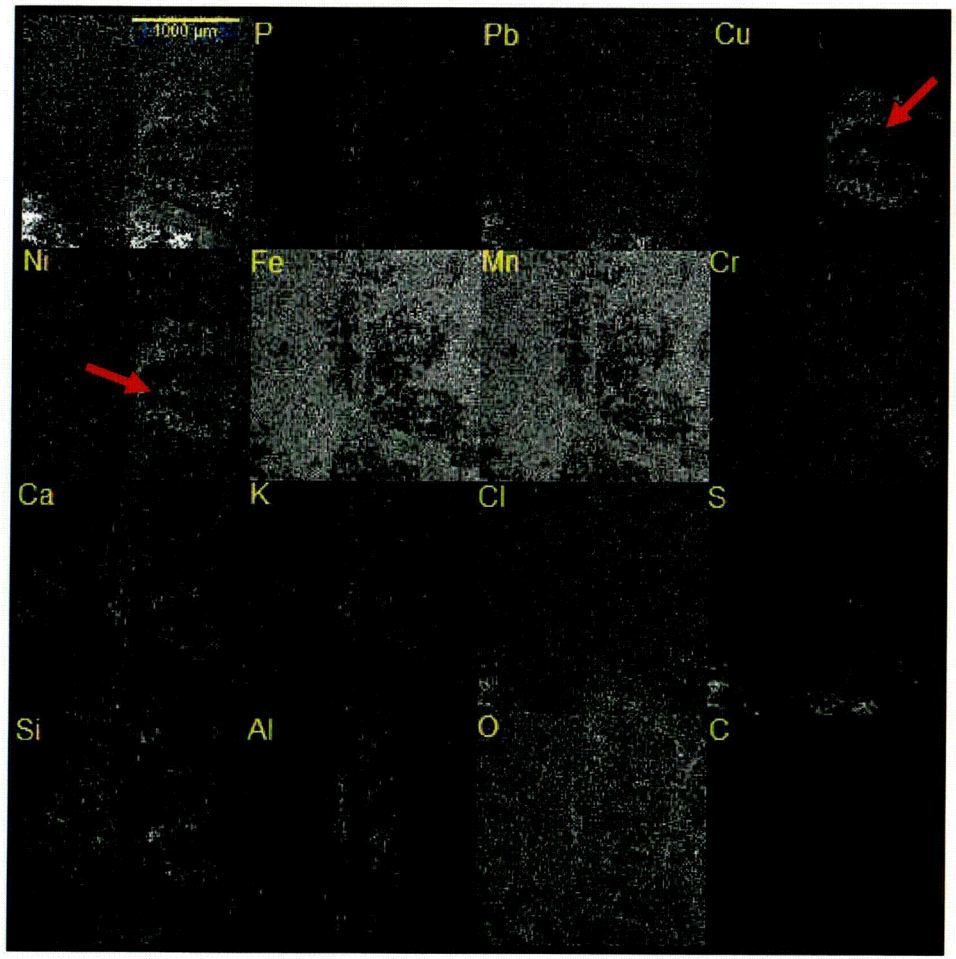

Figure 10-27 SEM Photograph and Backscatter EDS Area Maps Showing Concentration of Various Elements Identified on the OD Deposit at TTS Region of R11C60 Piece 2B at 327° Azimuthal Orientation (Field +Pt Signal Location). Note region of higher copper and nickel concentrations.

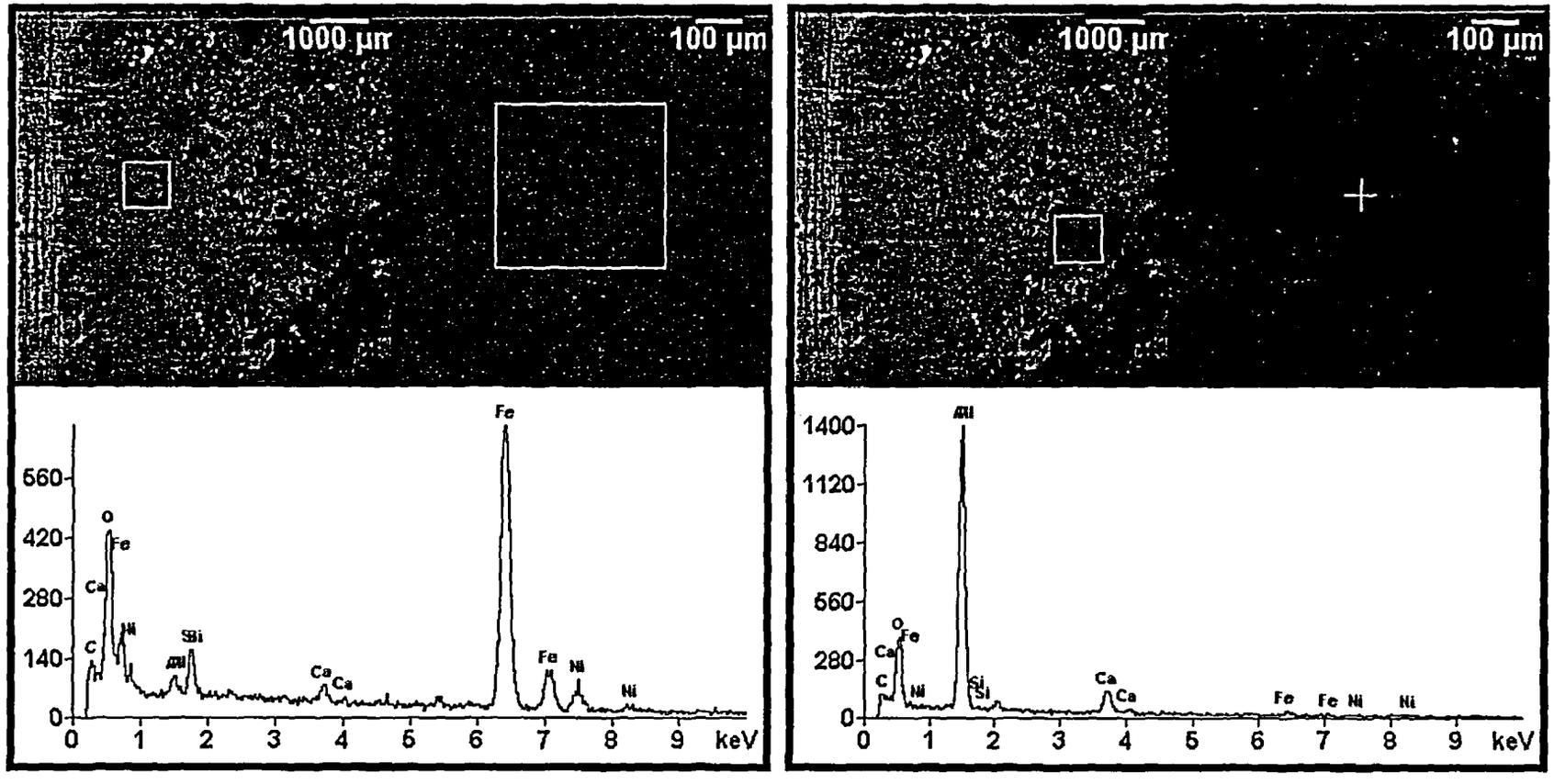

a) 6B-EDS2

b) 6B-EDS3

Figure 10-28 SEM Photography and EDS Elemental Trace of OD Deposit from TTS Region of R11C60 Piece 2B at 130° Azimuthal Orientation (Field UT signal location).

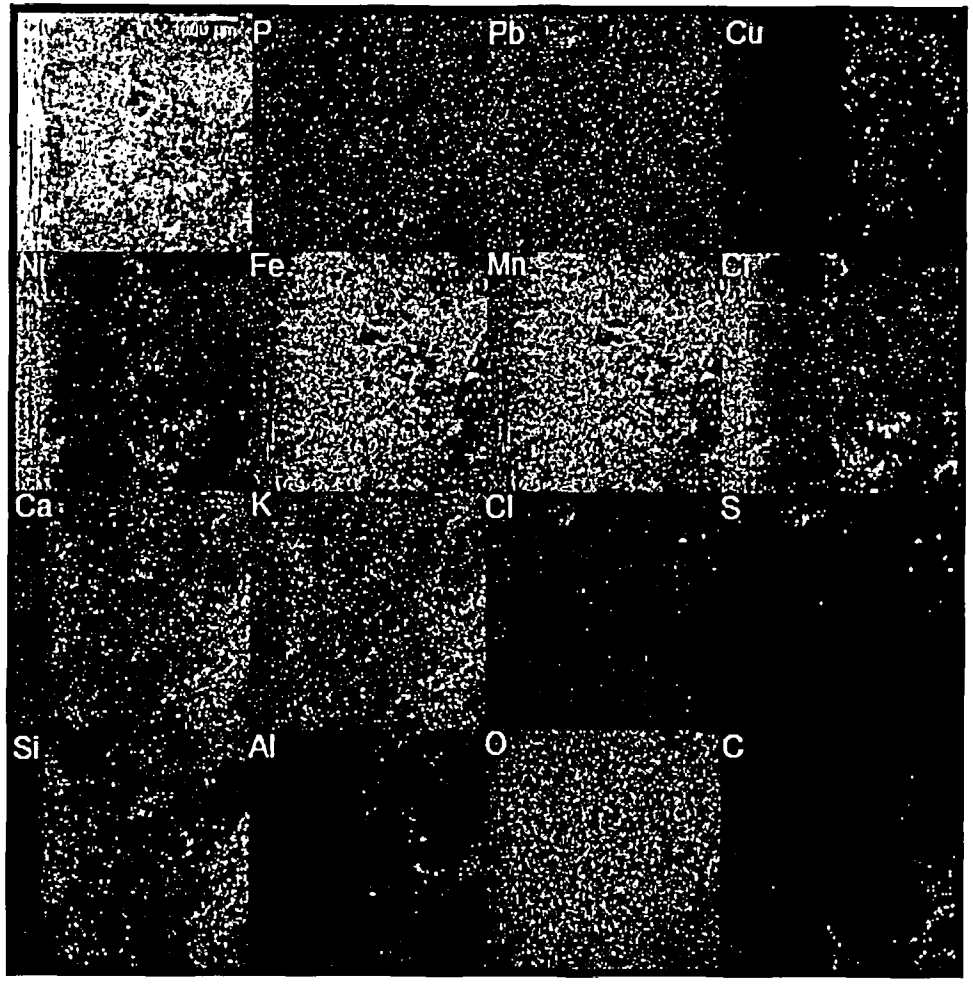

c) 6B – EDS Area Map

Figure 10-29 SEM Photography and EDS Elemental Maps of OD Deposit from TTS Region of R11C60 Piece 2B at 130° Azimuthal Orientation (Field UT signal location).

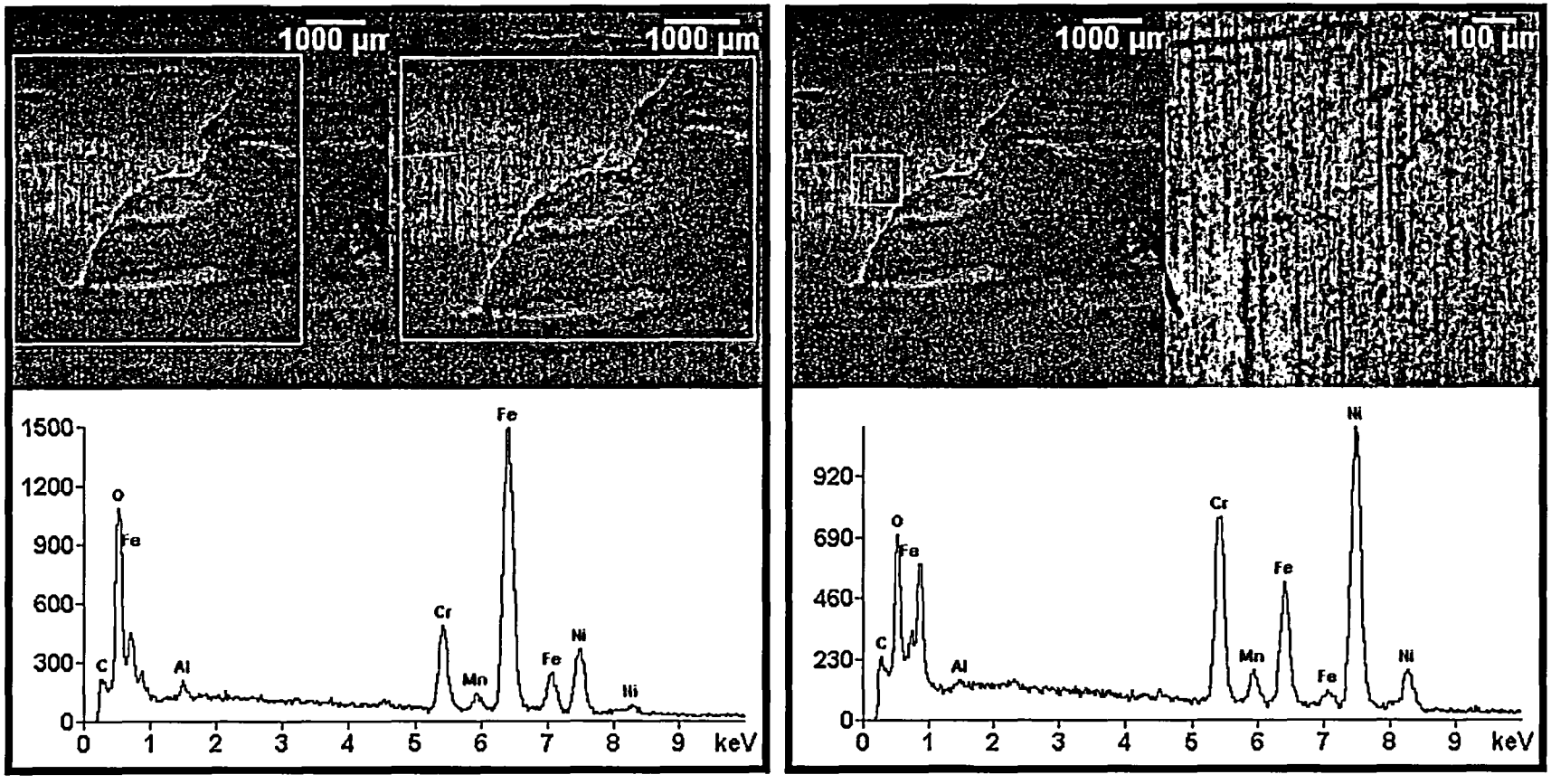

a) 6B-EDS1

b) 6B-EDS2

Figure 10-30 SEM photography and EDS elemental trace of OD deposit from 1st TSP region of R12C59 Piece 3B at quatrefoil land to tube intersection (10° azimuthal orientation).

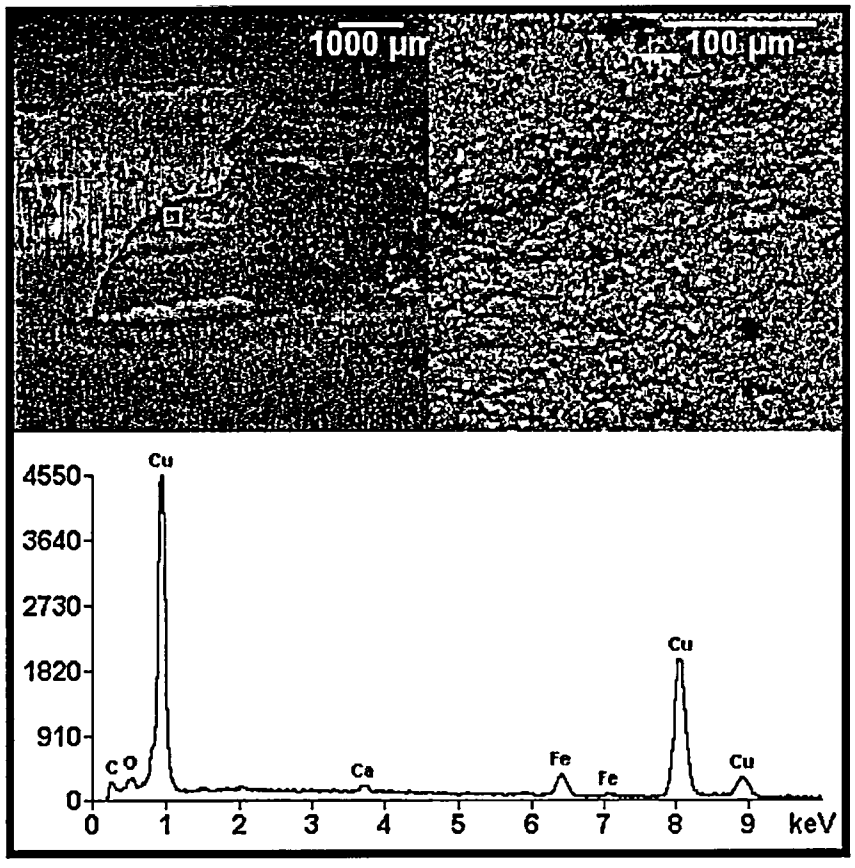

c) 6B-EDS3

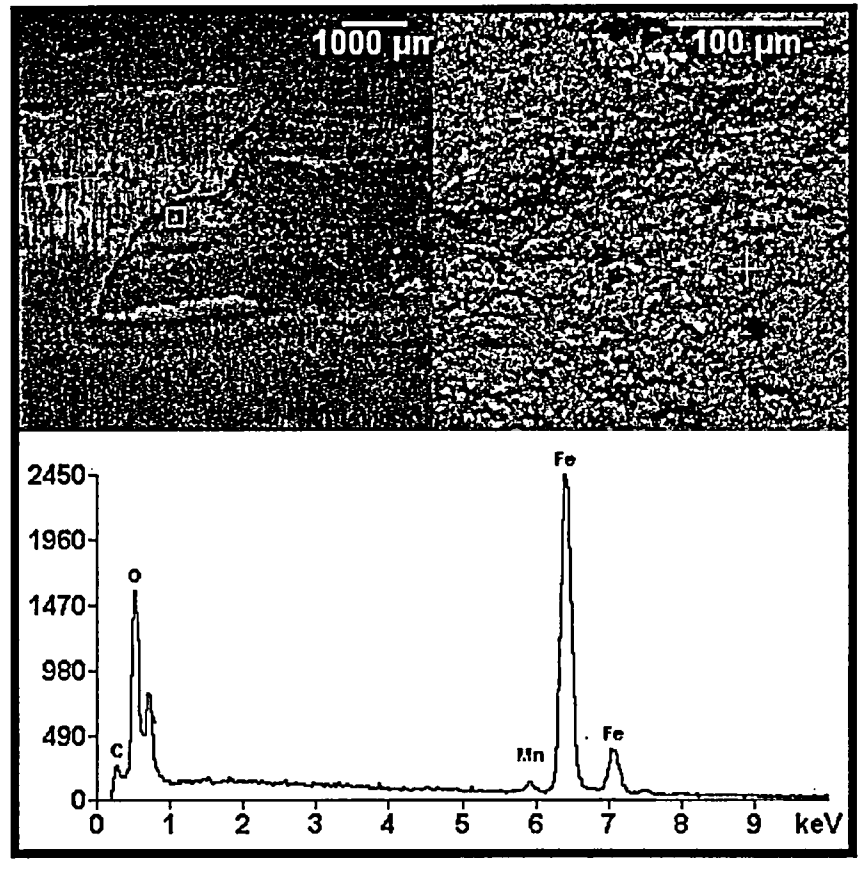

d) 6B-EDS4

Figure 10-30 (Cont'd) SEM photography and EDS elemental trace of OD deposit from 1st TSP region of R12C59 Piece 3B at quatrefoil land to tube intersection (10° azimuthal orientation).

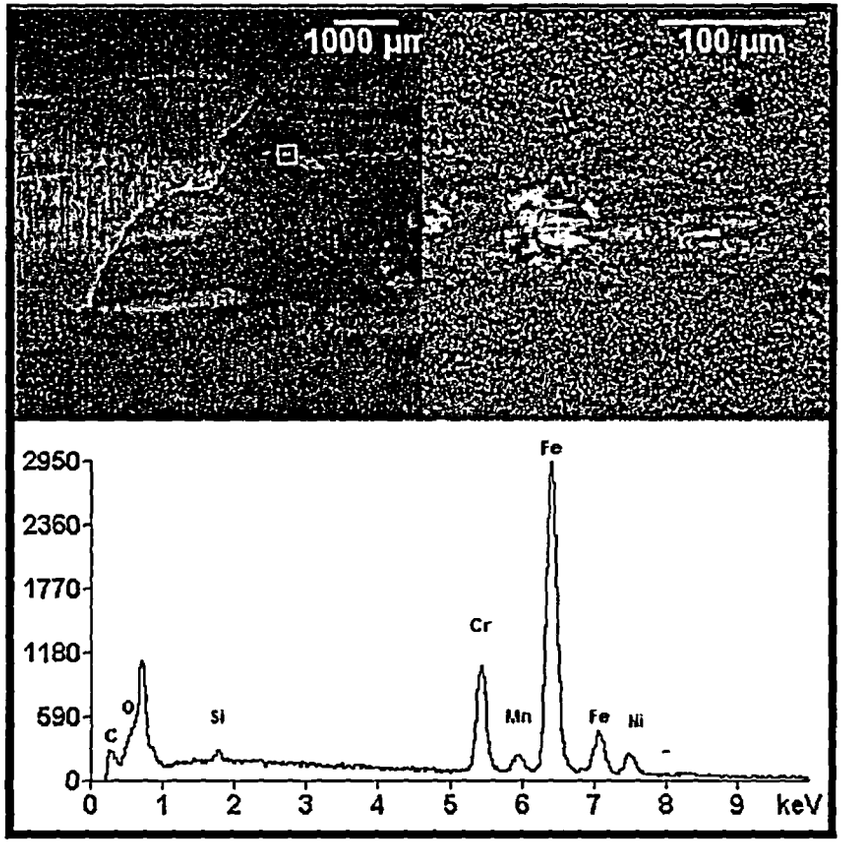

c) 6B-EDS5

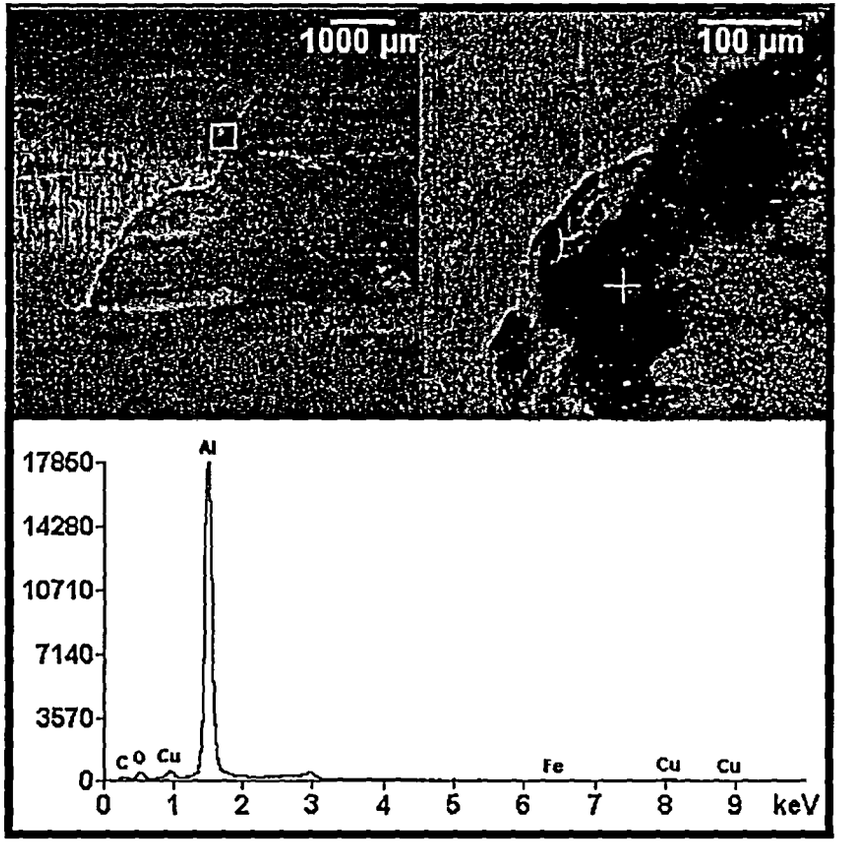

f) 6B-EDS6

Figure 10-30 (Cont'd) SEM photography and EDS elemental trace of OD deposit from 1st TSP region of R12C59 Piece 3B at quatrefoil land to tube intersection (10° azimuthal orientation).

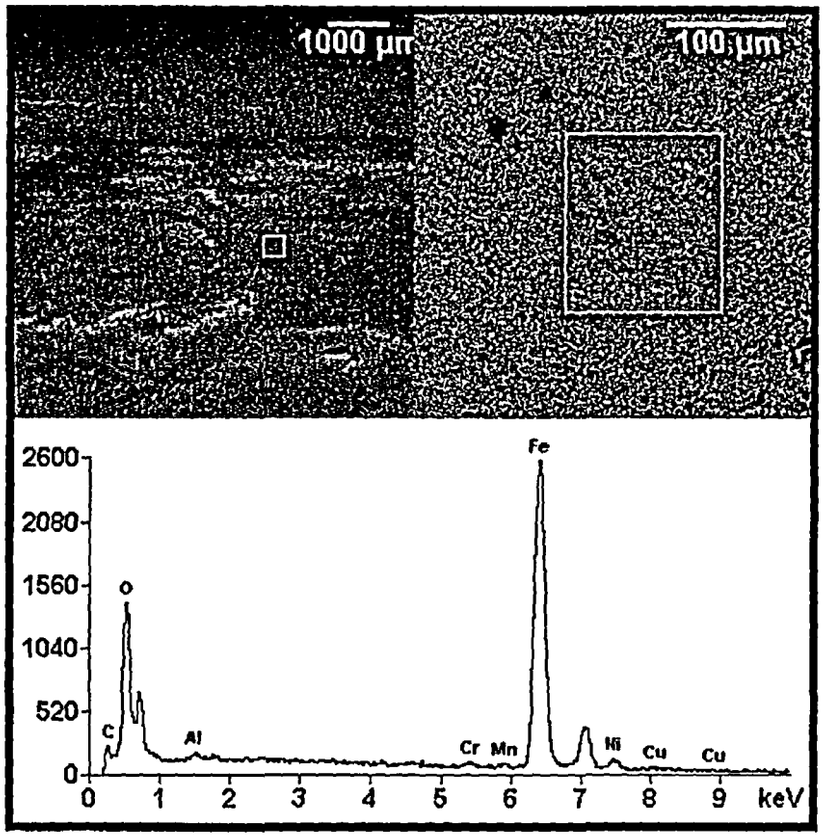

g) 7B-EDS1

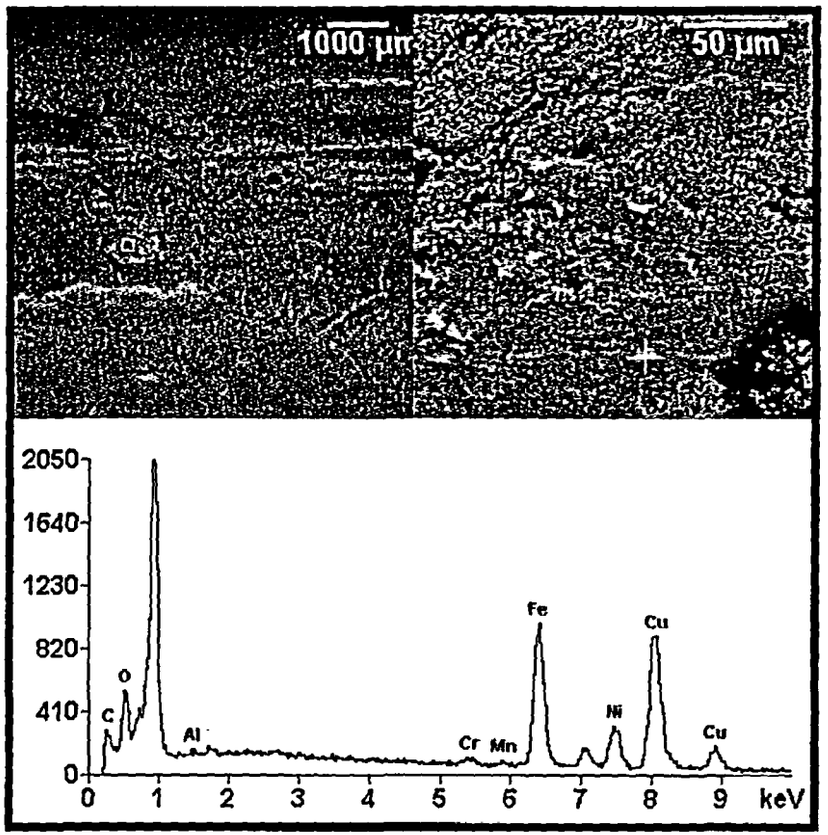

h) 8B-EDS1

Figure 10-30 (Cont'd) SEM photography and EDS elemental trace of OD deposit from 1st TSP region of R12C59 Piece 3B at quatrefoil land to tube intersection (10° azimuthal orientation).

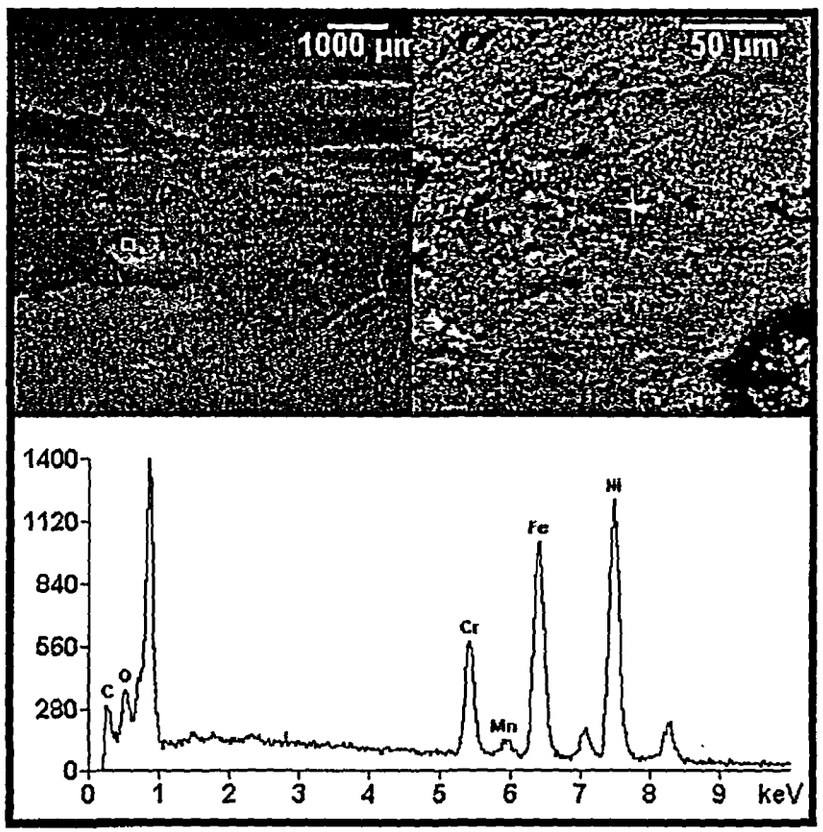

i) 8B-EDS2

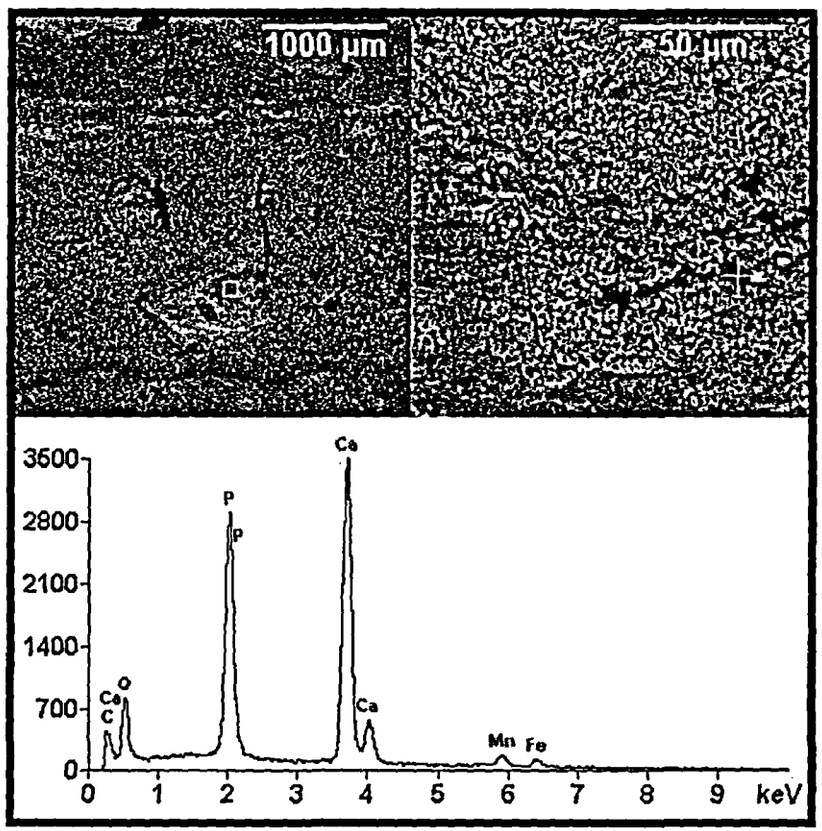

j) 8B-EDS3

Figure 10-30 (Cont'd) SEM photography and EDS elemental trace of OD deposit from 1st TSP region of R12C59 Piece 3B at quatrefoil land to tube intersection (10° azimuthal orientation).

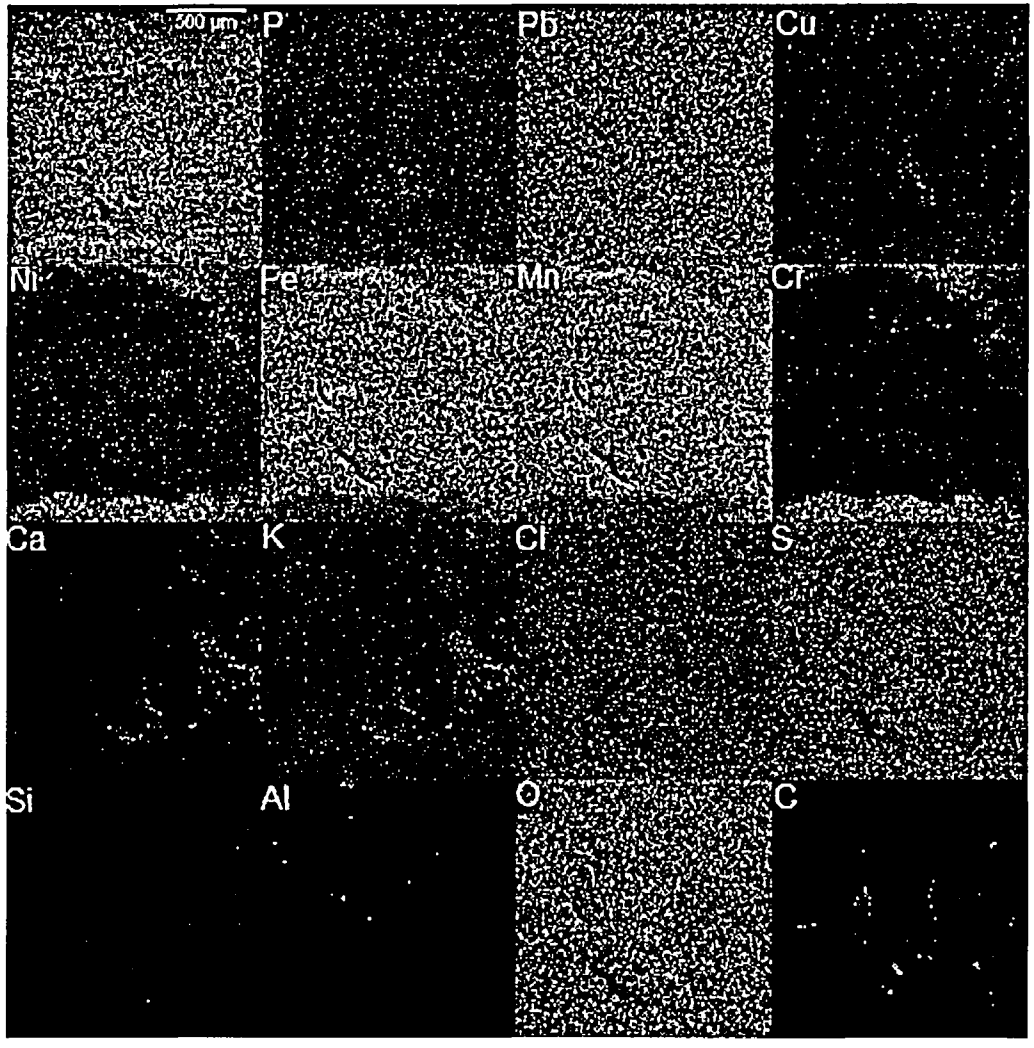

Figure 10-31 Backscatter EDS maps showing concentration of various elements identified on the OD surface of deposit at 1st TSP region of R12C59 Piece 3B at quatrefoil land tube intersection (10° azimuthal orientation).

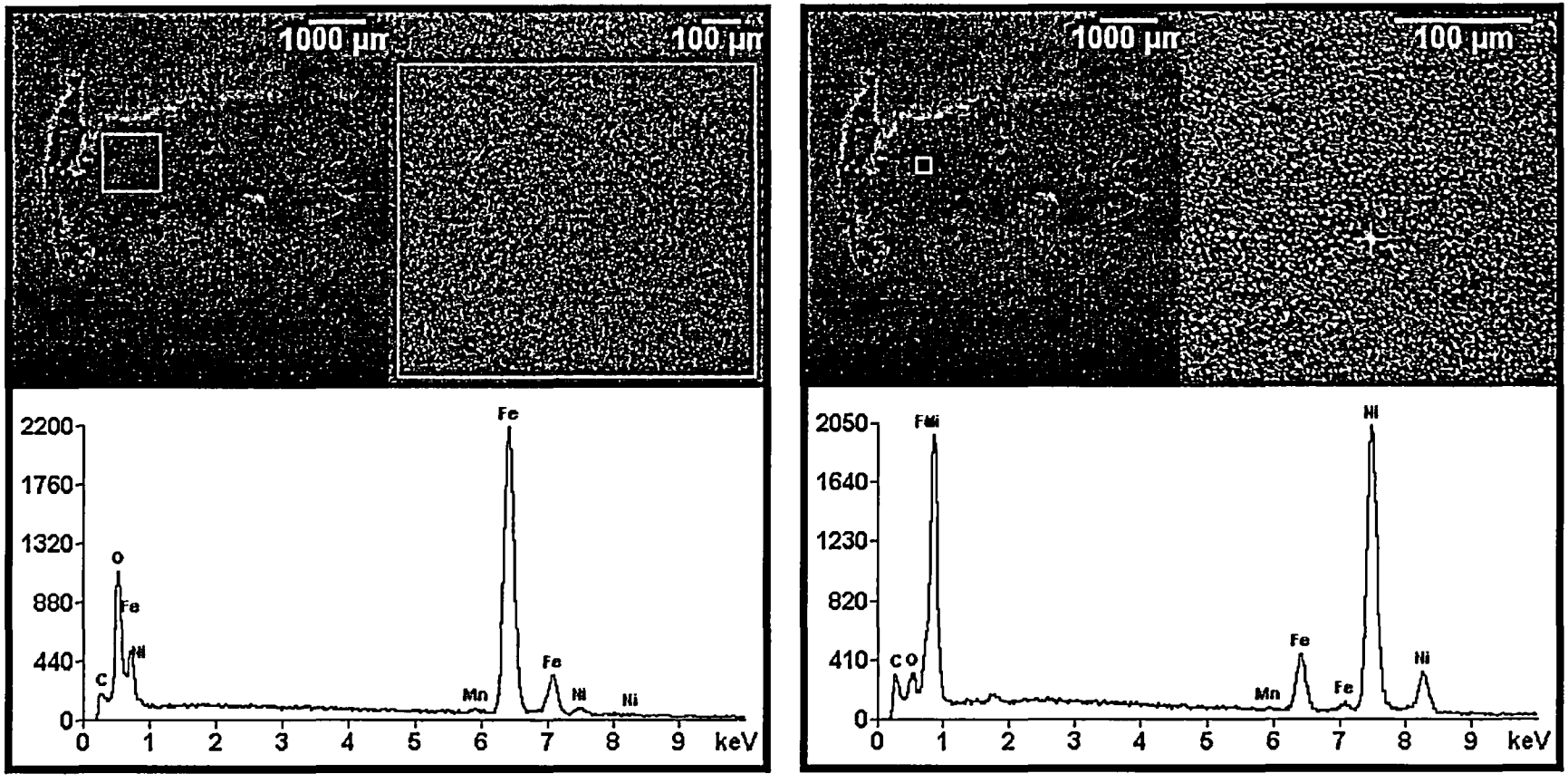

a) 7B-EDS1

b) 7B-EDS2

Figure 10-32 SEM photography and EDS elemental trace of OD deposit from 1st TSP region of R12C59 Piece 3B quatrefoil land to tube intersection (100° azimuthal orientation).

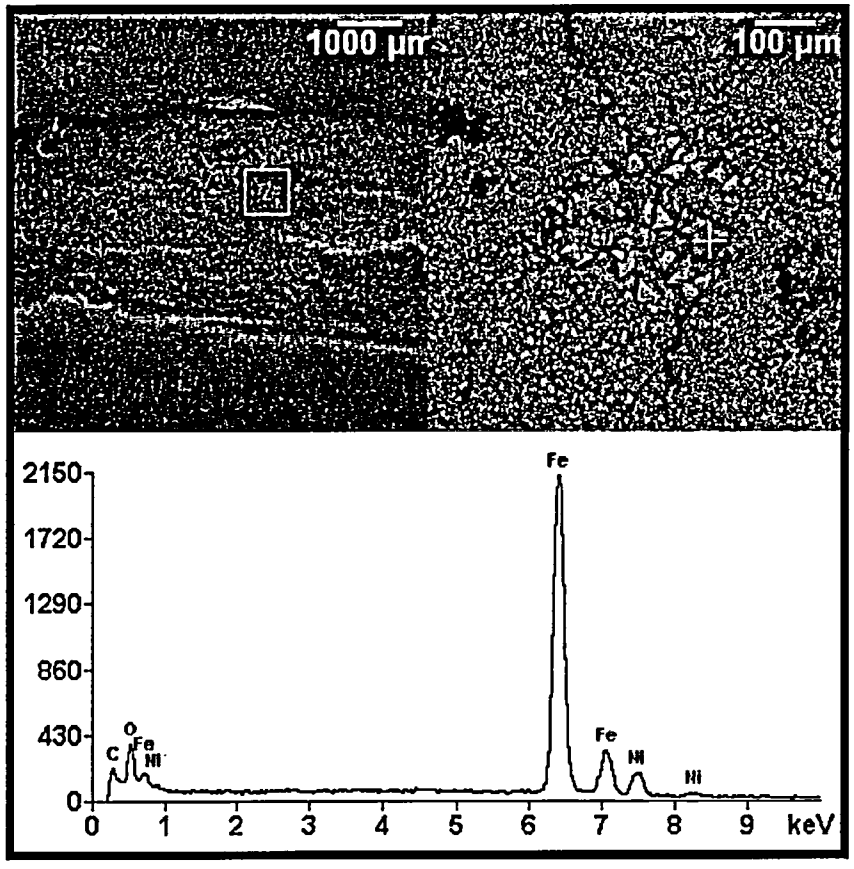

c) 8B-EDS2

Figure 10-32 Cont'd) SEM photography and EDS elemental trace of OD deposit from 1st TSP region of R12C59 Piece 3B quatrefoil land to tube intersection (100° azimuthal orientation).

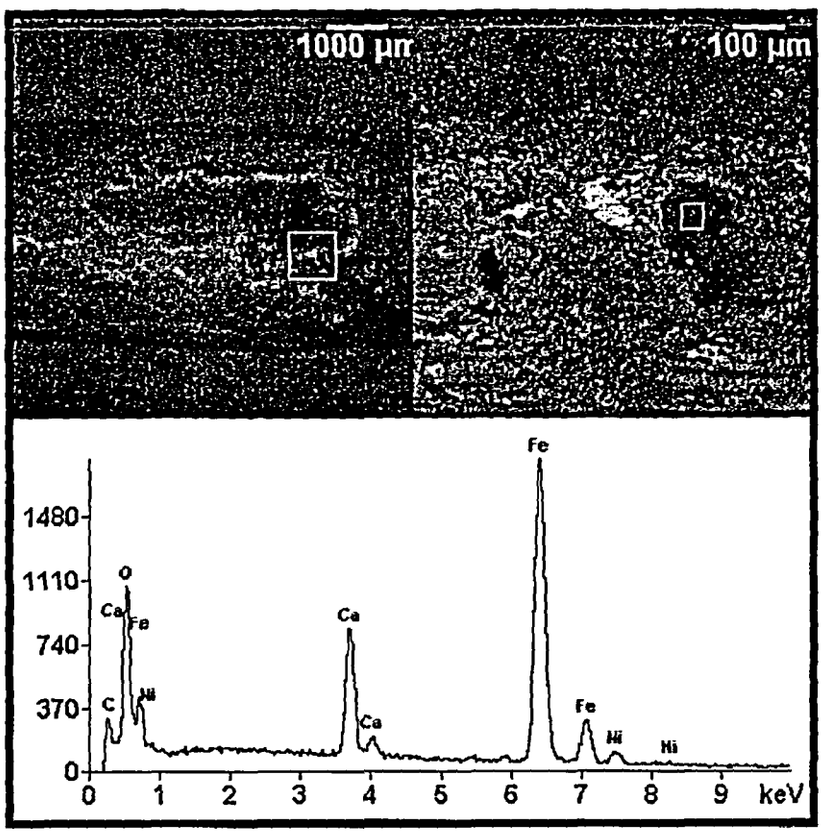

d) 9B-EDS1

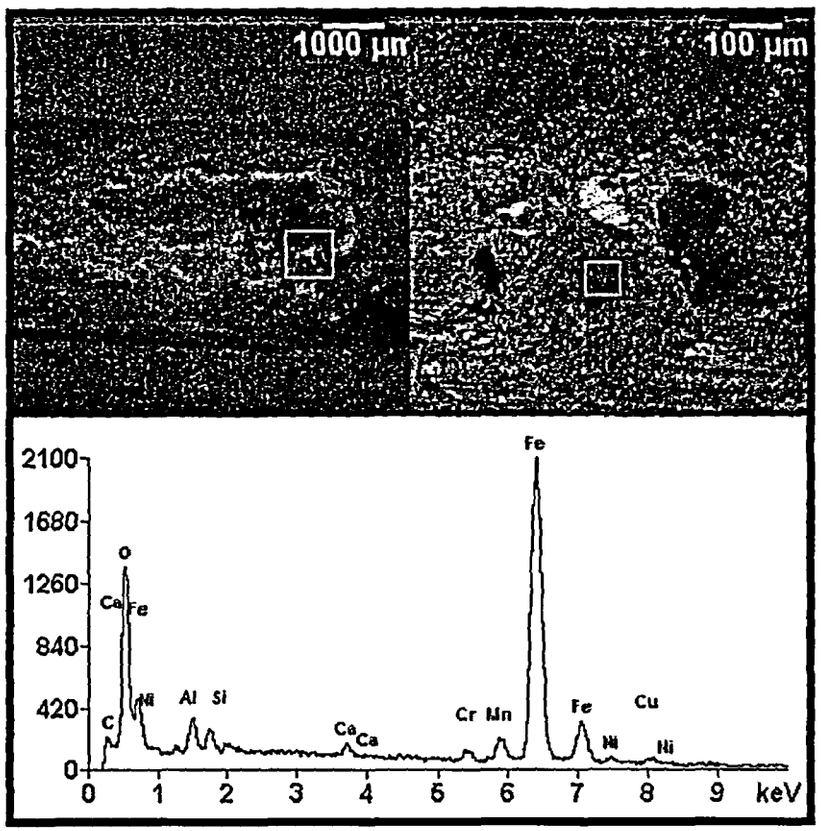

e) 9B-EDS2

Figure 10-32 Cont'd) SEM photography and EDS elemental trace of OD deposit from 1st TSP region of R12C59 Piece 3B quatrefoil land to tube intersection (100° azimuthal orientation).

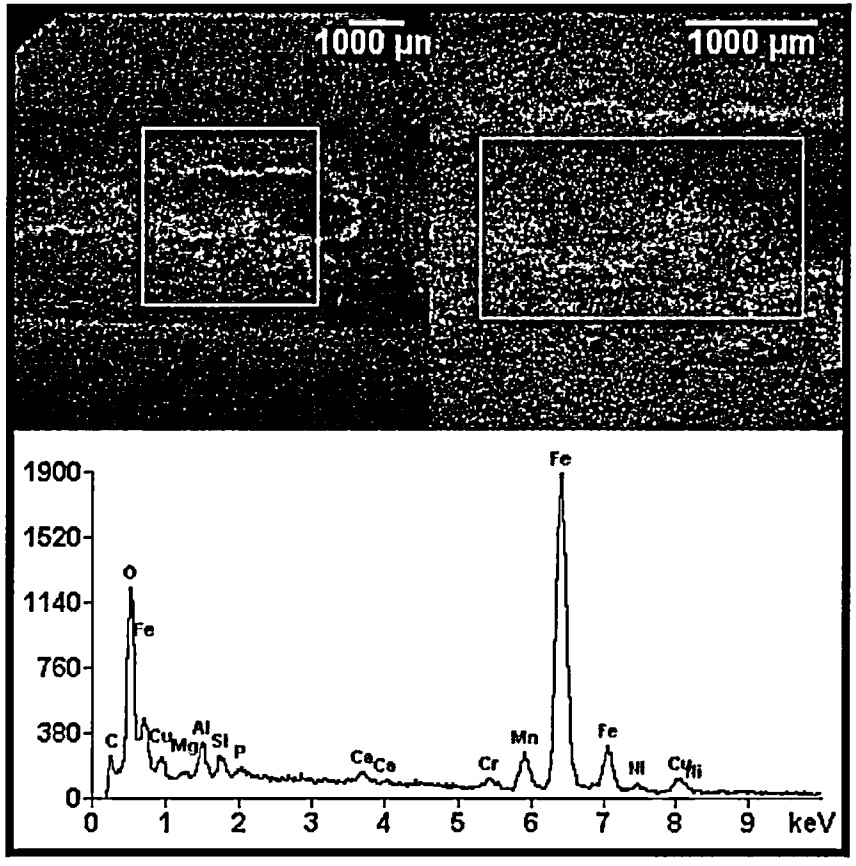

f) 9B-EDS3

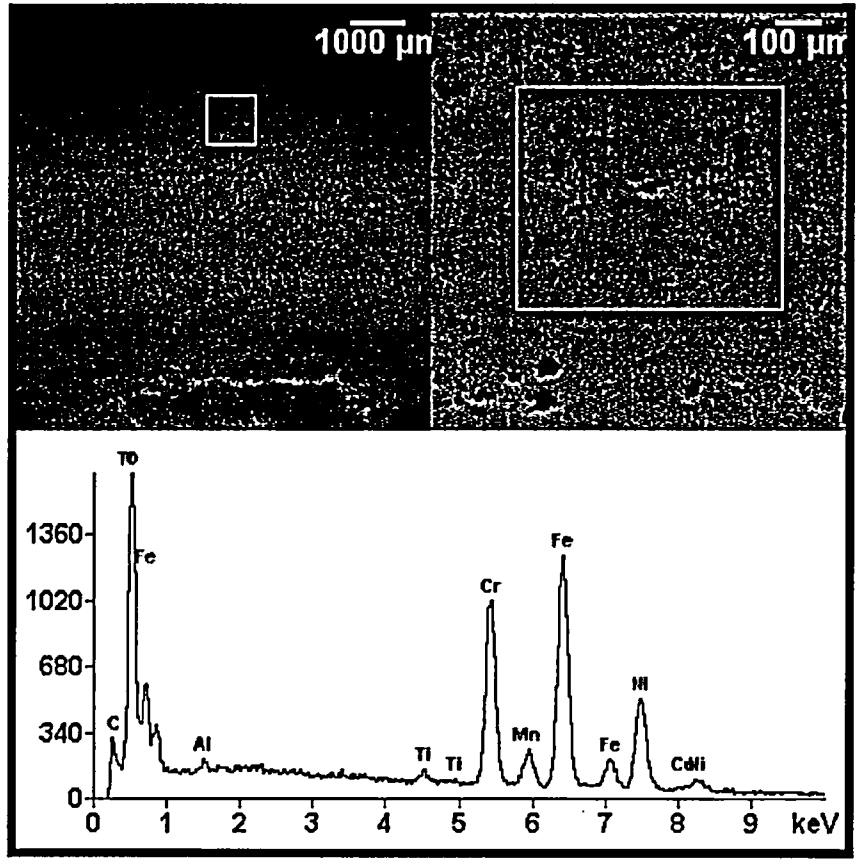

g) 10B-EDS1

Figure 10-32 Cont'd) SEM photography and EDS elemental trace of OD deposit from 1st TSP region of R12C59 Piece 3B quatrefoil land to tube intersection (100° azimuthal orientation).

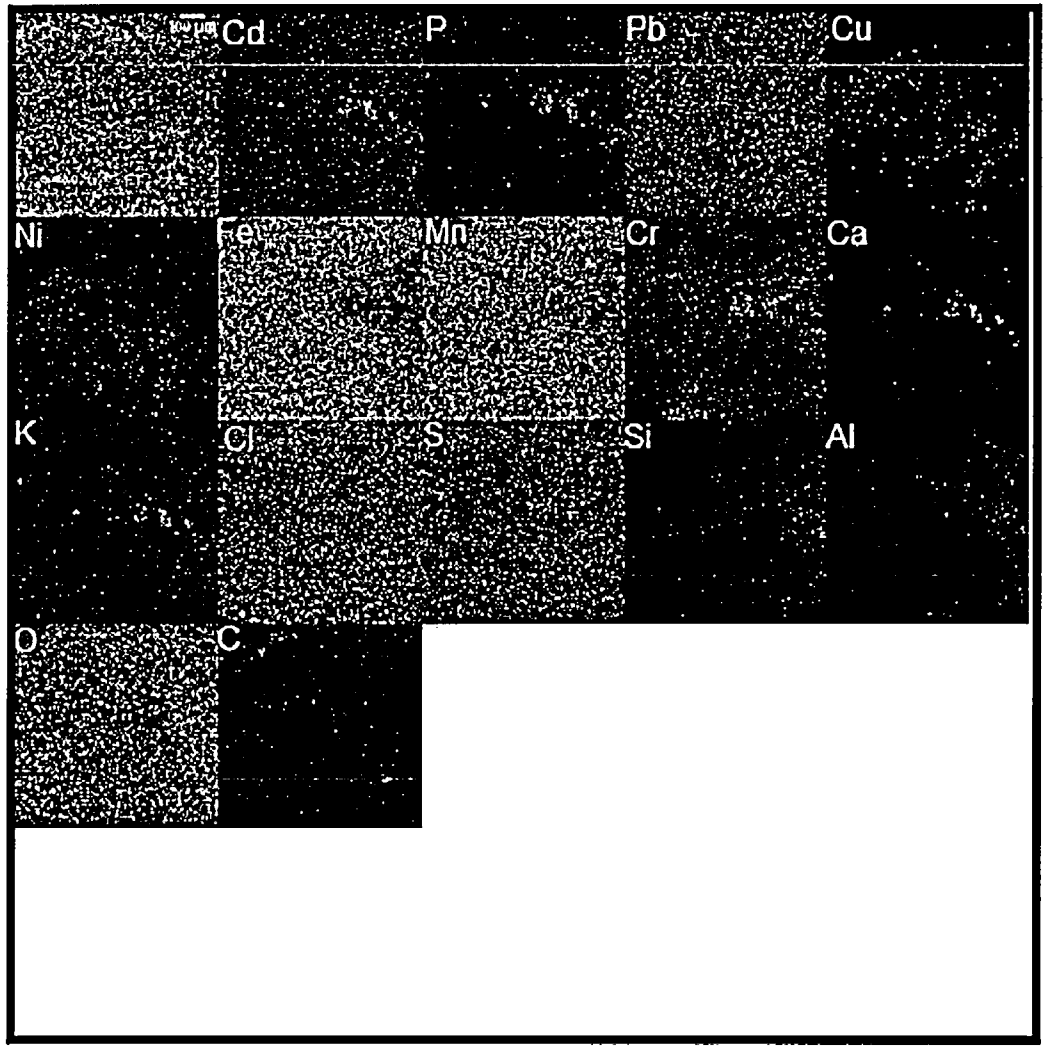

Figure 10-33 Backscatter EDS maps showing concentration of various elements identified on the OD surface at 1st TSP region of R12C59 Piece 3B at quatrefoil land tube intersection (100° azimuthal orientation).

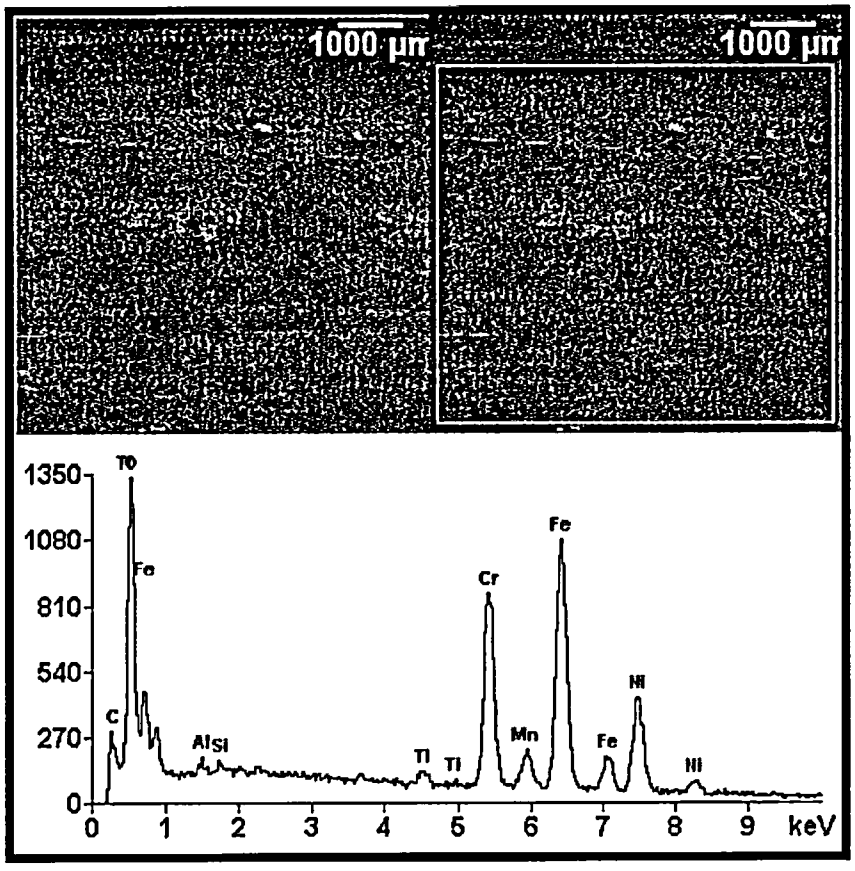

a) 4B-EDS1

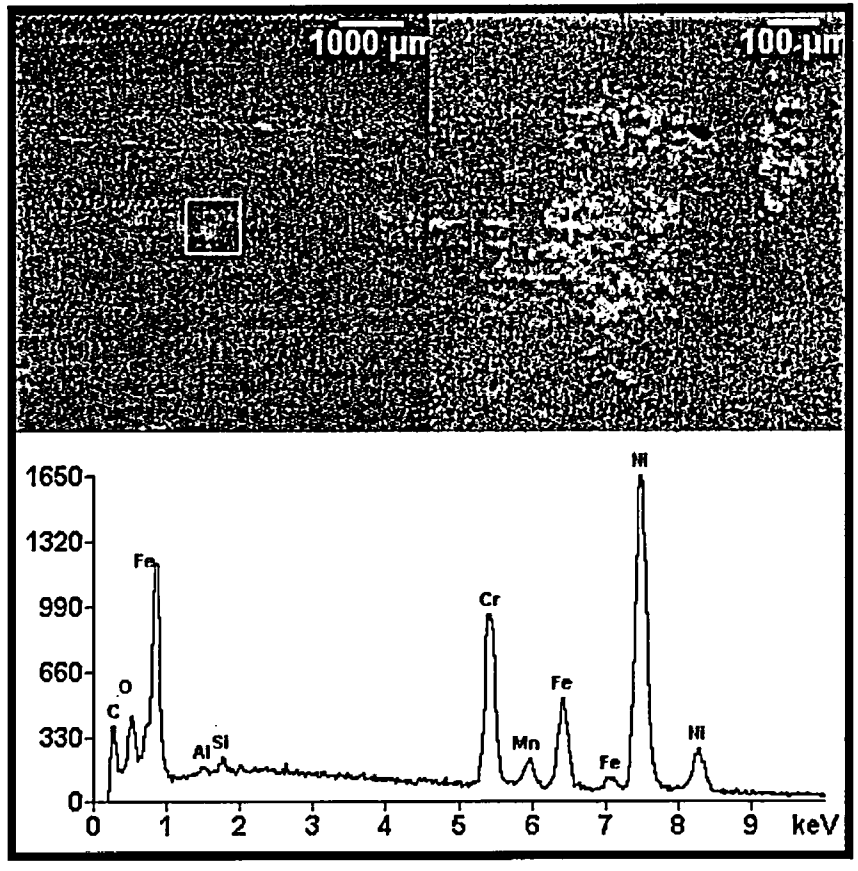

b) 4B-EDS2

Figure 10-34 SEM photography and EDS elemental trace of OD deposit from 1st TSP region of R11C60 Piece 3B quatrefoil land to tube intersection (10° azimuthal orientation).

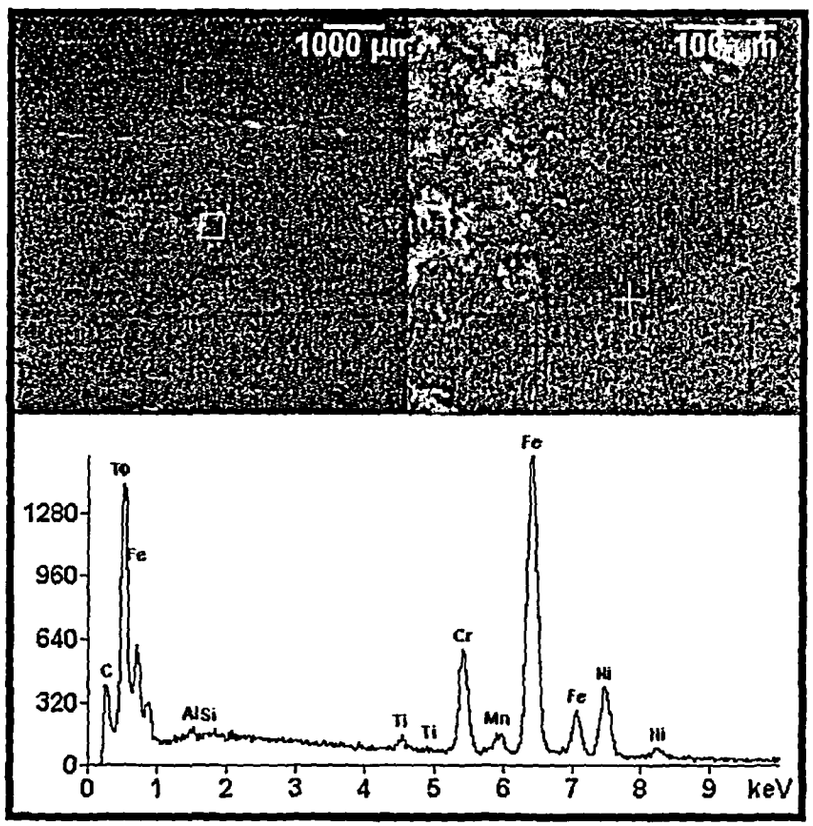

c) 4B-EDS3

Figure 10-34(Cont'd) SEM photography and EDS elemental trace of OD deposit from 1st TSP region of R11C60 Piece 3B quatrefoil land to tube intersection (10° azimuthal orientation).

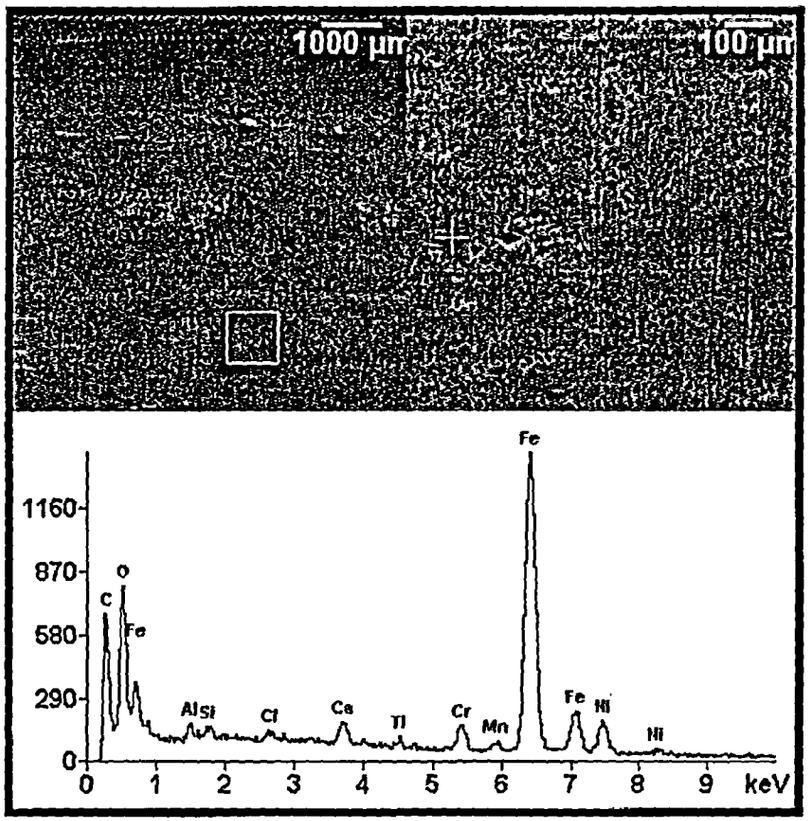

d) 4B-EDS5

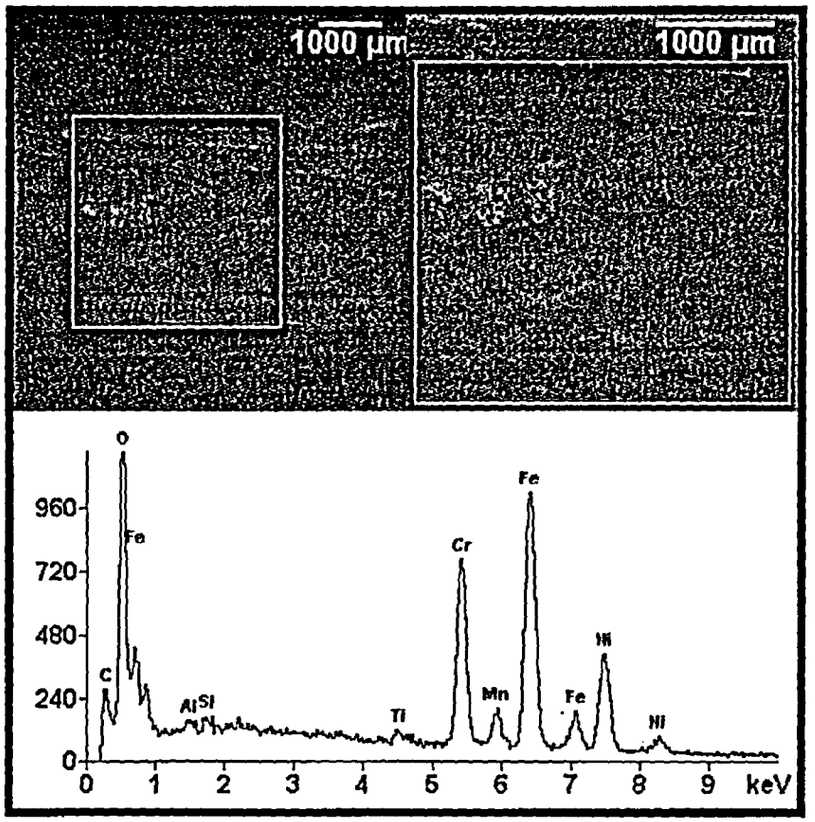

c) 5B-EDS1

Figure 10-34(Cont'd) SEM photography and EDS elemental trace of OD deposit from 1st TSP region of R11C60 Piece 3B quatrefoil land to tube intersection (10° azimuthal orientation).

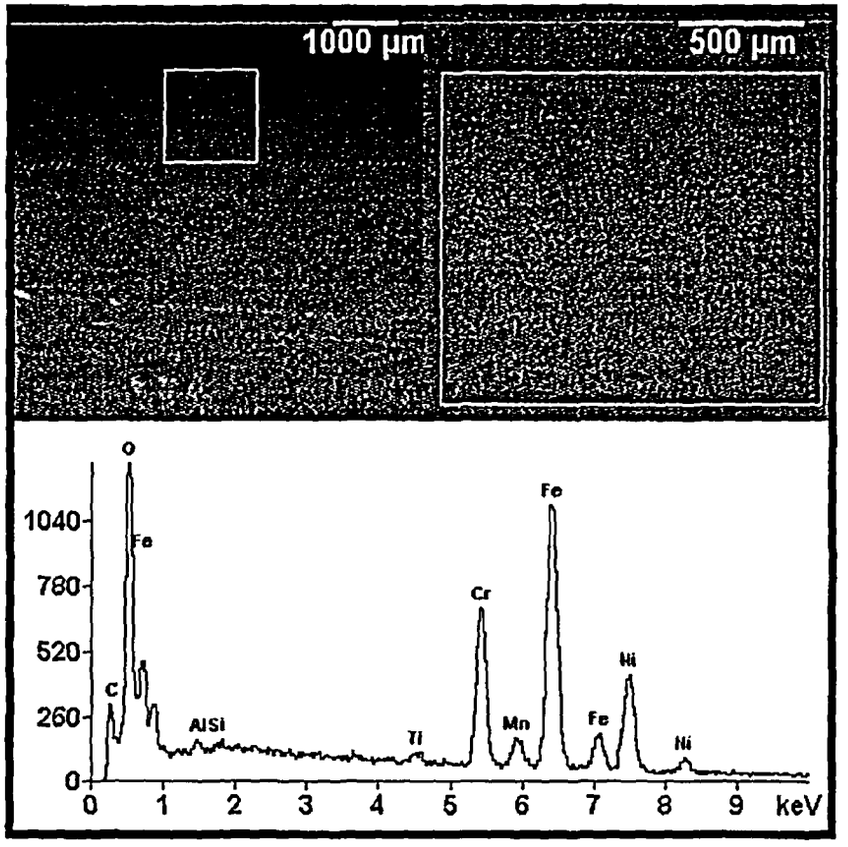

f) 6B-EDS1

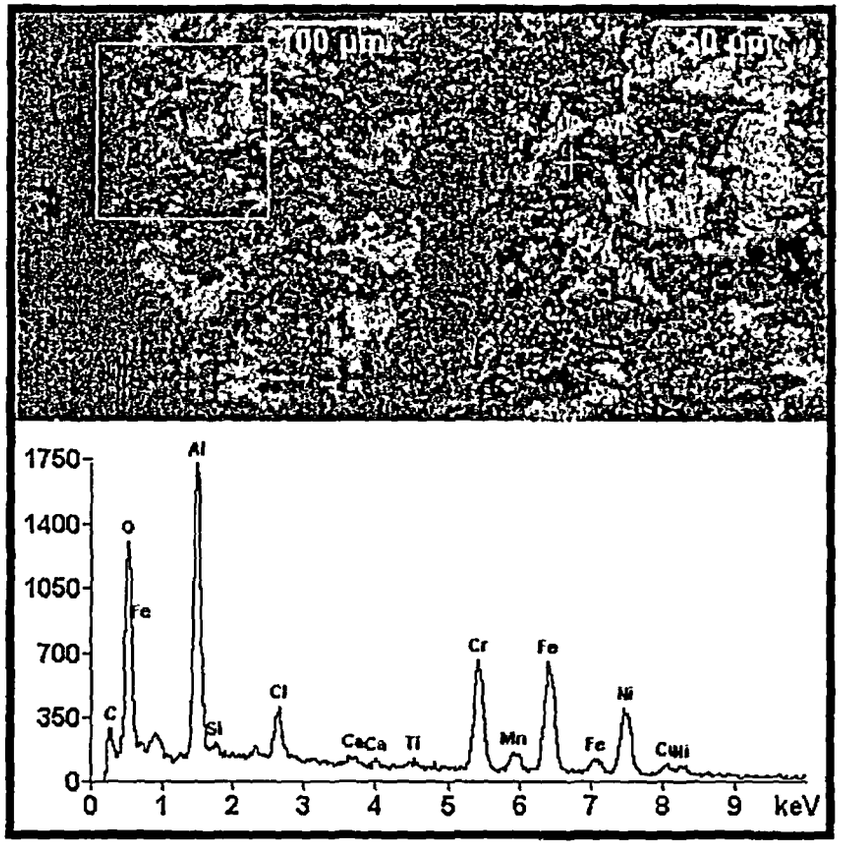

g) 7B-EDS1

Figure 10-34(Cont'd) SEM photography and EDS elemental trace of OD deposit from 1st TSP region of R11C60 Piece 3B quatrefoil land to tube intersection (10° azimuthal orientation).

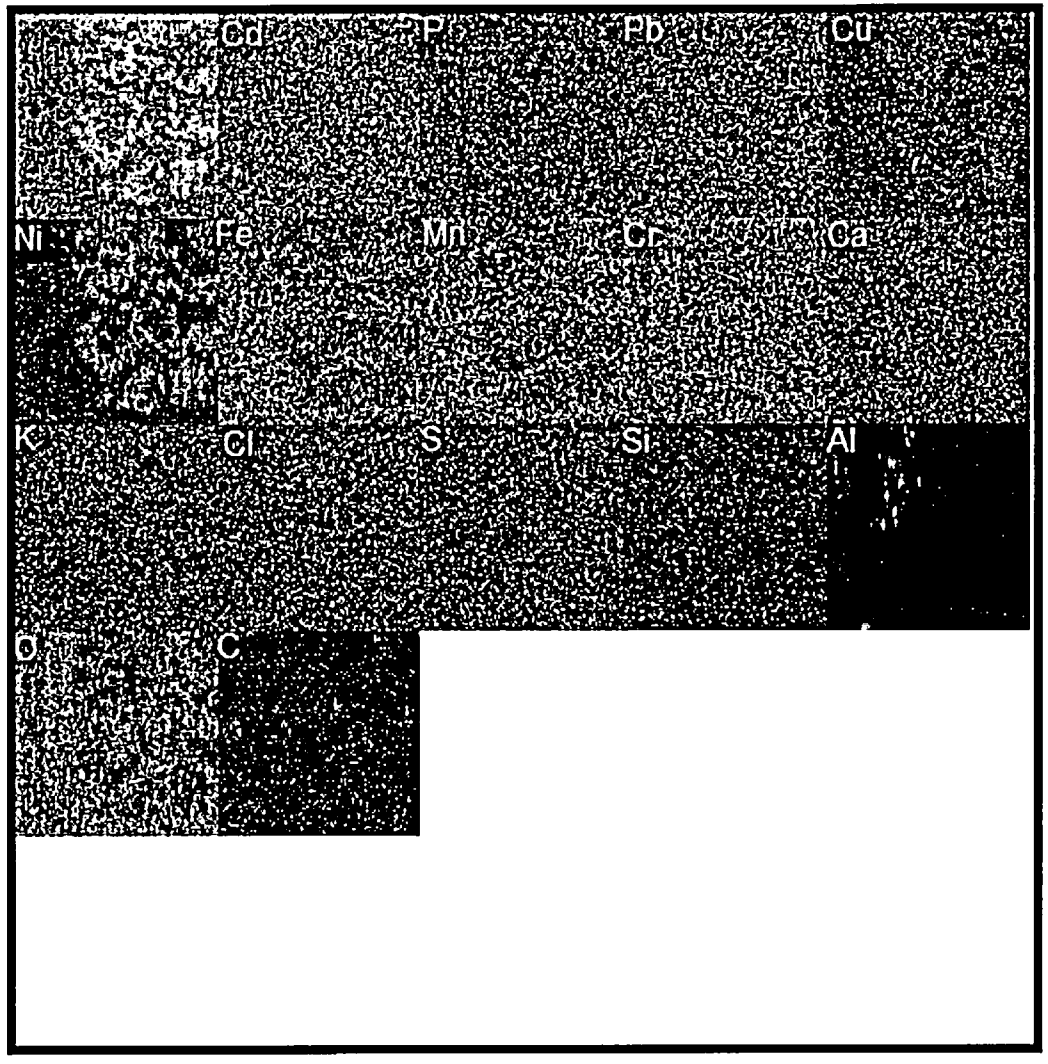

Figure 10-35 Backscatter EDS maps showing concentration of various elements identified on the OD surface of deposit at 1st TSP region of R11C60 Piece 3B at quatrefoil land tube intersection (10° azimuthal orientation).

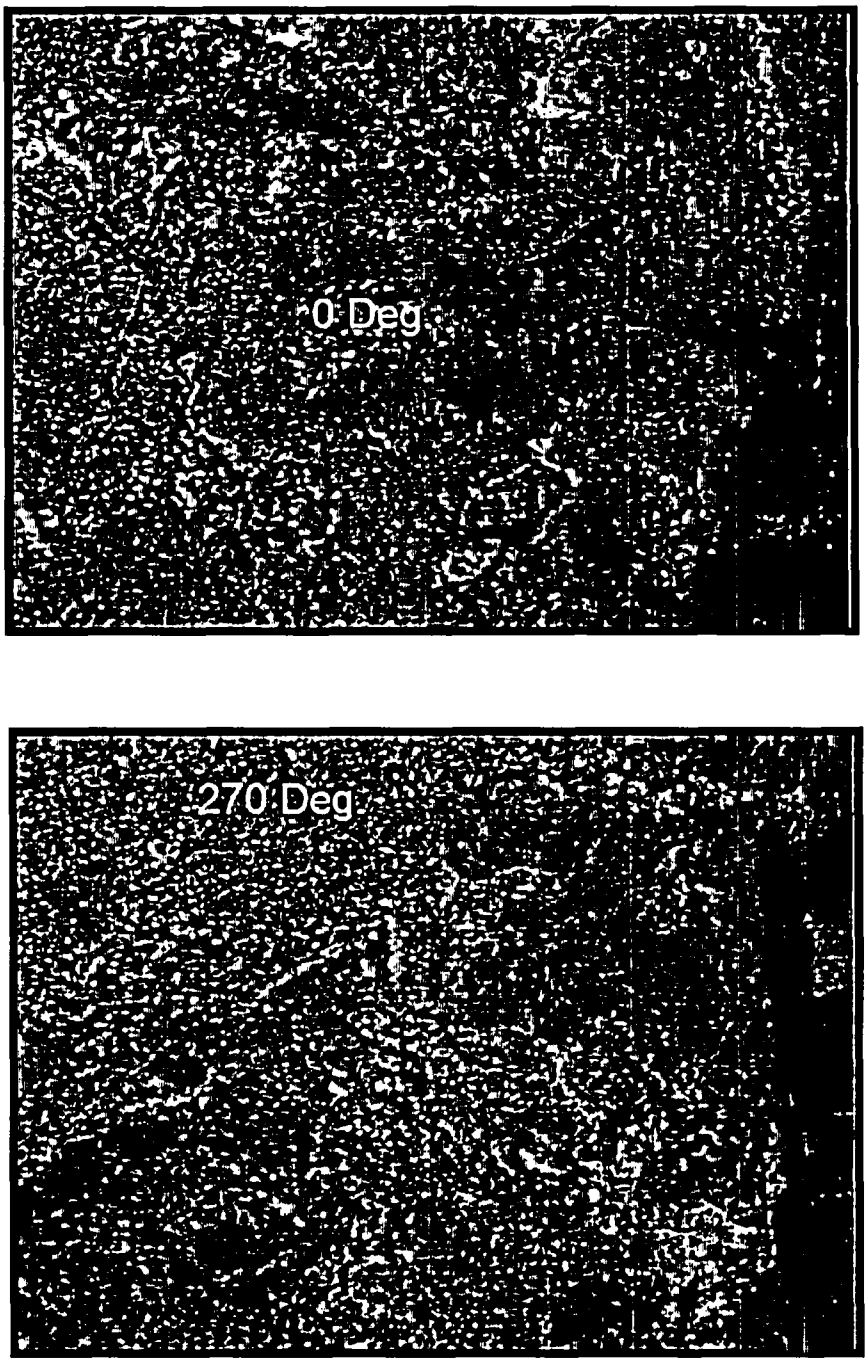

Figure 10-36 SEM micrograph of TTS area of R12C59 HL Piece 2B following ID pressurization to 9,000 psi at 0° and 270° azimuthal orientation. No evidence of cracking or "spalling" of the deposit is seen.

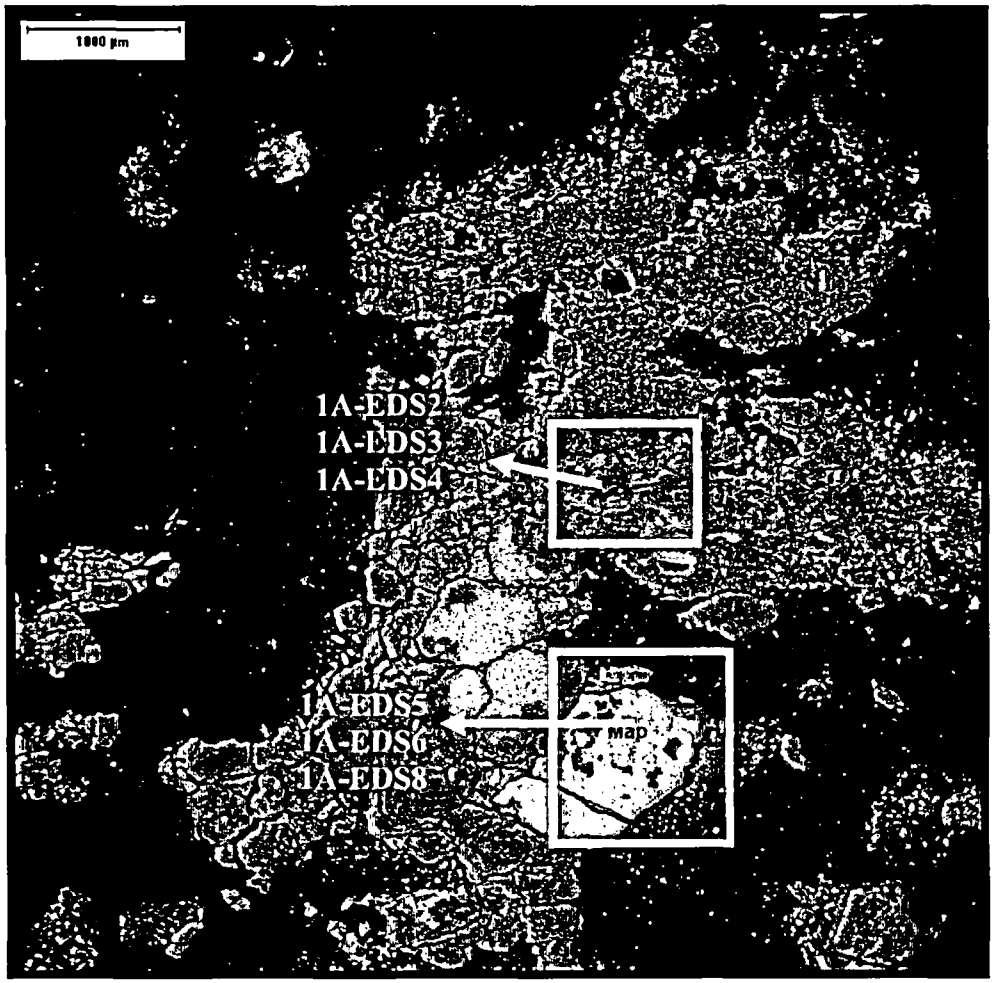

Figure 10-37 SEM micrograph of OD surface deposit removed from the TTS region of R12C59 HL Piece 2B after pressurization to 9000 psi. Refer to Figure 10-38 for EDS analyses.

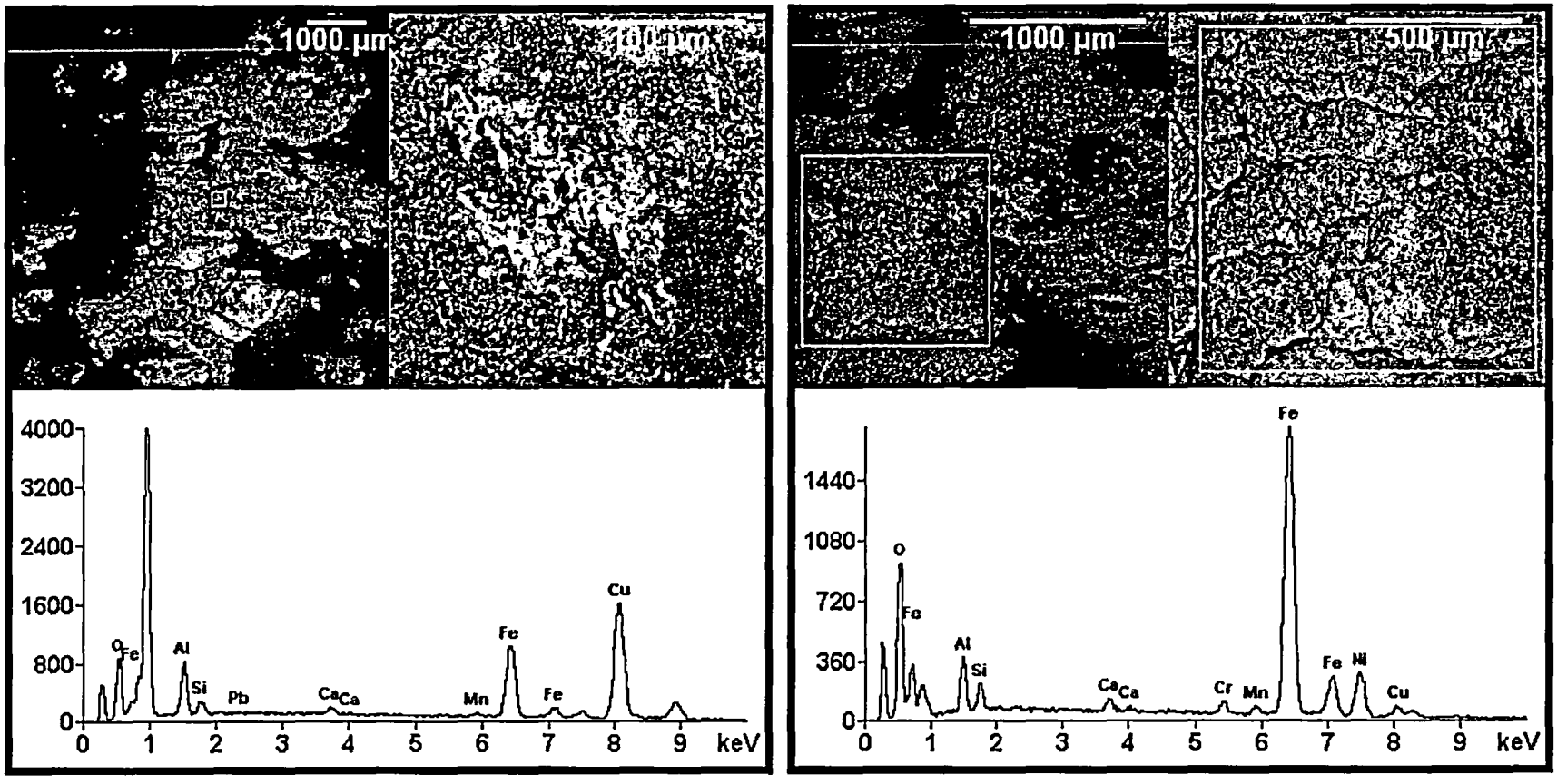

a) 1A-EDS2

b) 1A-EDS3

Figure 10-38 SEM photography and EDS elemental trace of OD deposit collected on tape from the TTS region of R12CC59 HL Piece 2B during ID pressurization to 9,000 psi.

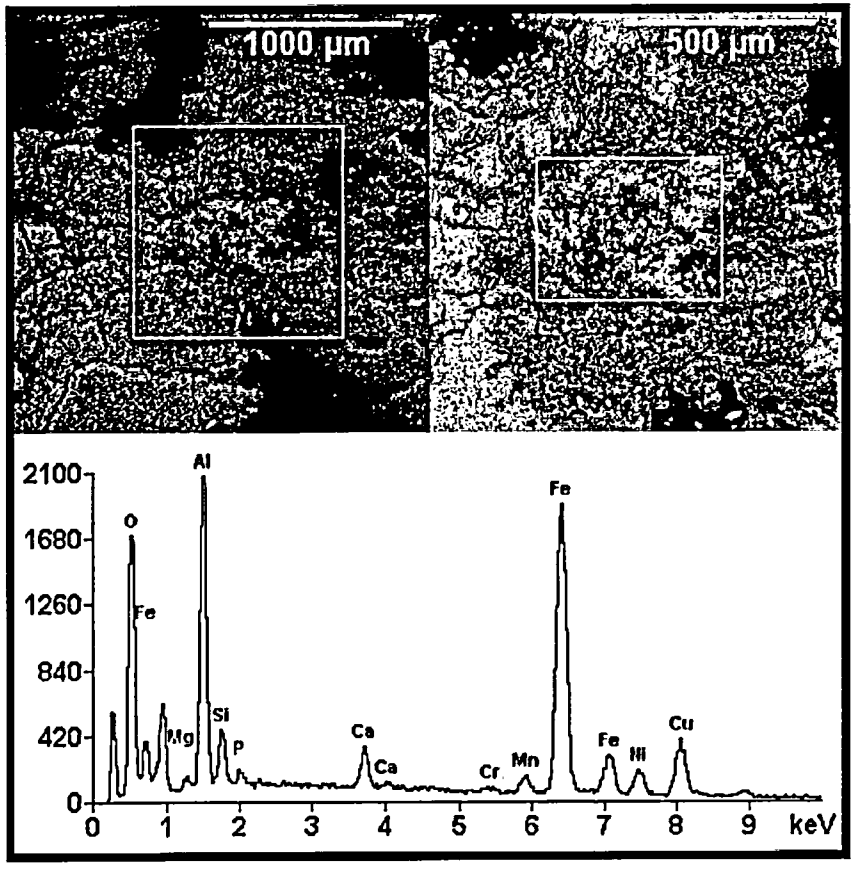

c) 1A-EDS4

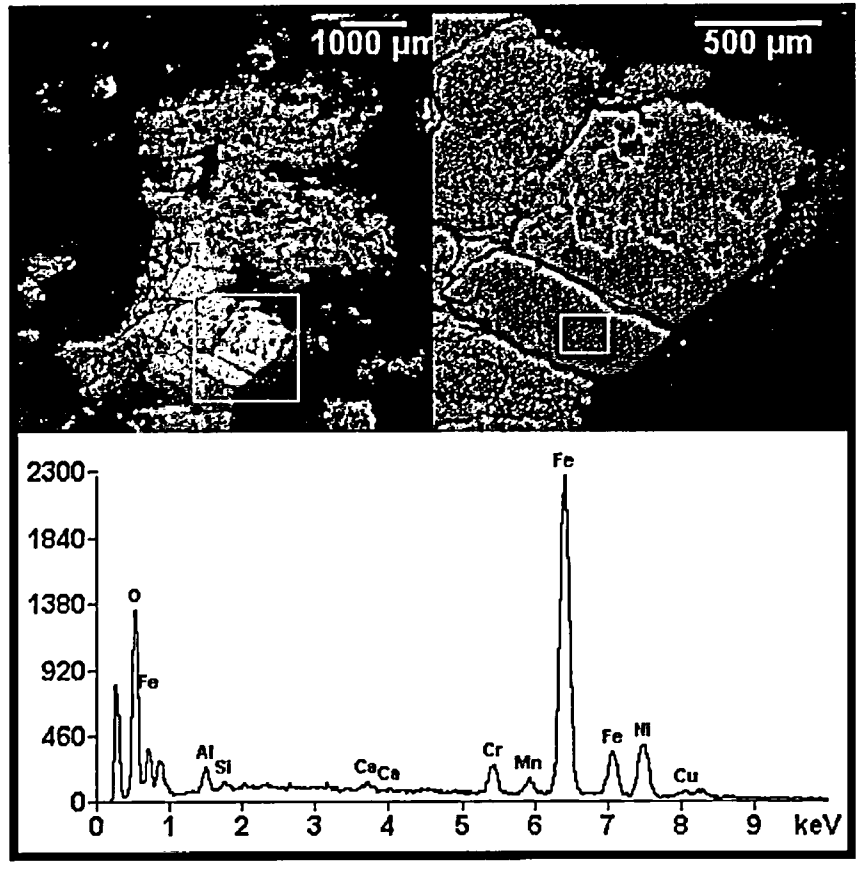

d) 1A-EDS5

Figure 10-38 (Cont'd) SEM photography and EDS elemental trace of OD deposit collected on tape from the TTS region of R12CC59 HL Piece 2B during ID pressurization to 9,000 psi.

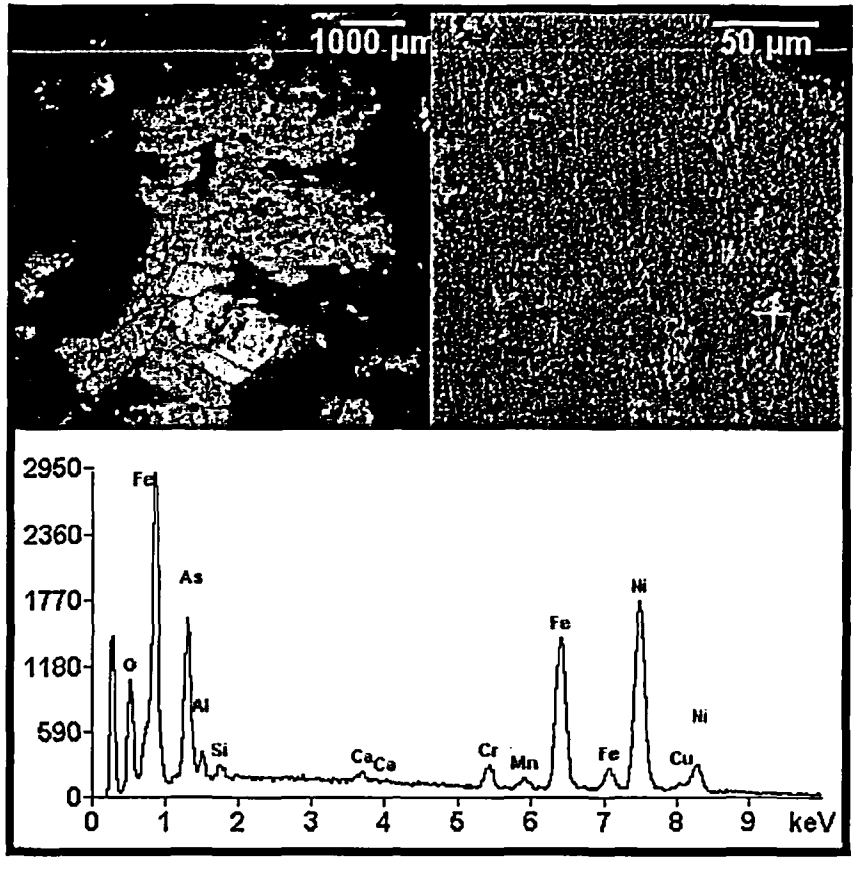

c) 1A-EDS6

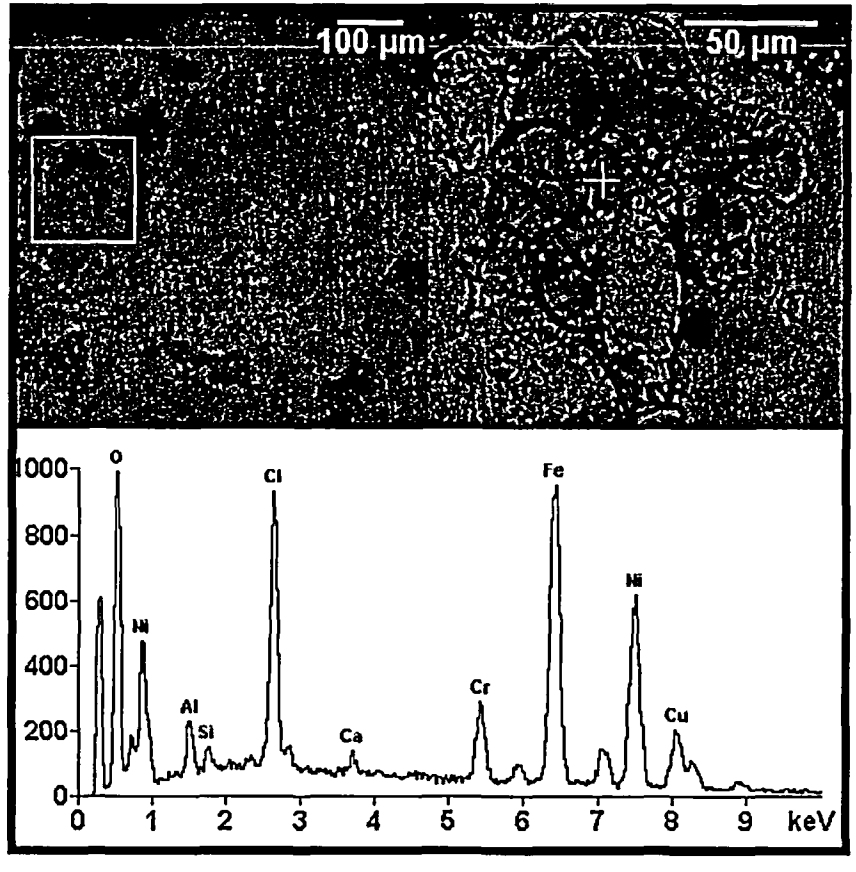

f) 1A-EDS8

Figure 10-38 (Cont'd) SEM photography and EDS elemental trace of OD deposit collected on tape from the TTS region of R12C59 HL Piece 2B during ID pressurization to 9,000 psi.

a) Pre-Pressurization

b) Post Pressurization

Figure 10-39 Backscatter Energy Mode montages showing the OD deposit at the quatrefoil land to tube intersection for R12C59 HL Piece 3B (10° azimuthal orientation). Note the areas where the deposit has "spalled" during the pressurization and collected on the carbon tape. EDS analyses of the deposit collected on the tape is provided in Figure 10-40. The 6, 7, and 8 shown on the pre-pressurization micrographs represents regions where EDS analyses were performed. Refer to Table 10-5 for the EDS analyses results for the pre-pressurization condition.

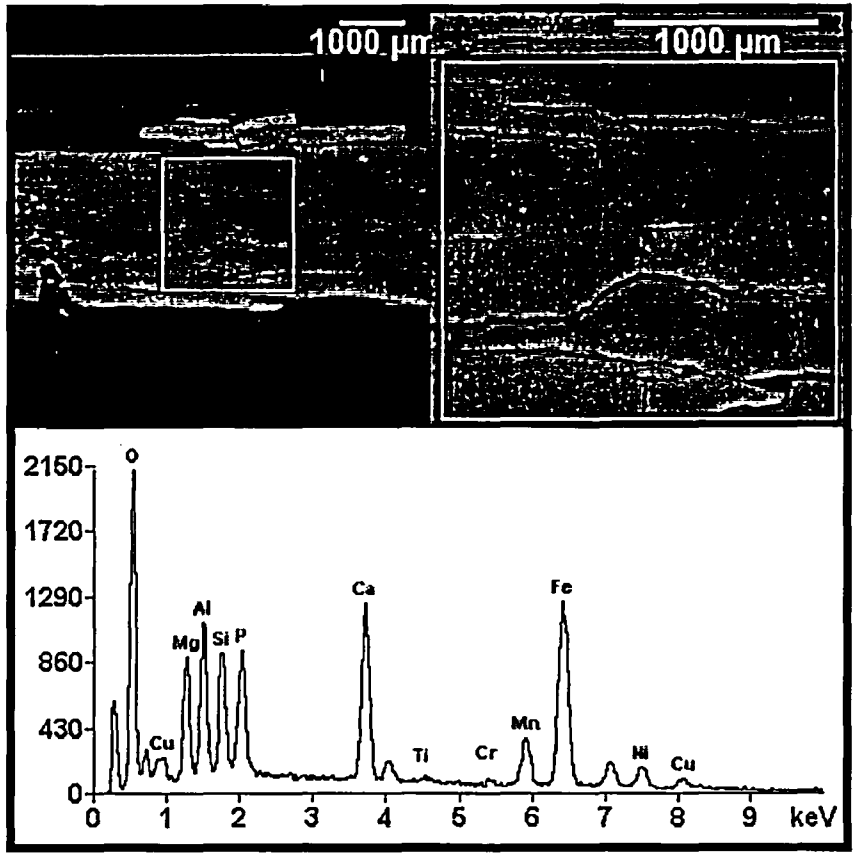

a) 1A-EDS1

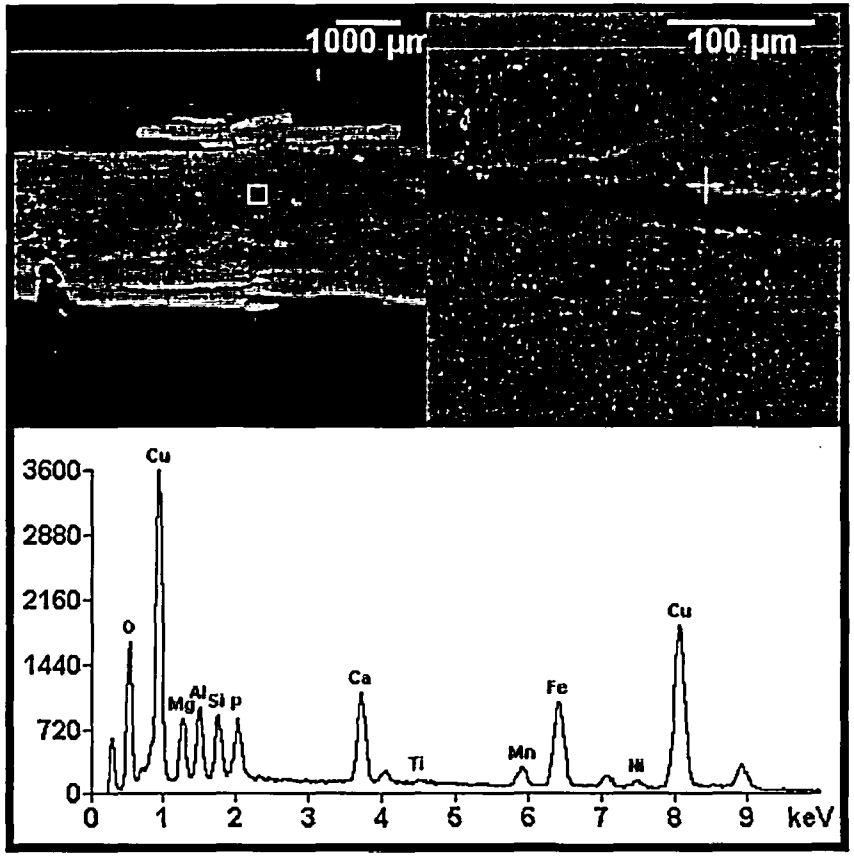

b) 1A-EDS2

Figure 10-40 SEM photograph and EDS elemental trace of OD deposit collected on tape from the 1st TSP region of R12C59 HL Piece 3B (10° azimuthal orientation) during ID pressurization to 9,000 psi.

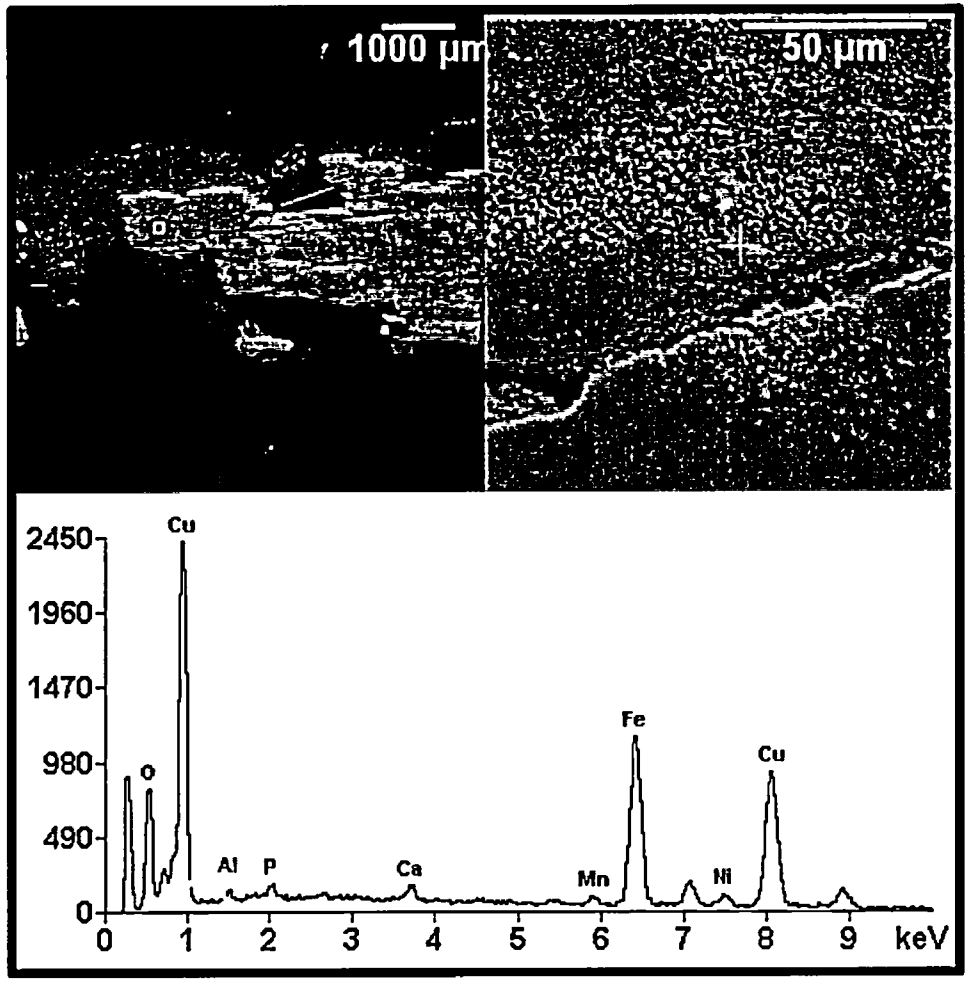

c) 2A-EDS1

Figure 10-40 (cont'd) SEM photograph and EDS elemental trace of OD deposit collected on tape from the 1st TSP region of R12C59 HL Piece 3B (10° azimuthal orientation) during ID pressurization to 9,000 psi.

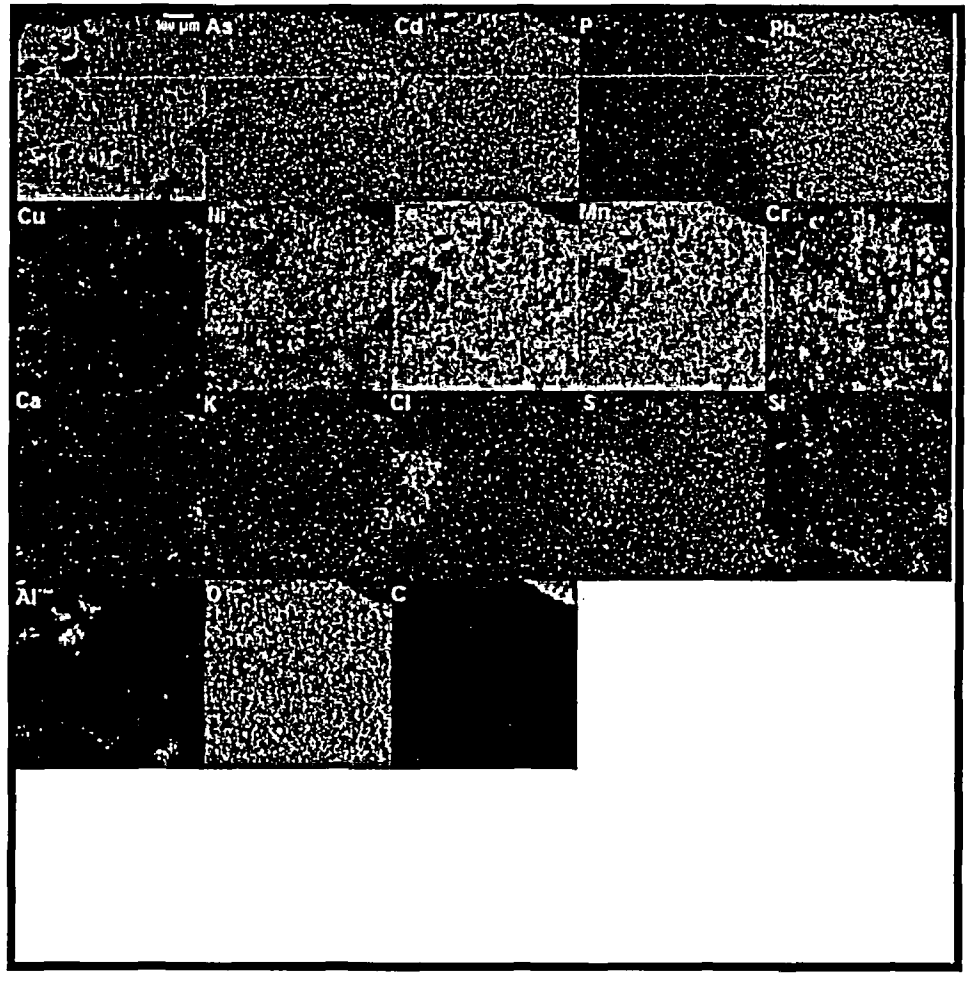

Figure 10-41 Backscatter EDS maps showing concentration of various elements identified on the deposit removed from the 1st TSP region of R12C59 Piece 3B at quatrefoil land tube intersection (10° azimuthal orientation) during pressurization to 9,000 psi.

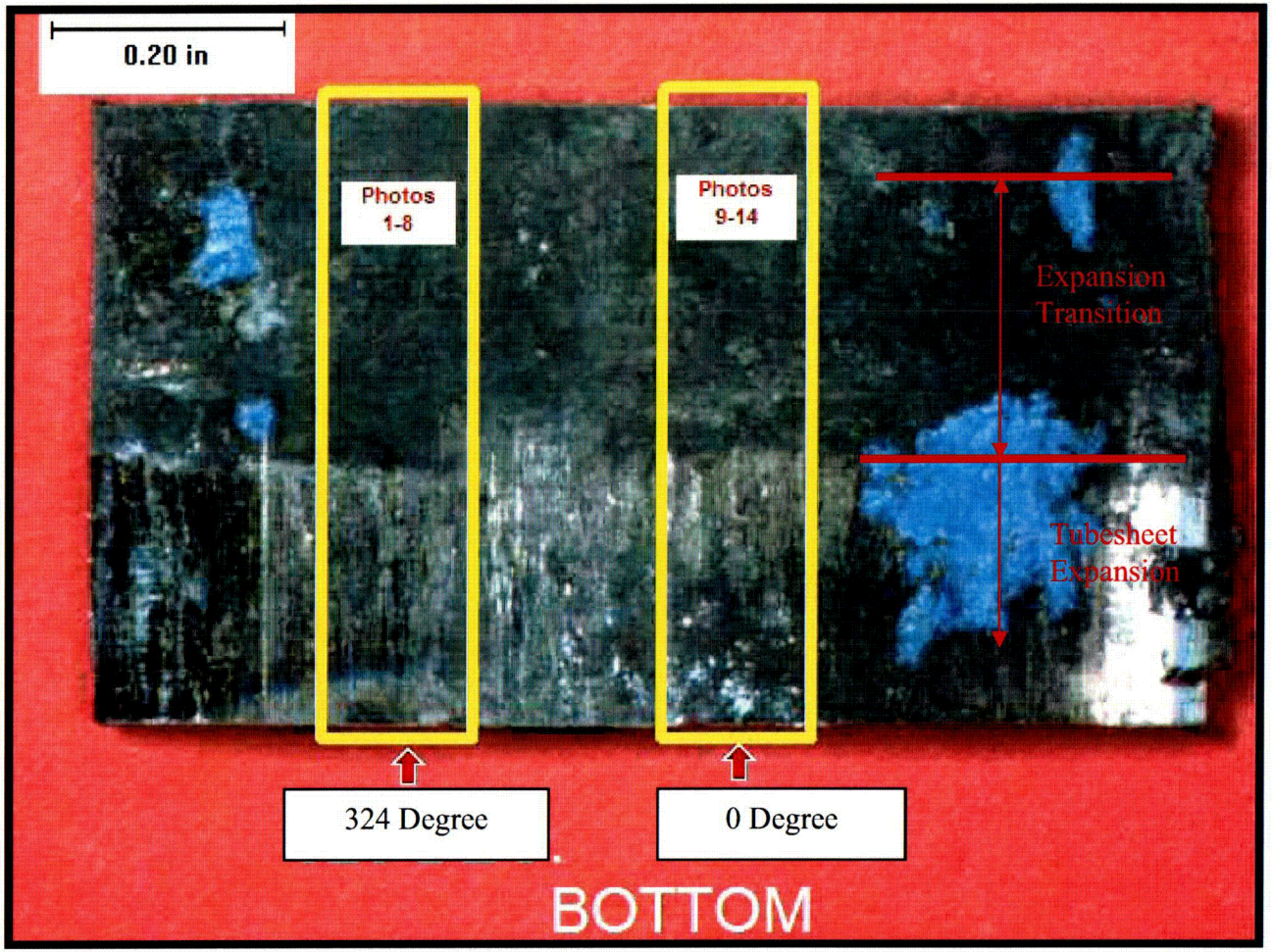

Figure 10-42 Light optical micrograph showing the OD surface appearance of Piece 2B2A removed from the TTS region of R12C59 HL. The micrograph shown is after the OD oxide was removed by 'flattening" of the ring. The deposit was collected on a carbon tape. The blue areas represent residual tape which remained on the ring.

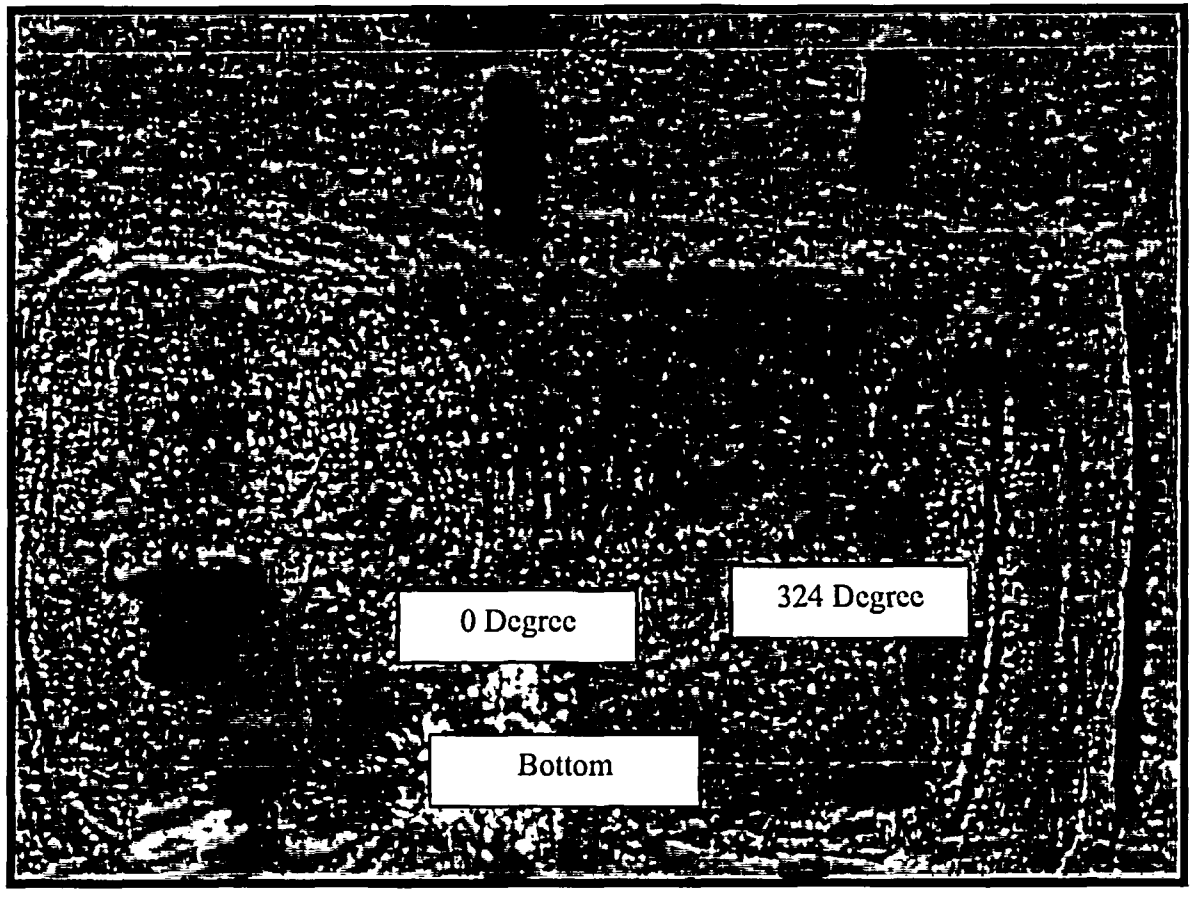

Figure 10-43 Light optical photograph showing deposit removed from the TTS region of R12C59 Piece 2B2A. The surface shown represents the interface between the deposit and the OD of the tube. The azimuthal orientations shown represents the location of the UT signal (0°) and the +Pt signal (324°).

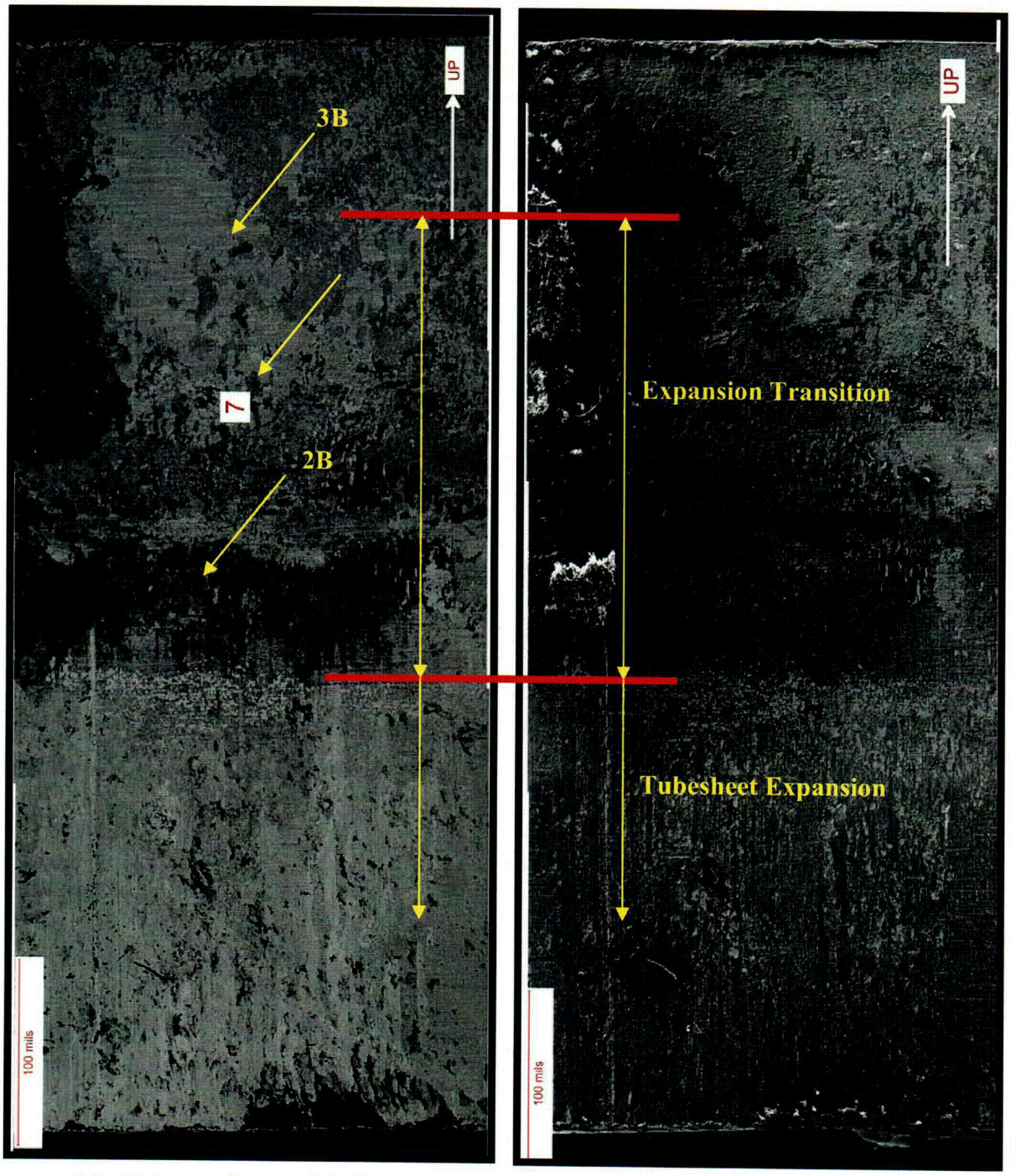

a) Backscatter Energy Mode

b) Reflective Energy Mode

Figure 10-44 Montage of OD surface of R12C59 Piece 2B2A at 324° azimuthal orientation following removal of deposits. Refer to Figure 10-45 for additional SEM micrographs of areas shown.

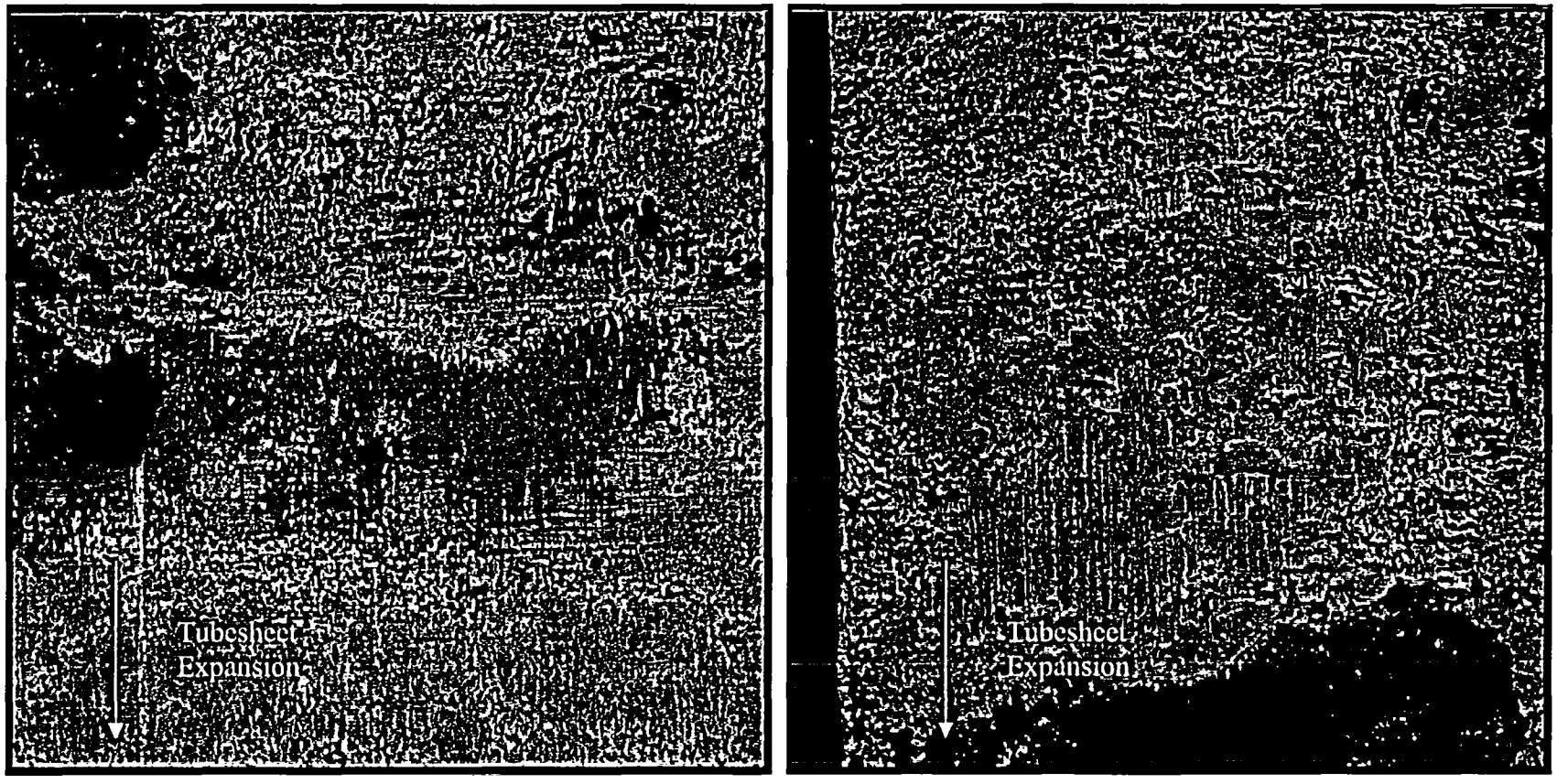

a) Area 2B

b) Area 3B

Figure 10-45 Backscatter Energy Mode SEM micrograph showing OD surface R12C59 HL Piece 2B2A at 324° azimuthal orientation following removal of OD deposits. Refer to Figure 10-44 for area locations.

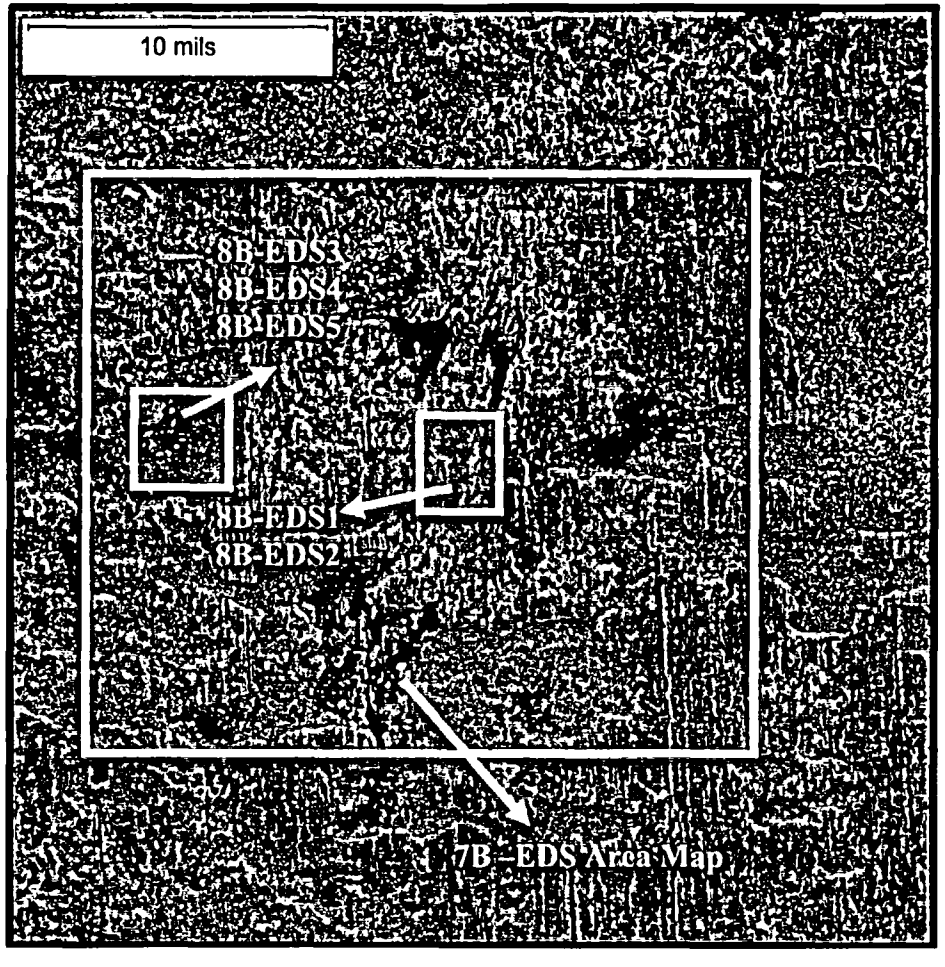

c) Area 7

Figure 10-45 (Cont'd) Backscatter Energy Mode SEM micrograph showing OD surface R12C59 HL Piece 2B2A at 324° azimuthal orientation following removal of OD deposits. Refer to Figure 10-43 for specific area locations. Results of EDS analyses are presented in Figure 10-46.

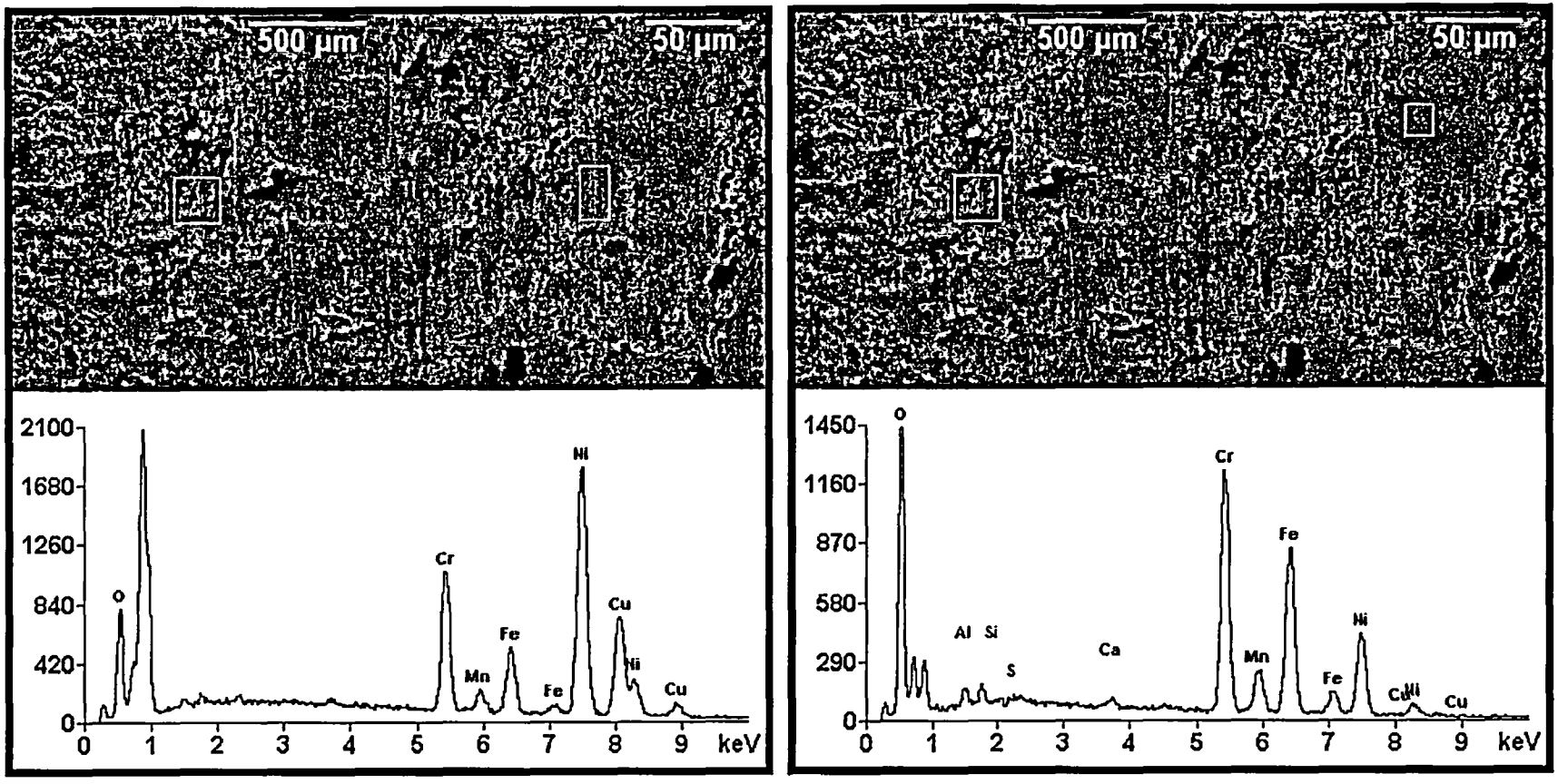

a) 8B-EDS1

b) 8B-EDS2

Figure 10-46 SEM photograph and EDS elemental trace on OD surface of R12C59 HL Piece 2B2A at 324° azimuthal orientation following removal of OD deposits. Refer to Figure 10-45 for specific area locations.

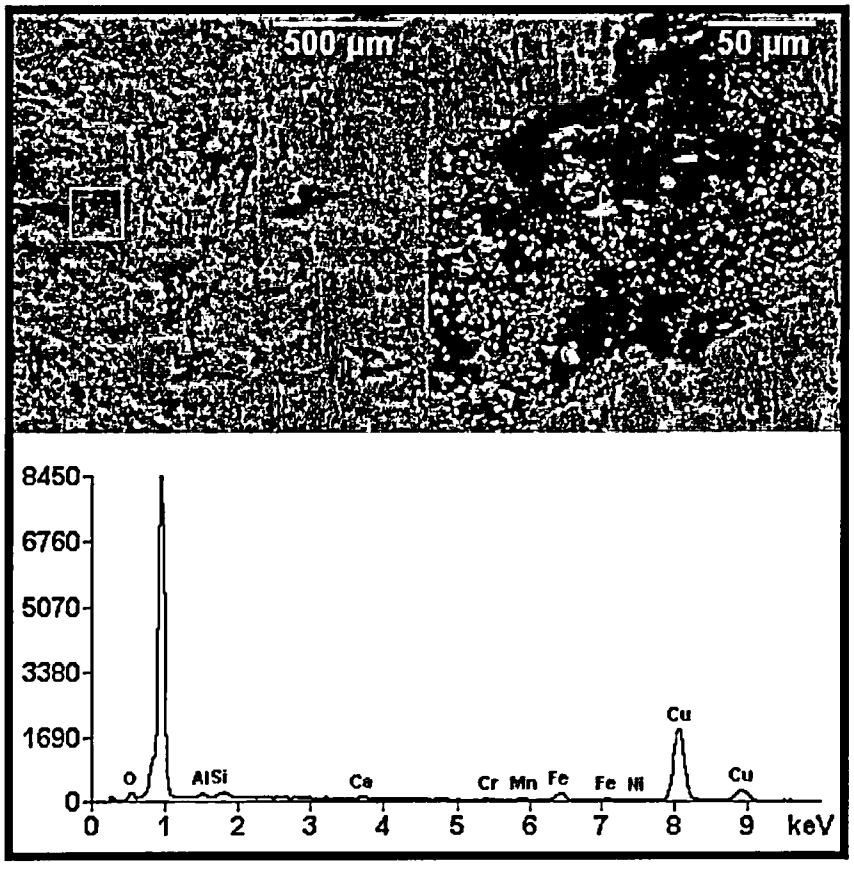

c) 8B- EDS3

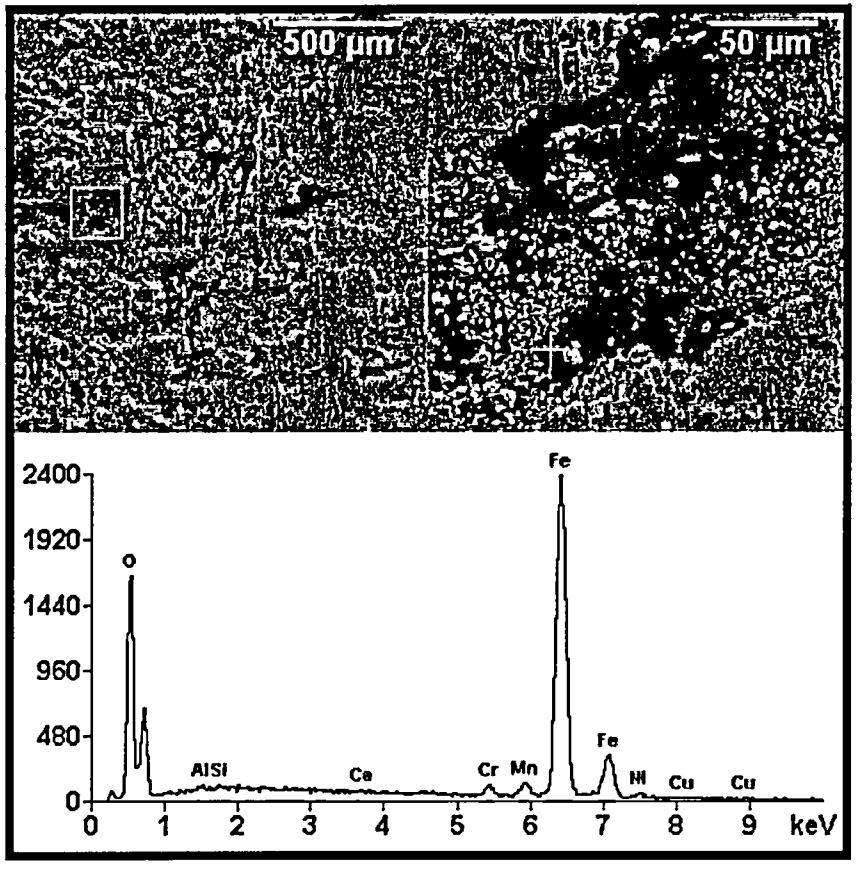

d) 8B-EDS4

Figure 10-46 (Cont'd) SEM photograph and EDS elemental trace on OD surface of R12C59 HL Piece 2B2A at 324° azimuthal orientation following removal of OD deposits. Refer to Figure 10-45 for specific area locations.

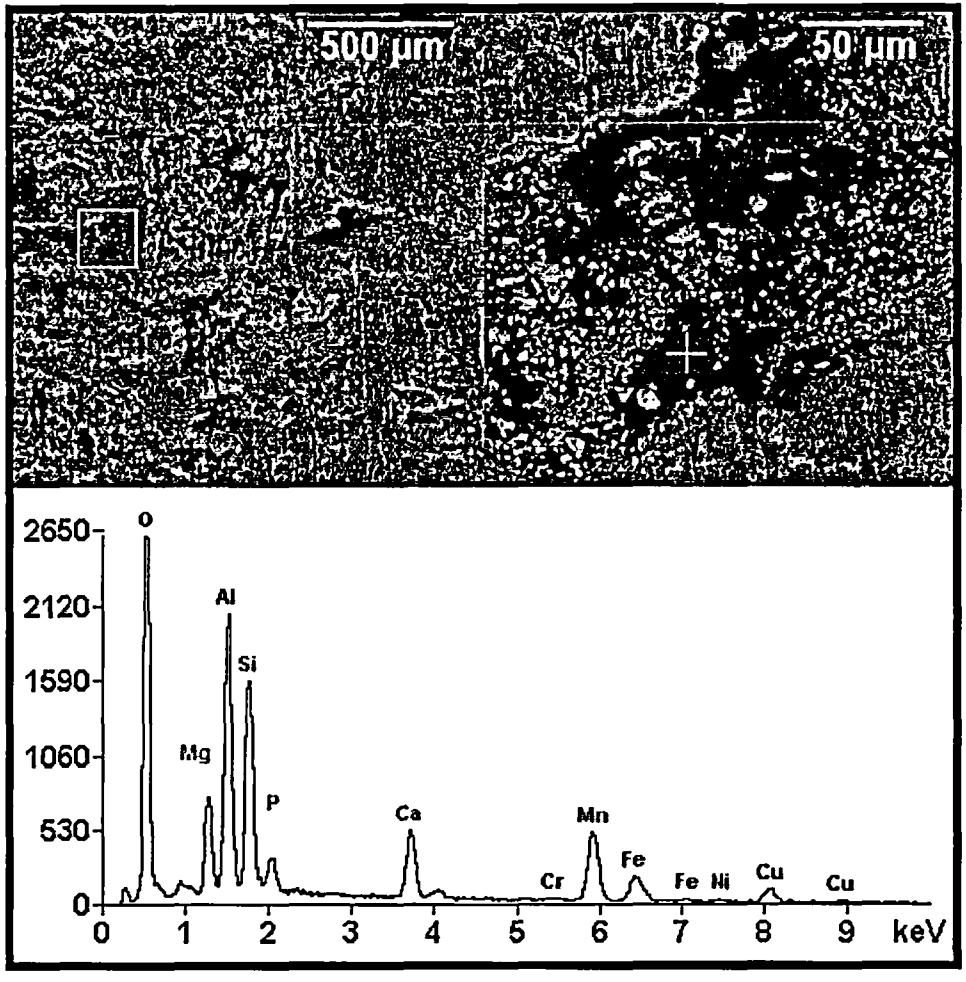

c) 8B-EDS5

Figure 10-46 (Cont'd) SEM photograph and EDS elemental trace on OD surface of R12C59 HL Piece 2B2A at 324° azimuthal orientation following removal of OD deposits. Refer to Figure 10-45 for specific area locations.

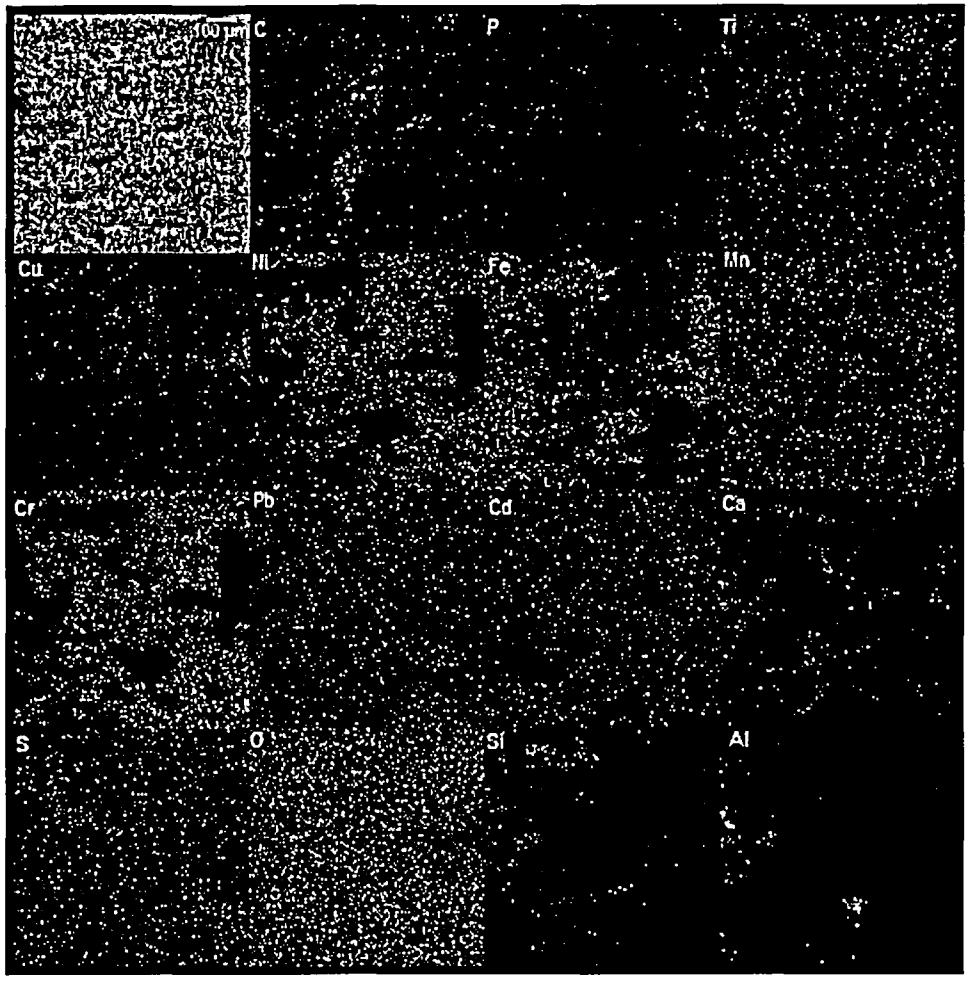

f) 7B-EDS Area Scan

Figure 10-47 SEM photograph and EDS elemental trace on OD surface of R12C59 HL Piece 2B2A at 324° azimuthal orientation following removal of OD deposits. Refer to Figure 10-45 for specific area locations.

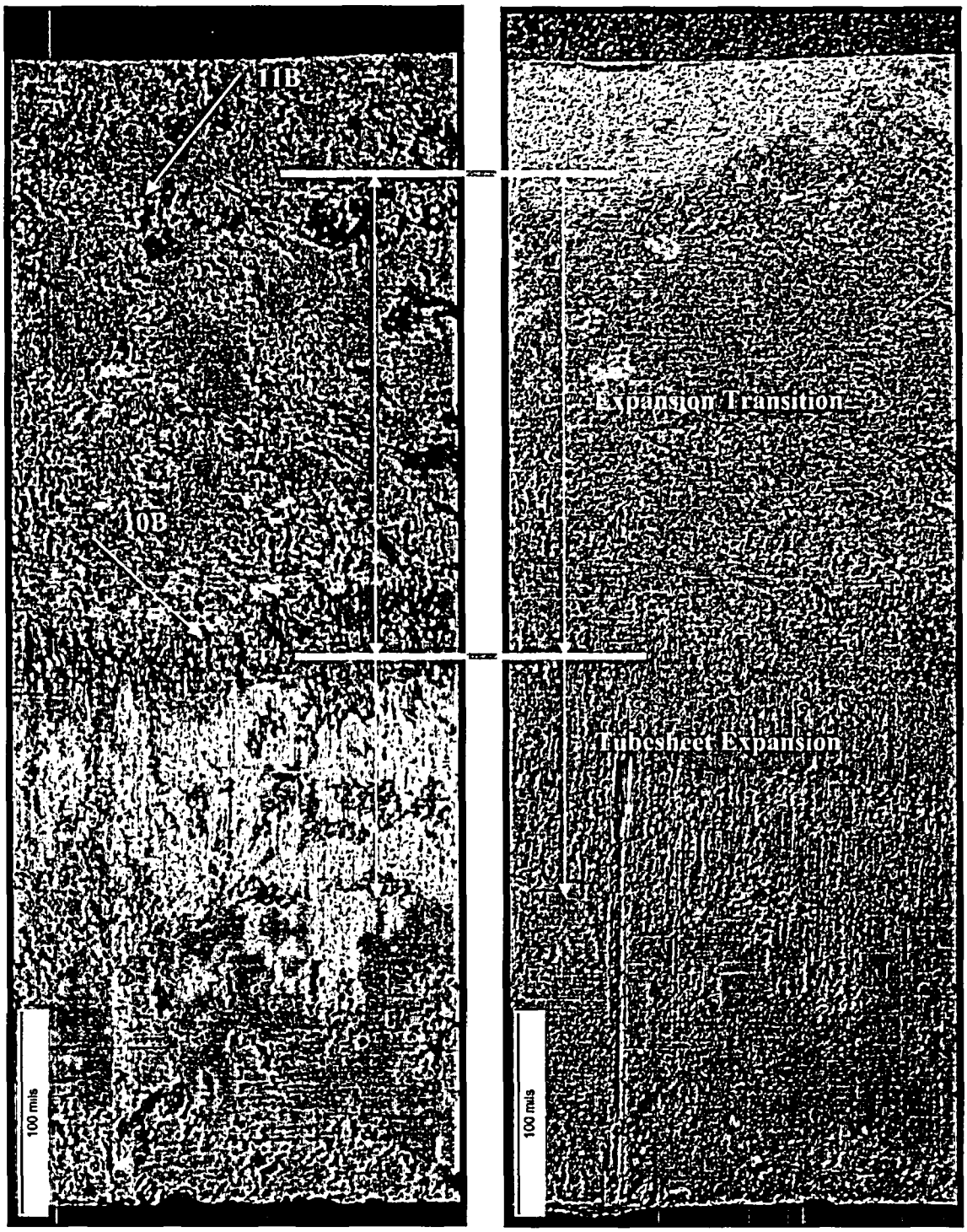

a) Backscatter Energy Mode b) Reflective Energy Mode

Figure 10-48 Montage of OD surface of R12C59 Piece 2B2A at 0° azimuthal orientation following removal of deposits. Refer to Figure 10-49 for additional SEM micrographs of areas shown.

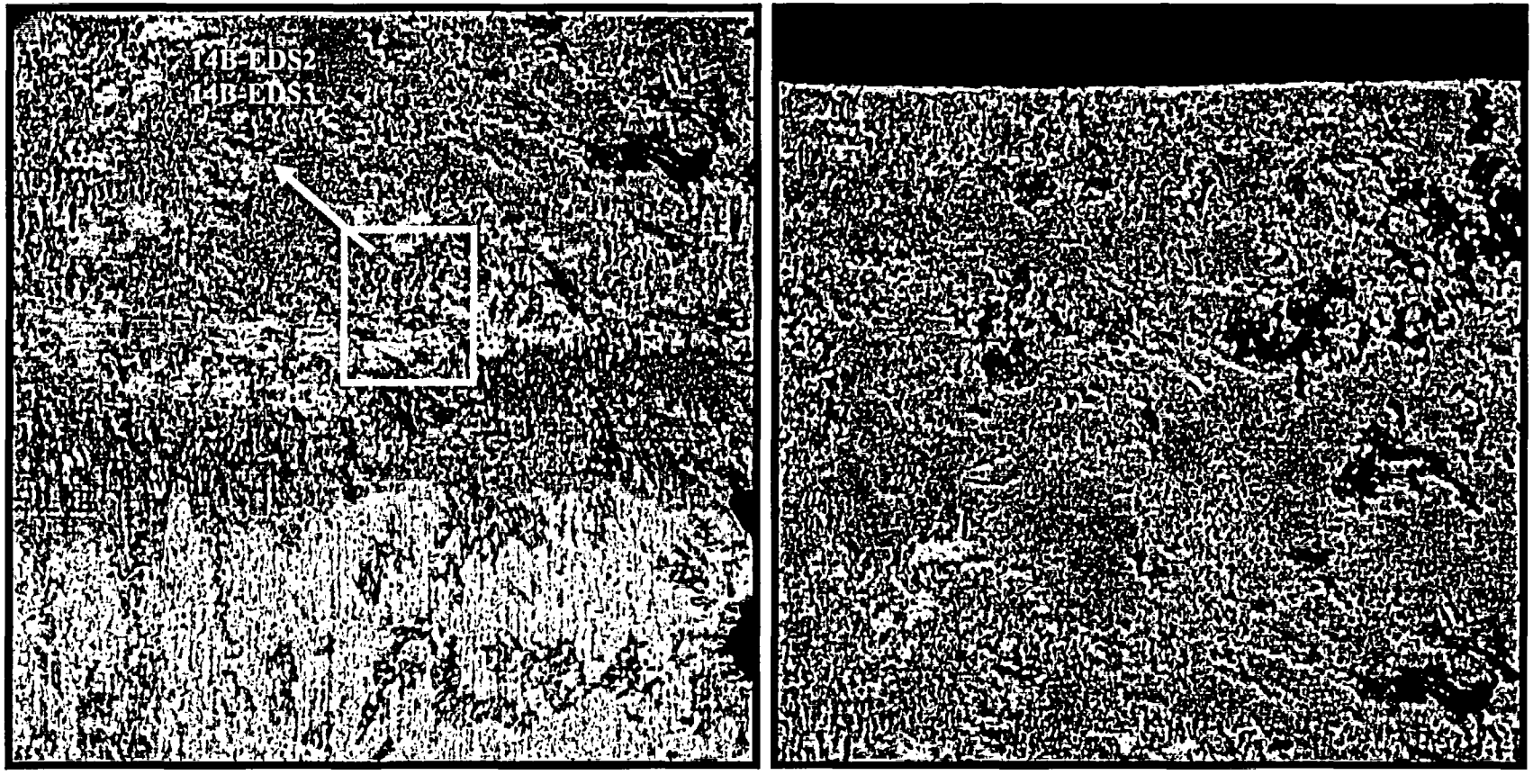

a) Area 10B

b) Area 11B

Figure 10-49 Backscatter Energy Mode SEM micrograph showing OD surface R12C59 HL Piece 2B2A at 0° azimuthal orientation following removal of OD deposits. Refer to Figure 10-48 for specific area location. Results of EDS analyses are presented in Figure 10-49.

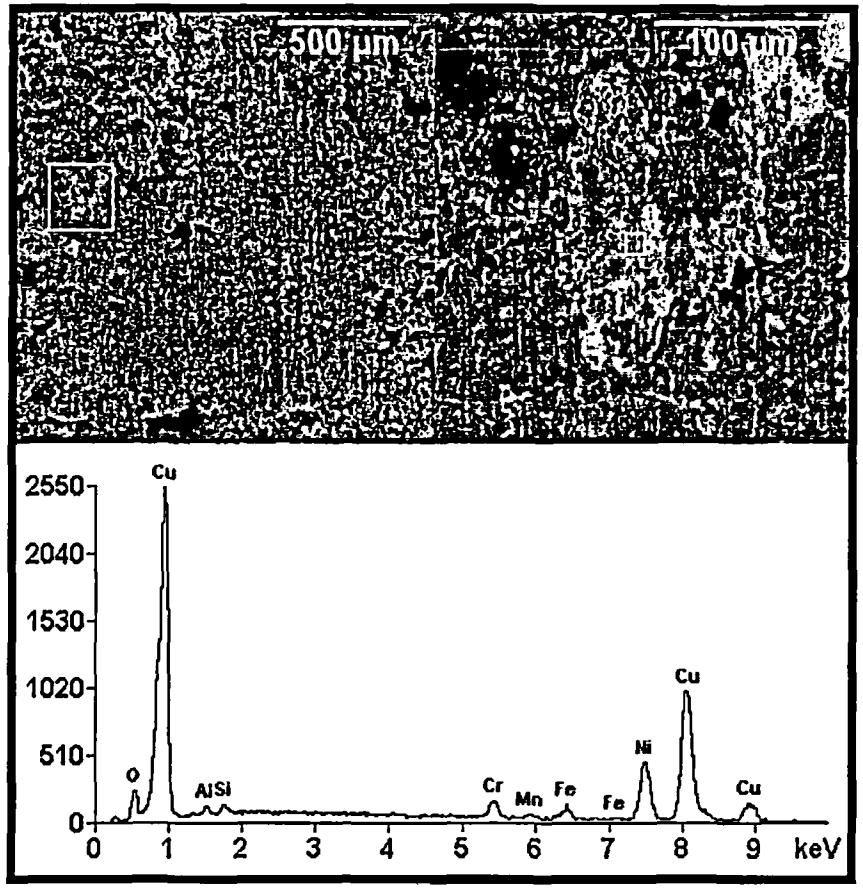

a) 14B EDS2

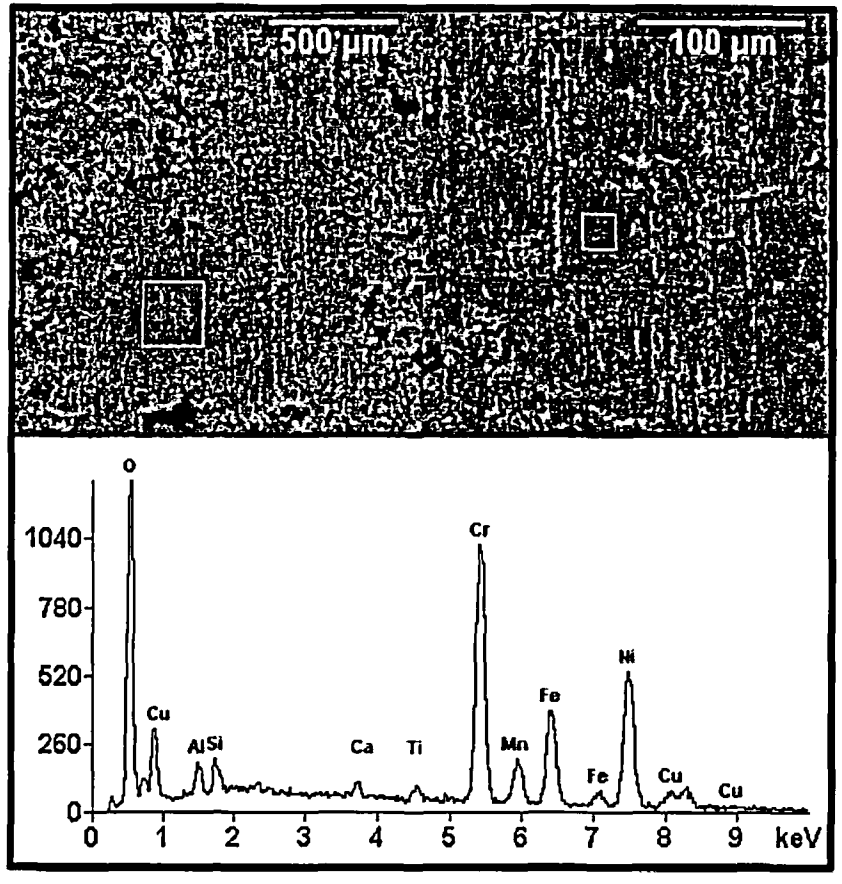

b) 14B-EDS3

Figure 10-50 SEM photograph and EDS elemental trace of OD surface on Piece 2B2A from R12C59 HL at 0° azimuthal orientation following removal of OD deposits. Refer to Figure 10-49 for location of EDS analyses.

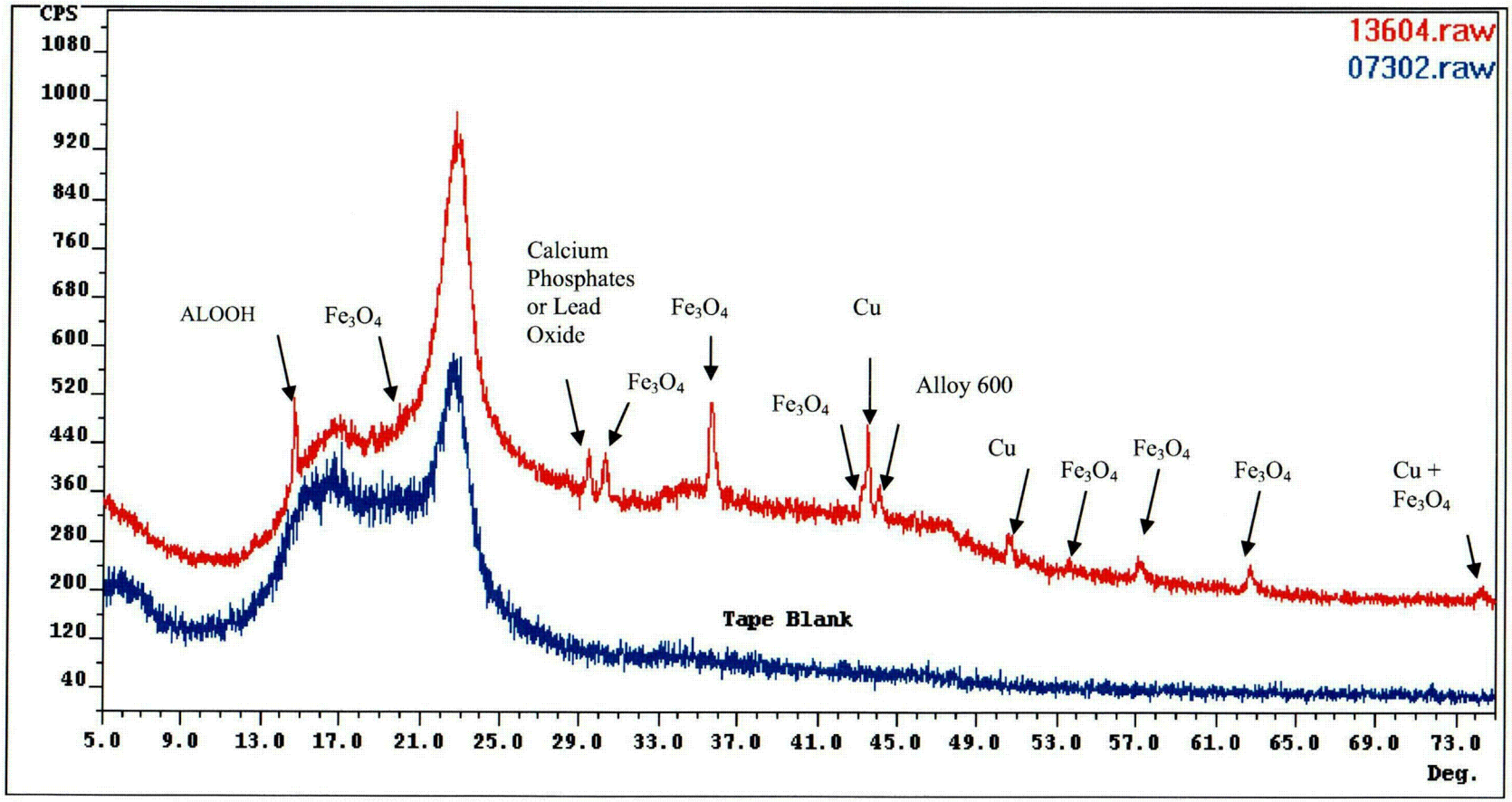

Figure 10-51 X-ray diffraction pattern of deposit from deposit removed from Piece 2B2A of R12C59 HL TTS region.

C25

SECTION 11

METALLOGRAPHIC EXAMINATIONS

11.1 Procedure

A ½ inch ring section containing the tube expansion transition from the top of tubesheet region of R12C59 HL was cut and split at 90° and 270°. The half ring section containing the reported field +Pt and UT indications was flattened to remove the OD deposit and visually examined prior to metallographic mounting. As discussed in Section 10, no evidence of degradation was noted on the flatten section. Following the completion of the OD deposit microchemistry effort, longitudinal sections were cut from the flattened ring section for metallographic examination to verify the lack of tube degradation and to determine if any other anomalies existed which could have contributed to the reported indications. The specimens were mounted and polished, etched in a Nital solution, and viewed with a light microscope. Low magnification photomicrographs were used to document the observed condition and if necessary, higher magnification was utilized to more clearly document the observed condition. Longitudinal mounts were prepared at the following azimuthal orientations: 270°, 300°, 324°, 0°, 30°, 60°, and 90°. Additional mounts were prepared to verify that the metallurgical conditions, i.e., grain size, carbide distribution, and microhardness, of the pulled tubes were consistent with vintage thermal treated Alloy 600 material. These results are presented in Section 12.

11.2 Results

The metallographic examination of the TTS region of the Vogtle Unit 2 steam generator tube R12C59 showed no evidence of corrosion degradation or other surface anomalies. No appreciable evidence of intergranular penetration was noted on the OD surfaces examined. Typical etched photomicrographs of the areas examined are shown in Figures 11-1 through 11-4. Longitudinal sections shown in Figure 11-1 were cut from Piece 2B2A at 60°, 90°, and 324° azimuthal orientations. The 324° location represents the azimuthal orientation where the field +Pt signal was reported, while the 60° and 90° sections represent the azimuthal orientation where the UTEC signals were reported. Higher magnification micrographs of the various locations shown in Figure 11-1 are presented in Figures 11-2, 11-3, and 11-4. In all cases, the only degradation seen is one to two grains deep of intergranular corrosion. This is typical of general secondary side corrosion observed for Alloy 600TT tubing material removed from operating plants.

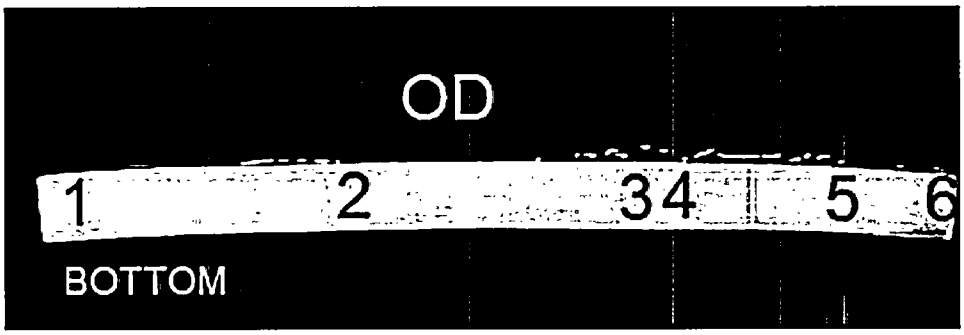

a) 324° Azimuthal Orientation (+Pt Field Indication)

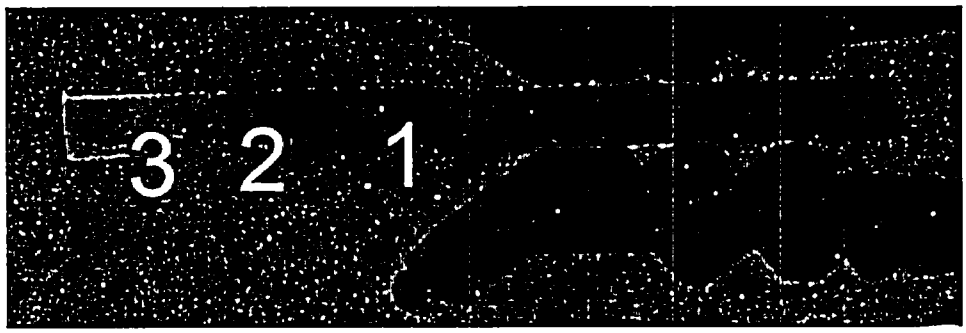

b) 90° Azimuthal Orientation

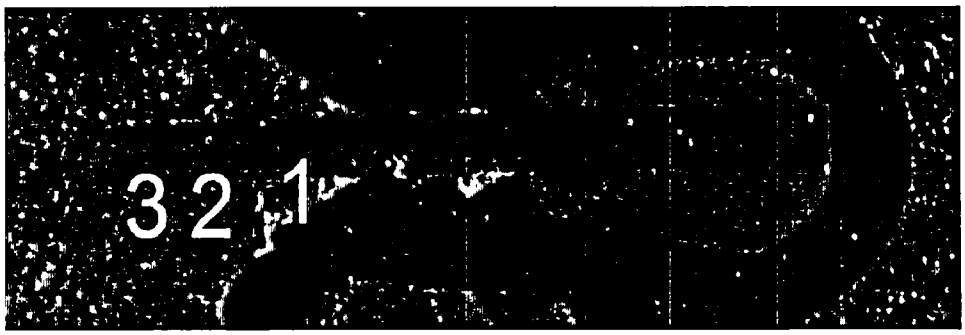

c) 60° Azimuthal Orientation

Figure 11-1 Longitudinal Metallographic Sections Through the TTS Region of R12C59 HL – Piece 2B2A1. Refer to Figures 11-2 through 11-4 For Etched Photomicrographs.

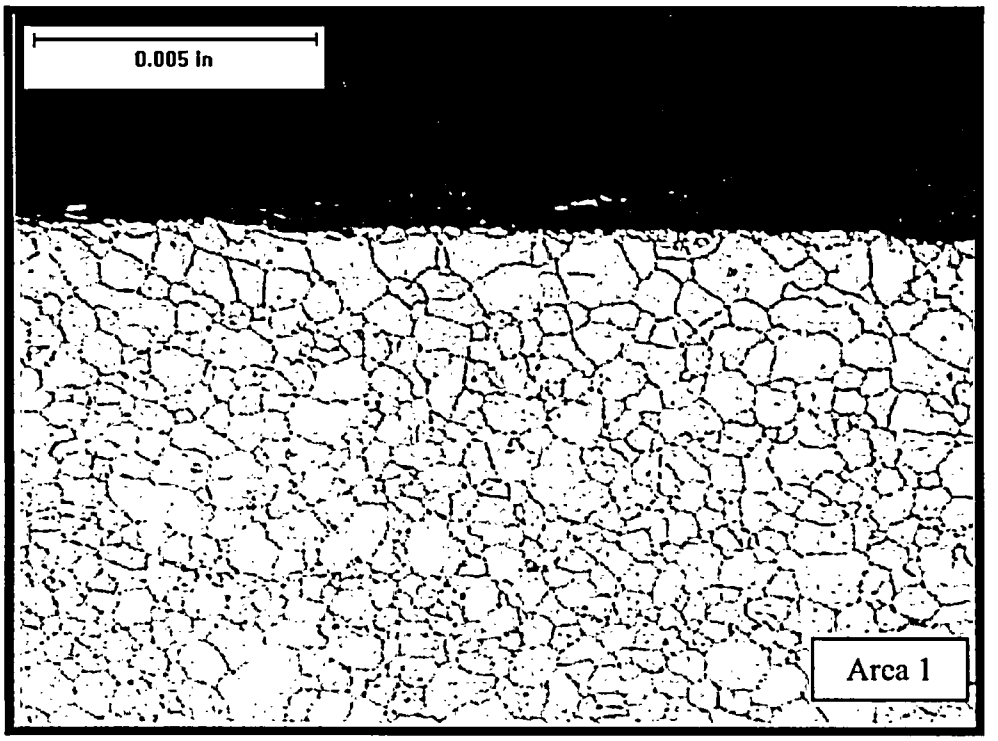

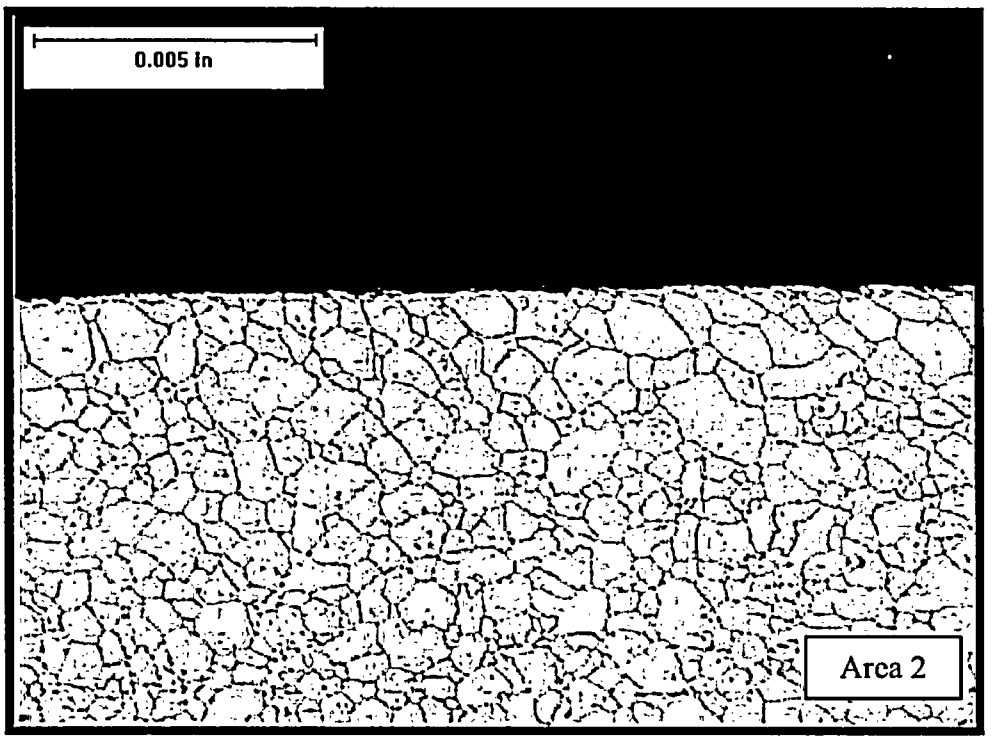

Figure 11-2 Etched Metallographic Sections Through the TTS Region of R12C59 HL – Piece 2B2A1 at 324° Azimuthal Orientation (Field +Pt Indication). Refer to Figure 11-1(a) For Location of Noted Area.

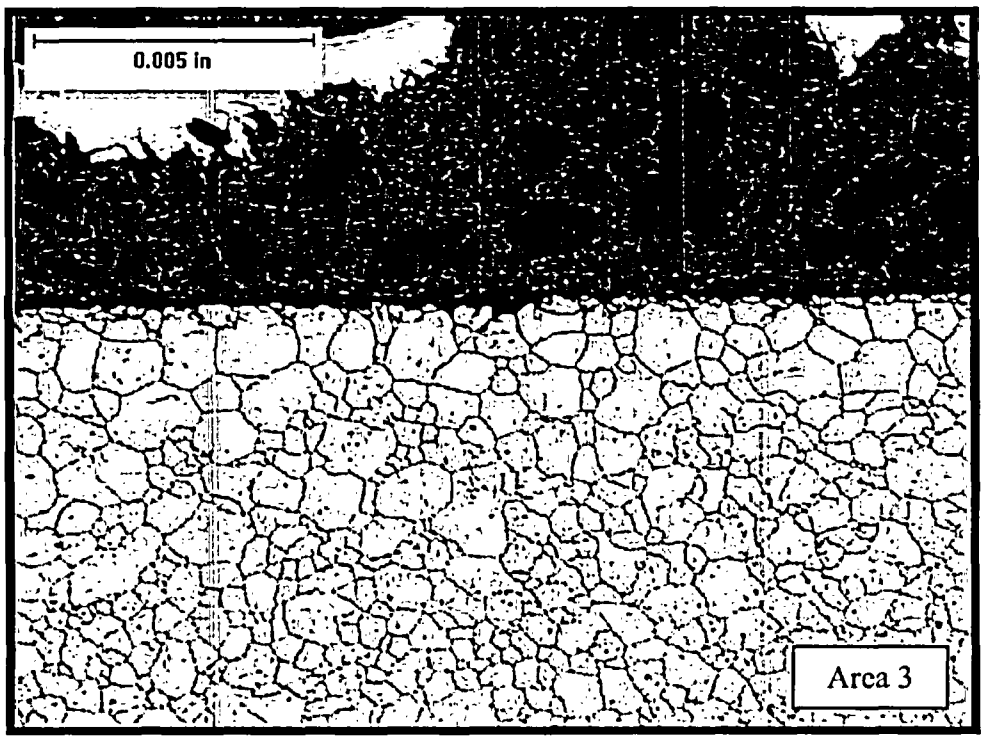

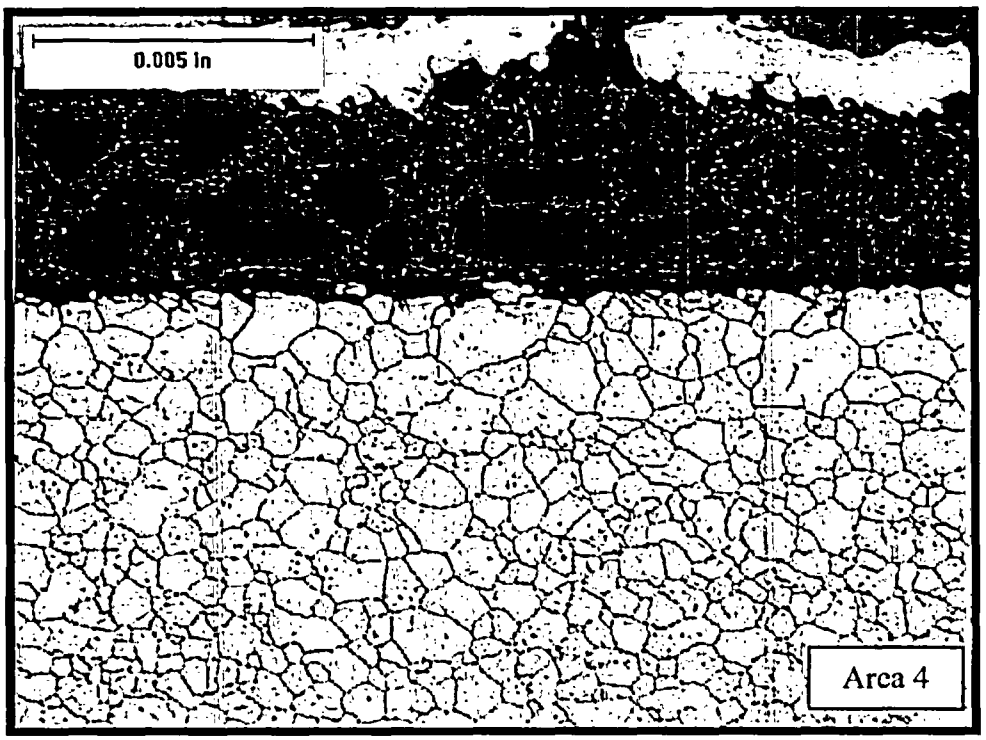

Figure 11-2 (Cont'd) Etched Metallographic Sections Through the TTS Region of R12C59 HL – Piece 2B2A1 at 324° Azimuthal Orientation (Field +Pt Indication). Refer to Figure 11-1(a) For Location of Noted Area.

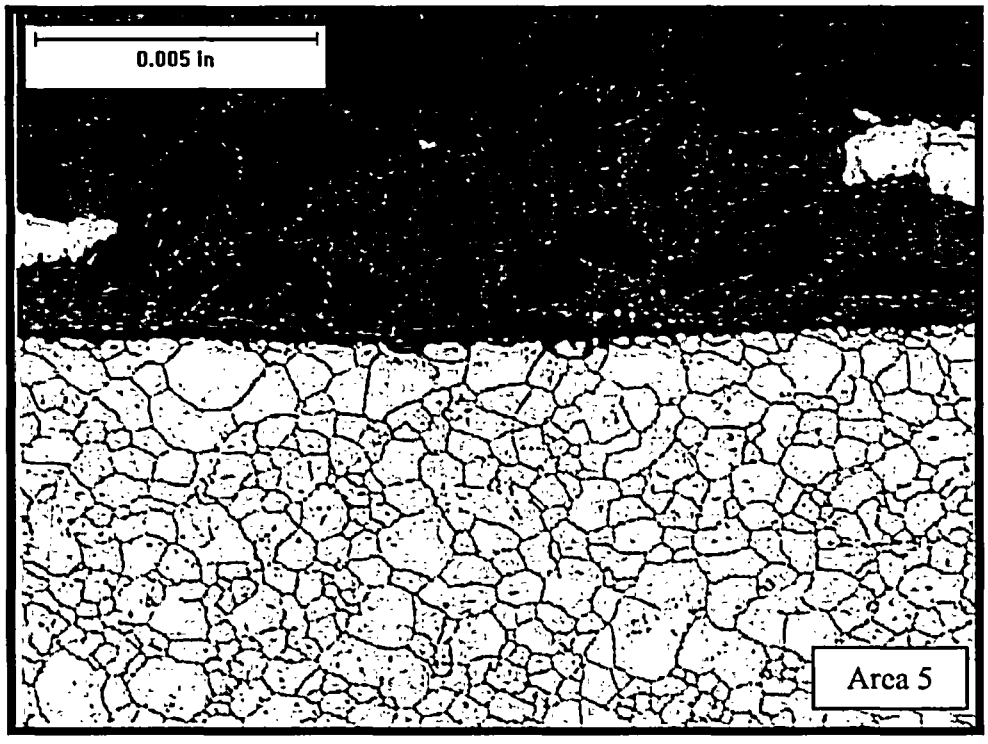

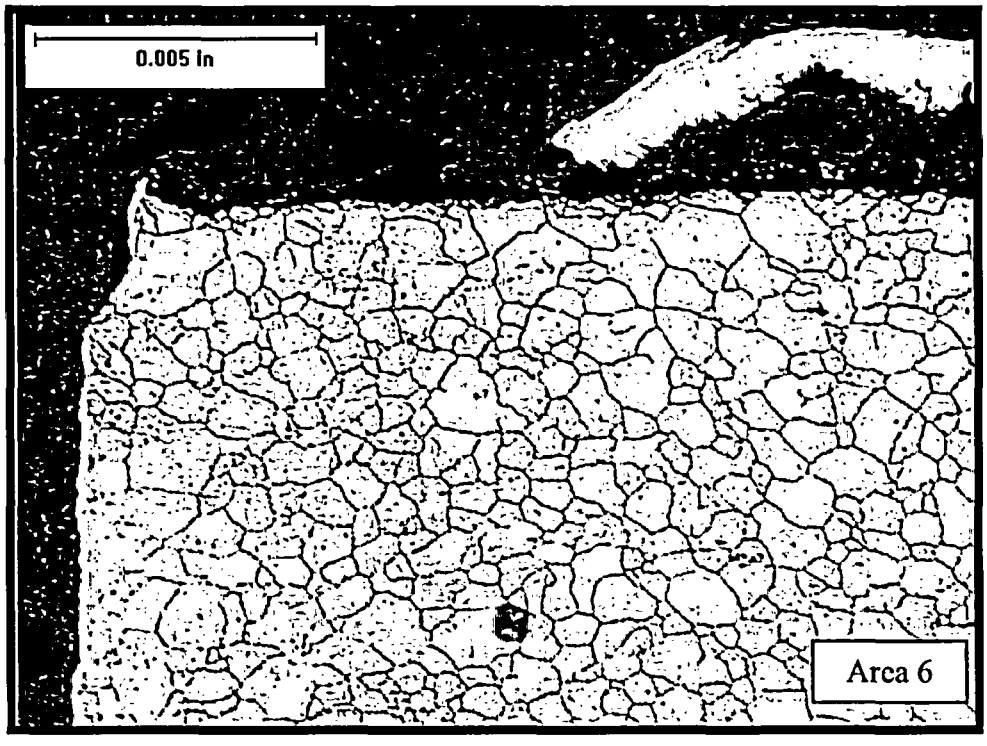

Figure 11-2 (Cont'd) Etched Metallographic Sections Through the TTS Region of R12C59 HL – Piece 2B2A1 at 324° Azimuthal Orientation (Field +Pt Indication). Refer to Figure 11-1(a) For Location of Noted Area.

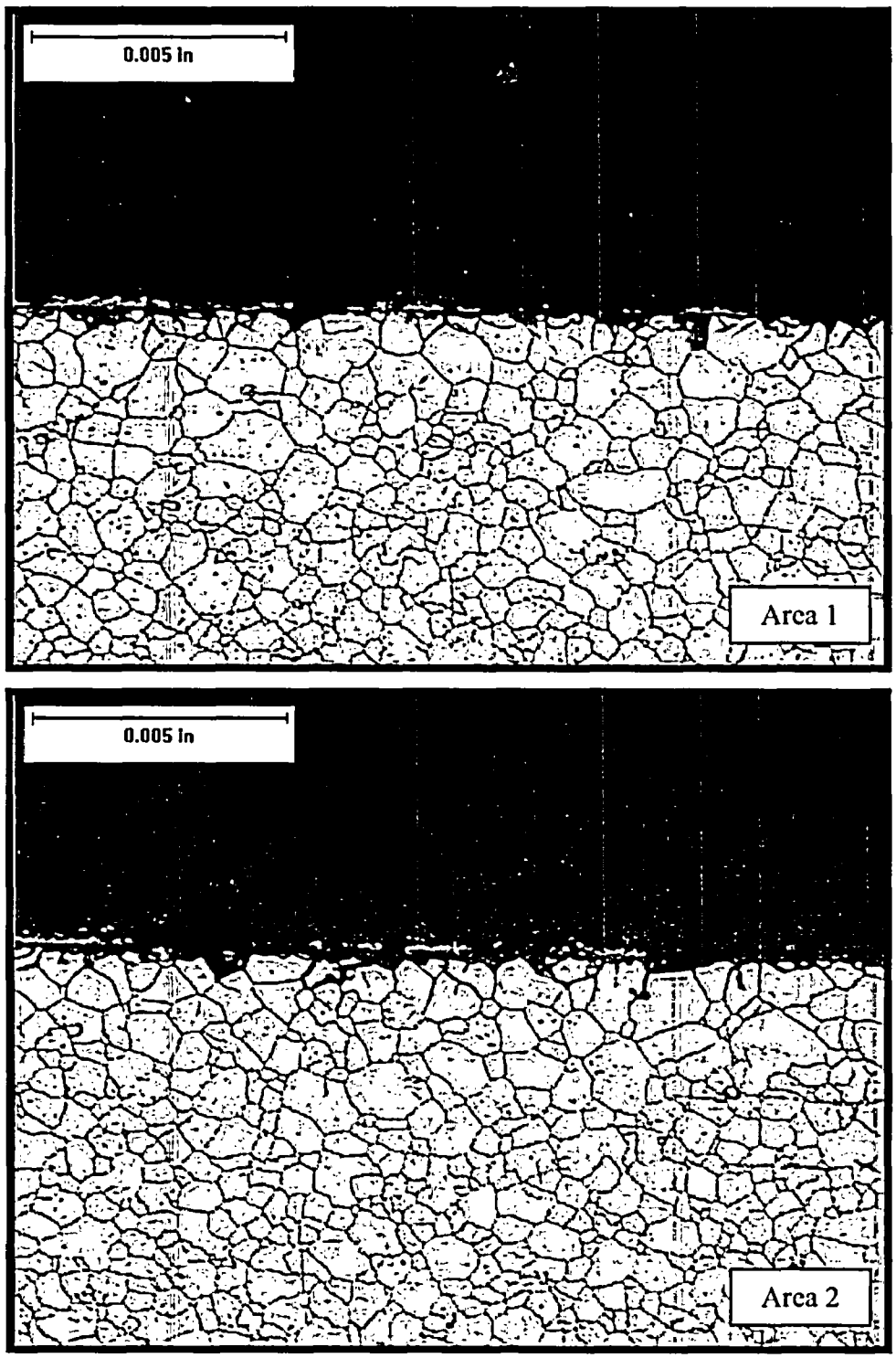

Figure 11-3 Etched Metallographic Sections Through the TTS Region of R12C59 HL – Piece 2B2A1 at 90° Azimuthal Orientation. Refer to Figure 11-1(b) For Location of Noted Area.

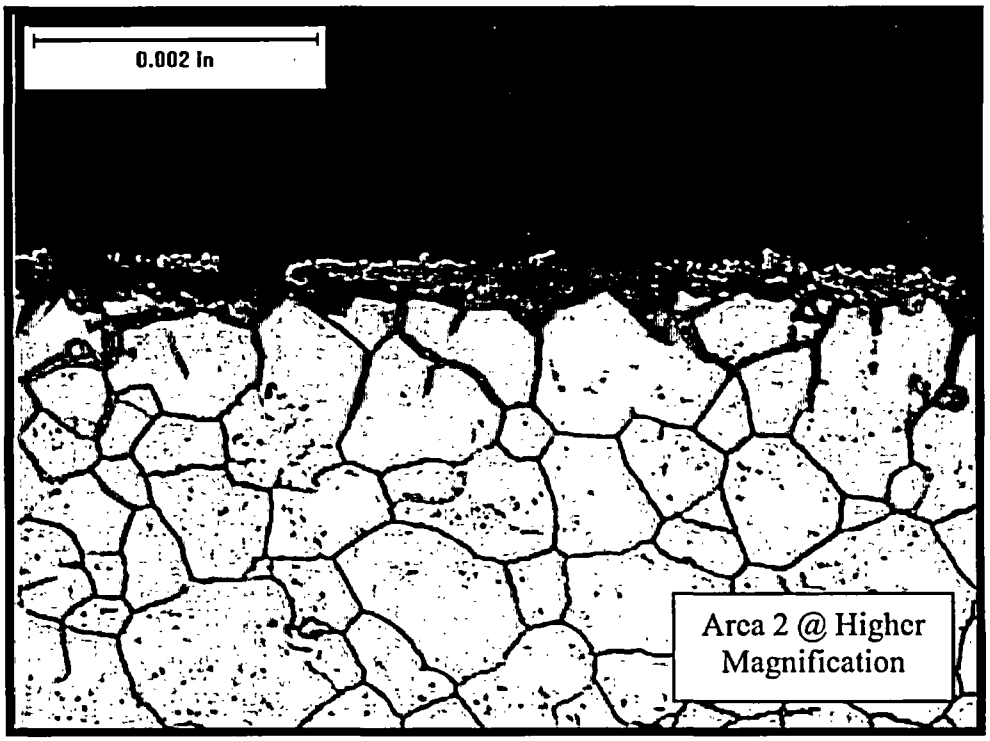

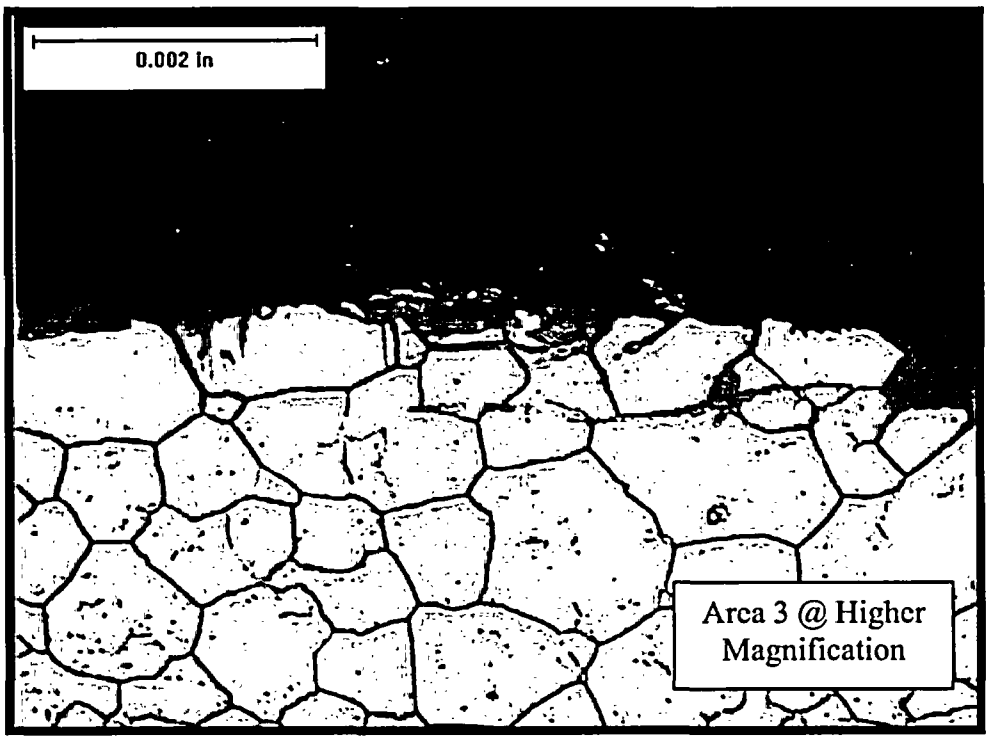

Figure 11-3(Cont'd) Etched Metallographic Sections Through the TTS Region of R12C59 HL – Piece 2B2A1 at 90° Azimuthal Orientation. Refer to Figure 11-1(b) For Location of Noted Area.

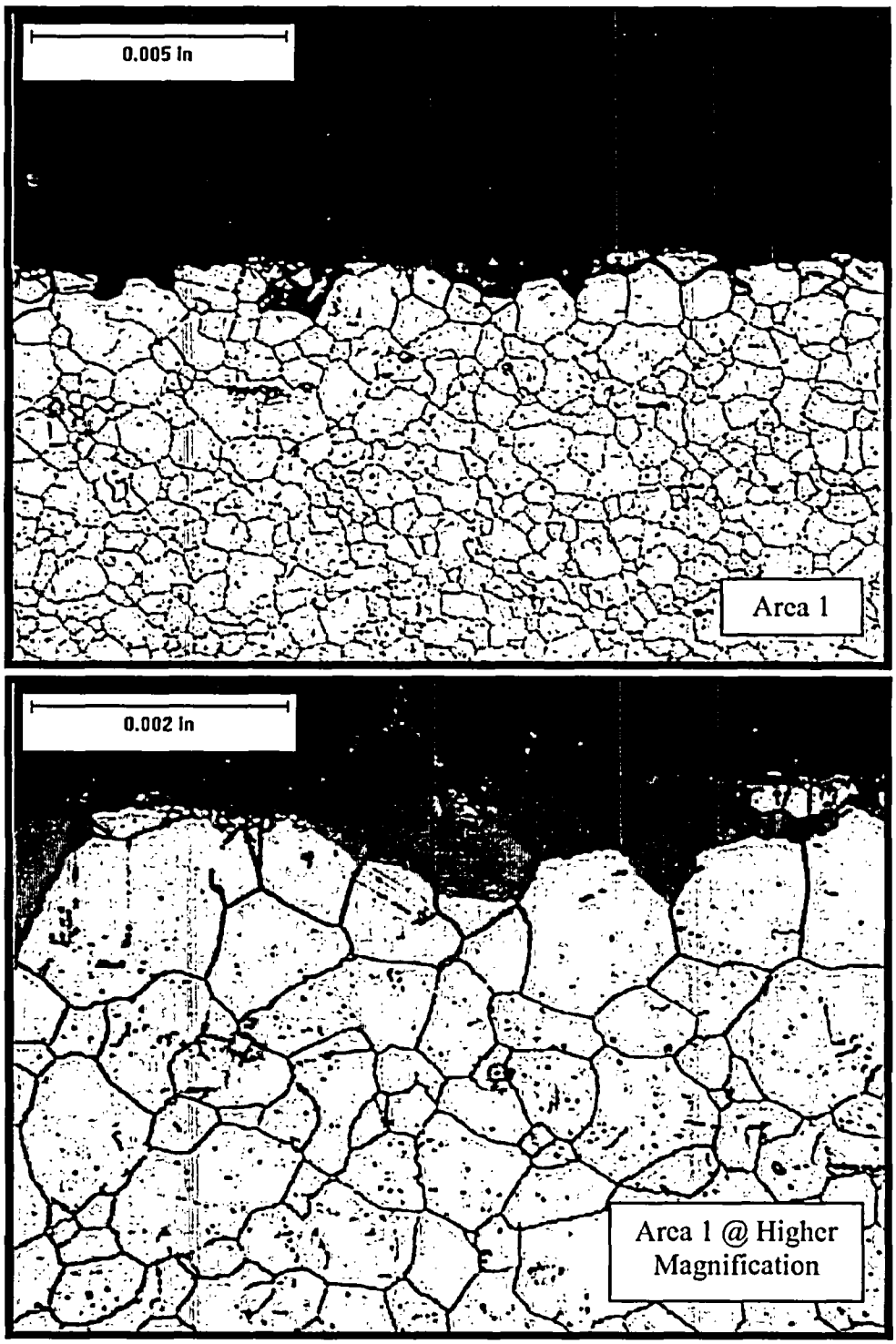

Figure 11-4 Etched Metallographic Sections Through the TTS Region of R12C59 HL – Piece 2B2A1 at 60° Azimuthal Orientation. Refer to Figure 11-1(c) For Location of Noted Area.

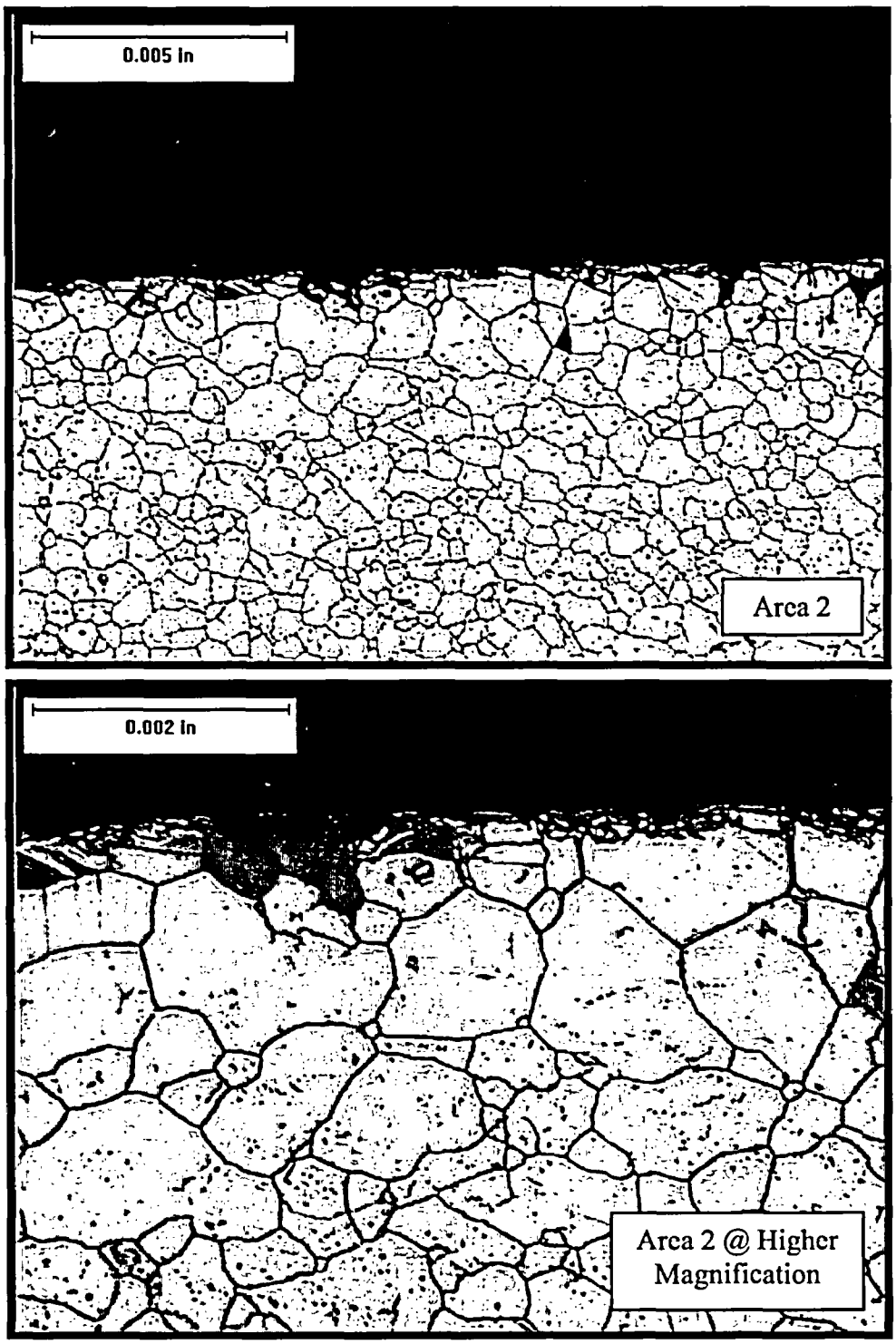

Figure 11-4 (Cont'd) Etched Metallographic Sections Through the TTS Region of R12C59 HL – Piece 2B2A1 at 60° Azimuthal Orientation. Refer to Figure 11-1(c) For Location of Noted Area.

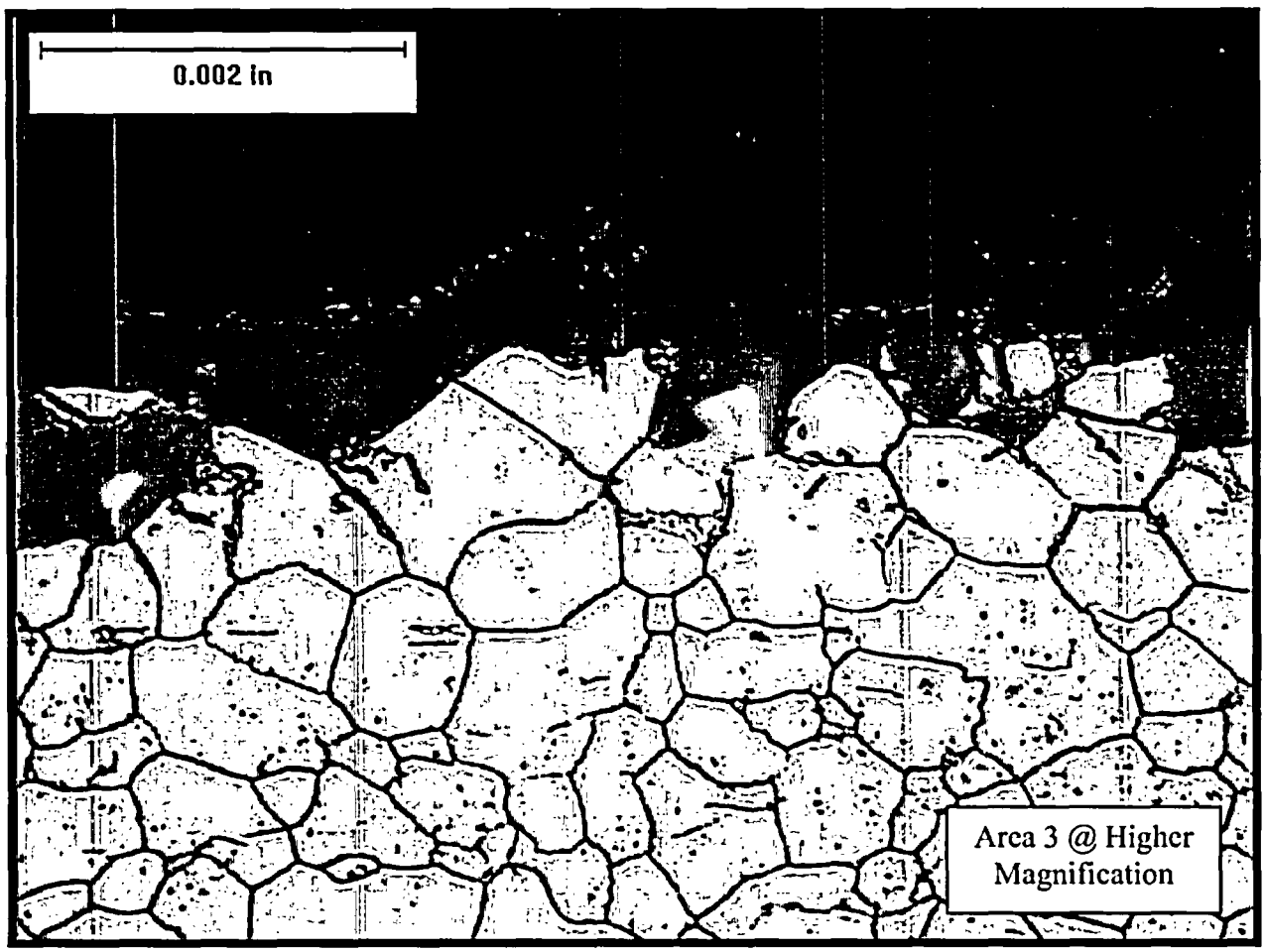

Figure 11-4 (Cont'd) Etched Metallographic Sections Through the TTS Region of R12C59 HL – Piece 2B2A1 at 60° Azimuthal Orientation. Refer to Figure 11-1(c) For Location of Noted Area.

SECTION 12
TUBING MATERIAL CHARACTERIZATIONS

12.1 Introduction

The material characterization tests were performed to determine the tensile, bulk chemistry, microstructural, modified Huey test, microhardness, and residual stress characteristics of the as-removed tube materials. The following sections detail the procedures and the results of each test performed.

12.2 Tensile Tests

Procedure

The tensile properties (i.e., yield strength, ultimate strength, percent elongation) for R12C59 HL - Piece 4A and for R11C60 HL - Piece 4A were determined by a room temperature tensile test of a full cross section tubular specimen approximately 12 inches in length. The full cross section tubular specimens were fitted with snug-fitting stainless steel plugs (mandrels) machined in accordance with ASTM Standard Method E8 to provide a minimum 2.000-inch gage length as prescribed by ASME SB-163. The crosshead speed was maintained at a 0.05 mils/minute rate until fracture.

Results

Figures 12-1 and 12-2 show the stress-strain curves for the two tubes. The results are consistent for thermal treated Alloy 600 steam generator tubing of this vintage. The yield and ultimate strength values measured for the Vogtle Unit 2 tubes are similar to the values listed in the Certified Materials Test Report (CTMR). The CMTR values for the respective heats are included on Figures 12-1 and 12-2.

During the preparation of the tensile test specimens dimensional measurements were taken to verify uniform wall thickness. OD and ID measurements were taken every 45° on both ends of each specimen. For both pulled tubes, all measurements showed the OD to be 0.688 inch and the ID to be 0.607 inch. This resulted in a uniform wall thickness of 0.039 inch.

12.3 Microstructure

Procedure

The microstructure of the pulled tubing was examined to determine the grain size and the general distribution of the carbide precipitation. Transverse metallographic mounts were prepared from R12C59 HL - Piece 4F and R11C60 HL - Piece 4F and were evaluated for grain size and carbide distribution. The specimens were etched in a 5% Nital solution and examined by optical microscopy for grain size rating per the ASTM procedures. The samples were also examined for carbide precipitation by Scanning Electron Microscopy following polishing and etching in a 2% bromine-methanol solution.

Results

The grain size for R12C59 HL is shown in Figure 12-3, while the grain size for R11C60 HL is shown in Figure 12-4. The ASTM grain size for R12C59 HL is 8.0 and the ASTM grain size for R11C60 HL is 9.0. These grain sizes are typical of thermal treated Alloy 600 tubing produced for Model F steam generators.

Representative SEM micrographs showing the carbide distribution in the R12C59 HL and R11C60 HL tubes are presented in Figures 12-5 and 12-6. The carbide distribution seen for both tubes is typical of thermal treated Alloy 600 tubing of this vintage. The carbide precipitates are predominantly intergranular with a low density of intragranular carbides. Based on prior laboratory test results, this microstructure has generally shown good resistance to stress corrosion cracking.

12.4 Bulk Chemistry

Procedure

The chemical composition of the base metal of both tubes was determined by quantitative chemical analysis. The radioactivity of each section was reduced by several cycles of immersion in a room temperature solution of 35% HNO_3 + 4% HF (by volume), plus surface abrasion with silicon carbide wheels. Quantitative analysis was performed using a combination of inductively coupled plasma, graphite furnace atomic absorption, inert gas fusion, and combustion methods.

Results

The results of the chemical analyses for R12C59 HL and R11C60 HL are provided in Table 12-1. Included also are the CMTR values for the respective heats. The CMTR values represent the mill analysis for the heat. The slight differences noted between the CMTR and pulled tube chemical analyses are within the expected variability based on industry experience.

12.5 Modified Huey Tests

Procedure

It has been Westinghouse practice in the manufacture of thermal treated Alloy 600 heat transfer tubing to ensure that the material was not sensitized. Westinghouse, along with the industry in general, adopted a modified Huey test (ASTM A262 Practice C) as the principal tool for the evaluation of grain boundary chromium depletion in Alloy 600. The test was modified to a single 48-hr exposure in boiling 25% nitric acid. This modification was necessary to enhance the sensitivity of the test for detecting chromium depletion. In view of this historical practice, it has been Westinghouse experience that thermal treated SG heat transfer tubing in Westinghouse PWRs is not sensitized, and therefore not prone to in-service degradation in faulted secondary environments due to this condition. This experience notwithstanding, in order to complete the assessment of the Vogtle Unit 2 tubing materials, the sensitization level of R12C59 HL and R11C60 HL tubing was determined using a modified Huey test (48 hours in 25% nitric acid). Two ½ inch rings were cut from each pulled tube and subjected to the test.

Results

The results of the test are presented in Table 12-2. The results are consistent for thermal treated Alloy 600 steam generator tubing and show that the Vogtle Unit 2 pulled tubes are not sensitized. The average weight loss observed for R12C59 HL specimens was 38.0 $mg/dm^2/day$, while the specimens for R11C60 HL exhibited an average weight loss of 30.3 $mg/dm^2/day$. Grain boundary chromium depletion is considered present if the weight loss is greater than 300 $mg/dm^2/day$.

12.6 Microhardness

Procedure

Microhardness tests are used to provide information such as general hardness, verification of specific heat treatment, random hardness variations, and hardness gradients caused by localized cold work. Microhardness measurements were performed across the tube wall for both R12C59 HL and R11C60 HL. Vickers hardness measurements were performed in accordance with Westinghouse Procedure MR 8111, Revision 1. Vickers hardness is determined by dividing the applied kg-force load by the surface area of the indentation in square millimeters, computed from the mean of the measured diagonals of the indentation. A 500-g load was used for through-wall (OD surface to ID surface) measurements.

Results

The results of the microhardness tests are presented in Table 12-3. No localized hardness variations were noted and the results are consistent with tubing of this vintage.

12.7 Residual Stress

12.7.1 Split Ring Technique

Introduction

The hoop stress was measured by a split tube method per Westinghouse Procedure MCT-003, Revision 1. The procedure was used to measure the net-section residual hoop stress for the pulled tubes. The resulting calculated residual stress assumes a linear distribution of residual stress through the tube wall and is an approximate average value of the stresses over the whole specimen surface. When the tube is split, a change in strain is observed on the OD surface and is inversely related to the residual strain in the tubing. Multiplying the observed strain by the elastic modulus (E) provides a value for the average residual stress.

Procedure

Two ring specimens from each tube were tested for residual hoop stress. The specimens were: R12C59 HL - Piece 4B and 4C, and R11C60 HL – Piece 4B and 4C. The length of the ring specimens was 2.25 inch. The residual stress was determined from change-in-diameter measurements.

The OD of the tubing was measured prior to and following the cut. The tube section was slit axially along one side of the tube and the hoop stress was calculated from the diameter changes of the tube. The residual stresses were calculated from the average of the four readings for the wall thickness values and the measured diameters with the following equation:

$$\sigma_R = \left[\frac{E}{1-\nu^2}\right] W \left[\frac{1}{D_o} - \frac{1}{D_f}\right]$$

where:

σ_R = residual stress
E = elastic modulus
ν = Poisson's Ratio
W = average wall thickness
D_o = average OD before splitting
D_f = average OD after splitting

Results

The experimental data are presented in Table 12-4. The calculated residual hoop stress range from 495 psi compressive to 295 psi tensile for R12C59 HL and 1404 to 1804 compressive for R11C60 HL. These values are within the range of residual stress levels expected for thermal treated Alloy 600 tubing produced by Westinghouse for Model F steam generators. Data obtained during the development of the thermal treatment process showed macro residual hoop stress levels from 0 to 3 ksi based on split ring methods.

Table 12-1

Chemical Composition of Vogtle Unit 2 Pulled Tubes

Element	R12C59 HL – Heat NX 2609		R11C60 HL – Heat NX 2613	
	Analysis	CMTR	Analysis	CMTR
C	0.032	0.028	0.035	0.031
Ni	72.622	73.94	72.376	74.14
Fe	9.0286	9.42	9.4611	9.53
Cr	14.535	15.84	14.639	15.65
Mn	0.168	0.27	0.192	0.25
Mo	0.179	-	0.204	-
Ti	0.18	0.22	0.202	0.24
Nb	0.125	-	0.157	-
Al	0.211	0.24	0.24	0.33
Si	0.106	0.23	0.334	0.11
Pb	0.023	-	0.029	-
S	0.001	0.002	0.002	0.001
Cu	0.209	0.27	0.246	0.29
P	-	0.010	-	0.011
Co	0.049	0.06	0.058	0.07
Mg	0.015	-	0.017	-
N	-	-	-	-
V	0.026	-	0.031	-
B	-	0.003	-	0.003

Table 12-2
Modified Huey Results

Specimen Identity	HNO_3 % (wt.)	Material Condition	Corrosion rate ($mg/dm^2/day$)
R12C59 HL Piece 4D	25	Alloy 600 TT – As pulled	36.8
R12C59 HL Piece 4E	25	Alloy 600 TT – As pulled	39.2
R11C60 HL Piece 4D	25	Alloy 600 TT – As pulled	31.3
R11C60 HL Piece 4E	25	Alloy 600 TT – As pulled	29.2

Table 12-3

Results of Vickers Microhardness Measurements
(500 gram Through-wall Measurements)

SPECIMEN	DISTANCE FROM OD, IN.	HARDNESS
R12C59 HL Piece 4F (Met #2662) @ 180°	0.006	181
	0.012	179
	0.018	174
	0.024	177
	0.030	186
	Avg.	179
R11C60 HL Piece 4F (Met @180°	0.006	191
	0.012	179
	0.018	174
	0.024	170
	0.030	172
	Avg.	177

Table 12-4

Net-Section Residual Stress – Pulled Vogtle Unit 2 Tubes

Split Ring Technique

TUBE	PIECE	AVERAGE TUBE WALL THICKNESS W (INCH)	AVERAGE OD BEFORE SPLITTING D_O (INCH)	AVERAGE OD AFTER SPLITTING D_O (INCH)	RESIDUAL HOOP STRESS
R12C59 HL	4B	0.0409 inch	0.6897 inch	0.6895 inch	-495 psi
	4C	0.0409 inch	0.6897 inch	0.6898 inch	295 psi
R11C60 HL	4B	0.0413 inch	0.6881 inch	0.6876 inch	-1404 psi
	4C	0.0412 inch	0.6880 inch	0.6874 inch	-1804 psi

Figure 12-1
Stress - Strain Curve for R12C59 - Piece 4A

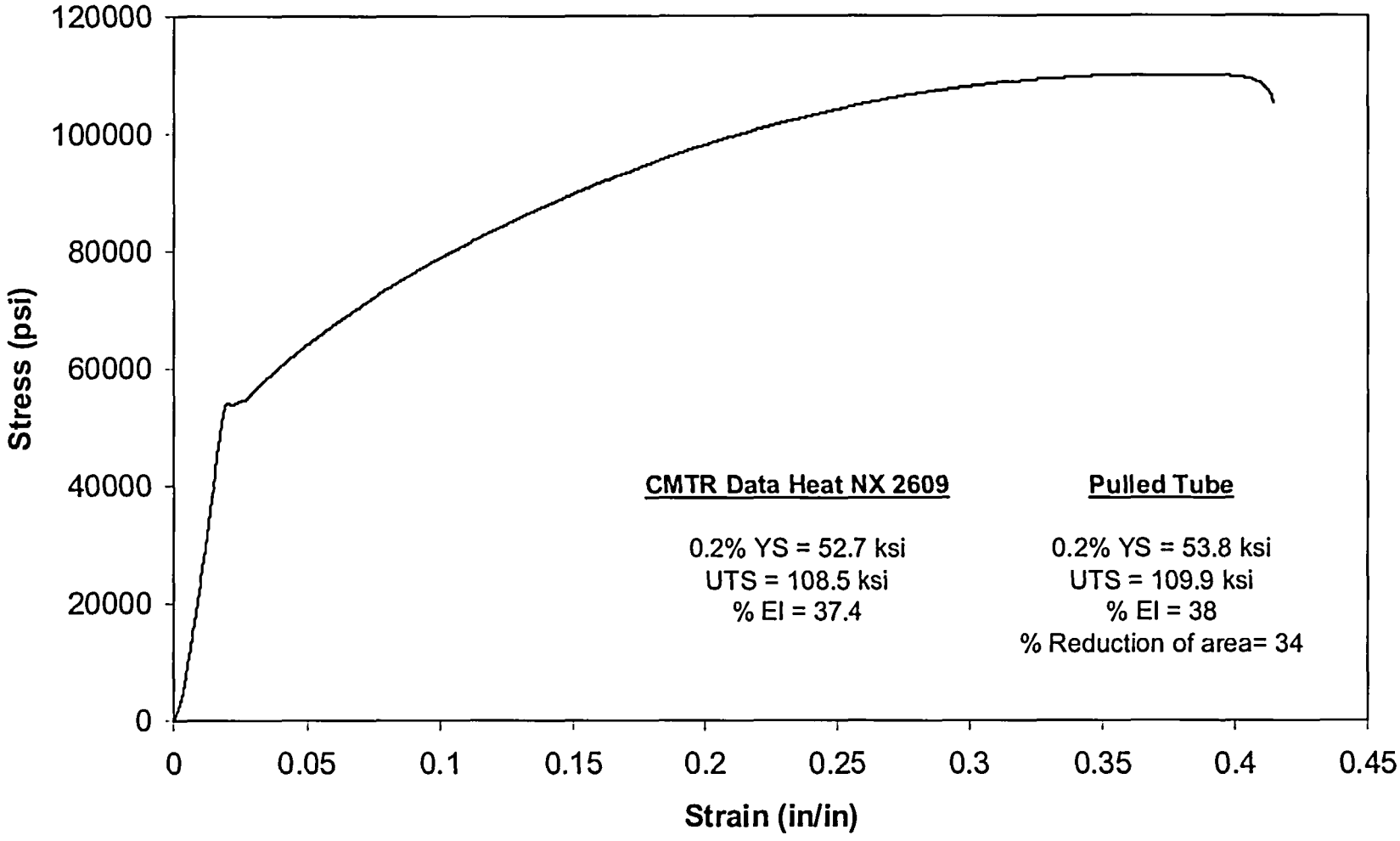

Figure 12-2
Stess - Strain Curve for R11C60 - Piece 4A

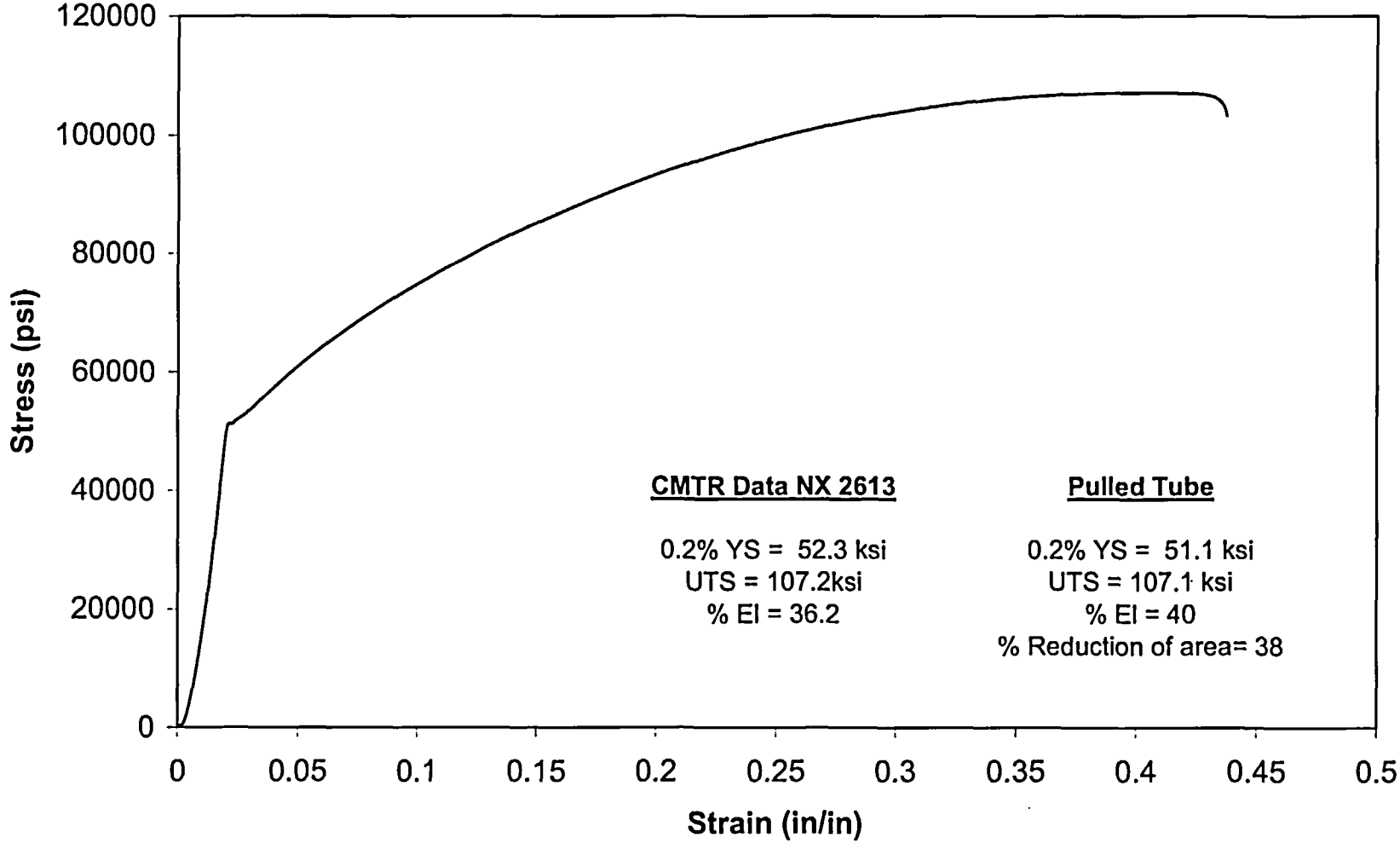

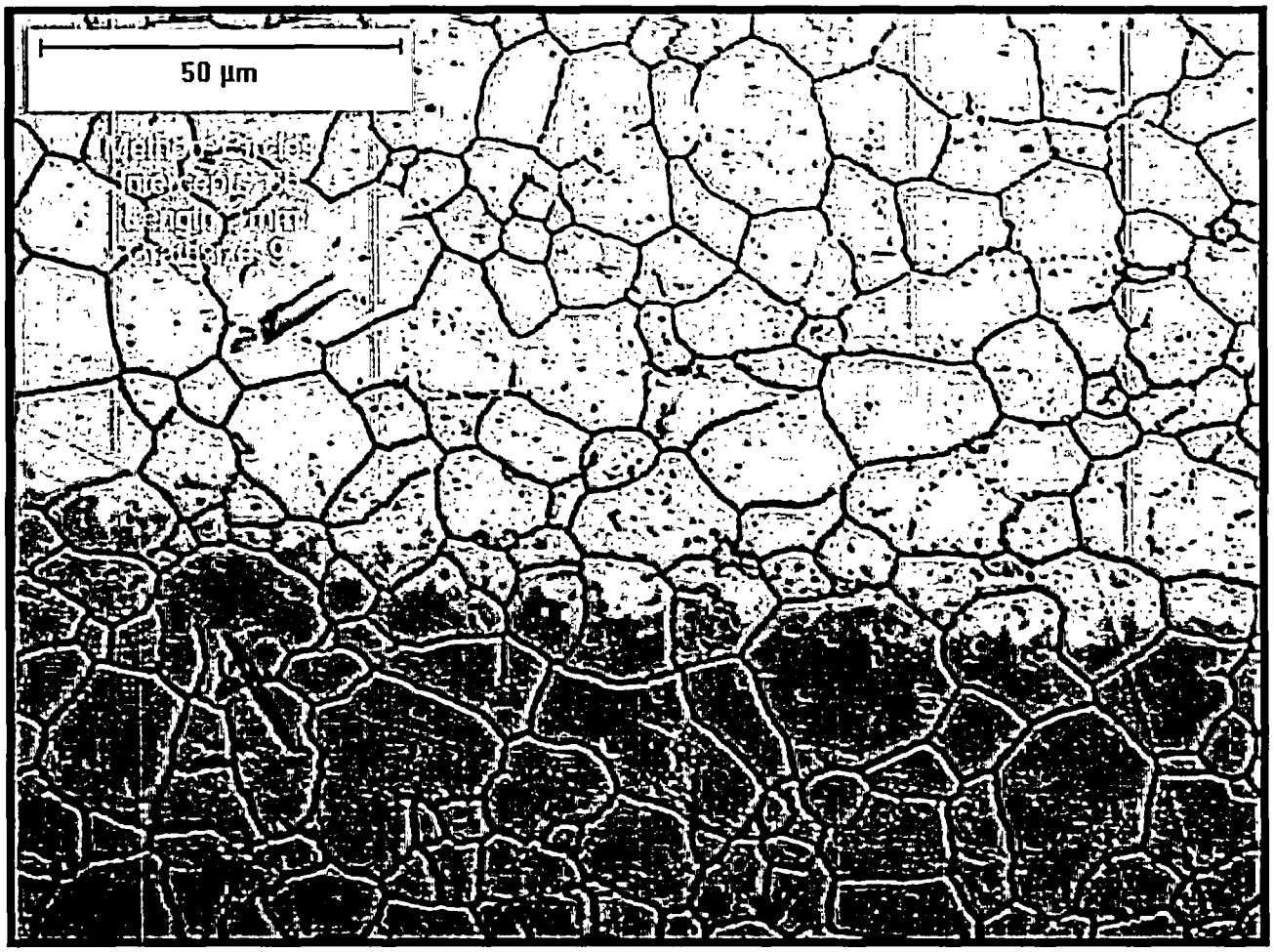

Figure 12-3 Photomicrograph Showing Grain Size of R12C59 HL – Piece 4F (Met #2663) 2% Nital Etch - ATSM Grain Size Number of 9.

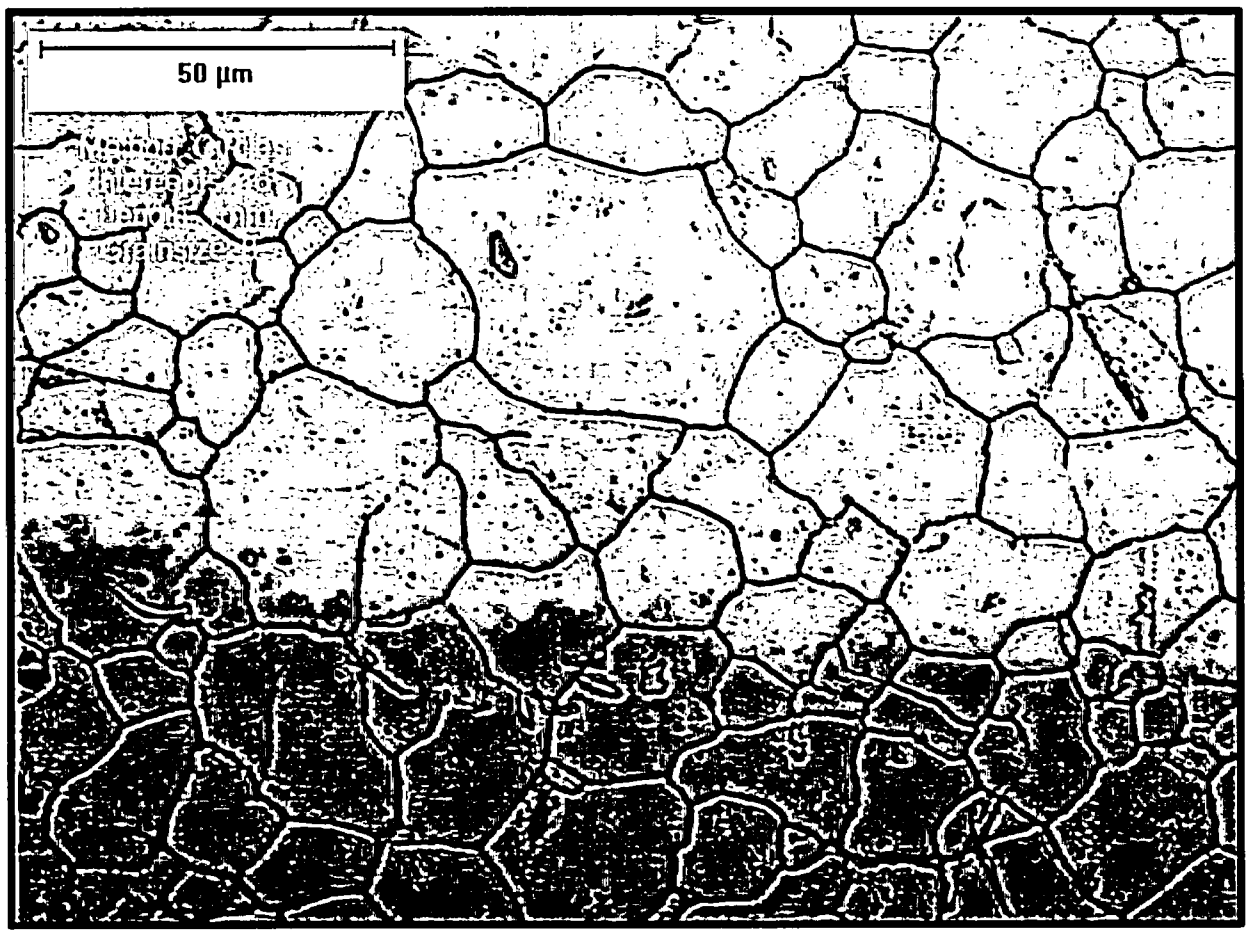

Figure 12-4 Photomicrograph Showing Grain Size of R11C60 HL – Piece 4F (Met #2662) 2% Nital Etch - ATSM Grain Size Number of 8.

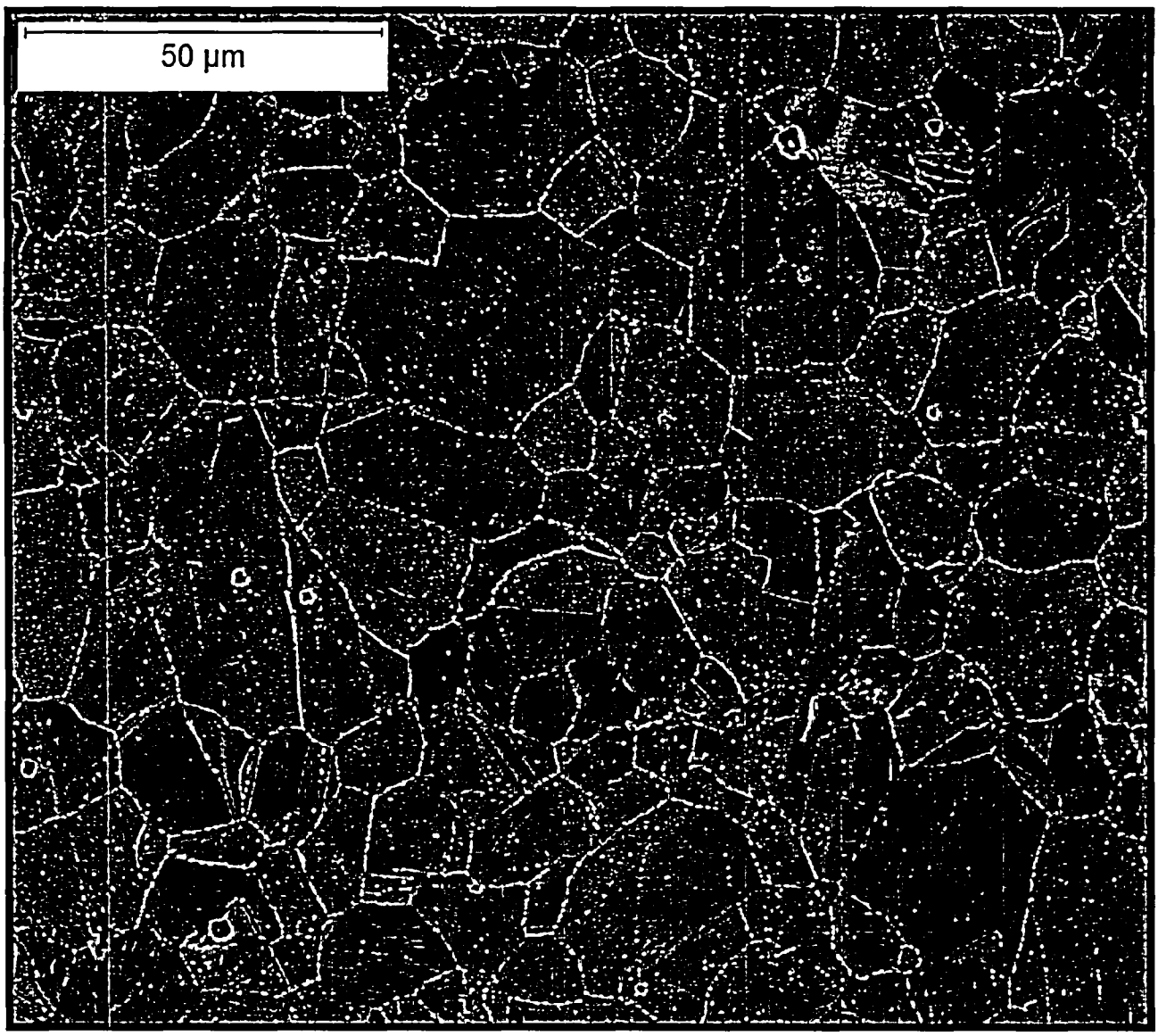

Figure 12-5 Scanning Electron Micrographs Showing Carbide Distribution of R12C59 HL – Piece 4F (Met #2663) Bromine-Methanol Etch. Carbide Precipitates Observed Mainly on Grain Boundaries and Minimal Intragranular Precipitates.

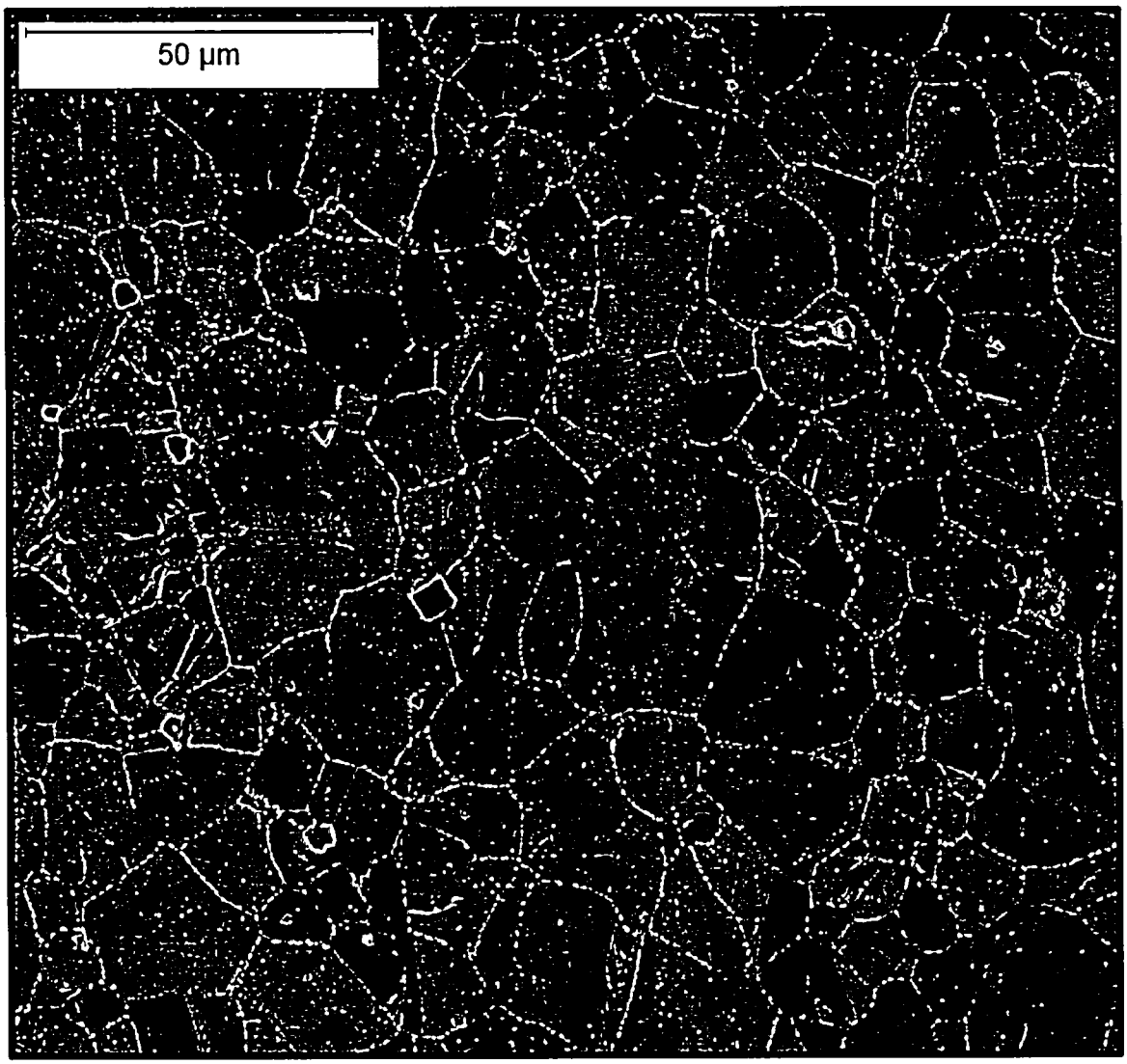

Figure 12-6 Scanning Electron Micrographs Showing Carbide Distribution of R11C60 HL – Piece 4F (Met #2662) Bromine-Methanol Etch. Carbide Precipitates Observed Mainly on Grain Boundaries and Minimal Intragranular Precipitates.